

**University of Nottingham
Department of Civil Engineering**

**AN INVESTIGATION INTO THE RESPONSE OF
PILES IN SAND
UNDER VERTICAL CYCLIC TENSILE LOADS**

**By
E. Sai Baba Reddy**

**Thesis Submitted to The University of Nottingham
for the Degree of Doctor of Philosophy
May 1996**

In memory of my Dad

ACKNOWLEDGEMENTS

The author wishes to thank all those who have given help and advice in this research as well as preparation of the thesis. The author is forever indebted to the following people for their contribution:

Professor S. F. Brown for his advice in times of need.

Dr. M. P. O'Reilly and Dr. D. N. Chapman for their constructive criticism and helpful supervision throughout the work;

Mr. Bob Collins for his expert workmanship in the construction of the experimental apparatus;

Mr. Darren Belcher who helped in the physical task of filling the test tank and setting up the apparatus several times.

Further acknowledgement is due to all the technicians, academic and research staff in the department for their friendship and advice.

The author expresses his sincere thanks to Prof. G. Rama Samy and Prof. Gopal Ranjan of University of Roorkee, INDIA for their help in final presentation of the thesis. Thanks are due to Prof. K. Ramasastri, Prof. A. Prasada Rao and Mr. M. Venkata Reddy of JNT University, INDIA for their help and support.

The financial support that enabled the author to complete the research was provided by the Commonwealth Scholarship Commission U.K. For this, the author is very grateful. It is appropriate to acknowledge the Jawaharlal Nehru Technological University, Hyderabad, India in the first place, for nominating the author for the above award.

Finally, special thanks are extended to authors in-laws for their support. To authors wife Sudha and sons Satish and Rakesh, very special thanks for the patience support in time of need.

C O N T E N T L I S T

ABSTRACT

List of Symbols and Abbreviations

List of Tables

List of Figures

CHAPTER ONE

Introduction

1.1	General	1
1.2	Scope of investigation	2
1.3	Outline of the thesis	3
1.3.1	Laboratory Model pile Tests	4
1.3.2	Theoretical studies	4

CHAPTER TWO

Literature Review

2.1	Introduction	5
2.2	Behaviour of sand under cyclic loading	5
2.2.1	Deformation of sand under cyclic loading	6
2.2.2	Change in density of sand under cyclic loading	8
2.3	Behaviour of pile under Monotonic Tensile loading	8
2.3.1	Shear stress distribution along the pile length	9
2.3.2	Load-displacement behaviour	12
2.4	Behaviour of pile under cyclic tensile loading	15
2.4.1	Accumulation of permanent displacement	15
2.4.2	Degradation of friction under cyclic loading	17
2.4.3	Mechanism of pile failure under cyclic loading	18
2.5	Summary	19

CHAPTER THREE

Experimental Apparatus

3.1	Introduction	21
3.2	Model pile test apparatus	22
3.2.1	Test tank	23
3.2.2	Surcharge pressure system	24
3.2.3	Model piles	24
3.2.4	Loading system	26
3.2.5	Measuring devices	27
3.3	Soil-pile-slip test apparatus	28
3.4	Display and Recording units	31
3.4.1	Digital Multimeters	31
3.4.2	Chart Recorder	31
3.4.3	Data Logger	32

CHAPTER FOUR

Properties of Test Materials

4.1	Introduction	33
4.2	Properties of sand	33
4.2.1	Selection of sand	33
4.2.2	Details of the tests conducted	33
4.2.2.1	Grain size distribution test	34
4.2.2.2	Tests to obtain Angle of Internal Friction (ϕ)	34
4.2.2.3	Minimum and Maximum density tests	35
4.3	Properties of the pile materials	35
4.3.1	Selection of the material	35
4.3.2	Details of the tests conducted	35
4.4	Soil-pile interface properties	36

CHAPTER FIVE

Experimental Investigation

5.1	Introduction	37
5.2	Preliminary experiments	38
5.3	Test programme on model piles	40
5.3.1	Filling of test tank	40
5.3.2	Installation of the model pile	41
5.3.3	Application of surcharge pressure	41
5.3.4	Load testing of piles	41
5.3.4.1	Monotonic load tests	41
5.3.4.2	Cyclic load tests	42
5.3.4.3	Recording of test data	44
5.4	Soil-pile-slip test	44

CHAPTER SIX

Analysis and Discussion of Experimental Results

6.1	Introduction	46
6.2	Stress in sand during pile installation	47
6.3	Results of monotonic tension tests	49
6.3.1	Load-displacement behaviour	49
6.3.2	Ultimate tensile capacity of pile	49
6.3.3	Load and shear stress distribution along the pile	50
6.4	Results of cyclic load tests	51
6.4.1	Displacement of pile under cyclic loading	52
6.4.2	Load and shear stress distribution along the pile	53
6.4.3	Deformation of sand surface during cyclic loading of pile	55
6.4.4	Variation of Radial stress in sand during	

	cyclic loading of pile	56
6.4.5	Mechanism of pile failure	56
6.4.6	Relationship between cyclic load level and number of cycles of failure	57
	6.4.6.1 Tests on a pile of a large diameter (76.2 mm)	58
6.4.7	Safe cyclic load	59
6.4.8	Effect of cyclic loading on pile capacity	59
6.4.9	Response of pile subsequent to peak loading	60
6.5	Soil-pile-slip test results	61
6.6	Concluding Remarks	63

CHAPTER SEVEN

Theoretical Studies on the Behaviour of Piles Under Tensile Loading

7.1	Introduction	66
7.2	Limitations of the Sulaiman and Coyle (1976) model	67
7.3	Estimation of load-displacement behaviour of pile under tensile loads- A modified method	69
	7.3.1 Algorithm	70
7.4	Results and Discussion	73
	7.4.1 Response of a pile under tensile loads	73
	7.4.2 Parametric study	74
	7.4.2.1 Effect of considering elastic deformation in shear mobilisation on the response of pile	75
	7.4.2.2 The effect of method of computing radial stress	76
	7.4.2.3 The effect of T-Z curves on pile reponse	77
	7.4.3 Prediction of load-displacement behaviour of a field pile	77

7.4.4	Estimation of safe cyclic load level - A critical appraisal	78
7.4.5	Suggested procedure to obtain safe cyclic load	80
7.4.6	A suggested design procedure for a pile under cyclic tensile loading	83
7.5	Concluding remarks	84

CHAPTER EIGHT

	Conclusions	85
--	--------------------	----

8.1	Recommendations for future work	88
-----	---------------------------------	----

	REFERENCES	90
--	-------------------	----

	BIBLIOGRAPHY	107
--	---------------------	-----

LIST OF RESEARCH PAPERS PRODUCED

Appendix A

Appendix B

Appendix C

A B S T R A C T

While most piles are subjected to compression during service, there are number of situations where piles are required to carry tension. These include foundations of transmission towers, gas holders, mooring systems for ocean surface or submerged platforms. However, serious attempts to understand the behaviour of piles under monotonic and cyclic tensile loading have been made with the development of Tension Leg Platforms for deep offshore oil fields. The piles used for TLP foundation are subjected to static pull-out force superimposed by a cyclic tensile force. Further, an offshore foundation is subjected, for the majority of the time, to small cyclic loads and at some times the load reaches a peak value. Thus, there is a need to understand the behaviour of pile not only under a constant cyclic tensile load but also subsequent to a peak loading.

A detailed review of the relevant literature presented in chapter two suggests that, there is very limited data available on the behaviour of piles under cyclic tensile loading, particularly for the case of piles embedded in sand. Further, the reported literature does not address on the response of the pile subsequent to peak loading. Hence, the present investigation is concerned with the behaviour of piles in sand under cyclic tensile loading particularly on the following aspects:

- (1) The displacement of pile under cyclic tensile loading
- (2) The mechanism of pile failure under cyclic tensile loading and
- (3) The response of pile subsequent to peak loading.

The objective was met through a comprehensive laboratory study on model piles. A model pile test apparatus was designed and developed during the present investigation. Using this apparatus, a number of monotonic and cyclic tensile load tests

were conducted on model piles (pile dia. 12.7 mm, 25.4 mm and 38.1 mm). Tests on an instrumented pile were also carried out to study the load distribution along the length of the pile. The results of these tests enabled understanding of the load-displacement behaviour and failure mechanism of pile under cyclic tensile loading. In a few tests, the pile was initially subjected to a large cyclic load for a few cycles and then the load was reduced to a small cyclic load. Results of these tests have thrown light on the behaviour of pile subsequent to peak loading.

Based on the results of the experimental investigation, the existing T-Z model suggested by Sulaiman and Coyle (1976) for the estimation of load-displacement behaviour of pile under monotonic tensile loads was modified. The results obtained from the modified T-Z model are compared with the observed values and with the results estimated by the existing T-Z model. Based on the modified T-Z model, a procedure of estimating the safe cyclic load for a pile has been suggested.

Further, an apparatus called soil-pile-slip test apparatus to obtain T-Z curves for tension piles was developed. The tests carried out using this apparatus, though they could not produce the desired T-Z curves, provided information on the changes in radial stress during pile loading.

Based on the investigation carried out, the following major conclusions have been drawn:

- (1) When a pile is subjected to a "safe" cyclic load, the response of the pile expressed as a plot between the displacement and the number of cycles exhibits insignificant increase in displacement with increase in number of cycles (stable zone of displacement curve) after an initial rapid increase in displacement for the first few load cycles.

(2) In tests carried out up to a maximum of 100,000 cycles, the safe cyclic load was observed to be 30% of ultimate tensile capacity of the pile.

(3) The failure of a pile in sand under cyclic loading is due to reduction in normal stress on the pile surface and the consequent reduction in shearing resistance.

(4) The behaviour of a pile subsequent to a peak cyclic loading is not adversely affected as long as the displacement of the pile is within the stable zone of the displacement curve. However, if the pile reaches a state of failure under the peak loading its response to a subsequent loading deteriorates substantially.

(5) The proposed modified model estimates the load-displacement behaviour of a tension pile better than the existing T-Z model.

(6) The proposed model leads to a procedure of estimating the safe cyclic tensile load and a design method for piles under cyclic tensile loads.

LIST OF SYMBOLS AND ABBREVIATIONS

SYMBOLS

A	= cross-sectional area
B	= breadth
C _u	= uniformity coefficient (D ₆₀ /D ₁₀)
dr	= change in radial distance
D ₁₀	= particle size below which 10% of material lies
D ₃₀	= particle size below which 30% of material lies
D ₅₀	= mean particle size below which 50% of material lies
D ₆₀	= particle size below which 60% of material lies
D _c	= diameter of test chamber
D _p	= diameter of pile
DR	= relative density
Dz	= length of the pile segment
e	= void ratio
e _{min}	= minimum e
e _{max}	= maximum e
e _{at test}	= e at test
E	= Young's modulus of material
G	= shear modulus
G _s	= Specific gravity of soil solids
h	= distance from pile tip
k	= coefficient of lateral earth pressure
L	= length
LL	= liquid limit
N	= number of cycles
N _f	= number of cycles to failure
p	= surcharge pressure
PL	= plastic limit
q	= load
q _c	= cyclic load
q _{csafe}	= safe cyclic load
q _{ct}	= ultimate cyclic tensile capacity

q_t = ultimate tensile load (tensile capacity)
 q_{ta} = average tensile capacity (obtained from a number of trials)
 R_I = internal radius
 R_o = external radius
 r = radial distance
 r_m = radial distance from the centre of the pile where the shear
= stress becomes negligible
 S = load shared by a pile segment
 S_L = ratio of radial stress at failure to the initial radial
stress ($\sigma_{rf} / \sigma_{rc}$)
 δ = soil-pile interface friction angle
 δ_p = peak δ
 δ_r = residual δ
 ϕ = angle of internal friction
 ϕ_p = peak ϕ
 ϕ_r = residual ϕ
 γ = unit weight (density)
 γ_{min} = minimum γ
 γ_{max} = maximum γ
 $\gamma_{at\ test}$ = γ at test
 σ = direct stress
 σ_r = radial stress
 σ_{rc} = initial radial stress
 σ_{rf} = radial stress at failure
 τ = shear stress
 τ_{av} = average shear stress
 τ_o = shear stress at the pile surface
 τ_f = shear stress at failure
 τ_{max} = maximum shear stress
 τ_{limit} = limiting shear stress

ABBREVIATIONS

CLA	= Central Line Average
DMM	= Digital Multimeter
FS	= Factor of safety
LC	= Load Cell
LSG	= Load cell Segment
LVDT	= Linear Variable Differential Transducer
OCR	= Over Consolidation Ratio
PC	= Pressure Cell
TLP	= Tension Leg Platform
T-Z	= Load-displacement
VP	= Vacuum Point

LIST OF TABLES

Table 1.1	The World's tension leg platforms to date
Table 1.2	Example of 18 hours storm composition
Table 2.1	Studies of cyclic load tests on sands
Table 2.2	Soil properties at Labenne
Table 2.3	Soil properties at Labenne, by layer
Table 2.4	Cyclic load tests on laboratory model piles
Table 2.5	Number of cycles to failure with cyclic load level (Chan and Hanna, 1980)
Table 3.1	Monotonic tests on laboratory model piles
Table 3.2	The ratios of the tank dimensions to pile diameters adopted in the investigation
Table 3.3	Details of the model piles used in the investigation
Table 3.4	Calibration factors for the measuring devices
Table 4.1	Soil properties: Classification
Table 4.2	Soil properties: Shear strength parameters
Table 4.3	Properties of pile material
Table 4.4	Direct shear interface test results
Table 5.1	Details of experiments on model piles
Table 5.2	Soil-pile-slip tests
Table 6.1	Tests for pressure distribution during installation of pile
Table 6.2	Variation of $\sigma_{r(\max)}$ and $\sigma_{r(\max)}/p$ at different radial distances during the installation of the pile
Table 6.3	The ultimate tensile capacity of steel model piles
Table 6.4	Ultimate tensile capacity of aluminium alloy model piles
Table 6.5	Recoverable displacement observed during tests with varying cyclic load
Table 6.6	Displacement of the sand surface during cyclic tension tests
Table 6.7	Number cycles to failure with cyclic load level

Table 6.8	Ultimate tensile capacity of 76.2mm diameter pile
Table 6.9	The pile capacity after cyclic loading
Table 6.10	Soil-pile-slip test results
Table 6.11	Comparison of observed and estimated τ_f values
Table 6.12	Back calculated vales of S_L
Table 7.1	Shear stress distribution along the pile
Table 7.2	Properties of soil and piles
Table 7.3	Comparison of the observed and computed pile head displacements (pile No.1)
Table 7.4	Comparison of the pile head displacement at half-load carrying capacity
Table 7.5	The ultimate cyclic tensile capacity of piles for different limiting stresses

LIST OF FIGURES

- Fig. 1.1 Schematic representation of forces and movements of TLP
- Fig. 1.2 Illustration of a possible loading pattern on TLP
- Fig. 2.1 Illustration of the deformation of soil during cyclic loading
- Fig. 2.2 Cyclic stress ratio versus permanent strain ratio
- Fig. 2.3 Changes in soil properties with shear strain
- Fig. 2.4 Mode of deformation of shaft
- Fig. 2.5 Displacement of a pile during cyclic tensile load
- Fig. 2.6 Features of cyclic stability diagram
- Fig. 2.7 Cyclic interaction diagram
- Fig. 2.8 Distribution of maximum and minimum shear stress during a cyclic tension test
- Fig. 2.9 Distribution of axial load during cyclic load test
- Fig. 2.10 Variation in horizontal pressure during a cyclic tension test
- Fig. 3.1 Model pile test apparatus (Abood, 1989)
- Fig. 3.2 Layout diagram of the model pile test apparatus
- Fig. 3.3 The model pile test apparatus
- Fig. 3.4 Details of the test tank
- Fig. 3.5 Details of the fittings for the pile access unit
- Fig. 3.6 Design details of the model piles
- Fig. 3.7 Design details of the load cell segment
- Fig. 3.8 The load cell segments
- Fig. 3.9 Pile cap design
- Fig. 3.10 Load frame
- Fig. 3.11 Pull-out loading unit
- Fig. 3.12 Cyclic loading equipment
- Fig. 3.13 Laboratory miniature pile test apparatus
- Fig. 3.14 Details of the soil-pile-slip test apparatus
- Fig. 3.15 Soil-pile-slip test apparatus
- Fig. 3.16 Top plate design for the 38.1mm dia. pile element
- Fig. 3.17 Details of the deformation measuring unit

- Fig. 3.18 A closed view of deformation measuring unit
- Fig. 4.1 Particle size distribution of sand used in the investigation
- Fig. 4.2 Test plates for interface testing
- Fig. 5.1 A schematic representation of the experimental programme
- Fig. 5.2 Location of the pressure cells to study the pressure distribution during the pile installation
- Fig. 5.3 Arrangements for the vacuum test
- Fig. 5.4 Cyclic load form
- Fig. 6.1 Sign conversion for load and shear stress
- Fig. 6.2 Variation of radial stress with depth of pile penetration (25.4mm dia.)
- Fig. 6.3 Variation of radial stress with depth of pile penetration (38.1mm dia.)
- Fig. 6.4 Stress distribution during the pile installation (an illustration)
- Fig. 6.5 Stress variation with radial distance during the pile installation (25.4mm dia.)
- Fig. 6.6 Stress variation with radial distance during the pile installation (38.1mm dia.)
- Fig. 6.7 Monotonic test results
- Fig. 6.8 Loads along the instrumented pile during a monotonic tension test
- Fig. 6.9 Load distribution during monotonic tension test (38.1^{*}-100-B)
- Fig. 6.10 Simple representation of the settlement of the sand due to a surcharge pressure
- Fig. 6.11 Average shear stress distribution during monotonic tension test (38.1^{*}-100-B)
- Fig. 6.12 Load-displacement during a constant cyclic load test
- Fig. 6.13 Variation of recoverable displacement with cyclic load
- Fig. 6.14 Total displacement with number of cycles (12.7mm)

- dia. pile)
- Fig. 6.15 Total displacement with number of cycles (25.4mm dia. pile)
- Fig. 6.16 Total displacement with number of cycles (38.1mm dia. pile)
- Fig. 6.17 Displacement of pile under cyclic loading (an illustration)
- Fig. 6.18 Load variation along the instrumented pile during cyclic loading (75% q_{ta})
- Fig. 6.19 Load distribution load-off condition (test 38.1^{*}-75-A)
- Fig. 6.20 Load distribution load-on condition (test 38.1^{*}-75-A)
- Fig. 6.21 Load distribution and shear stress condition during load-off and load-on conditions at $N = 100$
- Fig. 6.22 Shear stress distribution along the pile during a cyclic load test (38.1^{*}-75-A)
- Fig. 6.23 Aluminium tip used to monitor movement of the sand surface
- Fig. 6.24 Displacement of the sand surface during tensile cyclic load test (38.1mm dia. pile)
- Fig. 6.25 Variation of radial stress in sand around the pile during a cyclic load test)
- Fig. 6.26 Number of cycles to failure Vs q_c (as % q_{ta})
- Fig. 6.27 Comparison of cyclic load test results with existing literature
- Fig. 6.28 Effect of pile diameter on number of cycles to failure
- Fig. 6.29 Varying cyclic load test results for the 38.1mm dia. pile
- Fig. 6.30 Varying cyclic load test results for the instrumented pile (38.1^{*}-V-B)
- Fig. 6.31 Cyclic load test results for the 38.1mm dia. pile (38.1-38-A)
- Fig. 6.32 Pile element test results (25.4mm dia.)

- Fig. 6.33 Possible load transfer mechanism in soil-pile-slip test
- Fig. 7.1 Components of pile head displacement estimated by T-Z model
- Fig. 7.2 T-Z curves for the soil pile interface
- Fig. 7.3 Flow chart for the modified T-Z model
- Fig. 7.4 Load displacement computation along the pile
- Fig. 7.5 T-Z curves (an illustration)
- Fig. 7.6 T-Z curve used
- Fig. 7.7 Load-displacement curve
- Fig. 7.8 Load distribution along the pile length
- Fig. 7.9 Shear stress distribution under different pile head loads
- Fig. 7.10 Load displacement behaviour of piles of different lengths - effect of considering elastic deformation of pile
- Fig. 7.11 Shear stress distribution along the length of piles - effect of considering elastic deformation of pile
- Fig. 7.12 Radial stress distribution for different pile lengths
- Fig. 7.13 Variation of pile capacity - effect of method of computing radial stress
- Fig. 7.14 T-Z curves used for comparison
- Fig. 7.15 Load-displacement behaviour of piles of different lengths - effect of T-Z curves
- Fig. 7.16 Comparison of load displacement behaviour of a field pile
- Fig. 7.17 Flow chart to obtain an ultimate cyclic tensile load
- Fig. 7.18 Shear stress distribution with and without considering load transfer mechanism
($\tau_{\text{limit}} = 20\% \tau_{\text{max}}$)
- Fig. 7.19 Shear stress distribution with and without considering load transfer mechanism
($\tau_{\text{limit}} = 30\% \tau_{\text{max}}$)

- Fig. 7.20 Shear stress distribution with and without considering load transfer mechanism
($\tau_{\text{limit}} = 40\% \tau_{\text{max}}$)
- Fig. 7.21 Shear stress distribution with and without considering load transfer mechanism
($\tau_{\text{limit}} = 50\% \tau_{\text{max}}$)
- Fig. 7.22 Flowchart for the design of pile under cyclic tensile load

INTRODUCTION

1.1 General

While most piles are subjected to compression during service, there are a number of situations where piles are required to carry tension. These include foundations of transmission towers, gas holders, mooring systems for ocean surface or submerged platforms. However, serious attempts to understand the behaviour of piles under monotonic and cyclic tensile loading have been made with the development of Tension Leg Platforms (TLP) for deep offshore oil fields (beyond 300m depths of water) as an economical alternative structure (Dailey *et. al.*, 1979; Thornton, 1979; Perrett and Webb, 1980; Mangiavacchi *et. al.*, 1980; Hamilton and Perrett, 1986 and Patel, 1989).

The TLP configuration resembles that of a semi-submersible structure but is tethered to the sea-bed by vertical legs. These legs are kept in tension by excess buoyancy in the platform as shown in Fig.1.1. A list of the world's TLP structures to-date is shown in Table 1.1. Piles are considered to be a suitable type of foundation to provide anchorages to the tension legs (Lacy *et al.*, 1986 and Audibert and Bamford, 1989). The piles used for a TLP foundation are subjected to a static pull-out force superimposed by a cyclic tensile force keeping a net tensile force on the pile at all times (Andersen *et. al.*, 1982; Bea *et. al.*, 1982; St. John *et. al.*, 1983; Tetlow *et. al.*, 1983 and Bradshaw *et. al.*, 1984). A schematic diagram of loading on a TLP foundation can be illustrated as shown in Fig.1.2 and the general loading pattern for offshore structures in the North Sea is presented in Table 1.2. As can be seen from Fig.1.2 and Table 1.2 that, an offshore pile is subjected to cyclic loading of varying magnitudes. The majority of the time the pile is subjected to

small cyclic loads. However at some intervals the load reaches a peak value. Hence, there is a need to understand not only the behaviour of a pile under a constant cyclic load but also its response subsequent to peak loading.

There is very limited literature available on the behaviour of piles under cyclic tensile loading. The reported literature suggest the following:

(1) When a pile is subjected to cyclic tensile loading it undergoes recoverable and irrecoverable upward displacement.

(2) If the magnitude of the cyclic tensile load is greater than approximately 50% of its ultimate pull-out capacity, the irrecoverable displacement increases rapidly and the pile fails within a limited number of load cycles. If the magnitude of the cyclic load is less than about 30% of its ultimate pull-out capacity, the irrecoverable displacement is small and the rate of displacement decreases with the number of load cycles.

(3) Cyclic loading of piles is suspected to cause densification of the granular soil around the pile accompanied by a drop in the normal stress on the pile surface leading to the failure of the pile. However no attempt appears to have been made to measure the soil densification around the pile during cyclic loading.

1.2. Scope of Investigation

The available data is limited and scattered from laboratory and field tests. As can be seen from a review of literature presented in Chapter Two, very few tests have been reported on instrumented piles. There is a need to understand more clearly the mechanism of pile failure under cyclic loading. Furthermore, the reported literature does not address the response of the pile subsequent to a peak loading which is an important aspect to be

considered, for offshore pile foundations. In view of the above requirements a comprehensive study has been carried out to understand the behaviour of piles under cyclic tensile loading particularly on the following aspects:

- (1) The displacement of pile under cyclic tensile loading
- (2) The mechanism of pile failure under cyclic tensile loading and
- (3) The response of pile subsequent to peak loading.

1.3. Outline of the Thesis

In the present investigation laboratory experiments were conducted on small scale model piles. The tests were conducted under monotonic and cyclic tensile loading. Besides laboratory experiments, an analytical study was also carried out to estimate the behaviour of piles under tensile load.

1.3.1. Laboratory Model Pile Tests

An experimental apparatus was designed and developed to conduct tests on model piles. The apparatus was specially designed to increase the effective confining stress in sand around the pile to create an effect of overburden pressure experienced by a pile at a large depth. The details of the apparatus are presented in Chapter Three. The model tests were conducted on piles embedded in dry sand. The properties of test material are presented in Chapter Four. A set of preliminary experiments were conducted to ensure that the dimensions of the test tank were sufficient for the proposed maximum pile diameter and to study the working condition of the apparatus. In the main experimental programme, tests were performed on instrumented and un-instrumented model piles. The tests on model piles included monotonic and cyclic tensile loading. The effect of cyclic loading on monotonic pile

capacity was also studied. To study the response of the pile subsequent to a peak loading, a series of tests ~~wes~~ conducted under varying cyclic loads. The detailed experimental programme is presented in Chapter Five. The results obtained from laboratory model tests are analysed and discussed in Chapter Six.

1.3.2. Theoretical Studies

It was considered necessary to modify the existing T-Z model suggested by Sulaiman and Coyle (1976) for the estimation of load-displacement behaviour of pile under tensile loads. Accordingly, a modified T-Z model has been proposed. The load-displacement behaviour of a set of field piles estimated using the modified T-Z model has been compared with the observed values. Based on the present model developed, a procedure of estimating the safe cyclic load for a pile has been suggested. The details of these theoretical studies are presented in Chapter Seven.

In addition, an attempt was made to develop an apparatus called soil-pile-slip test apparatus, to obtain T-Z curves for tension piles. The tests carried out using this apparatus, though it could not produce the desired T-Z curves due to certain limitations realised at the analysis stage, provided information on the changes in radial stress during monotonic tensile loading of a pile.

The major conclusions drawn based on the experimental and theoretical studies carried out are presented in Chapter Eight.

Table 1.1 THE WORLD'S TENSION LEG PLATFORMS TO DATE

(Offshore Engineer, April, 1993)

Description of Item	Name of TLP (Country)				
	Hutton (UK)	Jolliet (US)	Snorre (Norway)	Auger (US)	Heidrun (Norway)
Water Depth, m	150	536	310	870	345
Installation Year	1984	1989	1992	1993	1995
Hull L x B m x m	96x92	55x55	101x101	103x88	110x110
Operator	Conoco	Conoco	Saga	Shell	Conoco

Table 1.2 Example of 18 Hour Storm Composition
(Andersen, 1991)

Load in % of Max. Load	Number of Cycles
0 - 10	2228
10 - 20	1450
20 - 30	645
30 - 40	324
40 - 50	161
50 - 60	74
60 - 70	34
70 - 80	11
80 - 90	4
90 - 92.5	1.4

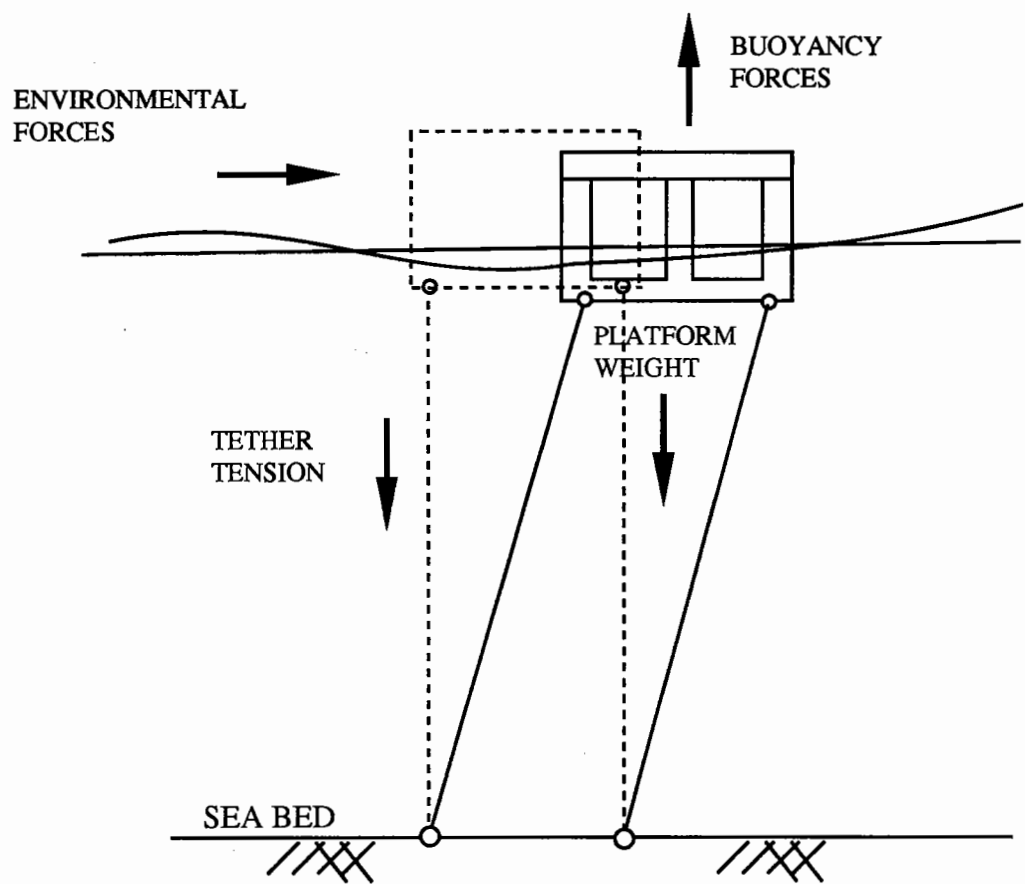


Fig.1.1. Schematic Representation of Forces and Movements of TLP
(Tetlow *et al.*, 1983)

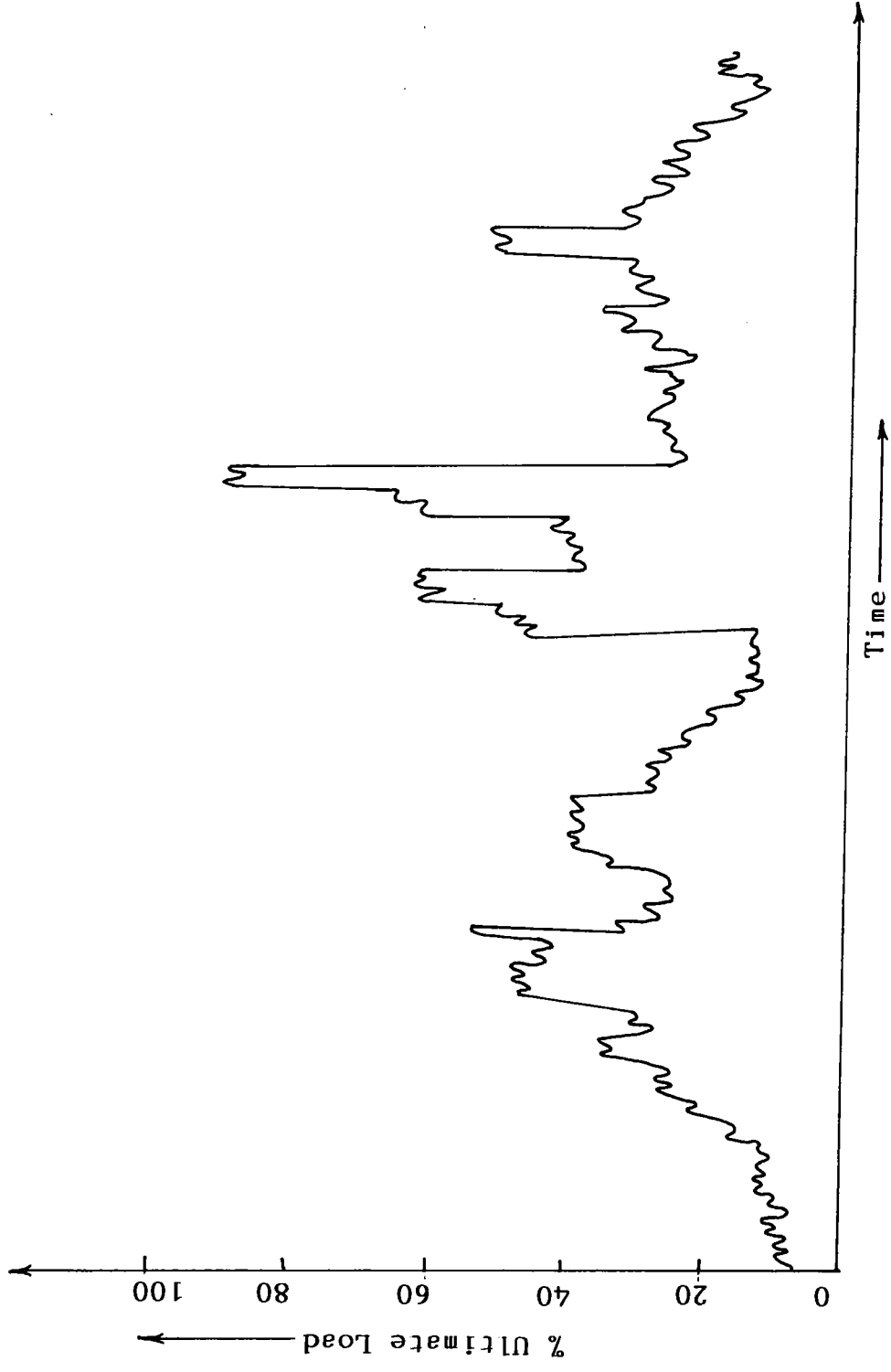


Fig. 1.2. Illustration of a Possible Loading Pattern on TLP

LITERATURE REVIEW

2.1 Introduction

A tension pile transfers the load to the surrounding soil by surface friction. The loads transferred create strains in the soil, which contribute towards the displacement of pile. When the shear stress at soil - pile interface reaches a maximum, the pile fails. Similarly, when a pile is subjected to cyclic loading, the surrounding soil experiences cyclic stress and strain. Hence, the response of a pile under cyclic loading depends on the response of soil and soil - pile interface under cyclic loading. Accordingly, the literature available on the following three aspects have been reviewed.

- 1) Behaviour of sand under cyclic loading
- 2) Behaviour of piles under monotonic tensile loading and
- 3) Behaviour of piles under cyclic tensile loading.

2.2 Behaviour of Sand Under Cyclic Loading

Investigations on the response of sand/crushed rock under cyclic loading have been reported in the literature. These studies show that a sand under cyclic loading undergoes recoverable and irrecoverable (permanent) strains frequently accompanied by a change in density. Hence the behaviour of sand under cyclic loading has been reviewed with reference to the following two aspects.

- i) Deformation of sand under cyclic loading and
- ii) Change in density of sand under cyclic loading.

2.2.1 Deformation of Sand Under Cyclic Loading

During cyclic loading, the sand undergoes recoverable and irrecoverable strains. Under a given cyclic load, the recoverable strain is reasonably constant and the irrecoverable strain accumulates with number of cycles (Fig. 2.1) (Boyce, 1976, 1980; Pappin, 1979; Lentz and Baladi, 1980; Luong, 1980; Shaw, 1980; Marr and Christian, 1981; Dyaljee and Raymond, 1982; O'Reilly, 1985; O'Reilly and Brown, 1992). Failure of foundations are generally associated with the irrecoverable strains in soils. Table 2.1 presents details of reported cyclic load tests on sand. It is generally reported that the rate of accumulation of irrecoverable strains in soil is a function of cyclic stress and strain levels.

a) Cyclic stress levels

Lentz and Baladi (1980) conducted a series of cyclic triaxial tests on uniform sand. The cyclic load tests were conducted under different cyclic load levels at a frequency of 1 Hz. In each cyclic load test, the total axial strain in soil was measured after 10,000 cycles. The strain under different cyclic load levels are presented in Fig.2.2. From the results it can be observed that,

(i) The total permanent strain increases with increase in cyclic stress level (Fig.2.2).

(ii) The rate of increase of permanent strain is gradual when the cyclic stress is a small percentage of its static capacity and is very rapid when the cyclic stress approaches the ultimate static capacity.

Marr and Christian (1981) carried out drained cyclic triaxial tests on alluvial sand. Their observations suggest that, the permanent strain in soil is not only a function of cyclic shear

stress, but also depends on the ratio of mean shear stress to mean normal stress and on initial porosity of the soil. Similar comments were made by Diyaljee and Raymand (1982) who analysed the cyclic triaxial test results obtained on sand by Lau (1975), Fitzpatrick (1977) and Abedi (1978).

Based on cyclic triaxial tests on sand, Luong (1980) reported that the rate of increase in the permanent deformation with number of cycles, decreases if the cyclic load level is lower than a threshold value and increases if the cyclic load is higher than the threshold value. However, no method has been suggested for obtaining the threshold value. Furthermore, the safe limiting stress level for the cyclic loading has not been identified.

b) Cyclic strain level

Recently Sagaseta *et. al.*, (1991) have presented a review of literature related to the behaviour of soil under different magnitudes of shear strain (Seed and Idriss, 1970; Ishihara, 1982; and Dorby and Vucetic, 1987). Fig. 2.3 illustrates different types of soil behaviour associated with the strain ranges. The review of Sagaseta *et. al.*, (1991) indicate that:

(i) Below a shear strain of the order of 10^{-5} the behaviour of soil is purely elastic.

(ii) For the shear strains in the range of 10^{-5} to 10^{-3} , the soil behaviour becomes elastoplastic but does not result in permanent strain (Fig.2.3)

(iii) Beyond a strain level of about 10^{-3} , soil properties tend to change with number of cycles leading to permanent strain.

From the above studies it appears that, during a cyclic loading, sand undergoes recoverable and irrecoverable strains.

The recoverable strains under a given cyclic load is constant with the number of cycles. The rate of increase of irrecoverable strain is very small at smaller cyclic stress and strains. It is very large and leads to failure, if the cyclic load reaches its static capacity and the cyclic strain is more than 10^{-3} .

2.2.2 Change in Density of Sand Under Cyclic Loading

During cyclic loading, sand undergoes a change in density. Studies related to change in density of sand under cyclic load have been made by Youd (1970 and 1972) and Airey *et. al.*, (1992). Youd (1972) studied the compaction behaviour of saturated Ottawa sand (DR=75-90%) under cyclic shear. The test results show that, during each load cycle, the sand undergoes a finite increase in the density and hence decrease in void ratio. The reduction in void ratio continues until a limiting minimum value of 0.412 was reached. This void ratio was less than e_{min} (0.484) determined for the same sand by ASTM method. Similar observations were reported by Airey *et. al.*, (1992), who conducted cyclic load tests on carbonate sand (DR= 90%). It was observed that, in the first cycle the soil expands but in all the subsequent cycles there was a net contraction. The rate of contraction was decreasing as the number of cycles increases. Compaction of granular material under repeated shear was also reported by Ansell and Brown (1978) and Chan (1990).

The above studies indicate that when sand is subjected to cyclic shear, it undergoes a net reduction in volume with number of cycles until it reaches a maximum density. Even if the initial relative density of sand is as high as 90%, during cyclic loading it undergoes compaction.

2.3 Behaviour of Piles Under Monotonic Tensile Loading

When a pile is subjected to a tensile loading it undergoes a

relative displacement from its surrounding soil. The relative displacement between the soil and pile creates shear stress and strain in the soil (Tan, 1971; Cooke and Price, 1973; Cooke, 1974; Tan and Hanna, 1974; Williams, 1979 and Gallagher, 1984). The shear strain in the soil and the elastic deformation of the pile contribute towards the displacement of the pile. The displacement of the pile under increasing loads continues until the shear stress on the pile surface reaches a maximum. When the shear stress along the length of the pile reaches the maximum, the pile fails.

2.3.1 Shear Stress Distribution Along the Pile Length

Shear stress on the pile surface increases with relative displacement between soil and the pile surface. The maximum shear stress (the skin resistance), at a given location, on the pile surface embedded in sand is estimated as

$$\tau_f = k \bar{\sigma}_v \tan \delta \quad (2.1)$$

where

τ_f = shear stress at failure

k = co-efficient of lateral earth pressure

$\bar{\sigma}_v$ = effective overburden pressure and

δ = friction angle between sand and the pile surface.

If k is constant, in Eq. (2.1), the skin resistance increases with depth. However, from the field and laboratory investigations (Vesic, 1963, 1964, 1970; Hanna and Tan, 1973; Mc Clelland, 1974; Meyerhof, 1970, 1976; Coyle and Castello, 1981; Hettler, 1982; Dennis and Olson, 1983; Toolan and Ims, 1988, Briaud and Audibert, 1990; Olson, 1990; Toolan *et. al.*, 1990 and Kraft, 1991) it has been observed that the skin resistance on driven piles increases with depth up to a certain critical depth, beyond which the average skin resistance attains a quasi-constant value. This critical depth varies with the density of sand. Hence, it has been inferred that the coefficient of lateral earth pressure(k) is

not a constant and is a function of soil state, density and the length of pile.

Lehane *et. al.*, (1993) carried out an investigation on the mechanism of shaft friction in sand. They conducted field tests on an instrumented pile at Labenne, France. The properties of the soil at the site are presented in Tables 2.2 and 2.3. The instrumentation details of the pile are presented by Bond *et. al.*, (1991). Their experimental results show that for a given soil conditions, the radial effective stress ($\bar{\sigma}_r$) is maximum near the pile tip and decreases as one moves above the pile tip. Hence, it is inferred that the radial stress at any point along the pile length depends not only on the soil properties but also on the position of the pile tip, in relation to that sub layer (i.e. h/R_0 , where h - distance of the point considered from pile tip and R_0 - pile radius). Accordingly, the shear stress on the pile surface is given as

$$\tau = \bar{\sigma}_r \tan \delta \quad (2.2)$$

Where $\bar{\sigma}_r$ = radial effective stress on pile surface which is a function of DR, $\bar{\sigma}_v$ and h/R_0

The reasons for the variation of $\bar{\sigma}_r$ with h/R_0 is explained as follows. During the installation of the pile, the advancement of pile tip creates an increase in lateral stress. Once the pile tip passes through a particular soil horizon, continued penetration causes strain reversal and hence the radial stresses at that level falls (Kavvas and Baligh, 1982; Nauroy and Le Tirant, 1983; Coop, 1987; Bond, 1989; Coop and Wroth, 1989; and Lehane, 1992). Hence, the radial stress is a maximum near the pile tip and reduces as one moves above the pile tip.

Lehane, (1992) and Lehane *et. al.*, (1993) further reported that, during pile loading $\bar{\sigma}_r$, on the pile surface increases such

that at peak shear resistance the radial effective stress ($\bar{\sigma}_{rf}$) is about 1.4 times its static equilibrium value after installation ($\bar{\sigma}_{rc}$). This increase in $\bar{\sigma}_r$ was observed both under compressive and tensile loading of pile. The reason for this increase in radial stress is explained as due to interface slip dilation (Boulon and Foray, 1986 and Uesugi and Kishida, 1986). Further it is reported that the effect of interface slip dilation and hence the increase in radial stress during pile loading is more in small diameter piles. This indicates that the average shear resistance at failure decreases with increase in pile diameter.

From the above observations, Lehane (1992) has suggested an expression for shear stress at failure (τ_f) by modifying the Eq. (2.2) as

$$\tau_f = S_L \bar{\sigma}_{rc} \tan \delta \quad (2.3)$$

where $S_L = \bar{\sigma}_{rf} / \bar{\sigma}_{rc}$

(Varies between 1 and 1.4)

$\bar{\sigma}_{rf}$ = effective radial stress at failure

$\bar{\sigma}_{rc}$ = effective radial stress at equilibrium after pile installation = $0.70 (\bar{\sigma}_v)^{0.89} e^{2.91DR} (h/R_o)^{-0.33}$

DR = relative density of sand

$\bar{\sigma}_v$ = effective overburden pressure

R_o = radius of pile and

h = distance of pile tip from the point of consideration.

The effect of compressibility of pile on the shear stress distribution along the pile length was brought out by Randolph (1983) Jardine and Potts (1988, 1992) and Jardine (1991). If the pile is short and incompressible the relative displacement between the soil and pile at different elevations is approximately constant. If the pile is very long and compressible, it undergoes elastic deformation. Therefore, the relative displacement of pile is maximum at the top and reduces with depth. Hence, in a compressible pile, the limiting shear stress

will be attained first in the upper layers and then in the lower layers.

2.3.2 Load-displacement Behaviour

The majority of studies on piles are directed towards its behaviour under compressive (downward) loads and several methods of estimating load-displacement behaviour of piles have been suggested under compressive loads (Coyle and Reese, 1966; Coyle and Sulaiman, 1967; Cooke, 1974; Randolph, 1977; Randolph and Wroth, 1978, 1979 and Vanimpe, 1991). Sulaiman and Coyle (1976) modified their method to obtain load-displacement behaviour of piles under tensile loads and the same is reviewed here. Randolph and Wroth (1978 and 1979) have suggested an elastic method for compression piles. The relationship between the friction and the pile displacement suggested in this method is of interest to the present study and therefore, the same is also discussed.

a) Load Transfer (T-Z) Method

This method is proposed by Sulaiman and Coyle (1976) for tension piles in sand. According to this method, the pile is divided into a number of segments. The relationship between the local displacement of the pile segment and the skin friction mobilized on the pile surface is estimated from laboratory tests. A value for upward pile tip movement is assumed and working progressively up the pile, the local displacement and skin friction mobilised for each segment are calculated. Accounting for elastic deformation of the pile the load and displacement at the pile head are obtained. By repeating the procedure with different values of pile tip displacement, the load-displacement curve is obtained for the pile.

Sulaiman and Coyle (1976) made the following assumptions:

1) The elastic deformation of the pile does not mobilise skin-frictional resistance, and this deformation equals $PL/(AE)$, where

P = tensile load applied to the pile

L = length of pile,

A = cross-sectional area of the pile and

E = Young's modulus.

2) The effective radial stress ($\bar{\sigma}_r$) on pile surface is given by

$$\bar{\sigma}_r = k \bar{\sigma}_v$$

where $k = 0.75$ and

$\bar{\sigma}_v$ = effective vertical pressure.

The above T-Z method is simple and easy to adopt but it suffers from the following limitations.

1) Elastic deformation of a long, compressible pile could be a significant component of pile displacement and needs to be considered in computing mobilised friction.

2) The radial stress on pile surface is computed assuming a constant value for k . However, Eq. (2.3) implies that k is not a constant and it is a function of relative density and location of the point under consideration from the pile tip.

3) In this method, the computation starts by assuming a tip displacement (the whole length of the pile undergoes displacement), which means, corresponding to the first point on the load displacement curve of the pile, load transfer to the full length of the pile is assumed. This results in the initial portion of the load-displacement curve not getting defined adequately.

b) Elastic Method

Randolph and Wroth (1978), proposed a method of estimating

the load-displacement behaviour of pile under compressive loads. The total displacement of the pile is obtained by superimposing the settlements due to deformation in surrounding soil and that due to the deformation below the pile tip. The method suggested for computing the relationship between the skin friction and the corresponding displacement of the pile is of interest to the present study and the same is reviewed below.

According to this method, the soil around the pile is divided into a number of concentric circles as shown in Fig. 2.4. A load on the pile head is assumed. By dividing the load on the pile head by the surface area of the pile ($2\pi R_0 L$), the shear stress on the pile surface (τ_0) is computed. The shear stress in the soil at a radial distance 'r' is calculated as

$$\tau = \tau_0 \frac{R_0}{r} \quad (2.4)$$

Where τ = shear stress in soil at a radial distance 'r' from the centre of pile
 τ_0 = shear stress on the pile surface and
 R_0 = radius of pile.

Considering the thickness of each soil ring as dr and the shear modulus of soil as G , the displacement of pile due to the displacement of the surrounding soil, under the assumed load, is computed as

$$(\tau_0 R_0 / G) \int_{R_0}^{r_m} \frac{dr}{r} \quad (2.5)$$

where r_m = the radial distance from the centre of the pile where the shear stress becomes negligible.

A new value of load on the pile head is assumed and the corresponding displacement is computed. By repeating the procedure, the skin friction load - displacement curve is obtained for the pile.

Based on the work carried out at Imperial College, London (Jardine *et. al.*, 1984, 1986 and Jardine, 1985), Jardine and Potts (1988) described an approach for the prediction of the load-displacement relationship for large piles. In their model, the effect of pile installation is also considered. An interface zone near the pile shaft was considered by limiting the friction angle at the soil-pile interface (Jardine *et. al.*, 1992b). The approach was demonstrated by employing it in a finite element analysis to predict the displacement of the pile foundation used for the Hutton tension leg platform and the Magnus steel-Jacket platform (Jardine, 1985, Jardine and Potts, 1988, 1992 and Jardine *et. al.*, 1988).

2.4 Behaviour of Piles Under Cyclic Tensile Loading

A number of studies on the behaviour of piles under cyclic tensile loading on piles in clay (Grosch and Reese, 1980; Mc.Anoy *et. al.*, 1982; Karlsrud and Haugen, 1983; Karlsrud *et. al.*, 1986, 1992 and Norwegian Geotechnical institute, 1987, 1988a, 1988b, 1989) and on piles in sand (Angemeer *et al.*, 1973; Chan, 1976; Chan and Hanna, 1980; Puech, 1982; and Abood, 1989) have been reported. Details of some of the laboratory studies are briefly presented in Table. 2.4. The results of these studies on the following aspects are discussed.

- i) Accumulation of permanent displacement,
- ii) Degradation of skin-friction under cyclic loading and
- iii) Mechanism of pile failure under cyclic loading.

2.4.1 Accumulation of Permanent Displacement

Chan and Hanna (1980) conducted cyclic tensile load tests on laboratory model piles in sand (Table 2.4). The performance of piles tested by them is presented in Fig. 2.5 and Table 2.5. These results suggest that:

1) When the applied cyclic tensile load is small, 15% to 20% of ultimate static tensile capacity (q_t), the pile undergoes small displacement and the rate of displacement with number of cycles decreases.

2) When the cyclic load is large (30 to 70% of q_t) the pile undergoes very large displacement and fails within a small number of load cycles.

The results of tests on laboratory model piles reported by Abood (1989) also agree with the above observations.

Puech (1982) reported the results of tests on instrumented steel piles embedded in silts and loose sands. These field tests were performed on 273mm diameter and 13m long piles. The piles were instrumented to record load, radial pressure and pore pressure on the pile. The results of these tests show that:

The displacement of piles under cyclic loading can be divided into a transitory phase, indicating an immediate response of the soil to the cyclic stresses and a cyclic creep phase, characterising the long-term behaviour of the pile

i) The transitory phase covers several tens of cycles and is characterised by an increase in pile displacement. This increase is fast at first and then gradually slows down.

ii) In the creep phase, each load cycle causes a tiny increase in the displacement. The rate at which this displacement is generated depends on the cyclic load level.

iii) For reduced load levels (less than 50% q_t), the rate of displacement decreases, indicating stability and for higher load levels (greater than 50% q_t), the rate of displacement increases

leading to failure, similar to those observed by Chan and Hanna (1980) and Abood (1989).

2.4.2 Degradation of Friction Under Cyclic Loading

Poulos has reported analytical studies (Poulos, 1979a, 1979b, 1983, 1988, 1989a and 1989b) and experimental studies on small model piles in clay (Poulos, 1981a, and 1981b) and in sand (Poulos, 1984). The degradation of skin friction under cyclic loading is evaluated by measuring the static capacity of piles before and after the cyclic loading. The results of these studies show that:

i) For piles in sand, the cyclic degradation of skin friction is controlled by the amplitude of cyclic displacement, relative to a critical displacement. This critical displacement is equal to the static displacement required for full slip. For large relative cyclic displacement, a reduction in skin friction of the order of 50% occurs.

ii) For piles in clay, the skin friction is not seriously affected when the cyclic load is less than 40% of its static capacity and the number of cycles is limited to 1000. For cyclic loads in excess of 40% of static capacity, a very marked decrease in skin friction occurs.

iii) The degradation of pile capacity under cyclic loading depends on (a) number of load cycles, (b) Mean load and (c) Cyclic load applied on the pile. The stability of the pile can be established with the help of cyclic stability diagram (Fig. 2.6). The stability can be characterised by one of the following three states:

i) Stable - Cyclic loading has no effect on pile capacity.

ii) Metastable - Cyclic loading causes a limited reduction in pile capacity but the pile does not fail within N-cycles.

iii) Unstable - Cyclic loading results in failure of pile within N-Cycles

Jardine (1991) has also suggested the concept of cyclic interaction diagram (Fig. 2.7). This concept is similar to the cyclic stability diagram suggested by Poulos, except that the co-ordinate axes in the interaction diagram are based on the shear stresses on the surface of the pile element as opposed to applied loads on the pile head as in the cyclic stability diagram of Poulos.

2.4.3 Mechanism of Pile Failure Under Cyclic Loading

Results of investigation reported by Karlsrud and Hauges, (1983) (Jardine, 1991), Chan and Hanna (1980) and Puech (1982) throw light on the mechanism of pile failure under cyclic loading. Karlsrud and Hauges, (1983) and Puech (1982) have conducted tests on large scale instrumental piles in clay and sand respectively. Chan and Hanna (1980) have performed tests on instrumented laboratory model piles in sand.

Karlsrud and Hauges (1983) have recorded the shear stress along the length of the pile both under loading and un-loading conditions. The results are presented in the form of shear stress variation with depth as shown in Fig. 2.8. The results of Chan and Hanna (1980) are presented in the form of load distribution with depth for different number of cycles in Fig. 2.9. The results shown in Figs. 2.8 and 2.9 suggest the following.

i) In a cyclic tensile test, on loading and un-loading, two-way shear takes place around the pile surface, primarily in

the upper part of the pile (Fig.2.8). The two-way shear leads to degradation of shearing resistance with number of cycles.

ii) The reduction of shearing resistance in the upper portion of pile leads to the transfer of load to lower portions of the pile (Fig. 2.8) results in progressive degradation in shearing resistance along the pile length and failure of pile.

Puech (1982) has recorded the variation in radial stress (σ_r) on the pile surface with number of cycles (Fig. 2.10). From these observation the mechanism of pile failure can be explained as follows:

(i) There is a reduction in radial stress with number of cycles. This reduction in radial stress is possibly due to the compaction of soil around the pile.

ii) The drop in radial stress leads to reduction in shearing resistance, ultimately resulting in the failure of the pile.

2.5 SUMMARY

The above review of literature can be summarised as follows:

1) Limited literature is available on the cyclic load behaviour of piles in sand.

2) Under cyclic loading, the pile undergoes recoverable and irrecoverable displacement. The irrecoverable displacement increases with number of cycles. The rate of this displacement decreases if the cyclic load is small and increases leading to failure, if the cyclic load is large. The literature puts the safe cyclic load levels varying from 20 to 50% of the static capacity of the pile. More experimental data on this aspect would enhance the understanding of the safe limiting load on piles.

3) Only a limited literature is available on the failure mechanism of piles under cyclic loading. The available literature suggests that the failure of piles take place because of the degradation of shearing resistance on the pile surface due to two-way shear in the soil and reduction in radial stress on the pile surface.

4) The response of piles subsequent to a peak tensile loading, which is one of the important aspects to be understood for the design of TLP foundations, appears to have not been studied so far.

5) The available method of estimating load-displacement behaviour of piles in tension (Sulaiman and Coyle, 1976) has a few limitations and needs to be modified for better predictions.

Table 2.1 Studies of Cyclic Load Tests on Sands

Reference	Soil Properties	Type of Test	Method of Loading	Maximum Number of Cycles
Yamanouchi and Aoto (1969)	Sand	Cyclic Tri-axial test. 35mm Dia. & 81.5-82.5mm high sample.	Cyclic loading was in a rectangular wave form at a frequency of 0.25Hz	50,000
Youd (1972)	Ottawa Sand $e_{min} = 0.484$ $e_{max} = 0.752$ $D_r = 75-79\%$	Cyclic Simple shear Test.	-	150,000
Lau (1975) and Abedi (1978)	Kingston sand $D_{10} = 0.09\text{mm}$ $D_{50} = 0.20\text{mm}$ $D_{60} = 0.26\text{mm}$	Cyclic Tri-axial Test.	The Triaxial test was conducted under a confining pressure of 35kPa	100,000
Fitzpatrick (1977)	Fine Ottawa sand. $D_{10} = 0.65\text{mm}$ $D_{50} = 0.70\text{mm}$ $D_{60} = 0.75\text{mm}$	Cyclic Tri-axial Test.	Tests were conducted at confining pressures ranging from 8.6kPa to 34.5kPa and under deviator stress level of 0.5 to 0.94 times static capacity.	100,000

Table 2.1 Continued.

Reference	Soil Properties	Type of Test	Method of Loading	Maximum Number of Cycles
Datta <i>et. al.</i> , (1979)	Calcareous Sand $e_{min} = 0.930$ $e_{max} = 1.390$	Cyclic Tri-axial Test. 38.1mm dia. & 76.2mm high Sample	The Cyclic load was applied at a frequency of 0.5Hz	400
Lentz and Baladi (1980)	Medium Sand $D_{10} = 0.25mm$ $D_{50} = 0.40mm$ $D_{60} = 0.50mm$ $D_r = 99\%$	Cyclic Tri-axial Test. 50.8mm Dia. & 137.16mm high sample.	Loads were measured using load cell beneath the sample; deformation was measured by a LVDT.	10,000
Uchida <i>et. al.</i> , (1980)	Sand $D_{10} = 0.165mm$ $e_{min} = 0.588$ $e_{max} = 0.910$ $D_r = 62-68\%$	Cyclic Tri-axial Test. 50mm dia. & 10mm high sample.	Samples were isotropically consolidated under a confining pressure of 50 & 100kPa and cyclic load was applied at frequencies of 1, 2 and 4Hz.	30
Marr and Christian (1981)	Uniform graded Aluvial sand $D_{50} = 0.17mm$ $e_{min} = 0.526$ $e_{max} = 0.846$ $D_r = 28\%$	Cyclic Tri-axial Test. 36mm dia. & 76mm high sample.	A nearly sinusoidal cyclic load was applied at a frequency of 0.125Hz.	10,000

Table 2.1 Continued.

Reference	Soil Properties	Type of Test	Method of Loading	Maximum Number of Cycles
Chen <i>et.al.</i> , (1988)	Glass spheres. sample is composed of 0.3-0.425mm and 0.18-0.25mm size particles $G_s = 2.472$ $D_r = 60\%$	Torsional simple shear resonant coulumn test. A hollow cyclinder of 71mm inner & 102mm outer diameter and 193mm high sample	Each specimen was isotropically consolidated under a pressure of 138kPa before the applica- tion of cyclic loading.	-
Georgiannou <i>et.al.</i> , (1991)	Clayey Sand $C_u =$ 102-147kPa $OCR = 1-2$	Computer controlled Cyclic tri-axial test	The deviator stress was applied at a frequency of 0.016Hz.	290
Airey <i>et.al.</i> (1992)	Carbonate Sand $e_{min} = 0.520$ $e_{max} = 1.090$ $D_r = 90\%$	Modified Cyclic shear box test. 60x60x2mm high Sample	Cyclic shear tests were conducted under a normal stress of 50-400kPa.	80

Table 2.2 Soil Properties at Labenne (Lehane *et. al.*, 1993)

Mean Particle size, D_{50} (mm)	Uniformity Coefficient D_{60}/D_{10}	Specific Gravity G_s	Maximum Void Ratio e_{max}	Minimum Void Ratio e_{min}
0.32± 0.02	1.85±0.05	2.65±0.01	0.81± 0.02	0.45±0.02

Table 2.3 Soil Properties at Labenne, by Layer (Lehane, *et. al.*, 1993)

Layer Number	Depth (m)	Relative Density D_r (%)	Void Ratio e	Bulk Density γ_b (kN/m ³)
1	0.0-2.2	60	0.60	16.9
1A	2.2-2.8	Transition zone	Transition zone	Transition zone
2	2.8-3.8	25	0.72	19.2
3	3.8-6.0	40	0.67	19.5

Table 2.4 . Cyclic Load Tests on Laboratory Model Piles

Reference	Soil Type	Diameter of Pile and Test chamber	Method of Pile installation. & Testing	Maximum Number of Cycles
Chan and Hanna (1980) & Chan (1976)	Sand Dr = 62%	Dp* = 19mm Dc = 380mm Dc/Dp = 20	Sand was placed in tank by rainfall method, 100kPa surcharge pressure was applied. Instrumented pile was then jacked-in and tested at a frequency of 0.0167Hz.	200,000
Poulos (1981b)	Clays LL = 65 PL = 20 & LL = 55 PL = 33	Dp = 20mm Dc = 152mm Dc/Dp = 7.6	Soil was placed in the container and the pile was jacked into it. Loading was applied at a frequency of 0.4 - 0.5 Hz.	1,000
Poulos (1984)	Calcareous soil. D ₅₀ = 0.3mm Carbonate content 88%	Dp = 20 Dc = 180 Dc/Dp = 9	Piles were jacked into the sand. Few tests were also conducted on burried pile, in which case the pile was initially positioned and the sand was rained around.	100

* Dp = Diameter of pile
Dc = Diameter of test Chamber

Table 2.4 Continued.

Reference	Soil Type	Diameter of Pile and Test chamber	Method of Pile installation. & Testing	Maximum Number of Cycles
Proctor and Khaffaf (1987)	Clay LL = 17% PL = 23%	Dp = 25mm Dc = 250mm Dp/Dc = 10	Soil was placed, the pile was jacked-in and 100kPa surcharge pressure was applied. Cyclic load frequency was 0.017 - 0.2 Hz.	500
Abood (1989)	Sand D ₁₀ = 0.162mm D ₆₀ = 0.254mm e _{max} = 0.845 e _{min} = 0.523 Dr = 75%	Dp = 25.4mm Dc = 584mm Dc/Dp = 23	Instrumented piles were tested. The pile was initially placed in position and the sand was compacted around it. A surcharge pressure of 0-200 kPa was applied. Loading frequency = 0.0167Hz	100,000

Table 2.5 Number of Cycles to Failure with Cyclic Load Level

(Chan and Hanna, 1980; D = 19mm, L = 570mm, p = 100 kPa)

q_c ($\%q_t$)	N_f
20	24347
30	3420*
50	157*
70	63*

* N_f Values estimated from the curves published

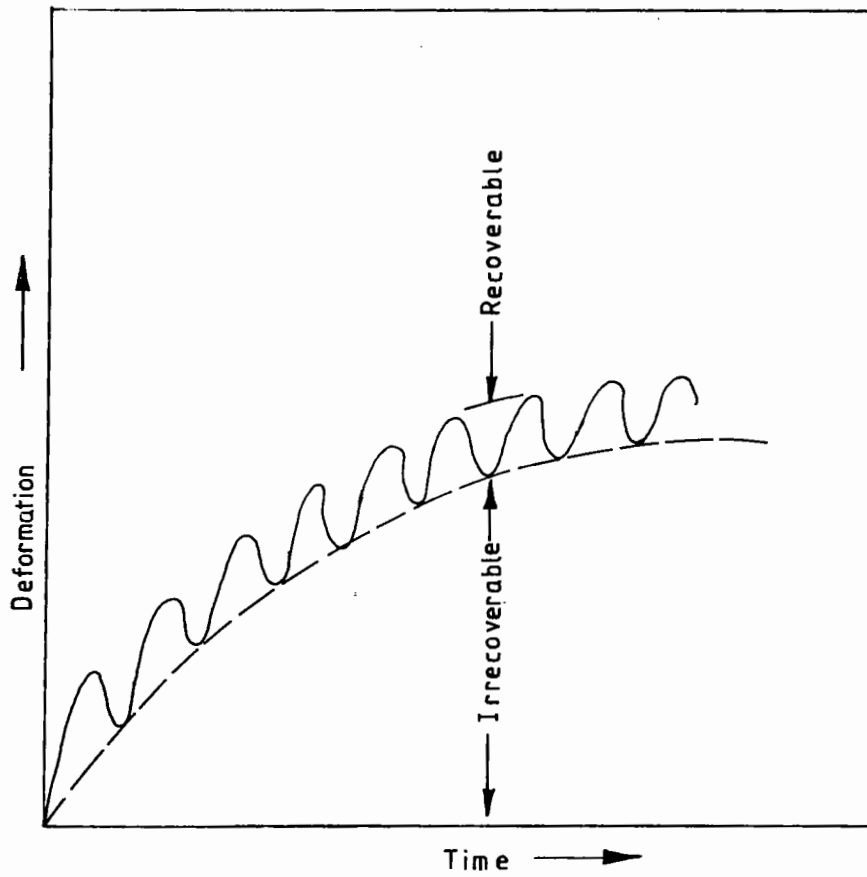


Fig.2.1. Illustration of the Deformation of Soil During Cyclic Loading
(Brown et al, 1975)

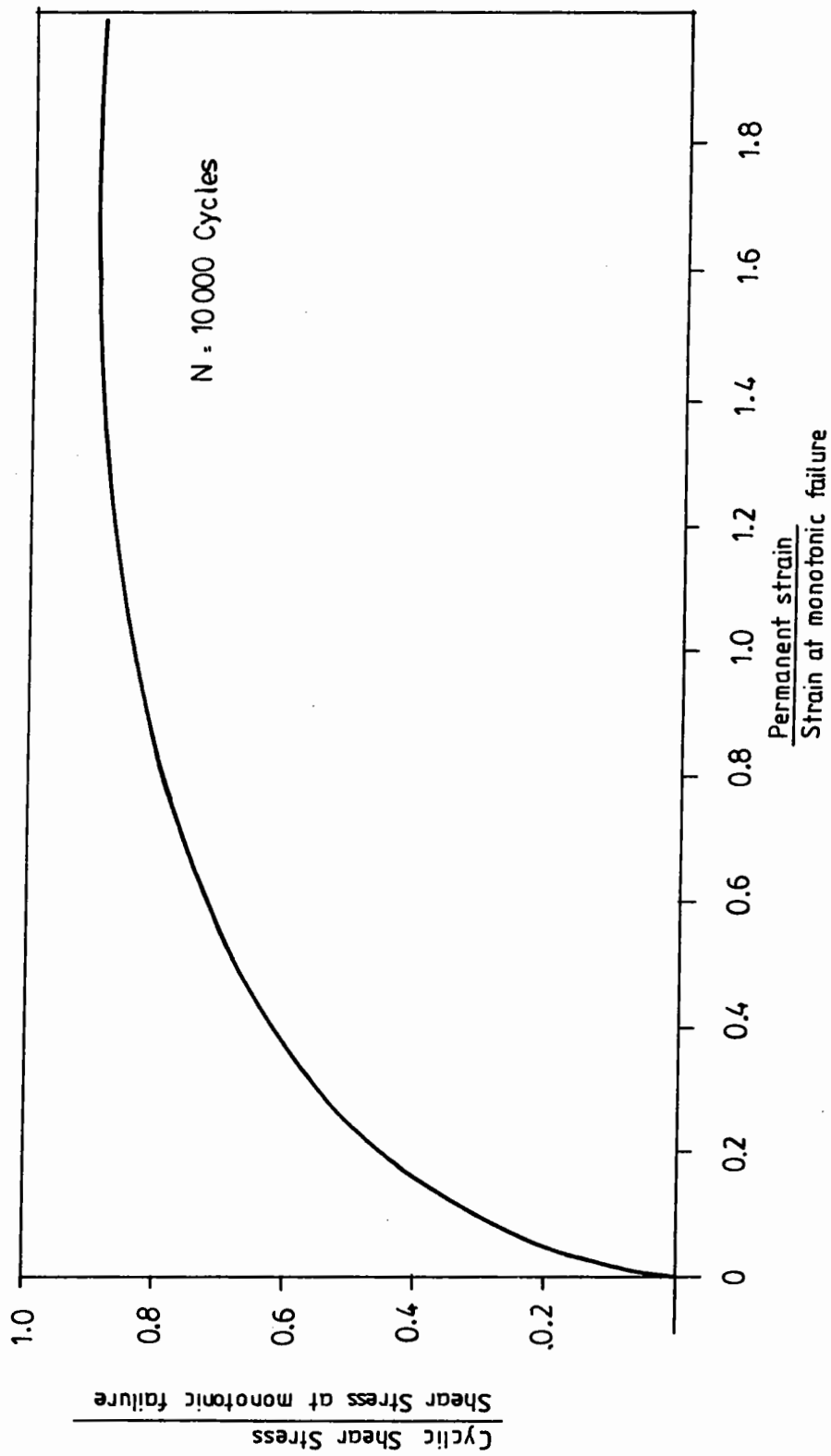


Fig.2.2. Cyclic Stress Ratio Versus Permanent Strain Ratio.
 (Lentz and Baladi, 1980)

Shear strain	10^{-6}	10^{-5}	10^{-4}	10^{-3}	10^{-2}	10^{-1}
	Small strain	Medium strain		Large strain	Failure strain	
Elastic						
Elasto plastic						
Failure						
Effect of load repetition						
Effect of loading rate						
Model	Linear elastic model		Visco elastic model		Load history tracing type model	

Fig.2.3. Changes in Soil Properties with Shear Strain
(Ishihara, 1982)

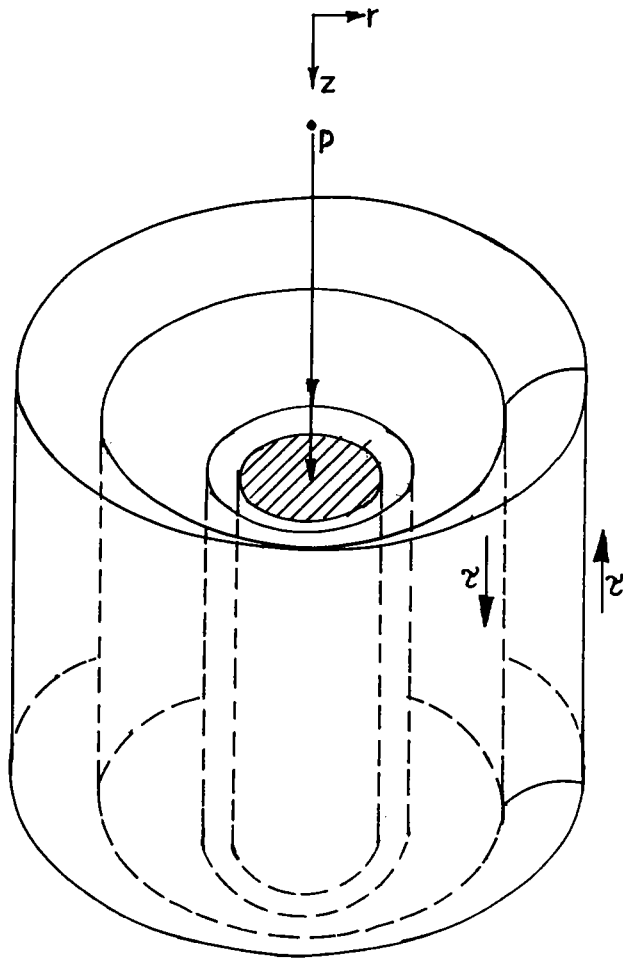


Fig.2.4. Mode of Deformation of Shaft.
(Randolph and Wroth,1978)

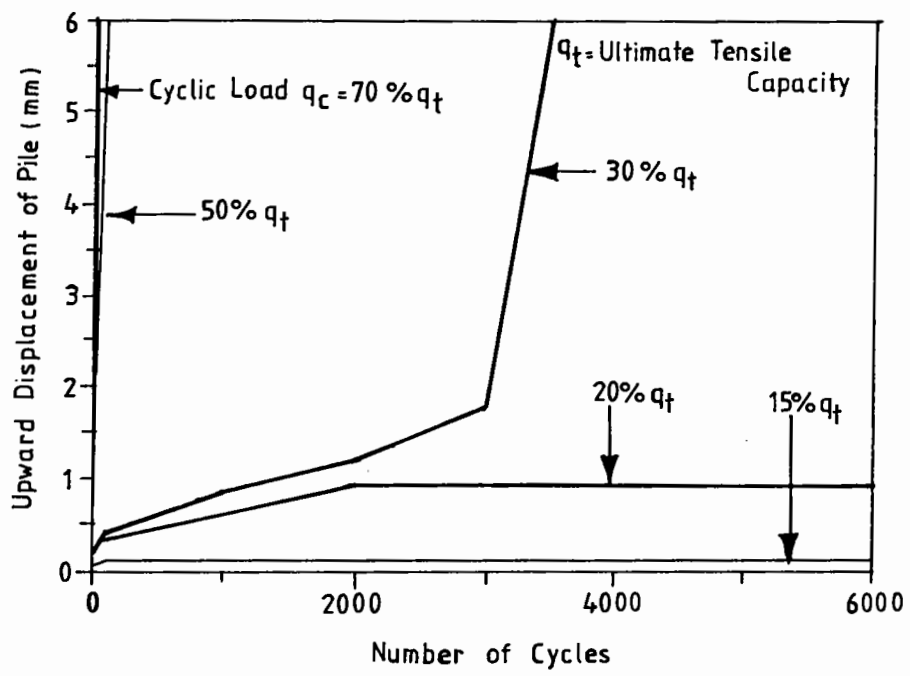


Fig.2.5. Displacement of Pile During Cyclic Tensile Load (Chan and Hanna, 1980)

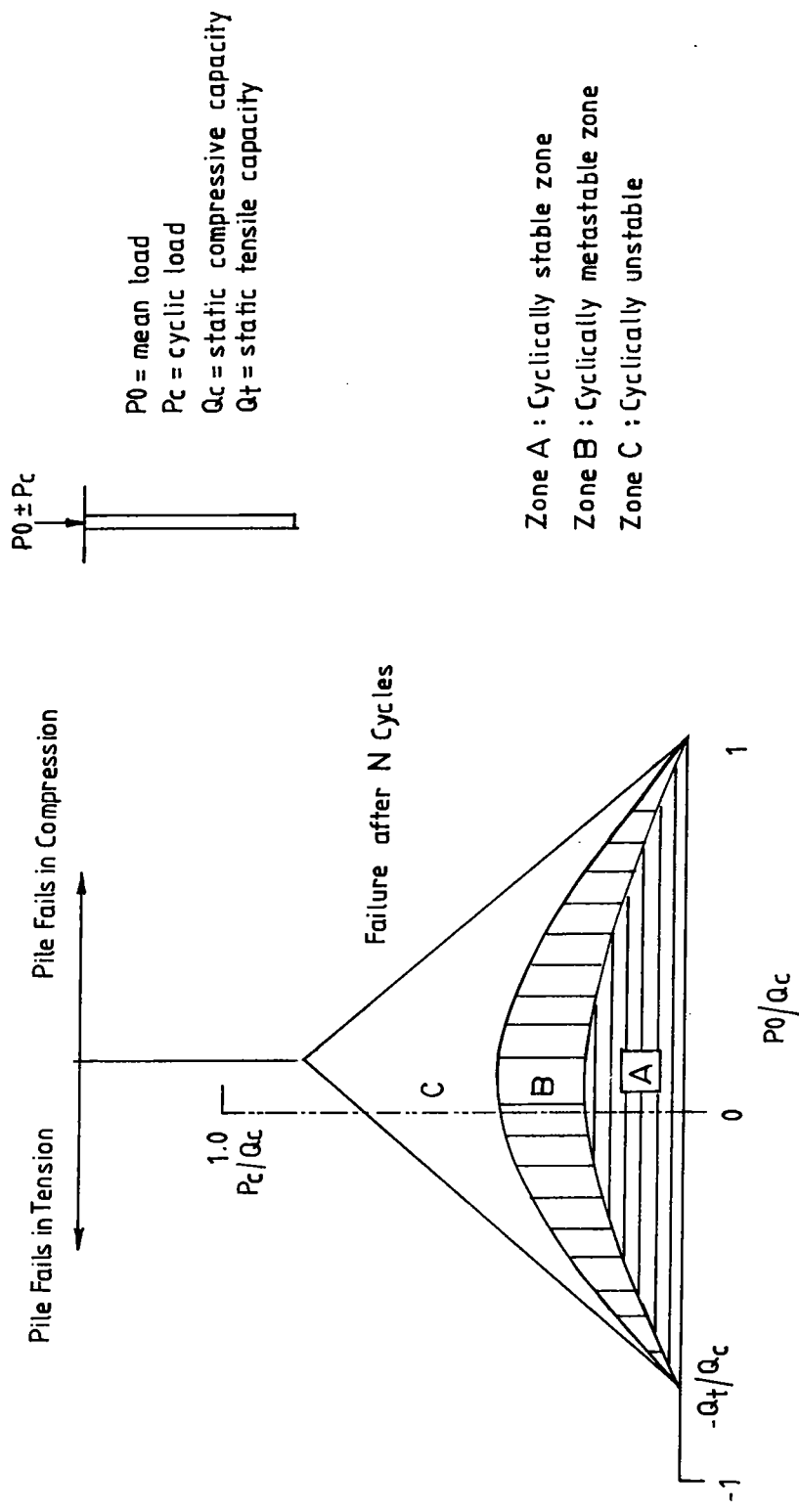


Fig.2.6. Features of Cyclic Stability Diagram (Poulos,1988)

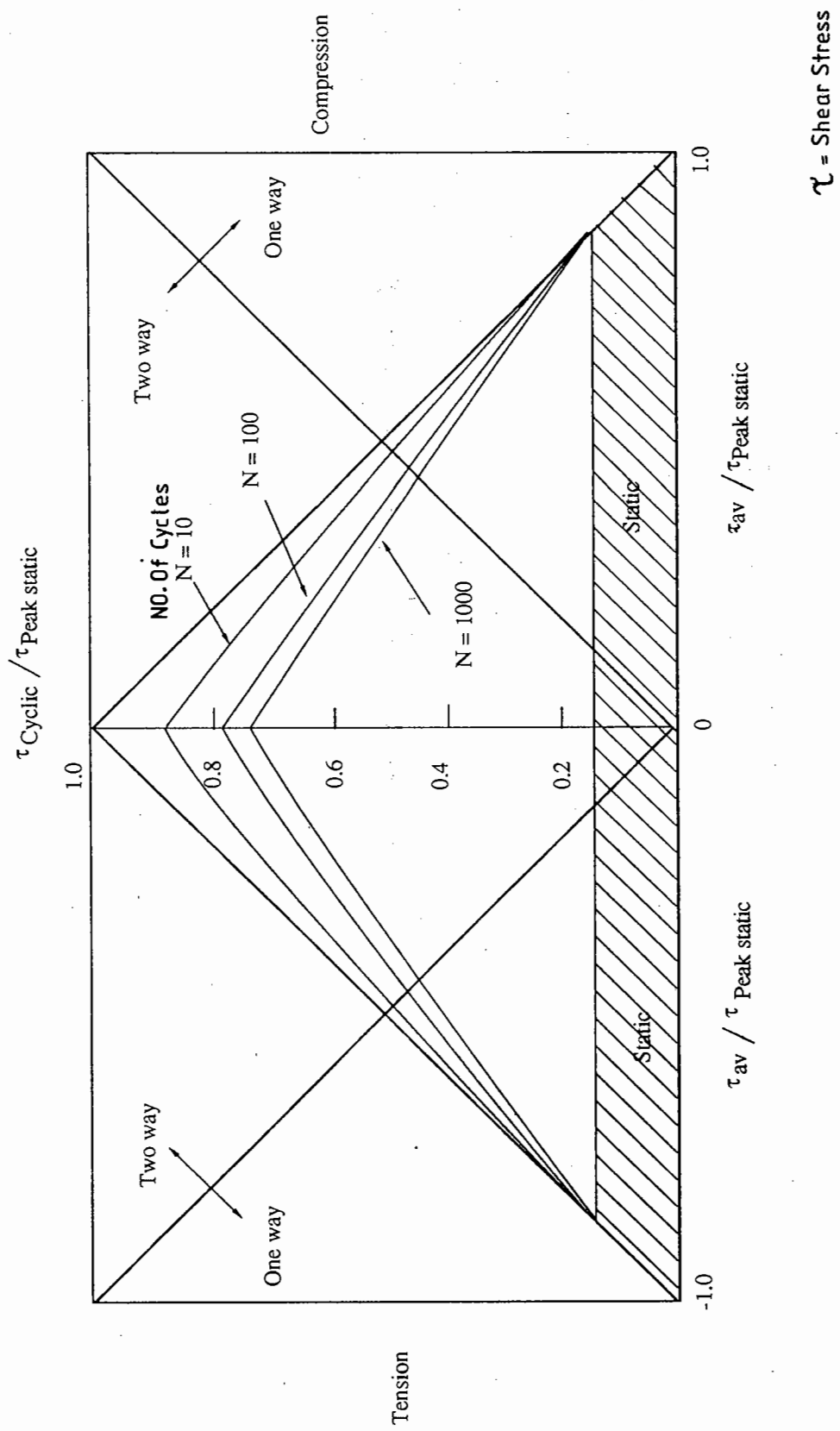


Fig. 2.7. Cyclic Interaction Diagram (Jardine, 1991)

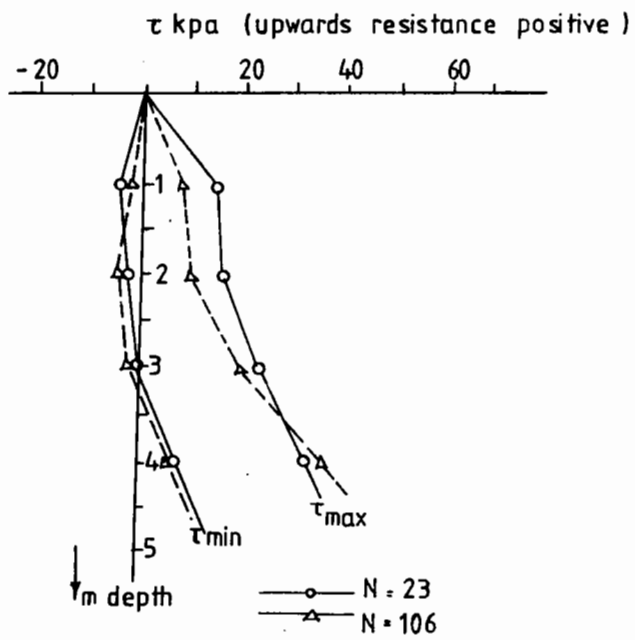
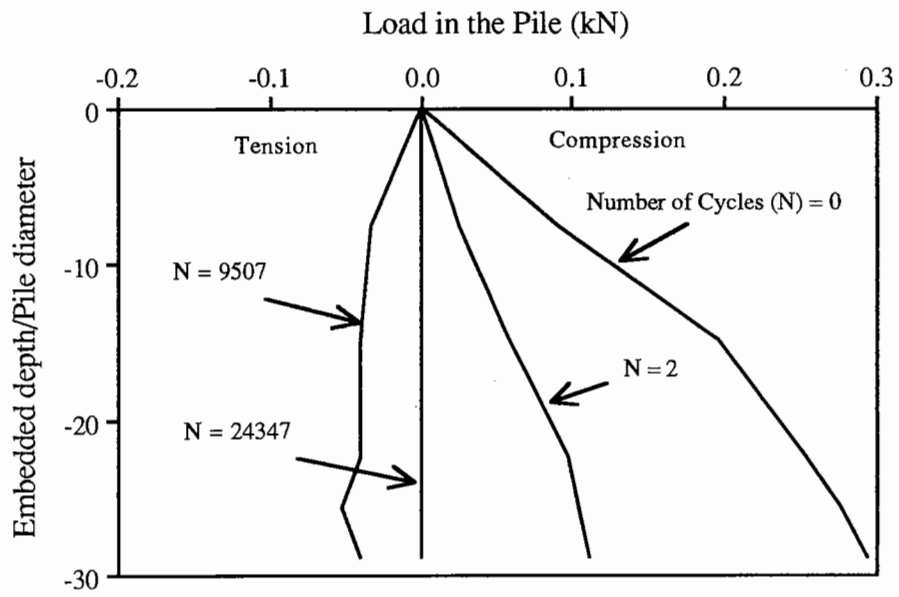
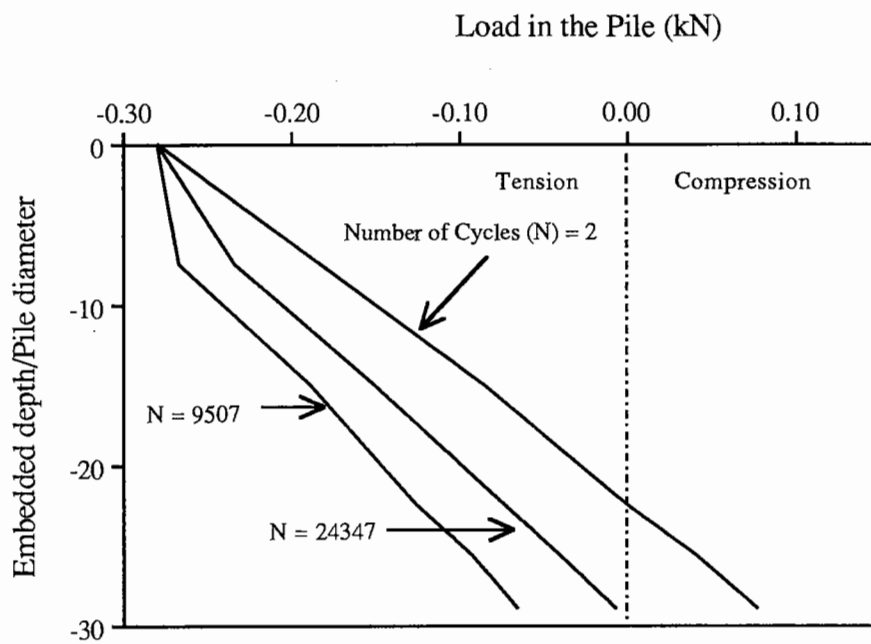


Fig.2.8. Distribution of Maximum and Minimum Shear Stress(τ)
 During a Cyclic Tension test
 (Karlsrud and Haugen, 1983).



(a) Load-Off Condition



(b) Load-On Condition

Fig. 2.9. Distribution of Axial Load During Cyclic Load Test (Chan and Hanna, 1980)

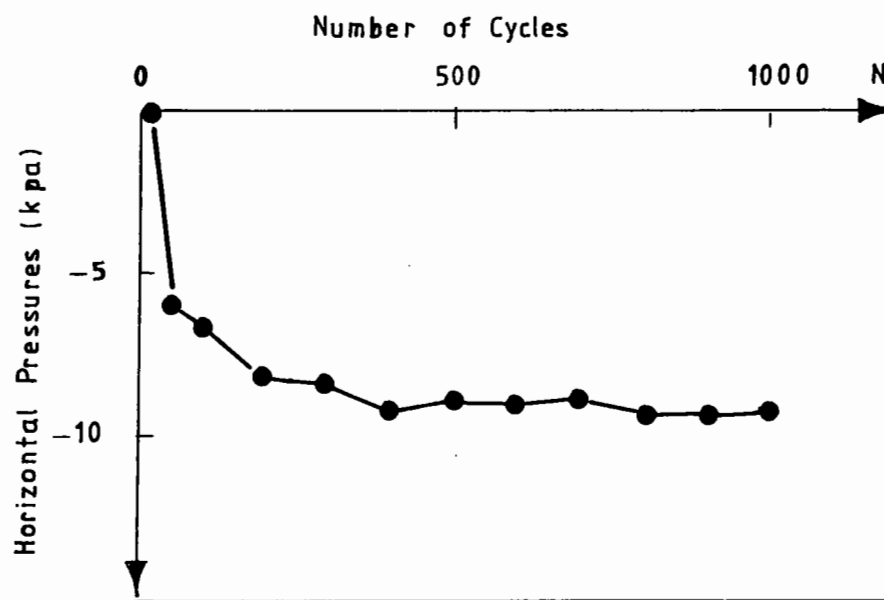


Fig.2.10. Variations in Horizontal Pressures During a Cyclic Tension Test. (Puech,1982)

EXPERIMENTAL APPARATUS**3.1 Introduction**

The review of literature presented in chapter two indicates there is a limited amount of work reported on the behaviour of piles in sand under cyclic tensile loading. Therefore, a comprehensive laboratory investigation was carried out on model piles in sand.

The investigation was carried out on model piles embedded in sand, mainly to understand the following:

- (i) The displacement of pile under cyclic tensile loading
- (ii) The mechanism of pile failure under cyclic tensile loading and
- (iii) The response of pile subsequent to peak loading.

This was achieved by conducting monotonic and cyclic tensile load tests on model piles embedded in sand. These tests were performed using the model pile test apparatus specially designed and developed during the present investigation. Further, soil-pile-slip test apparatus was developed to obtain T-Z curves for tension piles.

This chapter presents the details of the apparatus used in the investigation. The properties of the sand and the pile material are presented in chapter four. The major experimental apparatus developed during the present investigation includes:

- 1) Model pile test apparatus and
- 2) Soil-pile-slip test apparatus.

The details of the model pile test apparatus are presented in Section 3.2. The soil - pile-slip test apparatus is explained in Section 3.3. Information on the display and recording units used in this investigation is presented in Section 3.4.

3.2 Model Pile Test Apparatus

It was proposed to conduct monotonic and cyclic tensile load tests on model piles. The tests were proposed to be performed with the application of surcharge pressure, to create an effect of overburden pressure experienced by a pile element at a depth. In order to arrive at a proper design of the experimental set-up, the available literature on similar model pile test apparatus has been reviewed (Robinsky and Morrison, 1964; Williams, 1979; Ooi Teik Aun, 1980; Chan and Hanna, 1980; Abood, 1989; Baghdadi *et. al.*, 1991 and Schnaid and Houslby, 1991). The ratio of the dimension of the test tank to the model pile diameter adopted by the earlier investigators is summarised in Tables 2.4 and 3.1. The ratio varied from 6.8 to 50. Robinsky and Morrison (1964) have studied the movement of sand around a model pile as it was being jacked into the sand (Table 3.1) to examine the required tank dimension with respect to the pile diameter. Schnaid and Houslby (1991) analysed the results of cone pressuremeter and cone penetrometer tests, for assessing the effect of tank size. The above two studies revealed that, in model pile testing, unless the ratio of tank diameter to pile diameter is more than a minimum limit (i.e. 11 as per Robinsky and Morrison, 1964 and 25 as per Schnaid and Houslby, 1991) the soil-pile system experiences a confinement which affects the response of the model pile.

In the recent years, a number of model pile investigations have been reported where the test bed is subjected to a surcharge pressure (Chan, 1976; Chan and Hanna, 1980; Nauroy and Le Tirant, 1983; Proctor and Khaffaf, 1987; Abood, 1989 and Baghdadi *et. al.*, 1991). The design of the apparatus used in majority of these

investigations is similar to the one shown in Fig. 3.1. In this arrangement a rigid plate is used to apply surcharge pressure on sand surface. This causes stress concentration at the edges, leading to non-uniform pressure distribution.

With consideration of the above literature, the present test apparatus was designed. The layout of the apparatus is shown in Figs. 3.2 and 3.3. The major components of the testing apparatus are:

- i) Test tank
- ii) Surcharge pressure system
- iii) Model piles
- iv) Loading system and
- v) Measuring devices.

3.2.1 Test Tank

A galvanized steel tank available in the laboratory for immediate use, with internal dimensions 975mm x 695mm x 680mm, was used as the test tank. In order to examine the adequacy of the tank size, the ratio of tank dimension to pile diameter for various test piles has been computed and shown in Table 3.2. From Table 3.2 it can be observed that, the tank dimensions provide a ratio of tank dimension to pile diameter of 22 (average lateral dimensions of the tank: $(975 + 695)/2 = 835\text{mm}$ and maximum pile diameter 38.1mm) for the largest size of pile tested. This satisfies the minimum ratio suggested by Robinsky and Morrison, (1964) and is close to the value suggested by Schnaid and Housby (1991) to minimise the confining affects.

Further, radial stress in sand was measured with the help of pressure cells placed at different radial distances from the pile while the pile was being jacked into the sand bed (the details of

these tests are presented in Section 6.2). These results show that the radial stress becomes negligible beyond 300mm from the centre of the pile indicating the adequacy of the tank dimensions.

The tank walls were made of 3mm thick galvanised steel sheets. These were stiffened using steel angle sections (50mm x 50mm x 6mm) around the tank as shown in Fig. 3.4. A bottom stiffener was used to bolt the tank on to the floor. A top stiffener was provided to fix the top cover.

3.2.2 Surcharge Pressure System

To create an effect of overburden pressure experienced by a pile element at a depth, the effective stress in the sand was increased by creating a vacuum in the tank. The vacuum was created in the tank by connecting a pipe line from a remotely located vacuum pump. The top of the tank was covered with a polythene sheet tightly secured to the top flange of the tank to ensure an air tight sealing (Fig. 3.3 and 3.4). For installing the pile, a metal mounting with two nu-lip rings (pile access unit) was fitted on the polythene sheet (Fig. 3.5).

3.2.3 Model Piles

Seven model piles were fabricated. All piles were hollow, smooth surfaced (Central Line Average, (CLA) is about $0.5\mu\text{m}$ as obtained from the roughness tests conducted using Surfcom 20c/30c machine, see Section 4.3.2) and closed ended. The length of each pile was 500mm. Out of the seven piles, two were fabricated in steel and the remaining five in a high strength aluminum alloy. Reasons for the selection of pile material are discussed in Chapter Four. All the piles had a 60 degree cone. Details of the model piles are presented in Table 3.3.

The model piles used in the investigation are classified as:

- i) Plain pile
- ii) Semi-instrumented pile
- iii) Instrumented pile and
- iv) Large diameter pile.

i) Plain pile

A pile having no built-in instrumentation is referred to as a plain pile. The details of a plain pile are shown in Fig. 3.6 (a). The two steel piles (25.4mm and 38.1mm diameter) and two aluminium alloy piles (12.7mm and 25.4mm diameter) were fabricated as plain piles.

ii) Semi-instrumented Pile

A pile with one built-in load cell segment is referred to as a semi-instrumented pile. The details of this type of pile are shown in Fig. 3.6(a). The pile was of 38.1mm diameter and consisted of three detachable pieces.

iii) Instrumented Pile

A pile with three built-in load cell segments is referred to as an instrumented pile (Fig. 3.6(b)). The load cell segments were fabricated from the same aluminum alloy tube used for the pile. The wall thickness in the middle of the load cell segment was reduced to 0.7mm in order to obtain measurable strains in the strain gauges. Eight strain gauges (model FLA-3 350-23 of Techni measure) were mounted in each segment (Figs. 3.7 and 3.8). These load cell segments were identified as LSG1, LSG2 and LSG3 as shown in Fig. 3.6(b).

iv) Large Diameter Pile

A large (76.2mm) diameter pile was fabricated with no instrumentation. In view of its large diameter compared to other

piles used, a new method of pile installation, explained in chapter six, was adopted to reduce the installation effects. To facilitate this new method of installation, the pile was provided with a hole drilled centrally through the pile head upto the tip (Fig. 3.6(b)).

File Cap

A 200mm square steel plate was used as pile-cap for all the model piles. A 25mm diameter threaded hole was provided at the centre of the pile-cap to fix the pile head. All the piles, except the 76.2mm diameter pile, were designed to fit into this 25mm diameter hole. Four 5mm diameter holes were made as shown in Fig. 3.9 to fix the 76.2mm diameter pile using screws. In addition, four 3mm diameter holes (Fig. 3.9) were also made to facilitate mounting of a 25kN load cell.

3.2.4 Loading System

The loading system consisted of:

- (i) Load frame
- (ii) Pile jacking unit
- (iii) Pull-out loading unit and
- (iv) Cyclic loading unit.

i) Load Frame

A steel portal frame was used as the load frame (Fig. 3.10). Each column of the frame was made of two 150mm x 90mm steel channel sections welded to a base plate. The base plate was bolted to the laboratory floor. A cross beam, made of two channel sections welded to obtain a hollow rectangular beam of dimensions 250mm x 150mm, was used to support the different loading units.

ii) Pile Jacking Unit

A hydraulic jack was mounted upside down to the cross beam to carry out the pile jacking operation.

iii) Pull-Out Loading Unit

To conduct the monotonic pull-out (tension) tests, a hydraulic jack was placed upright on top of the cross beam. A connecting unit was fabricated to join the top of the jack to the pile cap such that hydraulic pressure in the jack provided a pull-out load on the pile (Fig. 3.11).

iv) Cyclic Loading Unit

For the application of cyclic loading, a single acting piston system was used (Fig. 3.12). Compressed air was used to drive the piston. A solenoid operated spool valve (model LB53013TF, of Economatics, Nottingham) was used to regulate the compressed air and to apply the cyclic load. The operation of the solenoid valve was controlled by an electronic signal which had a frequency range between 0.2Hz and 2 Hz in steps of 0.2 Hz. In the absence of an electronic signal a constant pull was built up on the pile. The magnitude of loading was controlled by regulating the pressure of the compressed air.

3.2.5 Measuring Devices

The measuring devices used for the model pile testing include:

- (i) Load Cell
- (ii) LVDT
- (iii) Pressure Cells

i) Load Cell

A 25 kN capacity, strain gauged, two way type load cell (U2000 model supplied by May Wood Instruments Ltd.) was used to measure the load applied to the pile. This load cell was mounted on top of the pile cap.

ii) LVDT

Two linear variable differential transducers (LVDT) (type DC 1000A from RDP electronics), were used to measure the displacement of the pile cap. Each LVDT had ± 25 mm travel and was positioned using a magnetic base supported on a channel section fixed to the tank.

iii) Pressure Cells

Four Nottingham pressure cells were used to study the pressure distribution in the sand. Each pressure cell had an overall diameter of 64mm and a thickness of 11mm. Design details of these pressure cells are available in the literature (Brown, 1977 and Brown and Brodrick, 1973). The pressure cells used are identified as PC1, PC2, PC3 and PC4.

The measuring devices used in the present investigation were calibrated (Appendix A). The calibration factors are presented in Table 3.4.

3.3 Soil-Pile-Slip Test Apparatus

A numerical model has been developed, and explained in chapter seven, to obtain load-displacement behaviour of piles using T-Z curves. In order to obtain T-Z curves from a pile element, a test apparatus (Soil-pile-slip test apparatus) was designed.

Coyle and Sulaiman (1967) used an apparatus shown in Fig. 3.13 to obtain T-Z curves. The apparatus was similar a to triaxial test apparatus, with a pile element embedded in the soil sample which could be pushed down through the base plate. The test was performed, after application of a confining pressure, with the gradual pushing down of the pile element. As the pile element was being pushed, the load on the pile element (T) and the corresponding displacement (Z) at the pile head were recorded using a proving ring and a dial gauge placed outside the cell. The test was repeated under different confining pressures and a T-Z curve was obtained for each confining pressure.

The apparatus used by Coyle and Sulaiman (1967) has the following limitations:

1) The measured displacement includes the displacement of the pile element and the slack in the apparatus. Similarly the measured load includes the load on the pile element and the frictional resistance between the pile element and the bearing system.

2) The measuring devices used, proving ring and dial gauge, are not considered to be sensitive enough to record very small variation in loads and displacements.

3) The rigid plates at the top and bottom of the sample restrained the soil from shear deformation.

With consideration of the above, a soil-pile-slip test apparatus was developed to obtain T-Z curves for tension piles. The details of the apparatus are shown in Figs. 3.14 and 3.15 and consists of:

- i) Triaxial Cell
- ii) Pile elements

- iii) Top plate
- iv) Deformation measuring unit and
- v) Loading system.

i) Triaxial Cell

A triaxial cell suitable for conducting tests on 100mm diameter samples was modified to perform the soil-pile-slip tests.

ii) Pile Elements

Three pile elements, with diameters 12.7mm, 25.4mm and 38.1mm, were fabricated. The pile elements were made from the same aluminum alloy tubes used for the model piles. Each pile element had a shaft length of 190mm to have an embedded length of 150mm. The pile elements had a smooth surface with a flat tip (Fig. 3.14). The head of a pile element was provided with a 10mm screw thread to mount the LVDT holder.

iii) Top Plate

The top plate was made of two sets of concentric aluminum rings as shown in Fig. 3.16. The inner rings had two nu-lip rings to provide a seal with the pile surface. The outer rings were used to support the rubber membrane on the sample. These two sets of rings were connected with a polythene sheet as shown in Fig. 3.16. This design of the top plate has allowed the soil to undergo shear deformation during testing.

iv) Deformation Measuring Unit

Details of the deformation measuring unit are shown in Fig. 3.17. This unit consists of a LVDT, LVDT holder and a soil clamp.

A LVDT (Type D5-100 AG, of RDP electronics Ltd.) having a 5mm

travel was used to measure the displacements. An aluminum holder was used to support the LVDT, which was screwed to the head of the pile element (Figs. 3.17 and 3.18).

A soil clamp was fabricated in brass to mount onto the soil sample as shown in Fig. 3.17. A screw rod was used to connect the clamp to the LVDT. This arrangement enabled the measurement of displacement between the soil and the pile element.

v) Loading System

A pull-out load was applied to the pile element through a steel rod, as shown in Figs. 3.14 and 3.18. A 25kN load cell was mounted on the LVDT holder to measure the load on the pile element.

3.4 Display and Recording Units

The display and recording units used in the investigation are:

- (i) Digital multimeters (DMM)
- (ii) Chart recorder and
- (iii) Data logger.

3.4.1 Digital Multimeters (DMM)

Two digital multimeters were used to observe the response of the LVDT and load cells during testing. One of these was supplied by Schlumberger Solartron, model No.7045. The other was a Keithley 177 microvolt DMM.

3.4.2 Chart Recorder

A chart recorder was used to record the wave form of load and

displacement during the cyclic load testing. The chart recorder used in the investigation was (type No.28000) supplied by Bryans Southern instruments, England.

3.4.3 Data Logger

The data logger used was a Schlumberger-Solartron ORION 3531D. It contained the software which provided a comprehensive and flexible logging capability. The data logger had facilities to record data on to a 3.5 inch computer diskette and to provide a hard copy as back up.

Table 3.1 Monotonic Tension Tests on Laboratory Model Piles

Reference	Soil Type	Diameter of Pile and Test Chamber	Method of Pile installation. & Testing	Surcharge Pressure (kPa)
Robinsky and Morrison (1964)	Sand $D_{10}=0.2\text{mm}$ $D_{60}/D_{10}=2$ $e_{\min}=0.474$ $e_{\max}=0.813$ $D_r=17-37\%$	$D_p^* = 29.5$ -37.6mm $D_c=606\text{mm}$ $D_c/D_p =$ $16-20.5$	Instrumented piles were tested. Sand was initially placed in the tank and then piles were pushed-in.	
Tan (1971) Tan & Hanna (1974)	Well graded sand. Average bulk density = 15.46 kN/M^3 $D_r = 41\%$	$D_p = 15.9-$ 38.1mm $D_c = 600\text{mm}$ $D_c/D_p =$ $15.8-37.7$	Instrumented piles tested. Piles were installed using two methods. (1) The pile was allowed to float freely as the sand bed was formed around it. (2) The pile top was restrained during sand placement.	-
Chaudhuri (1977) Chaudhuri & Symons (1983)	Medium fine sand. Grain size $0.15-0.40\text{mm}$ $D_{60}/D_{10}=1.7$ $D_r =$ $39.4-83.2\%$	$D_p = 25.4 -$ 50mm $D_c = 1100\text{mm}$ $D_c/D_p =$ $22-43.3$	Instrumented pile test. The pile was initially placed in position and sand was compacted around it.	-

* D_p = Diameter of pile; D_c = Diameter of test Chamber.

Table 3.1 Continued.

Reference	Soil Type	Diameter of Pile and Test chamber	Method of Pile installation. & Testing	Surcharge Pressure (kPa)
Francescon (1983)	Speeswhite Kaolin clay. LL = 69 PL = 38 PI = 31	Dp = 18.9mm Dc = 250mm Dc/Dp = 13.2	Instrumented piles were tested. Pore pressure transducers were positioned in the chamber before pouring clay slurry. The sample was consolidated under vertical stress. Then the pile was installed by jacking.	140 - 250 kPa
Martins (1983)	Speeswhite Kaolin clay LL = 62 PL = 32 PI = 30	Dp = 15mm Dc = 102mm Dc/Dp = 6.8	Instrumented and un-instrumented piles were tested. The soil sample was consolidated in a triaxial cell. A hole was then drilled whilst the radial total stresses were reduced to zero. A hollow pile was cast in the hole.	Max. Cell Pressure 260 kPa

* LL = Liquid Limit; PL = Plastic Limit; PI = Plasticity Index.

Table 3.1 Continued.

Reference	Soil Type	Diameter of Pile and Test chamber	Method of Pile installation. & Testing	Surcharge Pressure (kPa)
Nauroy and Le Tirant (1983)	Calcareous & Silica Sand. Dr = 80-100%	D _p = 20 - 30mm D _c = 650mm D _c /D _p = 21.7 - 32.5mm	Un-instrumented piles were tested. Sand was initially placed and the surcharge pressure was applied and then the pile was jacked in at a rate of 0.5mm/min. Earth pressure cells were used to record the lateral pressure in sand during pile penetration.	50 - 400 kPa
Wersching (1987)	Loose sands and clay	D _p = 114mm D _c = 3000mm D _c /D _p = 26	Instrumented pile tests.	----
Baghdadi et al. (1991)	Red Sea Carbonate sediments $\gamma_{min} = 14.03\text{kN/M}^3$ $\gamma_{max} = 16.97\text{kN/M}^3$	D _p = 16 mm D _c = 800 mm D _c /D _p = 50	Instrumented pile test. Sand was placed and a surcharge pressure was applied, the pile was then pushed into the soil at a rate of 2.8mm/min	0-138kPa

Table 3.2 The Ratios of Tank Dimensions to Pile Diameters Adopted in the Investigation

Pile Dia. (Dp) (mm)	Dc/Dp tank min. dimension (Dc = 695mm)	Dc/Dp tank average dimension (Dc = 835mm)	Dc/Dp tank max. dimension (Dc = 975mm)
12.7	55	66	77
25.4	27	33	38
38.1	18	22	26
76.2*	9	11	13

* Test data on 76.2 mm dia. pile was not used




-  Satisfies requirements of both Robinsky and Morrison (1964) and Schnaid and Housby (1991)
-  Satisfies requirements of Robinsky and Morrison (1964) but do not satisfies the limits suggested by Schnaid and Housby (1991)
-  Unsatisfactory

Table 3.3 Details of the Model Piles Used in the Investigation

Pile Diameter	Material Used
12.7	Aluminium alloy
25.4	Aluminium alloy
	Steel
38.1	Aluminium alloy*
	Aluminium alloy**
	Steel
76.2	Aluminium alloy

* Semi-instrumented pile; ** Instrumented pile

Table 3.4 Calibration Factors for the Measuring Devices

Measuring Devices	Calibration Factor
25kN Load Cell	680kN/ Volt
Load cell pile segment LSG1, LSG2 and LSG3	588kN/ Volt
LVDTs (± 25 mm travel)	5mm/ Volt
LVDT (5mm travel)	6.14mm/ Volt
Pressure Cells PC1, PC2, PC3 and PC4	220 kPa/ m Volt (at 10 Volt input)

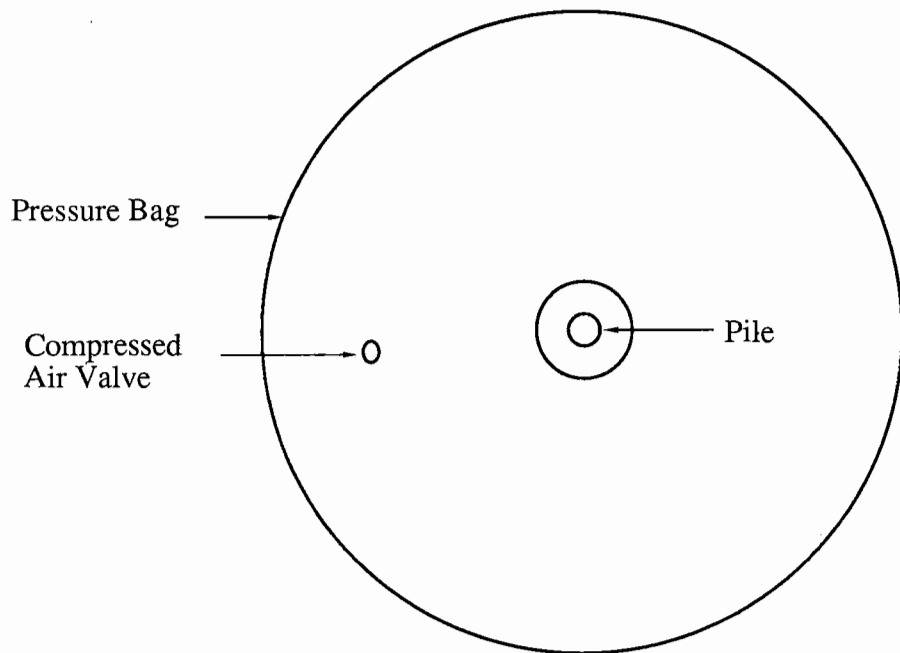
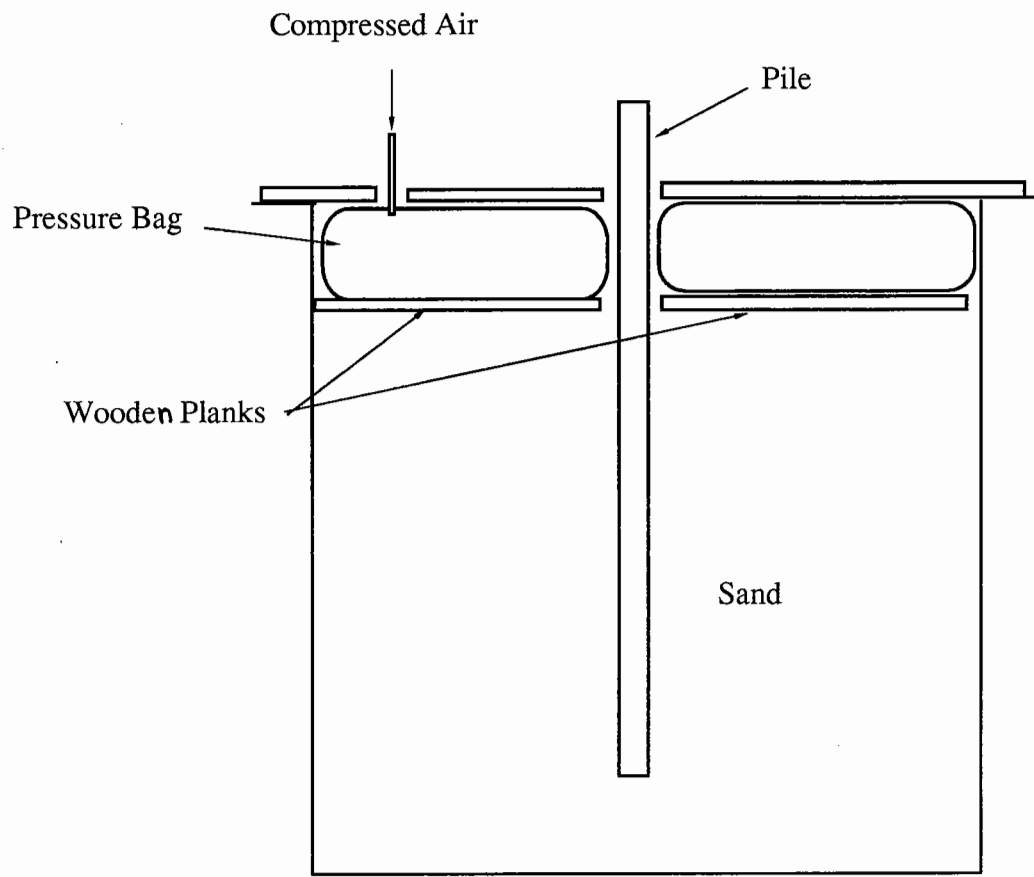


FIG.3.1. MODEL PILE TEST APPARATUS (Abood 1989.)

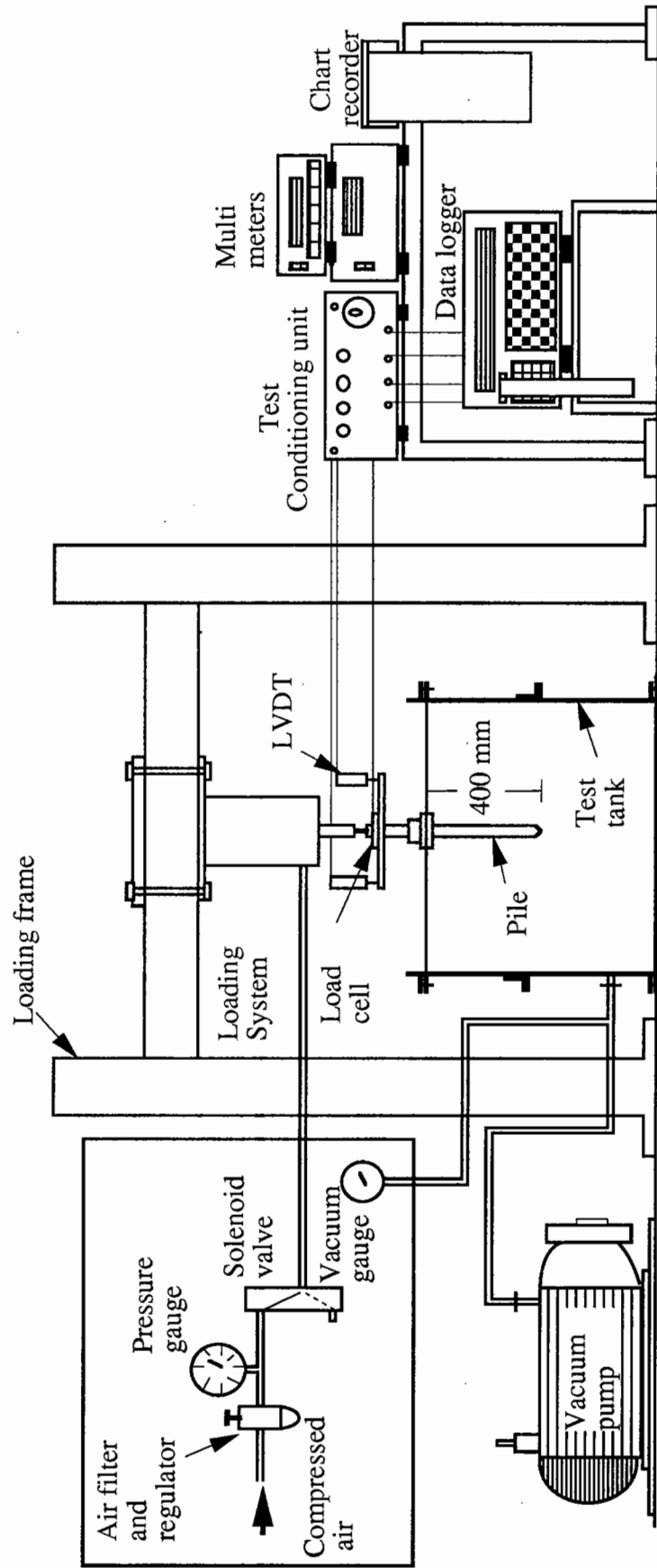


Fig.3.2. Layout Diagram of the Model Pile Test Apparatus

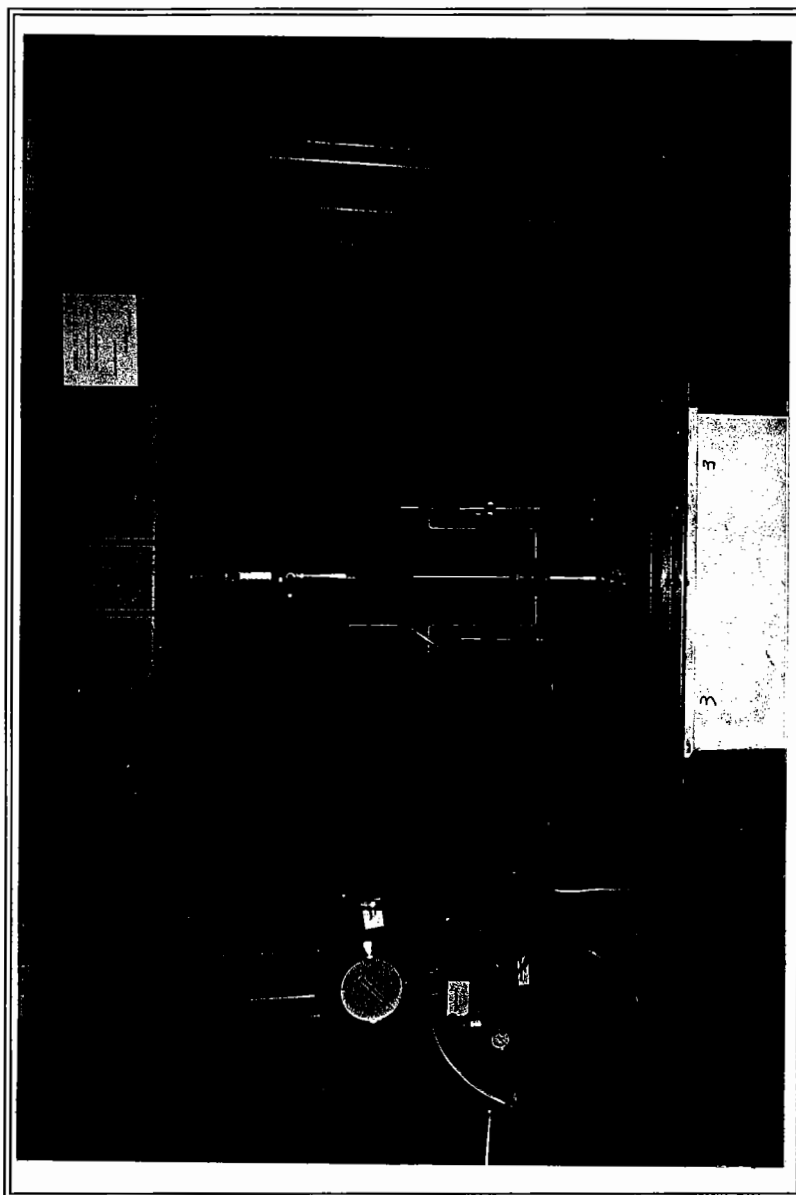
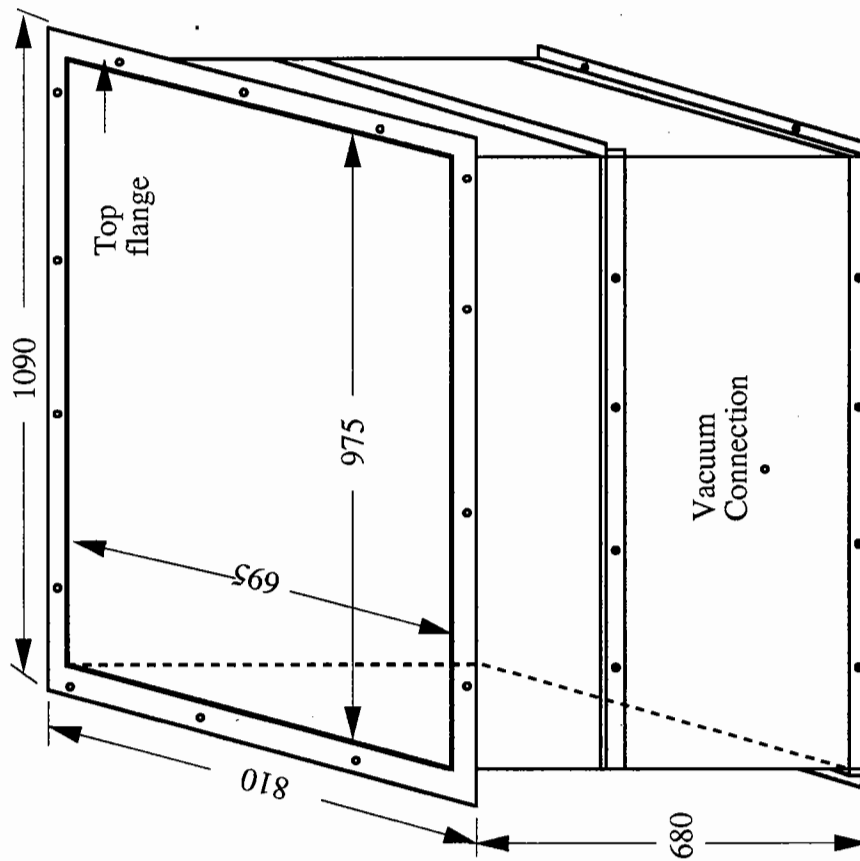
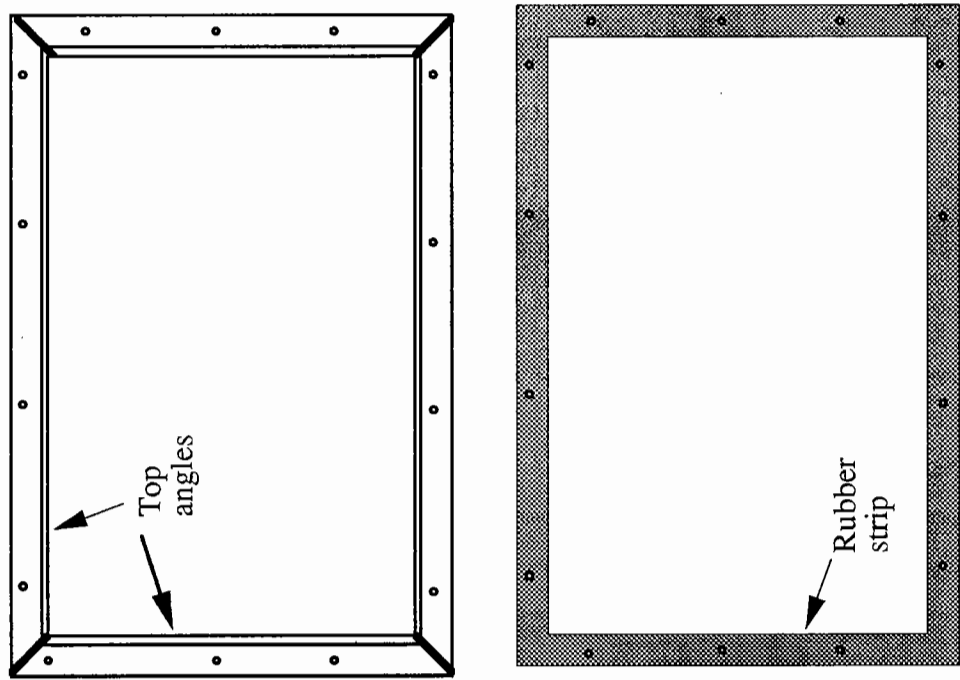
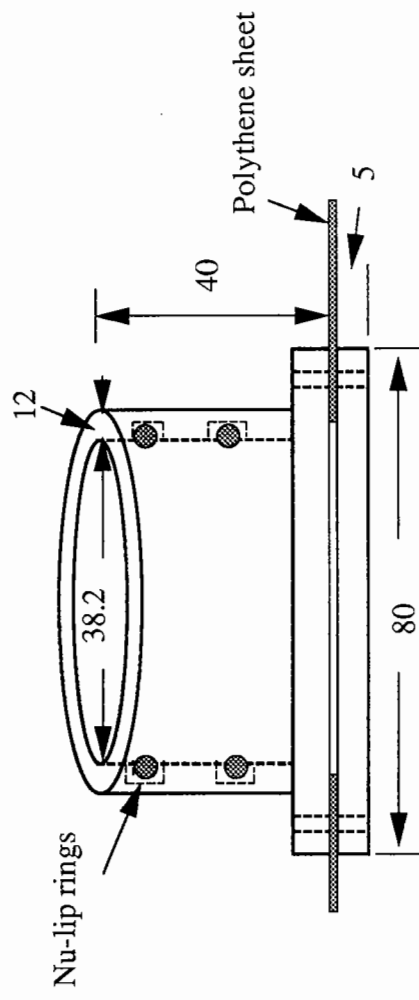


Fig. 3.3 The Model Pile Test Apparatus



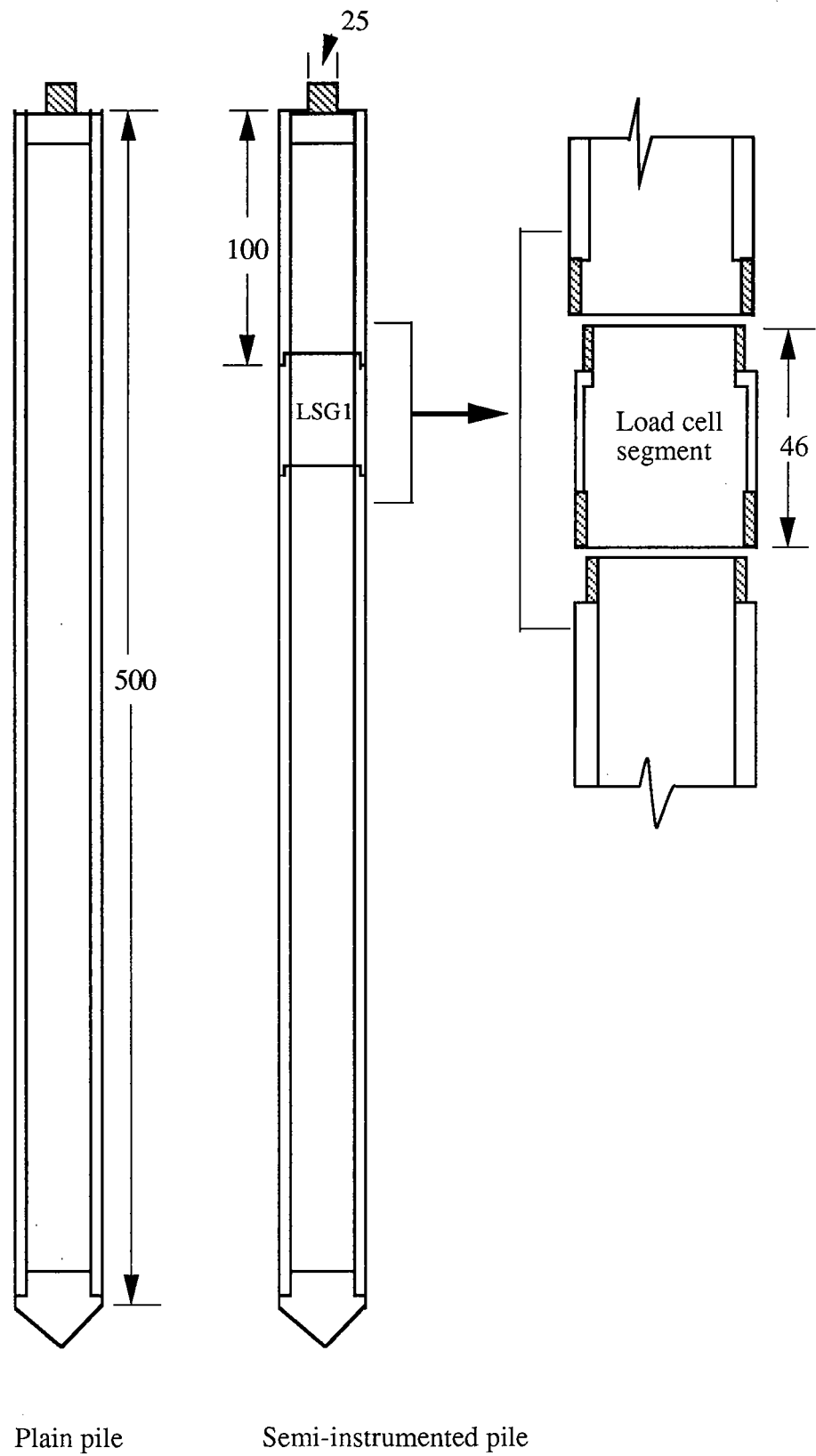
All dimensions are in mm

Fig. 3.4. Details of the Test Tank



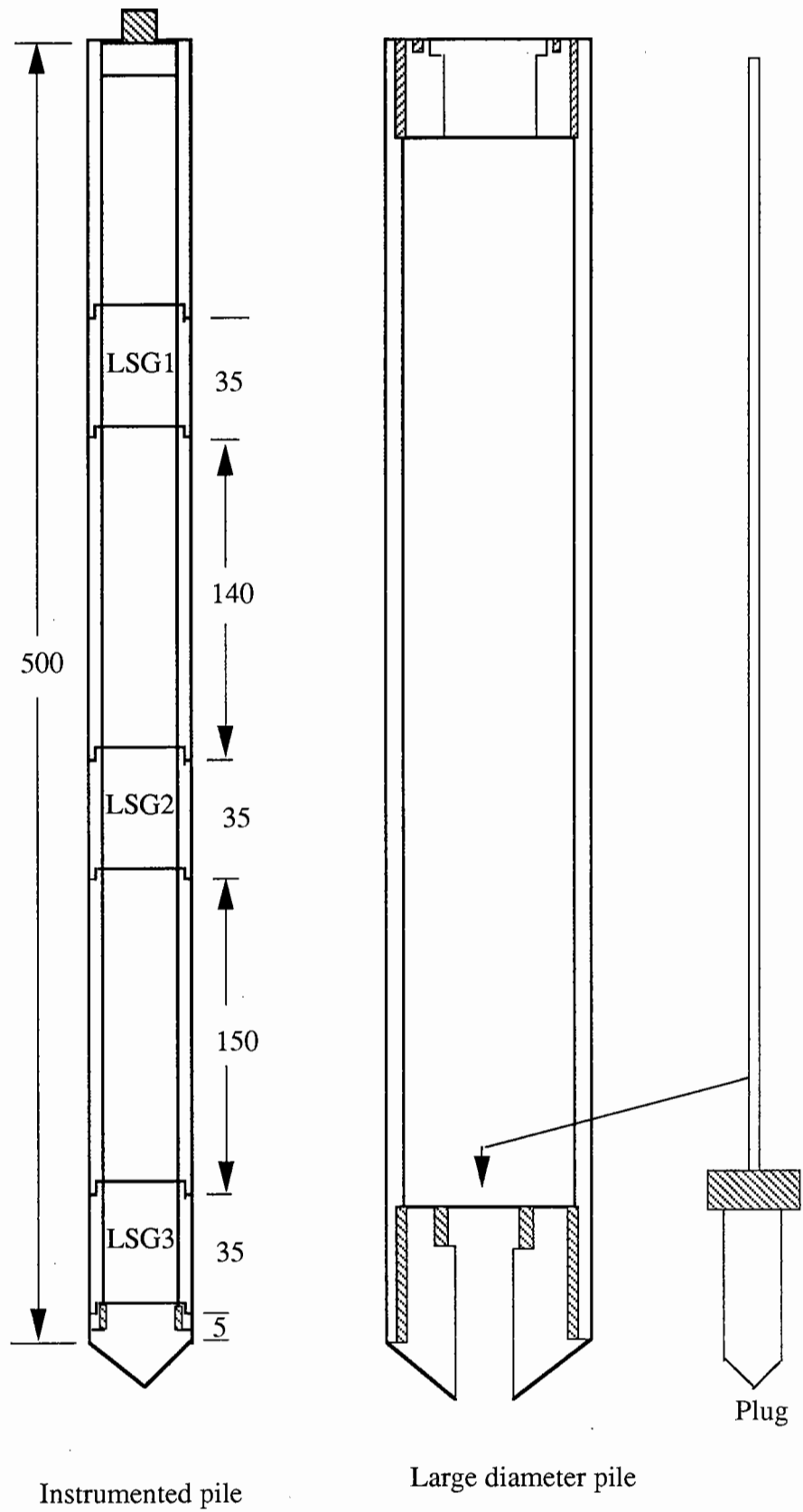
All dimensions are in mm

Fig . 3 . 5 . Details of the Fittings for the Pile Access Unit
(for the 38.1 mm Diameter Pile)



All dimensions are in mm

Fig. 3.6 (a). Design Details of the Model Piles



All dimensions are in mm

Fig.3.6(b). Design Details of the Model Piles

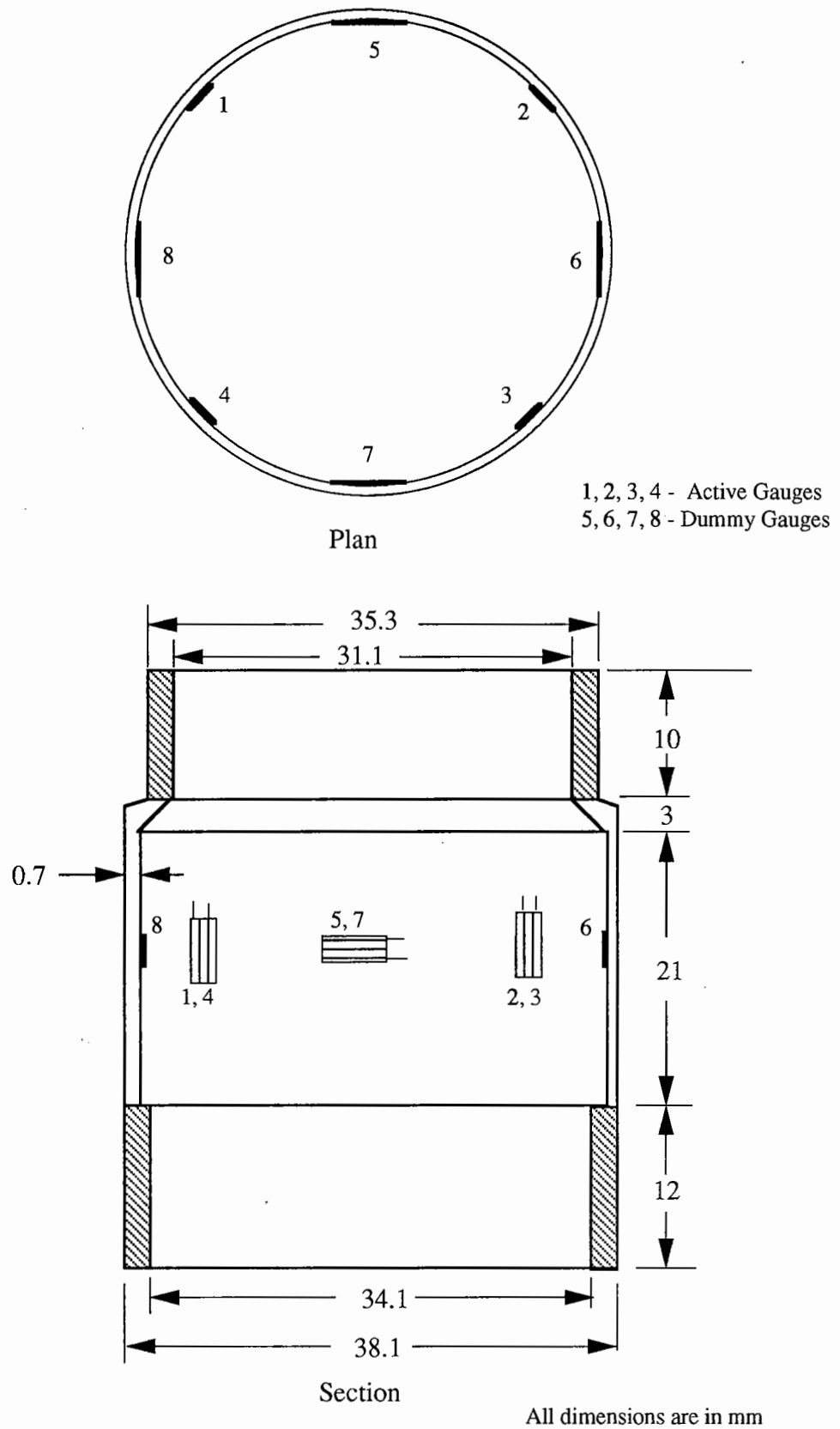
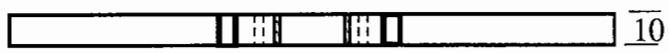
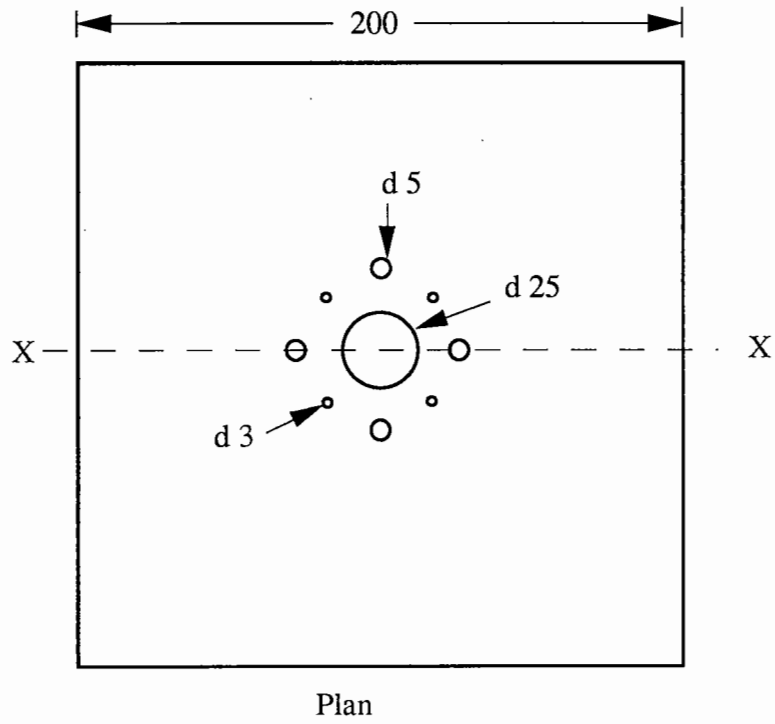


Fig. 3.7. Design Details of the Load Cell Segment

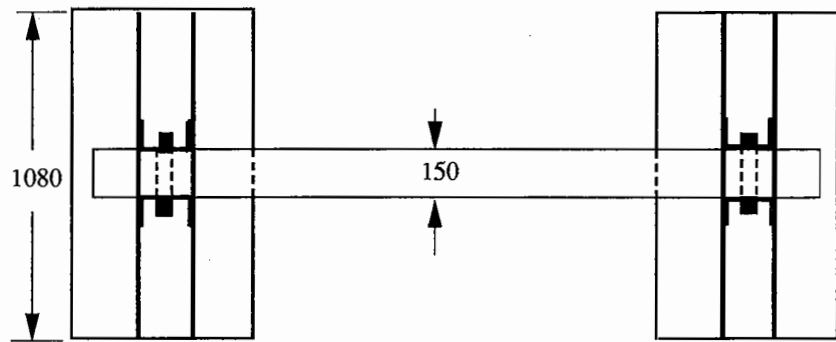


Fig. 3.8 The Load Cell Segments

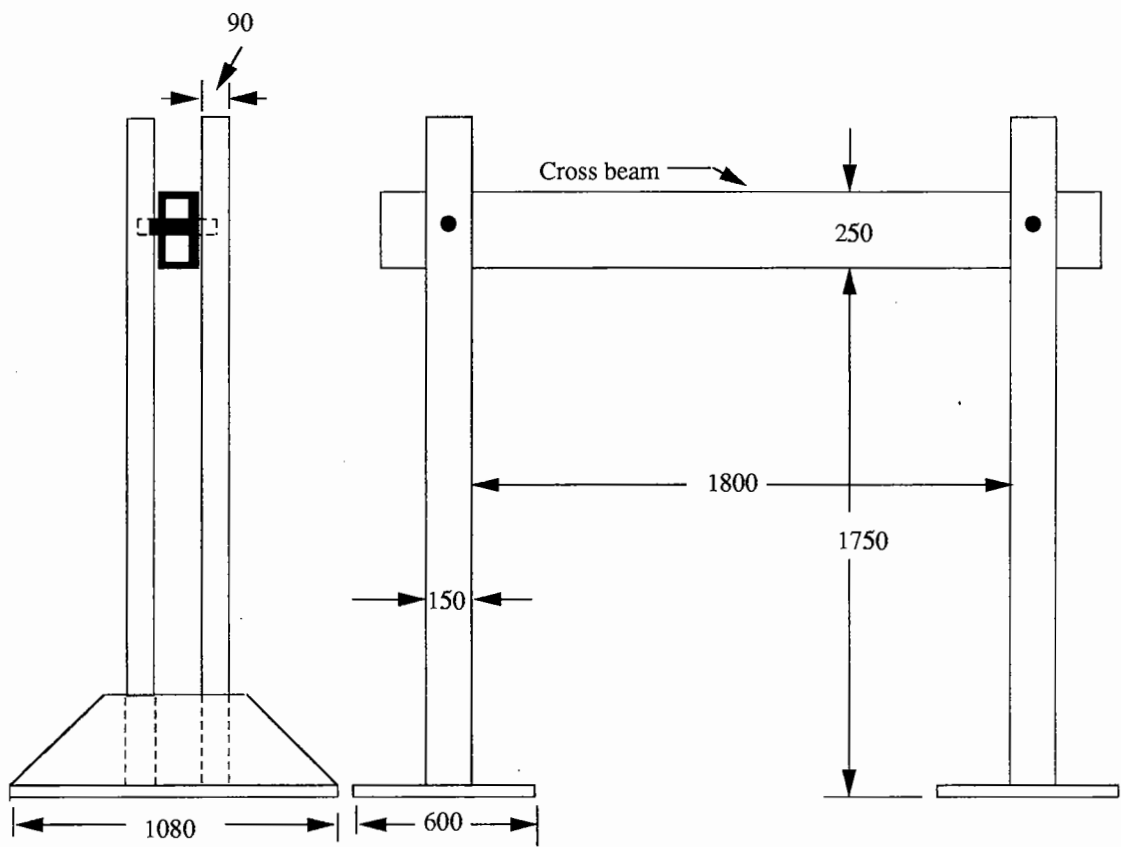


All dimensions are in mm

Fig.3 .9. Pile-Cap Design



Plan



Side view

Elevation

All dimension are in mm

Fig.3.10. Load Frame

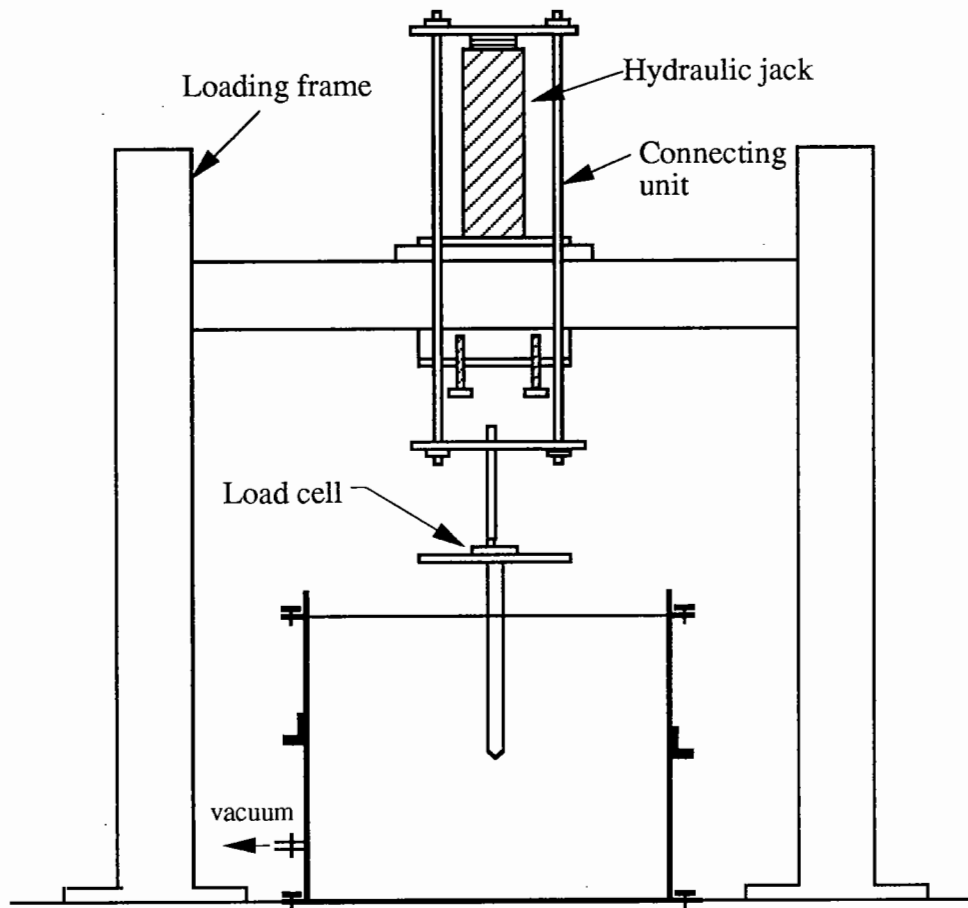


Fig.3.11. Pull-out Loading Unit

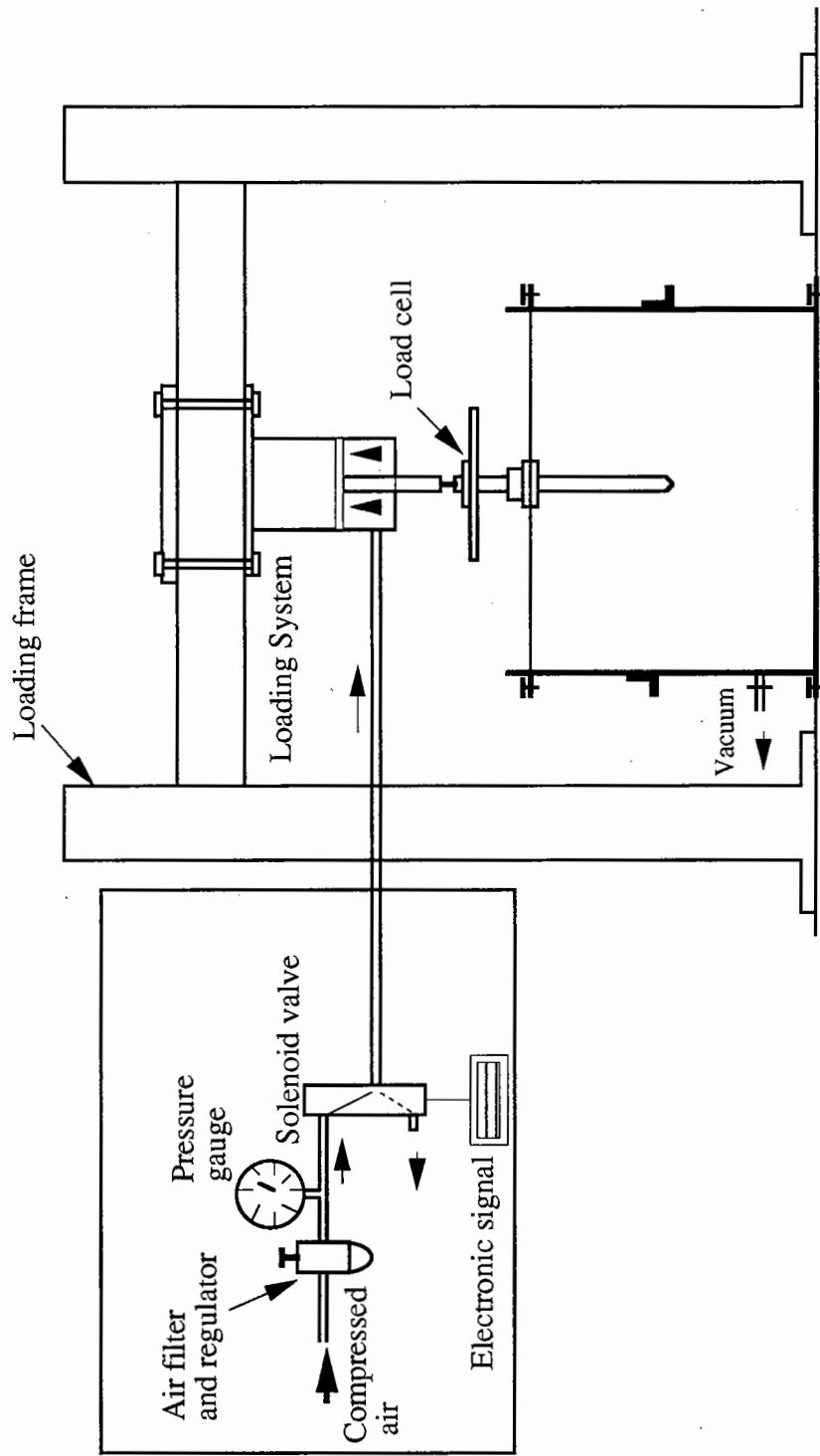


Fig.3.12 . Cyclic Loading Equipment

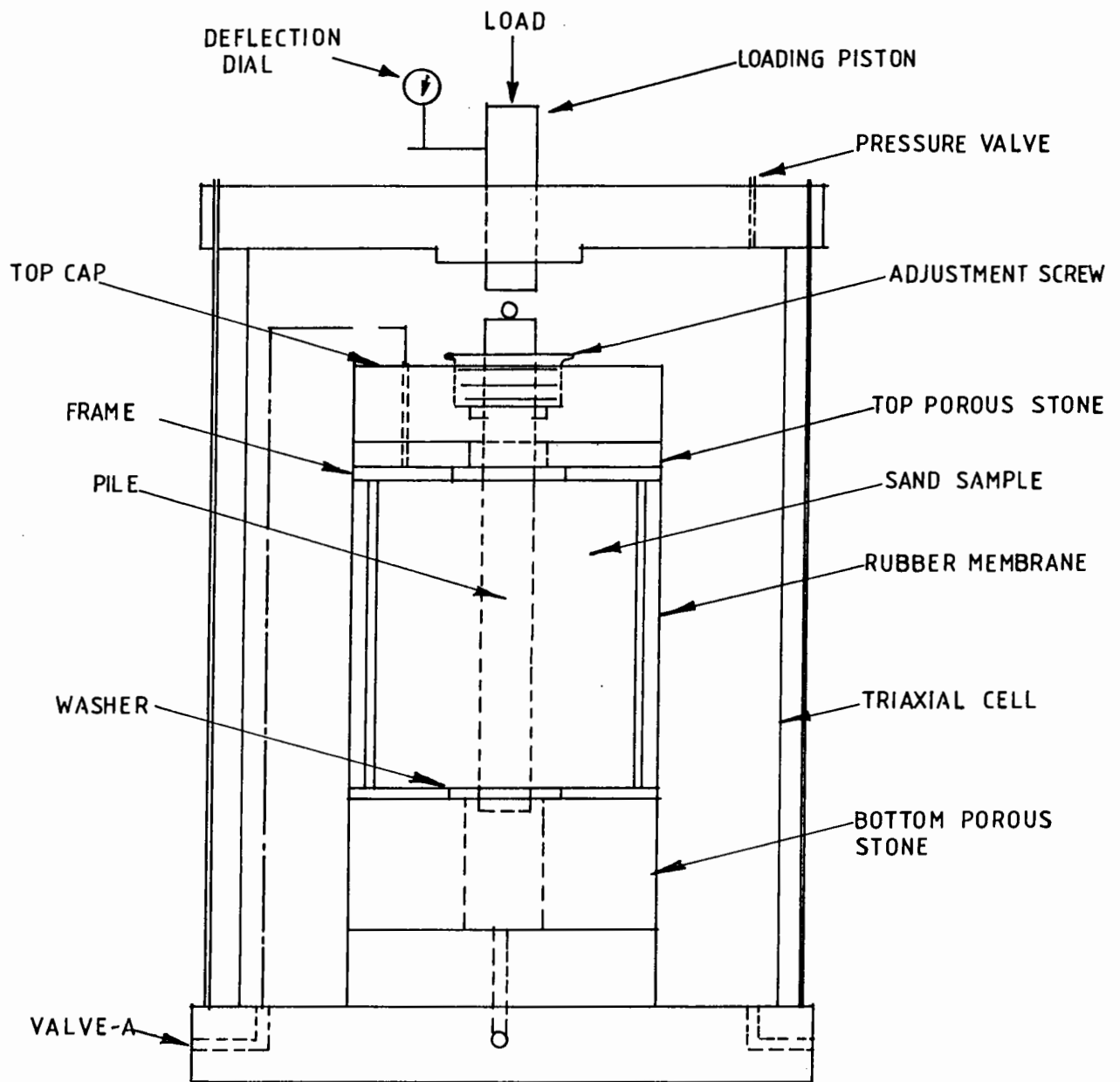
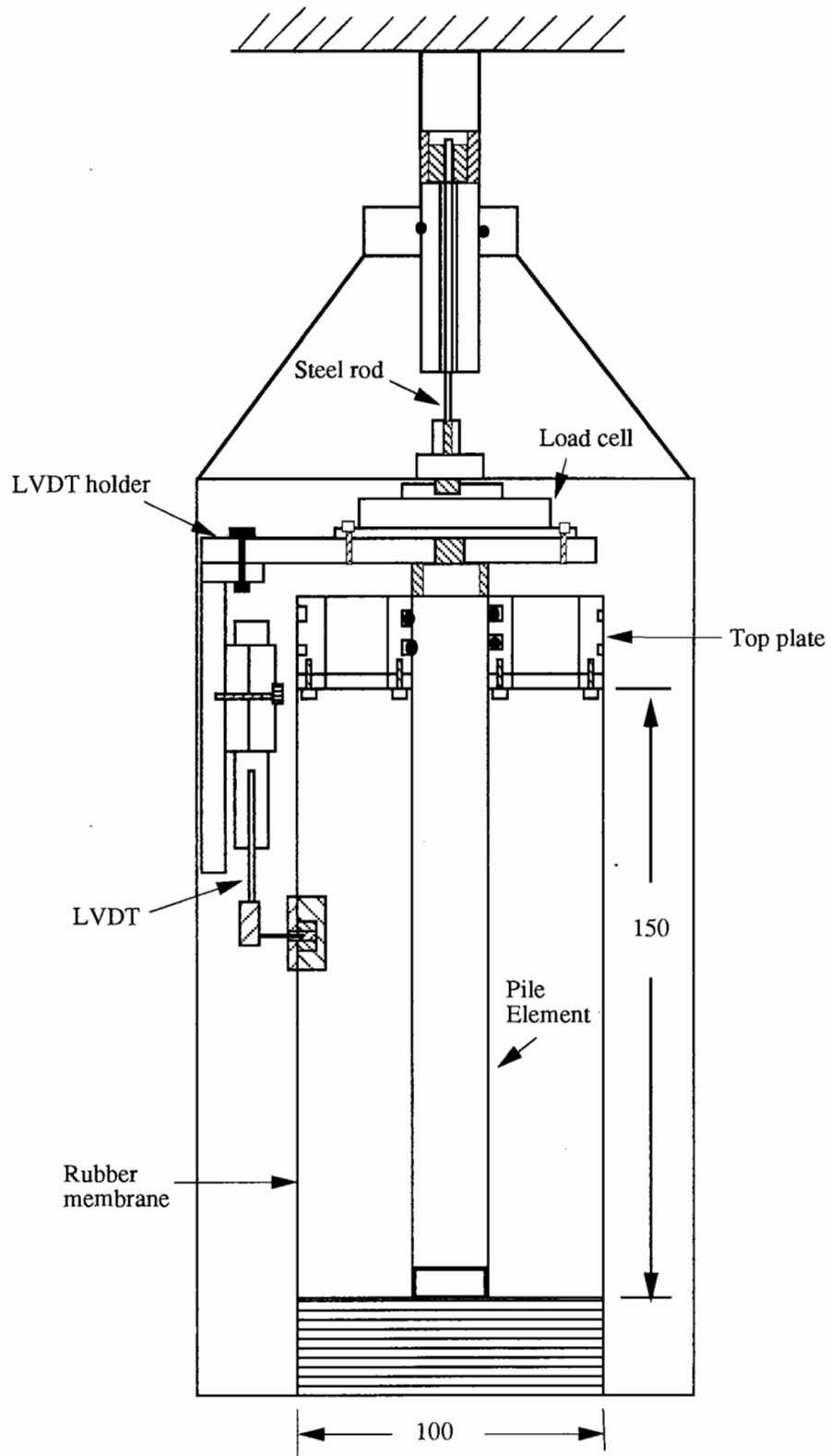


FIG. 3.13. LABORATORY MINIATURE PILE TEST APPARATUS
(Coyle and Sulaiman, 1967.)



All dimensions are in mm

Fig. 3.14. Details of the Soil-Pile Slip Test Apparatus

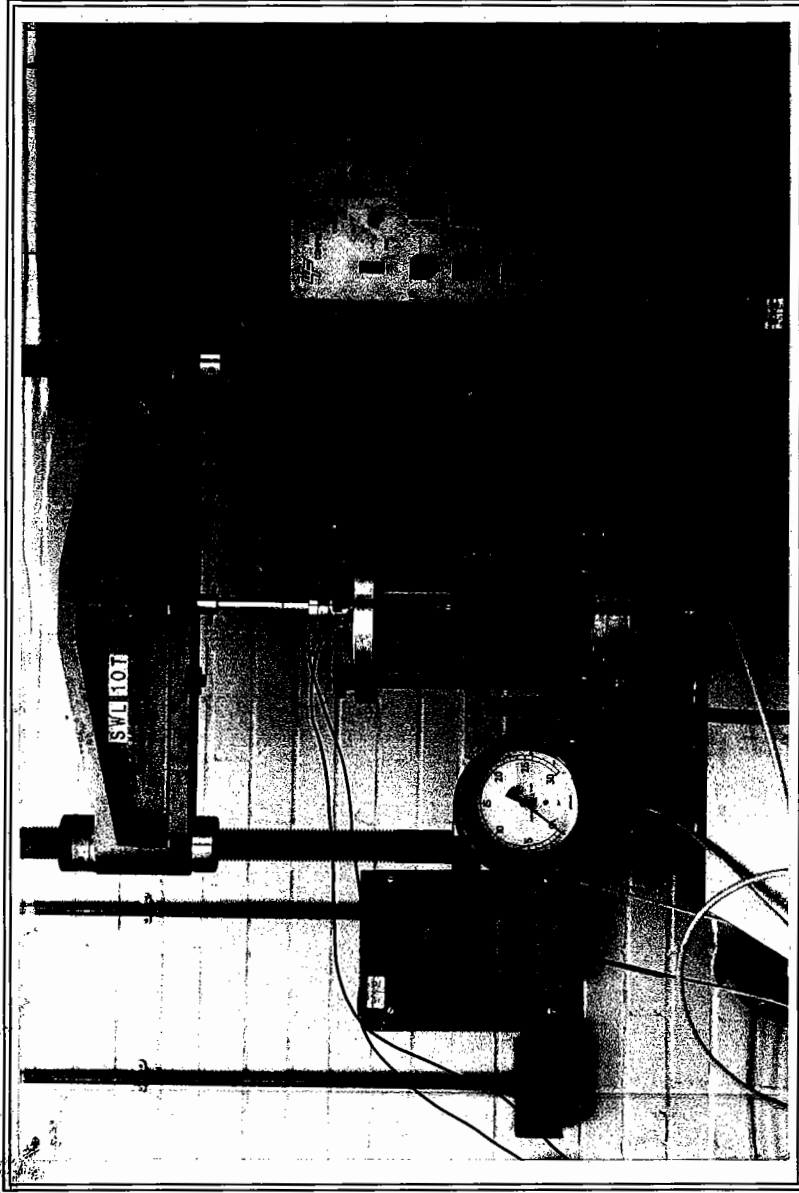
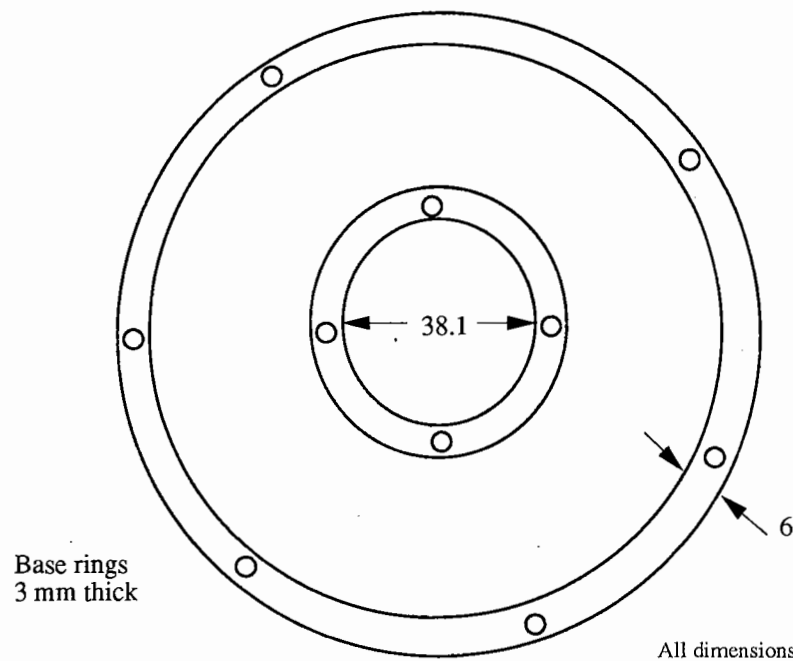
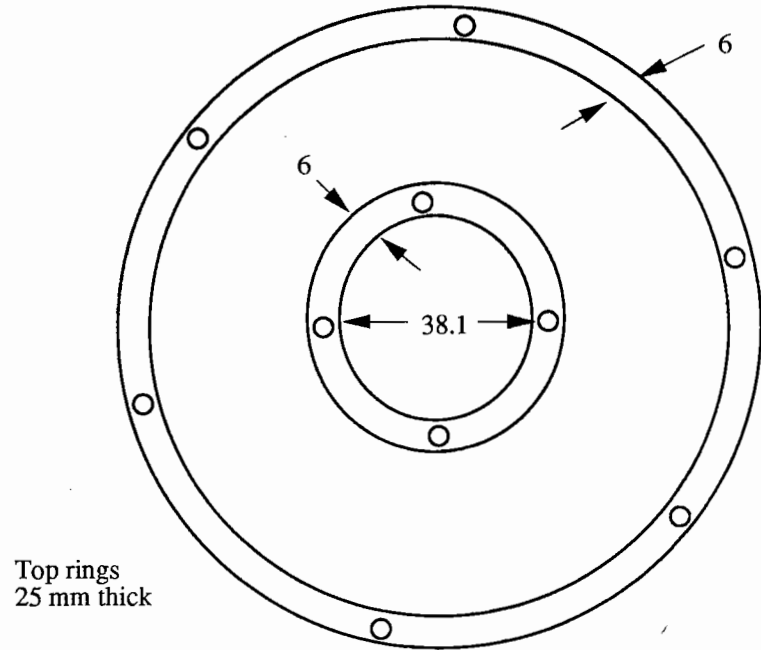
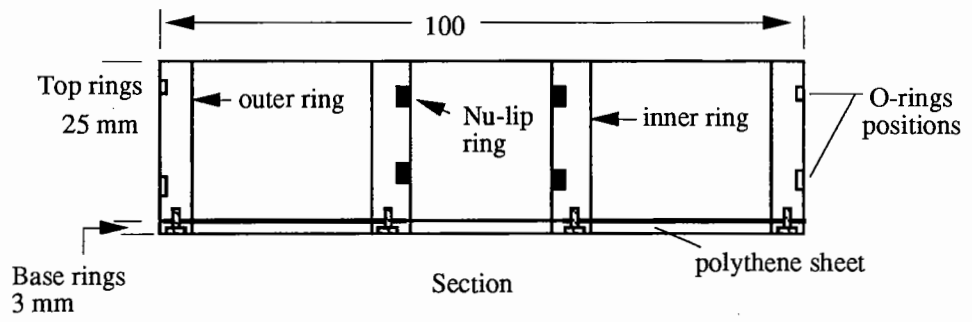
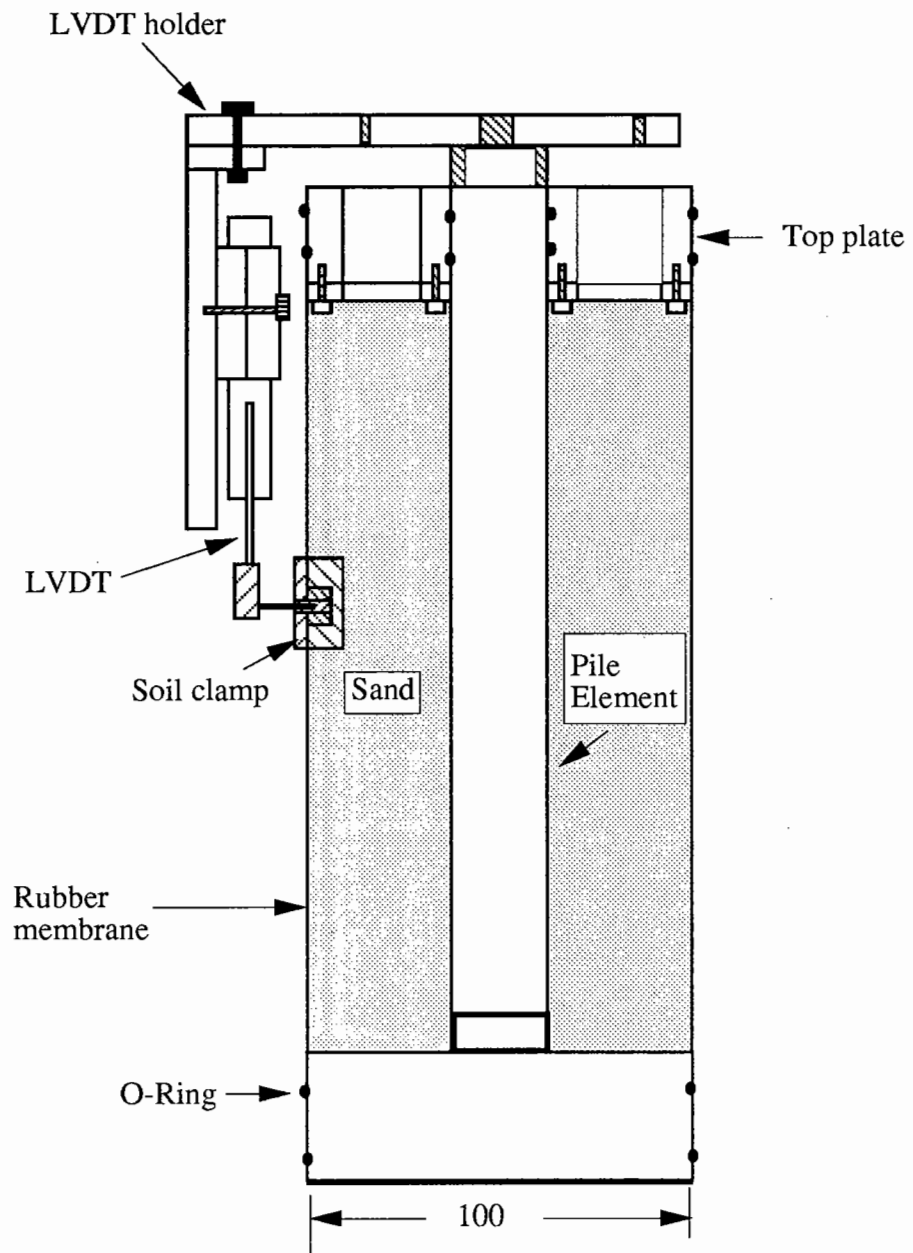


Fig. 3.15 Soil-Pile-Slip Test Apparatus



All dimensions are in mm

Fig.3.16. Top Plate Design for the 38.1 mm Diameter Pile Element



All dimensions are in mm

Fig. 3.17. Details of the Deformation Measuring Unit

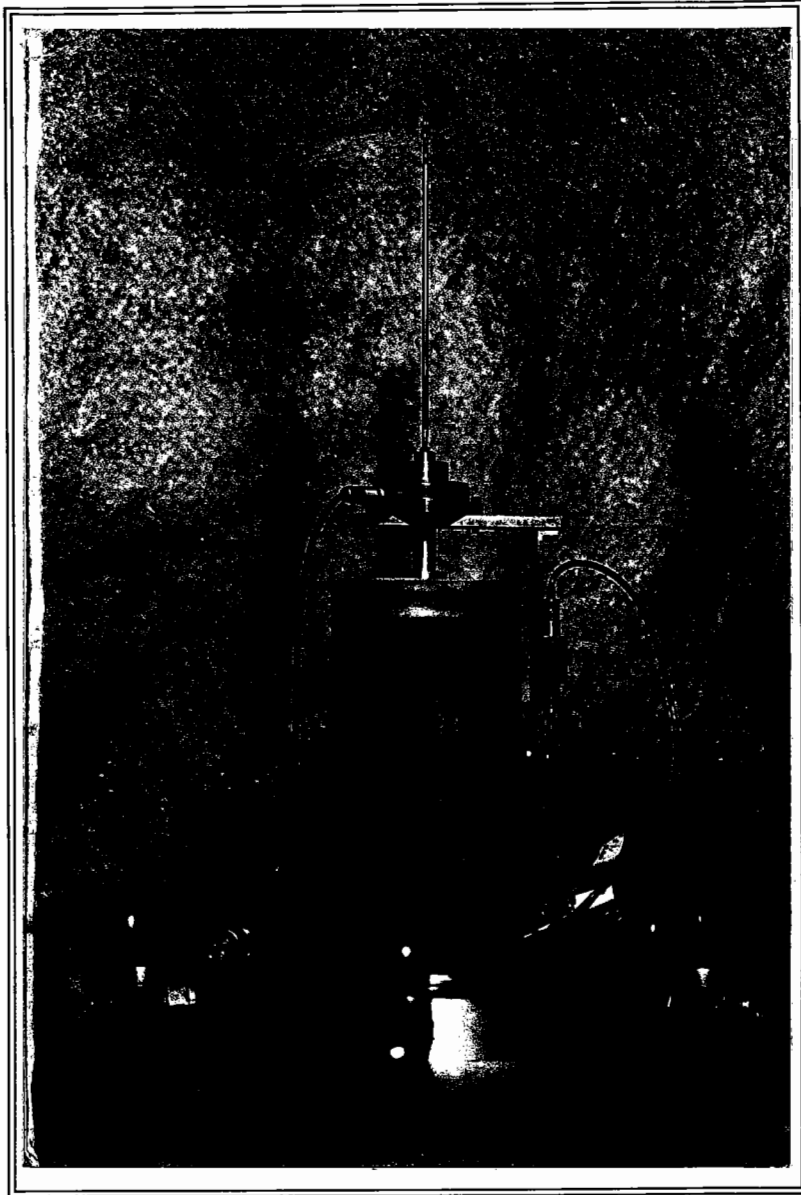


Fig. 3.18 A Close View of Deformation
Measuring Unit

PROPERTIES OF TEST MATERIALS

4.1 Introduction

The properties of the test material (the sand and the pile) used in the present investigation are presented in this chapter. The properties of sand and the pile material are presented in Section 4.2 and Section 4.3, respectively. The interface properties are presented in Section 4.4.

4.2 Properties of Sand

4.2.1 Selection of Sand

Concrete sand (i.e. sand to be used for making concrete) was used for the preliminary experiments and Leighton Buzzard sand was used for the main experiments. The reasons for using different sands are explained below:

The preliminary experiments were performed as the apparatus was being developed. The concrete sand, which was available in the laboratory, was used for the preliminary investigation. While working with concrete sand, a large amount of dust was created in the laboratory. In view of this, the environmental safety committee of the University advised to limit the minimum particle size of sand to 0.6mm. Accordingly a Leighton Buzzard sand having grain sizes between 0.6mm and 2mm was used for the main experiments.

4.2.2 Details of the Tests Conducted

Tests conducted on the sand include:

- i) Grain size distribution test
- ii) Test to obtain angle of internal friction and
- iii) Minimum and maximum density tests.

All the tests were performed according to the British Standards. The tests to obtain minimum and maximum densities of sand were performed by the author. The other tests were performed by laboratory technicians under the direct supervision of the author. In the following sections the test procedure in brief and their results are presented.

4.2.2.1 Grain Size Distribution Test

A dry sieve analysis was performed on the sand to obtain the grain size distribution. Fig. 4.1 shows the grain size distribution curves for the two sands. The properties of these curves are shown in Table 4.1

4.2.2.2 Tests to Obtain Angle of Internal Friction (ϕ)

Direct shear and triaxial tests were performed on the dry sand to obtain ^{the} angle of internal friction. The samples were prepared at a dry density of 17.20 kN/m^3 for concrete sand and 17.36 kN/m^3 for Leighton Buzzard sand which are equal to the densities obtained for the respective sands during the model pile testing.

The direct shear tests were performed under a normal stress of 50 kPa, 100 kPa and 150 kPa. The ratio of shear stress at failure to corresponding normal stress has been used to compute ϕ . The results are presented in Table 4.2.

Triaxial tests were conducted on 38mm dia. x 76mm high dry soil samples. The tests were performed at a confining pressure of 50kPa, 100kPa and 150kPa. By drawing Mohr's circles for the

results obtained at these three confining pressures, ^{the} failure envelope and hence the angle of internal friction (ϕ) was obtained for each sand. The values of angle of internal friction (ϕ) obtained from the triaxial tests are presented in Table 4.2.

4.2.2.3 Minimum and Maximum Density Tests

The minimum and maximum density tests were performed according to BS 1377: part 4:1990, Section 4. The results of these tests are presented in Table 4.1.

4.3 Properties of the Pile Materials

4.3.1 Selection of Pile Material

The mild steel tubes available in the laboratory were used to fabricate the model piles for the preliminary experiments. In the main experimental programme, a series of experiments were proposed on an instrumented pile with built-in load cell segments (Fig. 3.6(b)). For these tests, the pile material should have a low Young's modulus to produce measurable strain and high strength to withstand the forces during the pile installation. In view of the above requirements, a high strength aluminium alloy was selected as the pile material for the main experiments.

4.3.2. Details of the Tests Conducted

Properties of the pile materials are presented in Table 4.3. Hardness and roughness tests were performed during the present investigation and the other properties were provided by the material suppliers.

a) Hardness Test

Vickers hardness test was performed on the two pile materials

with an indentation mass of 10 kg. Based on the dimensions of the indentation, by referring to the chart, the corresponding Vickers hardness number was obtained. For each specimen, two trials were conducted and the average value was obtained (Table 4.3.(a)).

b) Surface Roughness Tests

After completing the experiments, a significant increase in roughness of the pile surface was observed. Hence, the roughness tests were performed on the pile surfaces using Surfcom 20c/30c equipment. The tests were conducted on the rough surface of the pile, after the pile tests, and on the polished surface, which indicate conditions before testing. The Central Line Average (CLA) values obtained for different pile surfaces are presented in Table 4.3.

4.4 Soil-Pile Interface Properties

A series of direct shear interface tests were performed to obtain the interface friction angle (δ) between the sand and the pile surface. In order to perform these tests four pieces of square plates, two in aluminium alloy and two in mild steel, were fabricated (Fig. 4.2). The plate was fitted into the lower half of the direct shear box and the top half was filled with sand to the required density. The whole assembly was placed in direct shear apparatus and loaded similar to that of a conventional direct shear test.

The steel plates were tested against the concrete sand (DR=48%) and the aluminium alloy plates were tested against Leighton Buzzard sand (DR=93%). The test results are presented in Table 4.4.

Table 4.1 (a) Soil Properties (Classification)

Soil Type	Grain Size Distribution				Specific Gravity
	D ₁₀ (mm)	D ₅₀ (mm)	D ₆₀ (mm)	D ₆₀ /D ₁₀	
Concrete Sand	0.221	0.452	0.530	2.400	2.656
Leighton Buzzard Sand	0.574	0.924	1.000	1.740	2.650

Table 4.1 (b) Soil Properties (Density tests)

Soil Type	Densities in kN/m ³			Void Ratios			Relative Density (DR)
	γ_{max}	γ_{min}	γ_{at} test	e _{min}	e _{max}	e _{at} test	
Concrete Sand	18.75	16.01	17.20	0.417	0.659	0.544	48%
Leighton Buzzard Sand	17.59	14.98	17.36	0.507	0.769	0.527	93%

Table 4.2 Soil Properties: Shear Strength Parameters
(All angles in degrees)

Normal Stress (kPa)	Direct Shear Test				Triaxial Test	
	Concrete Sand		Leighton Buzzard Sand		Concrete Sand	Leighton Buzzard Sand
	ϕ_p	ϕ_r	ϕ_p	ϕ_r	ϕ_p	ϕ_p
50	41.75	40.99	46.48	45.43		
100	40.30	39.94	46.31	44.82		
150	40.59	40.00	46.19	43.12		
Average	40.88	40.31	46.33	44.46	38	40

ϕ_p = Peak Shear angle;

ϕ_r = Residual Shear angle

Table 4.3(a) Properties of Pile Material

Pile Material	Young's Modulus (GPa)	Tensile Strength (N/mm ²)	Poisson's Ratio	Vickers Hardness Number
Mild Steel	210	250	0.30-0.35	245
Aluminium Alloy	70	310	0.32-0.34	42

Table 4.3 (b) Properties of Pile Material

Pile Material	Roughness of the Pile Surface (CLA, μm)							
	Before Test (Smooth)				After Test (Rough)			
	Trials				Trials			
	1	2	3	Average	1	2	3	Average
Mild Steel	0.53	0.69	0.66	0.63	1.28	0.87	1.37	1.17
Aluminium Alloy	0.44	0.60	0.38	0.47	2.09	2.14	1.80	2.01

Table 4.4 Direct Shear Interface Test Results

Normal Stress	Steel - Concrete Sand				Aluminium - Leighton B.Sand			
	Smooth		Rough		Smooth		Rough	
	δ_p	δ_r	δ_p	δ_r	δ_p	δ_r	δ_p	δ_r
50	17.8	16.8	21.1	20.5	21.7	21.3	28.4	27.0
100	15.4	14.4	20.0	19.7	23.7	23.3	28.9	27.3
150	18.9	18.6	21.2	20.7	25.3	24.3	32.1	31.0
Average	17.4	16.6	20.8	20.3	23.6	23.0	29.8	28.4

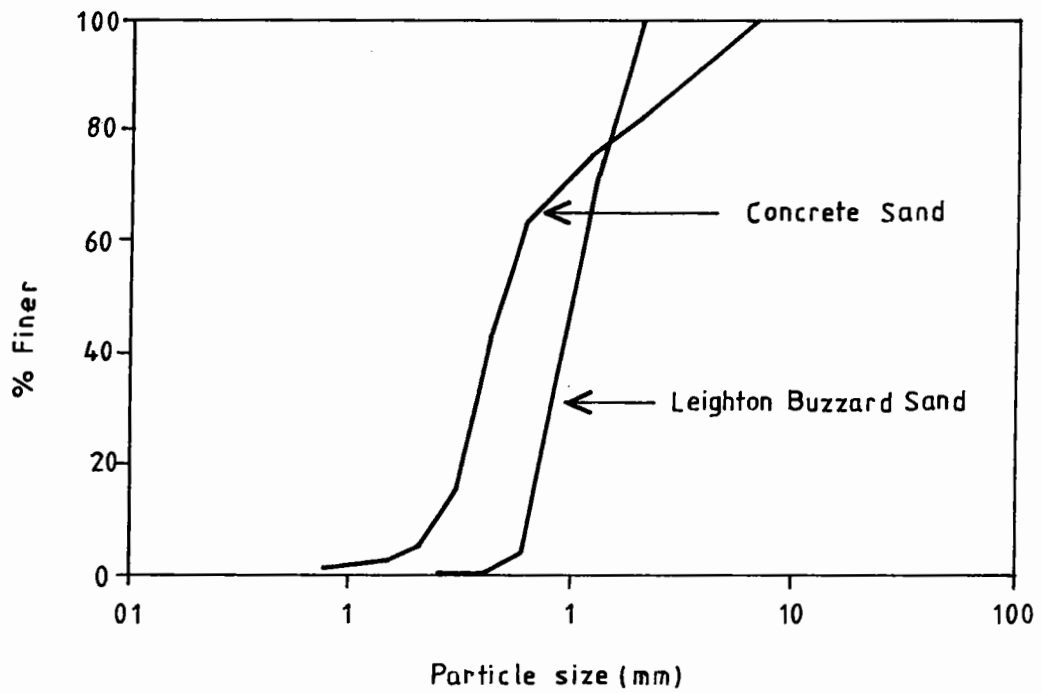


Fig.4.1. Particle Size Distribution of Sand Used in the Investigation

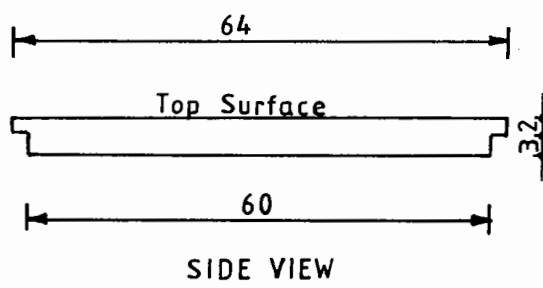
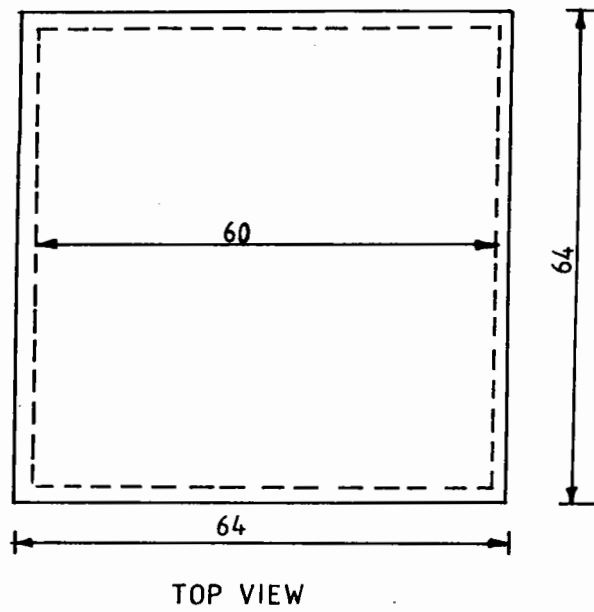


Fig.4.2.Test Plates For Interface Testing

EXPERIMENTAL INVESTIGATION**5.1 Introduction**

This chapter presents the details of the experimental programme and testing procedure used in the investigation. The experimental programme was divided into two parts.

- i) Tests on model piles and
- ii) Soil-Pile-Slip Tests.

The model pile test apparatus was completely designed and developed during present study. Therefore, a set of preliminary experiments were conducted to examine the working conditions of the apparatus and to arrive at a standard test procedure and programme. The details of these preliminary tests which led to improvements in the experimental set-up are discussed in Section 5.2. A number of tests on model piles were then carried out. The tests on model pile include monotonic and cyclic tensile load tests. The cyclic load tests were conducted under different cyclic load levels. During cyclic load tests, displacements of pile head, stress distribution along the pile, variation of radial stress in sand and settlement of sand surface were monitored. In several cyclic load tests, the response of the pile subsequent to peak loading was also studied. The procedure and the programme details of model pile tests are presented in Section 5.3. Besides tests on model pile, a set of experiments was conducted on soil-pile-slip test apparatus to obtain T-Z curves for tension piles. The details of soil-pile-slip tests are presented in

Section 5.4. A schematic representation of the entire experimental investigation carried out is shown in Fig. 5.1.

5.2 Preliminary Experiments

For the preliminary experiments, concrete sand and steel model piles were used. The test bed was prepared by placing sand in layers in the tank and compacting the same using a steel rod. Surcharge pressure was then applied by creating a vacuum in the tank and the pile was then installed by jacking. During the installation of the pile, the radial stress distribution in the sand was monitored by placing four pressure cells (PC1, PC2, PC3 and PC4) at different radial distances at a depth of 150 mm below sand surface as shown in Fig.5.2. The uniform distribution of the vacuum was also examined by measuring the vacuum pressure, with the help of vacuum gauges, at different locations (VP1, VP2, VP3 and VP4) in the test tank as shown in Fig.5.3. A number of monotonic and cyclic load tests were conducted on the model piles and load-displacement observations were made.

The following are the major observations made regarding the adequacy of the testing arrangements during the above preliminary tests and the modifications made to the apparatus and to the testing procedure for further pile tests.

1) The measured radial stress variation (Figs.6.5 & 6.6) shows that the stress becomes negligible beyond 300mm away from the pile location. This indicated that the tank dimensions are adequate to avoid any confining affects.

2) The radial stress in sand during the installation of the pile (installation stress) was observed to be proportional to

the applied surcharge pressure (vacuum pressure). Hence, in order to reduce the installation stress, it was decided to install the pile before the application of surcharge pressure.

3) The concrete sand used contained a significant amount of fines which created dust in the laboratory during the filling process. The concrete sand was therefore replaced by a relatively dust free, Leighton Buzzard sand for the rest of the testing programme.

4) The method of sand filling by compaction gave an average unit weight of 17.20 kN/m^3 and a relative density of 48%. Repeatability in the density of the test bed could not be achieved in different fillings because of the low relative density. Therefore, a vibration technique was adopted for the preparation of the sand bed which gave a higher relative density (93%) and repeatability to the sand bed.

5) The connection between the cyclic loading unit and the pile head became loose during the repeated loading of the pile. This was eliminated by sealing the nut connecting system by using Nut-Lock fluid before commencement of the loading.

6) Though, the vacuum pressure distribution within the test tank was observed to be uniform, the pressure got reduced over the long duration of testing (about a week). This was rectified by undertaking necessary repairs to the vacuum pump.

A period of 9 months was spent in carrying out the preliminary experiments and improving the experimental setup.

5.3 Test Programme on Model Piles

Tests were carried out on different diameter (12.7mm, 25.4mm and 38.1mm) aluminium alloy piles. A Leighton Buzzard sand was used for the investigation. The sequence of operation adopted for the conduct of tests on model piles were:

- (1) Filling of test tank
- (2) Installation of the model pile
- (3) Application of surcharge pressure and
- (4) Load testing of piles.

5.3.1 Filling of Test Tank

The sand was placed into the test tank using a vibration technique as explained in the following steps.

- Step 1: Place 200 kg of sand and level the surface with a wooden plank.
- Step 2: Vibrate the sand surface using a Bosch vibrating rammer, with a wooden plank 570mm x 240mm attached to its base, for 4 minutes.
- Step 3: Repeat steps 1 and 2 for the next two layers.
- Step 4: Place 160 kg of sand and level the surface.
- Step 5: Vibrate the sand surface for 3 minutes.
- Step 6: Place 40 kg of sand and level it.
- Step 7: Vibrate the surface for 3 minutes.

Using this method, 800 kg of sand was placed into the tank which gave an overall ~~unit weight~~ of 17.36 kN/m^3 and a relative density of 93%.

5.3.2 Installation of the Model Pile

After filling with sand, the test tank was made air tight by covering with a polythene sheet. The model pile was then installed by jacking it down gradually through the pile access unit, over a period of 15 minutes. During the entire jacking operation the verticality of the pile was monitored with the help of a spirit level. The final depth of penetration of the pile was 400 mm in all cases.

5.3.3 Application of Surcharge Pressure

The effect of surcharge pressure was created by applying vacuum in the tank. A constant vacuum pressure of 70 kPa was applied in all the tests conducted.

5.3.4 Load Testing of Piles

The load tests on piles include:

- (i) Monotonic load tests and
- (ii) Cyclic load tests.

The details of tests conducted are presented in Table 5.1.

5.3.4.1 Monotonic Load Tests

During the monotonic tension tests the load was applied in steps of 0.1 kN. Each load increment was maintained for a period of 2 minutes or until the time when the displacement under that load ceased, whichever was longer. The test was continued until

failure which took place with a large upward displacement under a small, or no incremental, load. Each test was repeated three times to obtain an average ultimate tensile capacity (q_{ta}) for each pile.

5.3.4.2 Cyclic Load Tests

The cyclic load was applied at a frequency of 0.2 Hz as shown in Fig. 5.4. The cyclic load level (q_c) was expressed as a percentage of q_{ta} . The tests were conducted both under constant and varying cyclic load conditions.

(a) Tests with Constant Cyclic Load

During these tests, the cyclic load was maintained constant throughout the test. The tests were conducted at cyclic loads ranging from 7% q_{ta} to 75% q_{ta} . Observations of displacement as a function number of cycles were recorded. The tests were conducted either until the failure of the pile or for a maximum of 100,000 cycles. If no failure was observed after 100,000 cycles, the pile was subsequently subjected to a monotonic tension test.

The number of cycles during a test was estimated from the loading frequency and the duration of the test. Application of 100,000 cycles took a continuous testing time of 6 days. The number of cycles was limited to 100,000 cycles bearing in mind the capacity of vacuum pump to run continuously and the time scale of the test programme.

(b) Tests with Varying Cyclic Load

In these tests, the cyclic load was varied at intervals until failure. The loading sequence followed in different tests is presented below:

Test identity

Loading sequence

1) 38.1-V-A

The test was started with a cyclic load level of 90% qta. When the pile reached a state of incipient failure (rapid increase in the rate of displacement) the cyclic load was reduced to 45% qta and the test was continued until failure.

2) 38.1^{*}-V-A

&

38.1^{*}-V-B

This is an instrumented pile test. The cyclic load level was kept as 15% qta at the start of the test. The load was increased approximately after every 600 cycles by 15%qta until the pile reached a state of incipient failure. At this point, the cyclic load was reduced to 15% qta and the test was continued by increasing the load after every 600 cycles by an increment of 15% qta until the pile failed.

5.3.4.3 Recording of Test Data

During the cyclic load tests on the pile, the pile head displacement and load at the pile head and at the load cell segments along the pile were recorded by a data logger on a 3.5 inch computer diskette. The logger was programmed to record a set of 30-60 scans, with a scan interval of 0.5 seconds. In each scan, the output signals from the LVDTs, load cell and load cell segments were recorded. The scanning process was repeated at regular intervals, varying from 12 to 1440 cycles, depending on the cyclic load level and the stability of the pile.

The data recorded by the logger was in the form of rolling numbers as shown in Appendix B. These numbers were processed on an IBM personal computer by using software available in the department. The monotonic test data was recorded manually and was processed using a Macintosh-II personal computer.

5.4 Soil-Pile-Slip Test

The soil-pile-slip test apparatus was developed to obtain load-displacement curves for a pile element. The details of the apparatus are shown in Figs.3.14 to 3.17. For these tests, the sample was prepared in a manner similar to that used for a conventional triaxial test.

A 100mm diameter mould was fitted with a rubber membrane and was positioned over the base of the triaxial cell. Keeping the pile element at the centre, the Leighton Buzzard sand was compacted around the pile element in three layers to give an overall density of 17.36 kN/m^3 . After filling the sample to a height of 150mm, the top plate was placed over the sample and the rubber membrane was transferred onto the sample. A vacuum was created within the sample, through the base plate, to keep the sample upright. The membrane was then clamped to the base of

triaxial cell at one end and to the top plate at the other end using O-rings.

The load cell and LVDT were mounted onto the sample as shown in Fig.3.17. The triaxial cell was then fitted over this assembly, a confining pressure was applied on the sample using compressed air and the vacuum pressure to the sample was disconnected. The whole of this assembly was placed in a triaxial load frame and the base of triaxial cell clamped to movable platform. The head of the pile element was connected to the rigid support at the top of the frame. The platform, along with the triaxial cell clamped on it, was moved down to create a tensile force on the pile element. The load cell and LVDT readings were recorded. The test was continued until failure exhibited by a large upward displacement of the pile element under a small, or no incremental, load.

The above tests were conducted on a 25.4 mm diameter pile element under confining pressures of 70 kPa, 120 kPa and 170 kPa. The tests carried out are listed in Table 5.2.

Table 5.1 Details of Experiments on Model Piles

Test No.	Diameter of Pile (mm)	Test Identity
1	12.7	12.7-100-A
2		12.7-100-B
3		12.7-100-30A
4		12.7-30-A
5		12.7-45-A
6		12.7-60-A
7		12.7-60-B
8		12.7-60-C
9		12.7-70-A
10	25.4	25.4-100-A
11		25.4-100-B
12		25.4-100-C
13		25.4-100-30A
14		25.4-30-A
15		25.4-45-A
16		25.4-60-A
17		25.4-60-B
18		25.4-60-C
19		25.4-75-A
20		25.4-75-B

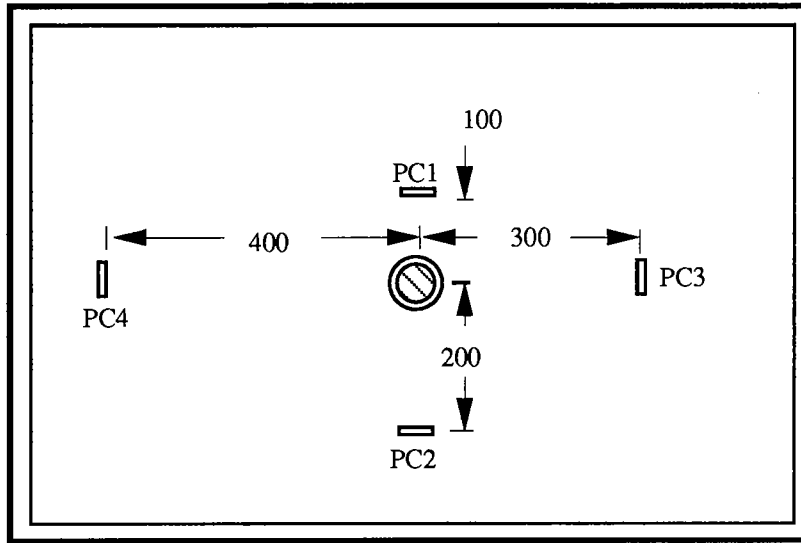
Note for reading Table: Test Identity: Pile Diameter - % q_u - Trial; * : Instrumented Pile ; + : The loading frequency was 0.4 Hz.; V: Varied loading; The test 38.1 - 100 - 45B Identifies a monotonic tension test conducted after the test 38.1 -45-B

Table 5.1 Continued

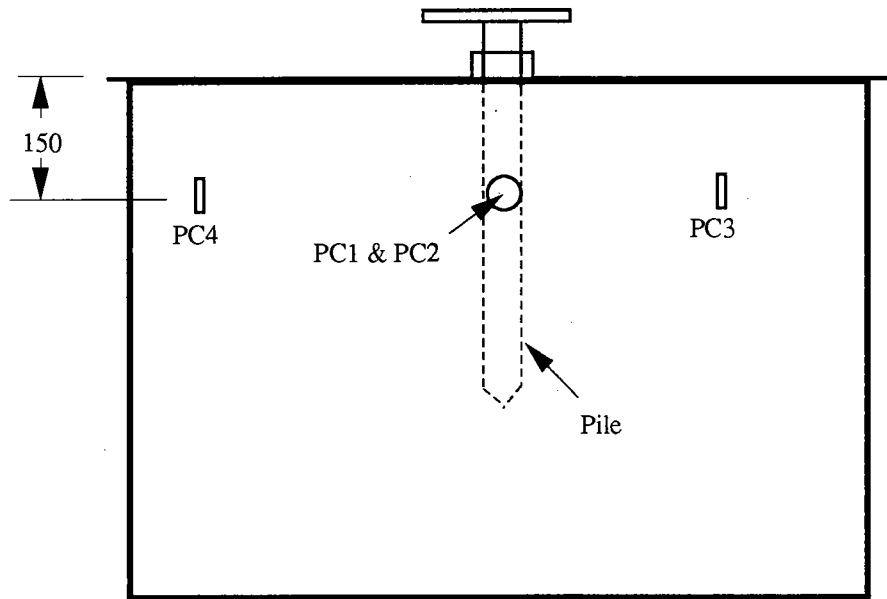
Test No.	Diameter of Pile (mm)	Test Identity
21	38.1	38.1-100-A
22		38.1-100-B
23		38.1-100-C
24		38.1-100-07A
25		38.1-100-15A
26		38.1-100-38
27		38.1-100-45
28		38.1-100-45
29		38.1-07-A
30		38.1-15-A+
31		38.1-38-A+
32		38.1-45-A
33		38.1-45-B
34		38.1-60-A
35		38.1-60-B
36		38.1-60-C
37		38.1-60-D
38		38.1-75-A
39		38.1-75-B
40		38.1-V-A
41		38.1 ^x -100-A
42		38.1 ^x -100-B
43		38.1 ^x -60-A
44		38.1 ^x -75-A
45		38.1 ^x -V-A
46		38.1 ^x -V-B

Table 5.2 Soil-Pile-Slip tests

Diameter of Pile Element (mm)	Confining Pressure (kPa)
25.4	70 120 170



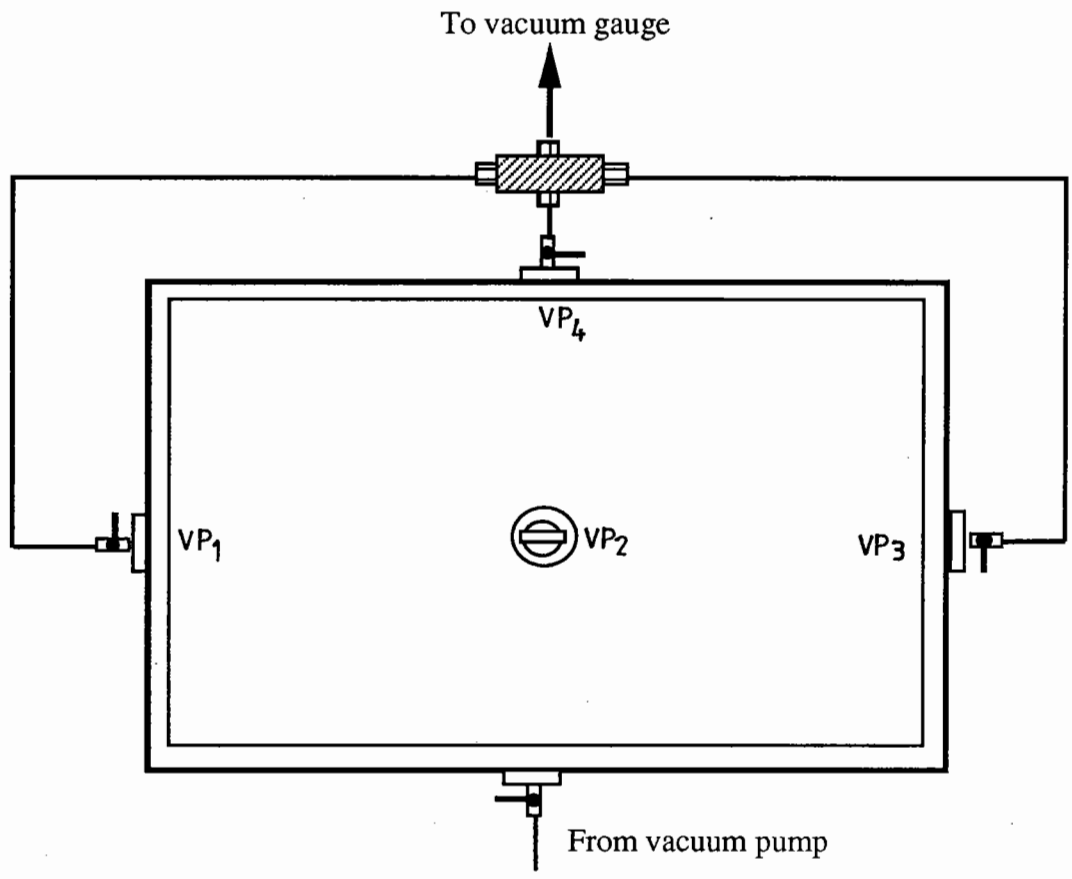
Plan view



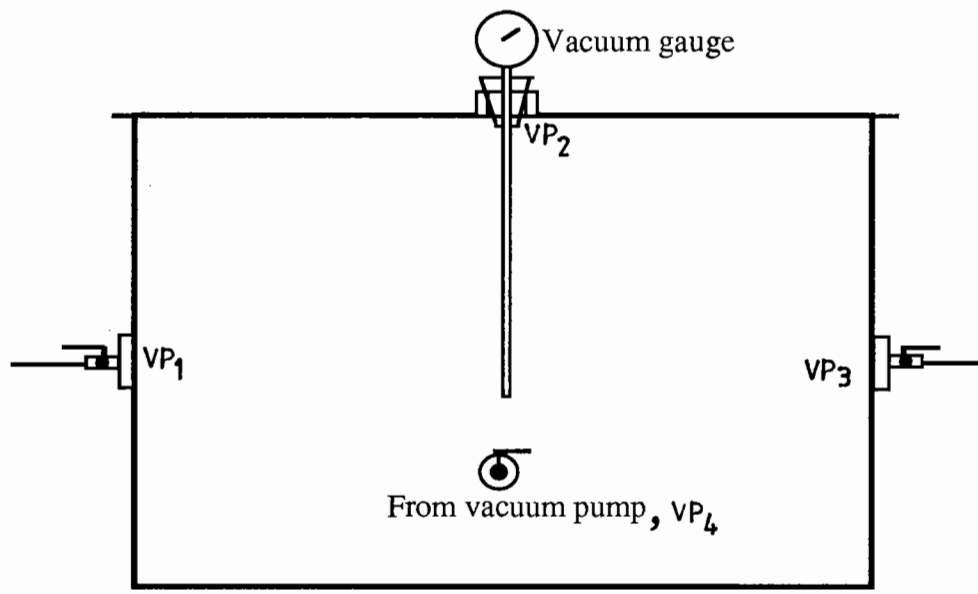
Front view

All dimensions are in mm

Fig.5.2. Location of the Pressure Cells to Study the Pressure Distribution During Pile Installation



Plan view



Front view

Fig. 5.3. Arrangement for the Vacuum Test

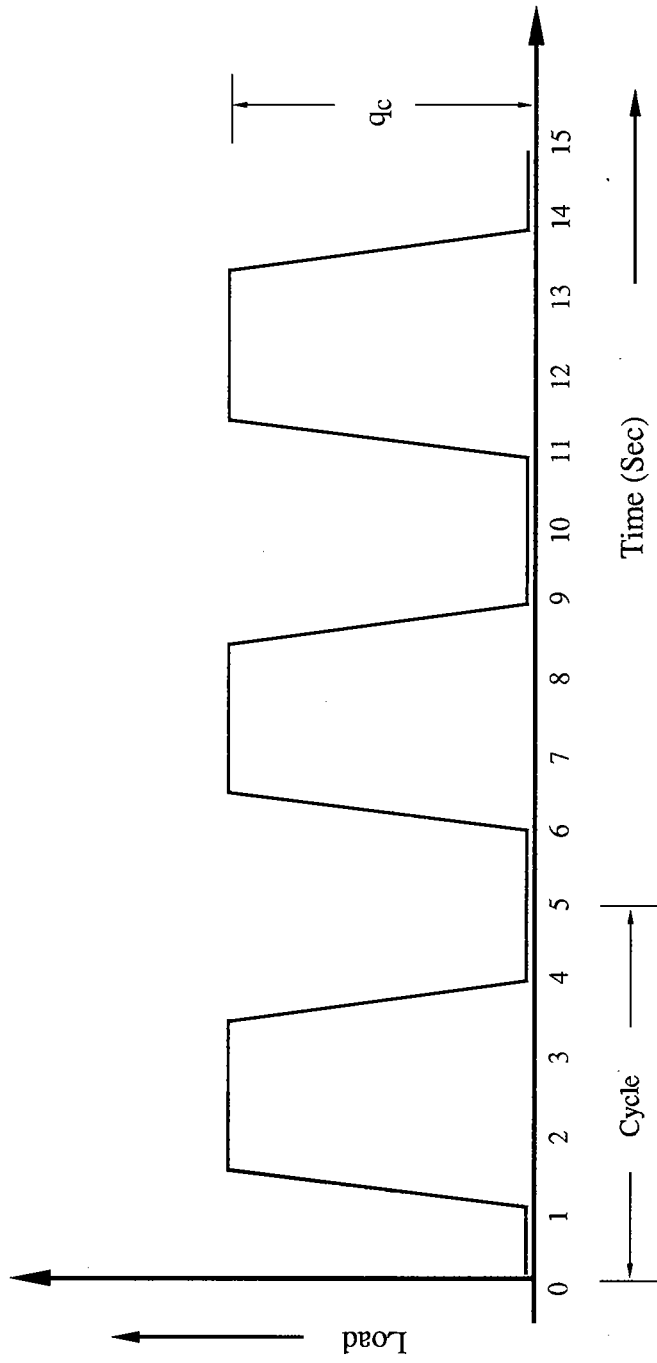


Fig. 5.4. Cyclic Load Form

ANALYSIS AND DISCUSSION OF EXPERIMENTAL RESULTS**6.1 Introduction**

During the present investigation, a comprehensive experimental programme was carried out on model piles to understand the behaviour of piles under vertical cyclic tensile loading. The tests were carried out on different diameter model piles under constant and varying cyclic loads. The ultimate tensile capacity of the piles, obtained from monotonic tension test, was used as a reference value for cyclic loads. The cyclic load tests were conducted under different cyclic loads in order to obtain safe cyclic loads and a relationship between cyclic load and number of cycles to failure. In a few tests, the pile was subjected initially to a peak cyclic loading and the load was then decreased to a smaller cyclic load to study the response of the pile subsequent to peak loading. A series of tests were also conducted on an instrumented pile to study the shear stress distribution along the pile. Besides the above, observations were also made on the settlement of the sand surface and variation in radial stress in the sand during cyclic loading which helped in the understanding the mechanism of pile failure. In addition to tests on model piles, a set of experiments were also carried out on the soil-pile-slip test apparatus. This chapter presents the analysis and discussion of these experimental results.

The sign convention adopted for load and shear stress in this thesis for the analysis of results, is shown in Fig. 6.1 and explained below.

Load: A load which compresses a pile element and tries to reduce its length is +ve load (Fig. 6.1(a)). A load which creates a tensile force on a pile element and tries to increase its length

is -ve load (Fig. 6.1(b)).

Shear Stress: The shear stress developed between the soil and the pile, while either the pile moving down relative to the surrounding soil or the soil moving up relative to the pile is considered +ve shear (Fig. 6.1(c)). The shear stress developed between the soil and the pile while either the pile moving up relative to the surrounding soil or the soil moving down relative to the pile is considered -ve shear (Fig.6.1(d)).

6.2 Stress in Sand During Pile Installation

During the tests on steel model piles, four pressure cells, PC1, PC2, PC3 and PC4, were placed in the sand-bed at radial distances of 100 mm, 200mm, 300mm and 400mm respectively from the centre of the pile, as shown in Fig.5.2. The pressure cells were placed, at a depth of 150 mm below the sand surface, to measure the radial stress (σ_r) in sand.

The test bed was subjected to a desired surcharge pressure and the pressure cell readings were set zero. The model pile was then installed gradually (by jacking) into the sand-bed. The depth of penetration of the pile and the corresponding pressure cell readings were recorded by the data logger. These observations were made during the installation of 25.4 mm and 38.1 mm diameter steel piles with the test bed subjected to different surcharge pressures as shown in Table.6.1.

The variation of radial stress (σ_r) due to the penetration of the pile is examined with respect to:

- (i) Location of the pile tip and
- (ii) Surcharge pressure.

i) Radial stress as a function of pile tip location

The radial stress (σ_r) recorded with the depth of penetration of 25.4 mm and 38.1 mm diameter piles are shown in Fig.6.2 and 6.3 respectively. The results show that the radial stress (measured at a radial distance from the pile) reaches a maximum when the tip is just above the pressure cell location (Figs.6.2 and 6.3). This is because, the stress dispersion below the pile tip is expected to be as shown in Fig.6.4 and therefore, the pressure cell located radially away from the pile experiences a maximum stress when the tip is slightly above its elevation. However, a pressure cell placed close enough to the pile surface can be expected to record the peak value when the tip reaches the elevation of the pressure cell. This indicates that the radial stress on the pile surface is maximum near the pile tip and decreases as one moves above the pile tip. Similar observations have been reported by a number of other investigators (Nauroy and Le Tirant, 1983; Wersching, 1987; Bond, 1989; Bond and Jardine, 1989, 1991 and Lehane, 1992).

ii) Radial Stress as a function of surcharge pressure

Figs.6.5 and 6.6 show the maximum stress recorded at different radial distances under different surcharge pressure during the installation of piles. The radial stress (σ_r) and the corresponding normalised stress (σ_r/p) at different radial distance are shown in Table 6.2. It can be observed from Table 6.2 that for a given pile diameter, the normalised radial stress at a given radial distance is approximately a constant. This suggests that the radial stress due to installation of pile at a given radial distance is directly proportional to surcharge pressure.

From the above observations it can be stated that, the radial stress (σ_r) at a point along the pile surface is a function of

(h/Ro) and the overburden pressure.

6.3 Results of Monotonic Tension Tests

6.3.1 Load-displacement Behaviour

Tension loads in small increments of 0.1 kN were applied on the model piles and the pile head displacements were recorded. The results of these tests carried out on 12.7 mm, 25.4mm and 38.1 mm diameter piles are presented in Figs. 6.7(a), (b) and (c) respectively. It may be noted from these results that the displacement before failure is very small (only about 1 to 2 mm) and the failure occurs suddenly with large displacements.

6.3.2 Ultimate Tensile Capacity of Pile

Since the pile failed suddenly, with a large displacement, the ultimate tensile capacity of pile was obtained as the load corresponding to a sudden increase in the displacement of the pile. The ultimate tensile capacity and the average shear stress at failure obtained are presented for steel and aluminium alloy piles in Tables 6.3 and 6.4 respectively. These results show that:

(i) The ultimate capacity obtained from repeated tests are close to each other indicating the repeatability of test results (Table. 6.4).

(ii) The ultimate capacity and shear stress on the pile surface at failure increase with surcharge pressure (Table 6.3).

(iii) Shear stress at failure varies with change in pile diameter. However, no definite relationship is observed between the shear stress at failure and the pile diameter.

6.3.3 Load and Shear Stress Distribution Along the Pile

A monotonic tension test on the instrumented pile was carried out and load measurements along the pile were made. Three load cell segments (LSG1, LSG2 and LSG3) located in the embedded portion of the pile provided observations of load variation along the length of the pile. A load cell at the pile head provided observations of applied load. These observations of load and displacement are presented in Fig. 6.8. The distribution of load along the length of the pile at several values of displacement is presented in Fig.6.9.

It may be noted from Figs. 6.8 and 6.9 that, initially the entire length of the pile is subjected to a compressive load. This is because of the settlement of the sand surface due to the application of the surcharge pressure which results in a negative skin friction along the length of the pile as shown in Fig. 6.10. As the tensile load was applied on the pile head, the pile moves up relative to the soil. This was resisted by negative skin friction of the soil resulting in gradual reduction in tensile load from top to tip of the pile as shown in Fig. 6.9.

In Fig. 6.9 the difference in load between LSG1 and LSG2 provides the load transferred through shearing resistance in the upper portion of the pile. Likewise, the difference in load between LSG2 and LSG3 provides the load transferred through shearing resistance in the lower portion of the pile. The average shear stress mobilised in these portions of the pile are calculated using the above observations (Fig.6.9) and is shown in Fig.6.11.

The results presented in Fig.6.11 show that, the average shear stress in the lower portion of the pile is more than that observed in the upper part of the pile. This is possibly due to increase in radial stress (σ_r) on the pile surface as one moves

towards the tip of the pile (Lehane et.al., 1993).

It is also noted from Fig. 6.8 that:

(i) The reduction in load observed between the load cell and the load cell segment LSG1, is more than the shear load that can be expected to be transferred between the sand surface and the location of LSG1. This suggests that there is some friction between the pile and the pile access unit.

(ii) The load cell segment LSG3 has recorded a load value which can not be fully attributed to the possible shear load between LSG3 and the tip of the pile. Though the exact reason could not be identified, it is possibly due to certain effects around the pile tip associated with the application of the surcharge pressure.

The above observations however, do not invalidate, the pattern of load-displacement shown in Fig. 6.8 or the load and shear stress distributions shown in Figs. 6.9 and 6.11 respectively.

6.4 Results of cyclic load Tests

A number of cyclic load tests were carried out under different cyclic load levels varying from 7% to 75% of the ultimate tensile capacity of the pile. The pile head displacement was observed as a function of the number of load cycles. Tests on an instrumented pile provided data on load distribution along the length of the pile. Pressure cells embedded in the test bed provided data on the radial stresses in the test bed. These results are presented and analysed to examine a number of aspects of pile behaviour under cyclic loading.

6.4.1 Displacement of Pile Under Cyclic Loading

During cyclic load tests, the load and the pile head displacements were recorded with the number of cycles. Observations made in a typical test are shown in Fig.6.12. From Fig.6.12 it can be observed that the pile underwent recoverable and irrecoverable displacements. Under a given cyclic load the recoverable displacement was constant and the irrecoverable displacement increased with the number of cycles.

In a small number of cyclic load tests, the load was varied after every few hundred cycles, and the pile head displacement was recorded. The cyclic load and the corresponding recoverable displacement observed during two such tests are shown in Table 6.5 and the same are plotted in Fig. 6.13. It can be seen from these observations that the recoverable displacement increases with increase in cyclic load level.

Under a given cyclic load, the irrecoverable displacement increases with the number of cycles. The plots of total displacement versus number of cycles obtained from different cyclic load tests are shown in Figs. 6.14, 6.15 and 6.16. From these figures it is observed that failure of pile occurs at cyclic load levels above 45% q_{ta} (q_{ta} = average tensile capacity, Table 6.4). Similar results are reported by Chan and Hanna(1980), Al-Jumaily(1981), Puech(1982), Karlsrud *et.al.*, (1986) and Abood(1989).

The results shown in Figs.6.14 to 6.16 suggest that, the relationship between the number of cycles and pile head displacement can be characterised to consist of three zones as shown in Fig.6.17(a). Initially, for a few cycles, the displacement increases rapidly and then becomes almost constant (zone-I). There then follows a stable zone (zone-II) where there is insignificant increase in displacement with number of cycles.

Beyond this, the pile head displacement increases at a faster rate until failure. This zone of large displacement may be termed as the unstable zone (zone-III).

The number of cycles in the stable zone depends on the magnitude of cyclic load. As the magnitude of the cyclic load increases, the width of the stable zone shrinks and becomes less well defined at high load levels (Fig.6.17(b)). For example, from Fig.6.16 it can be observed that, for 38.1 mm diameter pile under a cyclic load of $q_c=15\% q_{ta}$, the stable zone extends beyond 100,000 cycles. For the same pile, with $q_c=45\% q_{ta}$, the stable zone was observed only upto 60,000 cycles. At $q_c = 60\% q_{ta}$, no well defined stable zone was observed and the pile failed at about 30,000 cycles.

The reasons for the above displacement trend (Fig.6.17) can be explained as follows. Initially, the pile undergoes a large displacement in order to mobilise skin-friction (zone-I). As the skin friction increases, the rate of displacement decreases (zone-II). With further increase in number of cycles, permanent changes take place in the sand properties (Sections 6.4.3 and 6.4.4) leading to reduction in skin resistance and pile failure (zone-III).

6.4.2 Load and Shear Stress Distribution Along the Pile

During cyclic load tests on an instrumented pile, the pile head displacement and the loads along the pile were recorded. The results obtained from the tests are shown in Fig.6.18. The pile head displacement versus number of cycles is shown in Fig.6.18(a). Figs.6.18(b) and (c) show the load recorded, by the load cell (LC) mounted on the pile cap and the load cell segments (LSG1, LSG2 and LSG3) in the pile, during load-off (no-load) and load-on (maximum load) conditions respectively.

From Fig. 6.18 the following observations can be made:

1) Initially the entire length of the pile experiences compression, which is due to the application of the surcharge pressure as explained in Section 6.3.3.

2) Under load-off condition, there was a certain amount of tensile load near the pile tip (LSG3). Similar observations have also been reported by Jardine (1991) and Chan and Hanna (1980) (Fig. 2.9). This could be due to the soil resistance against the elastic recovery of the pile. This soil resistance is particularly more in magnitude, due to relatively large radial stress, near the pile tip.

3) Just before failure of the pile, the load near the pile tip (LSG3) was reducing with increase in number of cycles. This indicates that the shearing resistance in the lower portion of the pile reduces resulting in the redistribution of load to the upper portion of the pile bringing the pile to failure.

The distribution of load along the length of the pile at a few typical ($N=5, 100$ and 120) number of cycles, during load-off and load-on conditions, is presented in Figs.6.19 and 6.20 respectively. In order to compare the load distribution during load-off and load-on conditions, the results corresponding to $N=100$ have been reported in Fig.6.21. It can be seen from Fig.6.21 that, during load-off condition the tensile force reduces from the pile tip to the pile head. This is due to a positive shear stress (resistance against elastic recovery of pile) acting along the length of the pile as shown in Fig.6.21(b). In the case of load on condition the tensile force reduces with depth due to a negative frictional resistance as shown in Fig. 6.21(b). It may be noted from Fig. 6.21(b) that, the direction of the shear resistance along the length of the pile was changing from load-off to load-on condition.

The difference in load between LSG1 and LSG2 provides the load transferred through shear resistance in the upper portion of the pile. Similarly, the difference in load between LSG2 and LSG3 provides the load transferred in the lower portion of the pile. The average shear stress mobilised in these portions of the pile, during load-off and load-on conditions, at 100th cycle, are calculated (from Fig.6.21) and shown in Fig.6.22.

From Fig.6.22, it can be observed that:

(i) The average shear stress in the lower portion of the pile is more than that observed in the upper portion of the pile. This is similar to that observed under monotonic loading of the pile.

(ii) Under the load-off condition, the shear stress along the pile is positive (dotted line) and under load-on condition, it becomes negative (continuous line) (for sign convention see Figs. 6.1 and 6.21). This means, even under one-way cyclic loading, the soil around the pile experiences two-way shear. Similar observations are reported by Jardine(1991) who analysed the results of cyclic tension tests on a 5m long instrumented pile, carried out by Karlsrud and Haugen(1983). It has been reported (St. John *et al.*, 1983; Poulos, 1988; Chan, 1990; and Jardine, 1991) that, two-way shear brings the shearing resistance along a shear surface down to its lowest residual value more quickly than one-way shear.

6.4.3 Deformation of the Sand Surface During Cyclic Loading of Pile

During a cyclic load test, the settlement of the sand surface was measured. This was achieved by monitoring the settlement of aluminium tips mounted on the polythene sheet, covering the sand surface (Fig.6.23), at different radial distances. The observed

settlement of the sand surface is shown in Table 6.6 and Fig.6.24. From Fig.6.24 it can be observed that, with an increase in the number of cycles, the sand around the pile undergoes settlement (compaction). This is due to the fact that when a pile is subjected to cyclic loading, the sand around the pile undergoes repeated two-way shear (Fig.6.22) which results in compaction of the sand (Youd, 1972 and Airey et. al., 1991). This compaction was a maximum near to the pile and reduced as one moved away from the pile. This is due to the fact that the shear stress is a maximum near the pile surface and reduces as one moves away from the pile.

6.4.4 Variation of Radial Stress in Sand During Cyclic Loading of Piles

During a cyclic load test, the radial stress was measured by placing a pressure cell in the sand bed at a depth of 150mm below the sand surface and at a radial distance of 100mm from the centre of the pile. The variation of radial stress observed as a function of the number of cycles during a test on the 38.1mm diameter pile is shown in Fig.6.25. From Fig.6.25 it can be seen that, the radial stress in sand and hence on the pile surface reduces as the number of cycles increases. A similar observation is also made by Puech (1982) in cyclic load tests on a 13m long and 273mm diameter prototype pile embedded in silts and loose sands. He attributed the reduction in radial stress to a possible compaction of soil around the pile. No measurement, however, was made on the compaction of the soil.

6.4.5 Mechanism of Pile Failure

The results presented in Sections 6.4.2, 6.4.3 and 6.4.4 suggest that the sequence of events leading to pile failure is as follows:]

The application of cyclic loading causes two-way shear along the pile surface (Section. 6.4.2) leading to compaction of the sand around the pile (Section 6.4.3). This compaction of sand results in the reduction in the radial stress (6.4.4) on the pile surface causing a reduction in the shearing resistance leading to failure of the pile.

6.4.6 Relationship Between Cyclic Load Level and Number of Cycles to Failure

The cyclic load tests were conducted under different cyclic load levels varying from 7% to 75% of ultimate tensile capacity of the pile (q_{ta}). The results of these tests are shown in Table 6.7. and plotted in Fig.6.26. The results obtained during the present investigation on 25.4mm diameter pile are compared with the results reported by Chan and Hanna (1980) and Abood (1989), in Fig.6.27. It can be observed from Fig.6.27 that, during the results obtained during the three investigations are following a similar trend.

From Table 6.7 and Fig.6.26 it can be observed that:

(i) For a pile of given diameter, the number of cycles to failure decreases with an increase in cyclic load level.

(ii) Under a given cyclic load level, the number of cycles to failure increases with an increase in pile diameter. For example, under a cyclic load level of 60% of q_{ta} , the number of cycles to failure was 372 for the 12.7 mm dia. pile, 658 for the 25.4 mm dia. pile and 12,550 for the 38.1 mm dia. pile.

The effect of pile diameter on the number of cycles to failure was further examined by making a plot of pile diameter versus number of cycles to failure (Fig. 6.28) under a cyclic load of $q_c=60\% q_{ta}$. The results show that the curve becomes almost

asymptotic to a vertical line. In order to confirm this observation an attempt was made to perform cyclic load tests on a 76.2 mm diameter pile.

6.4.6.1 Tests on a Pile of a Large Diameter (76.2mm)

In order to confirm the effect of pile diameter on the number of cycles to failure (Fig.6.28), an attempt was made to perform cyclic load tests on a pile of diameter 76.2mm. The pile was installed using a non-displacement technique in order to minimise the installation stresses. For this purpose, the pile was provided with a hole drilled centrally through the pile head and tip (Fig.3.6(b)) in order to pass a vacuum tube (taken from a vacuum cleaner) to the tip. The pile was positioned on the sand bed through the pile access unit and the sand was sucked by application of vacuum pressure through the pile. Simultaneously, the pile was pushed into the sand bed using a jack. The process of suction of sand and pushing of the pile into the sand bed was carried out in stages. After installation of the pile, the vacuum tube was withdrawn from the pile and the hole at the tip was plugged (Fig.3.6(b)).

Two trials of monotonic test were conducted on this pile which gave values of ultimate tensile capacity which differed significantly (Table 6.8). It was realised that this large difference was due to the fact that a controlled process of sand suction and pile installation was not achieved with the available equipment. As consistent results could not be observed in the monotonic test, the planned cyclic load tests on this large diameter pile were abandoned.

In view of the above, the available data on the effect of pile diameter was limited to those observed on piles of 12.7mm, 25.4 mm and 38.1mm diameter. Further, there is no data reported in the literature on the effect of pile diameter on the number of

cycles to failure. Hence, with this limited data from a narrow range of pile diameters, it is not feasible to obtain a meaningful extrapolation for large (1 to 2m) diameter field piles. More cyclic load test data obtained from a large range of pile diameters would help increase the understanding on the effect of pile diameter on cyclic load response of piles which may lead to a meaningful extrapolation of the response of prototype piles.

6.4.7 Safe Cyclic Load

It can be noted from the results presented in Table 6.7 that, failure has not occurred when the cyclic load was limited to 30% qta. The safe cyclic load could also depend upon the number of cycles applied. As the number of cycles applied was limited to 100,000, in the present investigation it can be stated that a cyclic load level of 30% qta is safe for a cyclic loading of the order of 100,000 cycles for piles of 12.7mm or greater diameters.

6.4.8 Effect of Cyclic Loading on Pile Capacity

In cases where a pile remained stable up to 100,000 cycles, the pile was then subjected to a monotonic tension test. The tensile capacity of piles thus obtained are presented, as a percentage of ultimate tensile capacity (qta) of the respective piles, in Table 6.9. From Table 6.9 it can be observed that, due to cyclic loading, the pile capacity reduced, but only marginally, in most cases. Two of the seven observations, however, showed values of pile capacity more than the ultimate tensile capacity (qta).

From the above limited data, it can be stated that as long as the pile remains in the stable zone (zone-II, Fig.6.17) under cyclic loading, the tension capacity of the pile is likely to be reduced, but only marginally. This may be due to the fact that though the cyclic loading reduces the radial stress, it leads to

densification of sand (Fig.6.24). Consequently, when a monotonic test on the pile is performed, large displacements cause dilation in this compacted sand thereby restoring its capacity.

6.4.9 Response of a Pile Subsequent to Peak Loading

Three tests were carried out to study the response of the pile subsequent to peak loading. The loading sequence and observations made in each of these tests are discussed below.

Test: 38.1-V-A: The pile was subjected to a cyclic loading of 90% qta until it reached a failure state. Subsequently, the load was reduced to 45% qta and the test continued (Fig.6.29). Under this load, the pile failed at 20,000 cycles. It was observed in earlier tests (38.1-45-A and 38.1-45-B) that, the same pile under a cyclic load of 45% qta remained stable at 100,000 cycles. Therefore, there was a deterioration in the pile behaviour subsequent to the type of peak loading applied in this case.

Test: 38.1* -V-B: The test was carried out under varying cyclic load levels. The observations of load and displacement are shown in Fig.6.30. The cyclic load level was increased in steps of 15% qta and at each load level, the pile was subjected to about 600 cycles. The failure of the pile was noticed at a load level of 60% qta. The load was then brought down to 15% qta and the test repeated. During this sequence of loading the pile failed at 45% qta. Thus, a definite deterioration in the pile performance was noticed subsequent to peak loading.

Test: 38.1-38-A: In a test under a constant cyclic load, the pile was subjected to a peak loading inadvertently due to a freak behaviour of the apparatus. The peak loading was about 75% qta and this got applied for a few cycles and subsequently the load was reduced to the intended constant load of 38% qta and the test

continued. The observations of the load and displacement are shown in Fig.6.31.

The pile continued to remain stable (zone-II, Fig.6.17) even after 100,000 cycles as can be seen from Fig.6.31. This result shows that the peak loading applied for a few cycles does not impair the performance of the pile on subsequent cyclic loading. It can be seen from the Fig.6.31 that subsequent to peak loading, there is no increase in displacement as the pile gets subjected to a further 70,000 cycles under 38% q_{ta}. Furthermore, it can be noted from Table 6.9 that the tensile capacity of pile obtained through a monotonic tension test carried after 100,000 cycles, has not been significantly affected. This shows that the performance of the pile has not been impaired due to a few cycles of peak loading.

From the above three tests it appears that, if the pile reaches a failure state under the peak load, the subsequent performance of the pile under a safe cyclic load may be adversely affected. However, if the peak loading is applied only for a few cycles and the pile has not reached a state of failure under this peak loading, the subsequent performance under safe cyclic load level appears to be not adversely affected.

6.5 Soil-Pile-Slip Test Results

The soil-pile-slip test apparatus was developed to obtain T-Z curves for a pile element embedded in sand. Tests were conducted in a large triaxial cell (Section 5.4), on a 25.4 mm diameter aluminium alloy pile element, embedded in Leighton Buzzard sand, at a cell pressure of 70 kPa, 120 kPa and 170kPa. The load and the relative displacement between the sand and the pile element, observed during these tests are shown in Fig.6.32. From Fig.6.32, it can be observed that, there was no relative displacement until the applied load reached the ultimate pile capacity and the pile

element failed suddenly with a large relative displacement.

The possible reasons for the above observation can be stated as follows:

Since there is no restraining surface (for the vertical movements) on the outer face of the soil sample and the sample being small, the stress transfer possibly taking place near the base of the pile element as shown in Fig. 6.33. At the ultimate resistance possibly the pile might have mobilised full friction and moved out of the sample resulting in a sudden relative displacement.

Thus, the soil-pile-slip test could not provide the intended T-Z curves. However, the tests provided the ultimate tensile capacity of the pile element under different confining pressures which are shown in Table 6.10. The results presented in Table 6.10 are examined further by comparing the observed shearing resistance on the pile surface, with the estimated values. The shear stress at failure (τ_f) on a pile element, in a dry sand, can be estimated as follows (after Lehane, 1992):

$$\tau_f = SL \sigma_{rc} \tan \delta \quad (6.1)$$

where

τ_f = shear stress at failure

SL = $\sigma_{rf} / \sigma_{rc}$

σ_{rf} = radial stress on pile surface at failure

σ_{rc} = initial radial stress on pile surface
(cell pressure in the present case)

δ = friction angle for soil-pile interface
(23.6 from Table 4.4)

By assuming $SL = 1$ and $\delta = 23.6^\circ$ (obtained from the direct shear interface test), the values of τ_f are obtained using Eq. (6.1) and these values are shown in Table 6.11. From Table 6.11 it can be

observed that the measured values are consistently more than the estimated values. The possible reason for this could be due to the value of S_L being more than 1. Therefore, the value of S_L is back calculated from the shearing resistance of the pile element for values of $\delta=23.6^\circ$ and $\delta=25.3^\circ$ (average and maximum respectively, of test values for smooth aluminium pile; Table 4.4). The values of S_L so obtained are shown in Table 6.12. From the values presented in Table 6.12 it can be seen that the value of S_L is more than unity indicating σ_{rf} is more than σ_{rc} . Wersching (1987) and Lehane (1992) have also reported that the radial stress at failure (σ_{rf}) along the pile surface can be higher than the initial radial stress (σ_{rc}) due to the phenomena of interface slip dilation. The results of the present investigation confirms this phenomena of increase in σ_{rf} due to interface slip dilation.

6.6 Concluding Remarks

The results of the investigation presented in this chapter, confirmed some of the earlier observations reported in the literature in addition to throwing light on some other aspects of pile behaviour under cyclic loading which are presented below.

(1) Under cyclic loading, the pile undergoes recoverable and irrecoverable displacement. With increase in the number of cycles, the recoverable displacement remains constant and irrecoverable displacement increases.

(2) The displacement curve, for a pile under cyclic loading, exhibits three distinct zones. Initially, for a few cycles, the displacement increases rapidly and then becomes almost constant (zone-I). A stable zone (zone-II) follows where there is insignificant increase in displacement with increase in the number of cycles. Beyond this, the pile head displacement increases at a faster rate until failure. This zone of large displacement is

termed the unstable zone (zone-III).

(3) The safe cyclic load level, in tests carried out upto a maximum of 100,000 cycles, is observed to be 30% of ultimate tensile capacity of the piles.

(4) Even under one-way (tensile) cyclic loading, the soil around the pile undergoes two-way shear.

(5) The failure of a pile under cyclic loading is due to the reduction in normal stress on the pile surface and the consequent reduction in shearing resistance.

(6) The reduction in the normal stress on the pile surface due to cyclic loading is accompanied by the compaction of the sand around the pile. This was also observed by Puech (1982).

(7) The cyclic load response of a pile subsequent to a peak cyclic loading does not get adversely affected as long as the displacement of the pile is within the stable zone of the displacement curve. However, if the pile reaches a state of failure under the peak cyclic loading its response to a subsequent reduced cyclic load level deteriorates substantially.

(8) Under a given cyclic load level q_c (expressed as a percentage of ultimate tensile capacity of the pile), the number of cycles to failure was observed to increase with pile diameter. This observation however is made on a limited number of tests on model piles having diameters of 12.7mm, 25.4mm and 38.1mm and needs further investigation.

(9) The results of the soil-pile-slip test indicate the phenomenon of interface slip dilation occurring along the pile surface leading to an increase in radial stress under the application of monotonic tensile loads. This was also reported by Wersching (1987), Jardine *et al.* (1992), Lehane (1992) and Lehane

et.al. (1993).

(10) Based on the results of the present investigation and those reported in the literature, it can be stated that under monotonic tensile loading, the sand around the pile undergoes slip dilation resulting in an increase in radial stress on the pile surface whereas under cyclic tensile loading, the sand around the pile undergoes compaction accompanied by a reduction in radial stress on the pile surface.

**Table 6.1 Tests for Pressure Distribution During
Installation of Pile**

Pile diameter (mm)	Surcharge pressure, p (kPa)
25.4	0 20 40
38.1	0 20 45

Table 6.2 Variation of $\sigma_r(\max)$ and $\sigma_r(\max)/p$ at different radial distances during the installation of the pile

Pile Diameter (mm)	Surcharge Pressure p (kPa)	$\sigma_r(\max)$ in kPa and $\sigma_r(\max)/p$ at radial distance, r							
		r = 100 mm		r = 200 mm		r = 300 mm		r = 400 mm	
		$\sigma_r(\max)$	$\sigma_r(\max)/p$	$\sigma_r(\max)$	$\sigma_r(\max)/p$	$\sigma_r(\max)$	$\sigma_r(\max)/p$	$\sigma_r(\max)$	$\sigma_r(\max)/p$
25.4	20	33.70	1.69	10.50	0.53	3.10	0.16	1.60	0.08
	40	55.50	1.39	21.20	0.53	6.60	0.17	6.50	0.16
38.1	20	83.30	4.17	9.80	0.49	3.50	0.18	2.70	0.14
	45	150.00	3.33	22.90	0.51	10.40	0.23	6.00	0.13

**Table 6.3 The Ultimate Tensile Capacity of Steel Model Piles
(Preliminary Experiments)**

Pile Diameter (mm)	Surcharge pressure (kPa)	Ultimate Capacity (q_t) (kN)	Average Shear Stress at Failure (τ_f) (kPa)
25.4	55	0.736	23.06
38.1	Zero	0.218	4.55
	20	0.345	7.21
	35	0.818	17.09
	45	0.836	17.46

**Table 6.4 Ultimate Tensile Capacity of Aluminium Alloy Model Piles
(Surcharge Pressure = 70 kPa)**

Pile Diameter (mm)	Test Identity	Pile Capacity q_t (kN)	Average q_t (q_{ta}) (kN)	Average Shear Stress at Failure τ_f (kPa)
12.7	12.7-100-A	0.742	0.740	46.368
	12.7-100-B	0.738		
25.4	25.4-100-A	2.149	2.122	66.482
	25.4-100-B	2.135		
	25.4-100-C	2.081		
38.1	38.1-100-A	2.650	2.720	56.811
	38.1-100-B	2.760		
	38.1-100-C	2.750		

Table 6.5 Recoverable Displacement Observed During Tests with Varying Cyclic Load

Pile Diameter	Test Identity	q_c (% q_{ta})	Recoverable Displacement (mm)
38.1	38.1 ^x -V-A	15	0.0170
		30	0.0575
		45	0.0893
		60	0.1330
	38.1 ^x -V-B	15	0.0194
		30	0.0531
		45	0.0918
		60	0.1320

Table 6.6 Displacement of the Sand Surface During Cyclic Tension Test
(38.1 mm Diameter pile at $q_c = 60\% q_{ta}$)

No. of Cycles	Total upward displacement of the pile head (mm)	Downward displacement of the sand surface (mm) at a radial distance r (mm) from the pile surface			
		$r = 55$	$r = 130$	$r = 180$	$r = 280$
0	0.000	0.000	0.000	0.000	0.000
120	0.483	0.100	0.040	0.012	0.006
840	1.362	0.236	0.132	0.116	0.054
2280	4.480	0.380	0.256	0.186	0.096
3000	8.532	0.464	0.336	0.242	0.110
Failure	320.000	2.966	1.332	1.104	0.440

Table 6.7 Number of Cycles to Failure with Cyclic Load Level

Pile Dia. (mm)	Test Identity	Cyclic Load q_c (% q_{tc})	No. of Cycles to Failure N_f	Average Value of N_f
12.7	12.7-30-A	30	Not Failed	---
	12.7-45-A	45	1680	1680
	12.7-60-A	60	480	372
	12.7-60-B	60	390	
	12.7-60-C	60	245	
12.7-70-A	70	170	170	
25.4	25.4-30-A	30	Not Failed	---
	25.4-45-A	45	47900	47900
	25.4-60-A	60	450	658
	25.4-60-B	60	1160	
	25.4-60-C	60	364	
	25.4-75-A	75	140	145
25.4-75-B	75	150		

continued...

Table 6.7 continued

Pile Dia. (mm)	Test Identity	Cyclic Load q_c (% $q_{t\alpha}$)	No. of Cycles to Failure N_f	Average Value of N_f
38.1	38.1-07-A	07	Not Failed	---
	38.1-15-A	15	Not Failed	---
	38.1-38-A	38	Not Failed	---
	38.1-45-A	45	Not Failed	---
	38.1-45-B	45	Not Failed	---
	38.1-60-A	60	29600	12550
	38.1-60-B	60	7000	
	38.1-60-C	60	8600	
	38.1-60-D	60	5000	
	38.1-75-A	75	900	743
	38.1-75-B	75	1270	
	38.1-75-C	75	60	
^x 38.1-60-A	60	18600	18600	
^x 38.1-75-A	75	130	130	

Table 6.8 Ultimate Tensile Capacity of
76.2 mm Diameter Pile

Test Identity	Pile Capacity q_t (kN)
76.2-100-A	3.264
76.2-100-B	6.528

Table 6.9 The Pile Capacity After Cyclic Loading

Diameter of pile (mm)	Cyclic load (% q_{ta})	Ultimate tensile capacity q_{ta} (kN)	Monotonic test identity	Pile capacity after cyclic loading as (% q_{ta})
12.7	30	0.740	12.7-100-30A	94.92
25.4	30	2.122	25.4-100-30A	152.22
38.1	7	2.720	38.1-100-07A	89.50
	15		38.1-100-15A	79.56
	38		38.1-100-38A	95.72
	45		38.1-100-45A	106.91
	45		38.1-100-45B	91.50

Table 6.10 Soil-Pile-Slip Test Results

Confining Pressure σ_c (kPa)	Ultimate Tensile Capacity q_t (kN)	Shear Stress at Failure τ_f (kPa)
70	0.405	33.84
120	0.756	63.16
170	0.998	83.38

Table 6.11 Comparison of Observed and Estimated τ_f Values

($SL = 1.0$; $\delta = 23.6^\circ$)

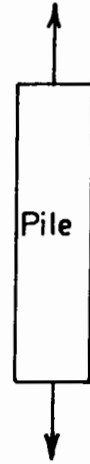
Confining Pressure σ_c (kPa)	τ_f Observed (kPa)	τ_f Estimated (kPa)
70	33.84	30.58
120	63.16	52.43
170	83.38	74.27

Table 6.12 Back Calculated Values of SL

Confining Pressure σ_{rc} (kPa)	τ_f Observed (kPa)	SL Value (for $\delta=23.6^\circ$)	SL Value ($\delta=25.3^\circ$)
70	33.84	1.14	1.05
120	63.16	1.21	1.12
170	83.38	1.16	1.07



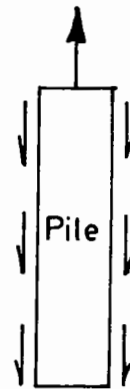
(a) Compression
+ve Load



(b) Tension
-ve Load



(c) +ve Shear



(d) -ve Shear

FIG. 6.1. SIGN CONVENTIONS FOR LOAD AND SHEAR STRESS

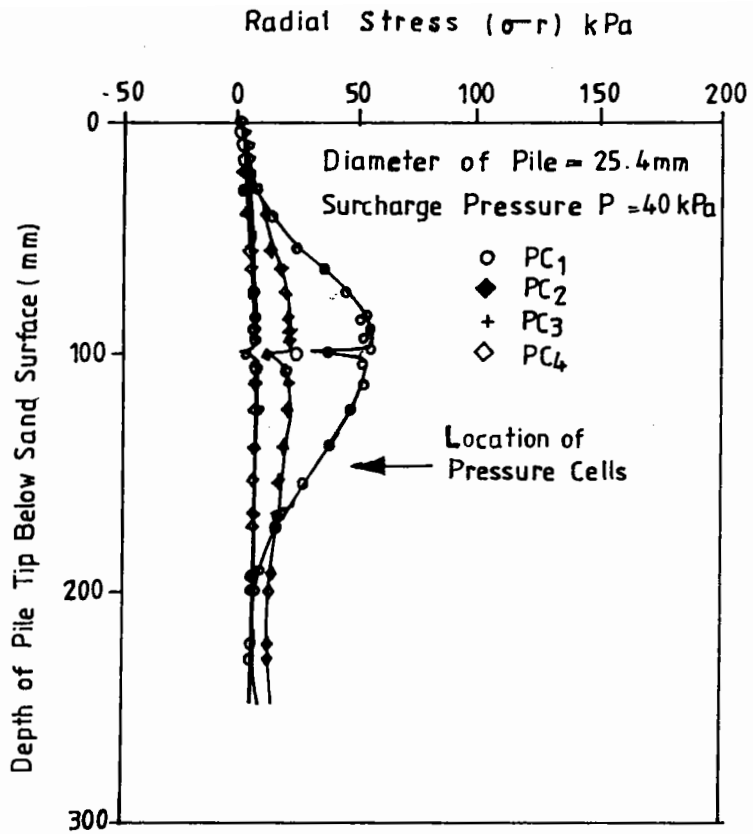


FIG. 6.2. VARIATION OF RADIAL STRESS WITH DEPTH OF PILE PENETRATION (25.4 mm dia)

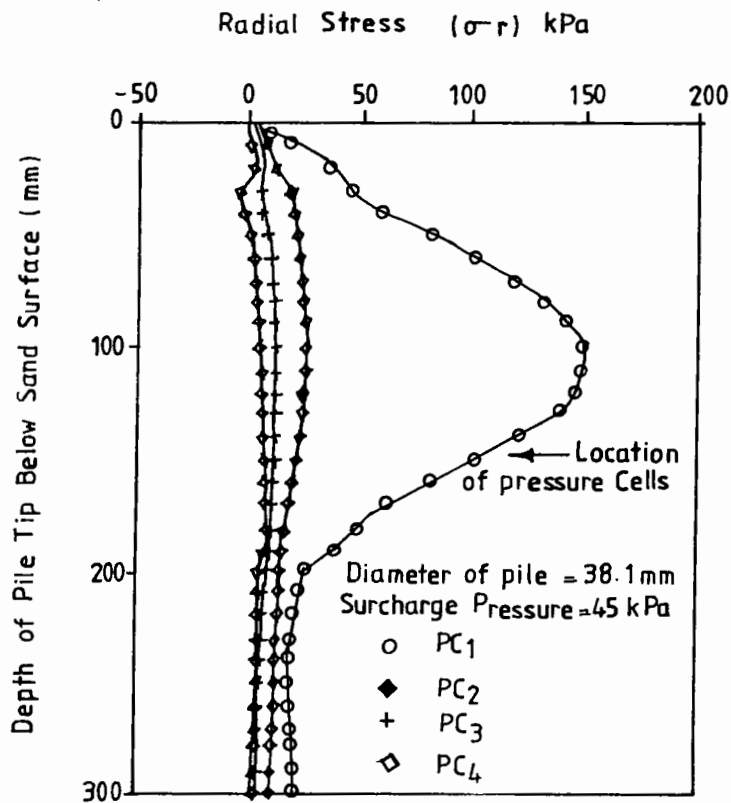


FIG. 6.3. VARIATION OF RADIAL STRESS WITH DEPTH OF PILE PENETRATION (38.1 mm dia)

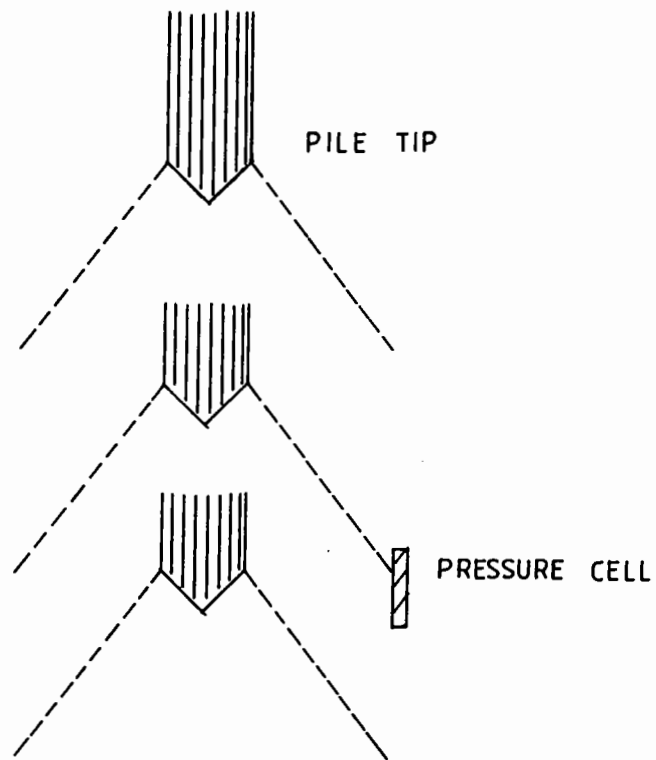


FIG. 6.4 · STRESS DISTRIBUTION
DURING THE PILE INSTALLATION
(AN ILLUSTRATION)

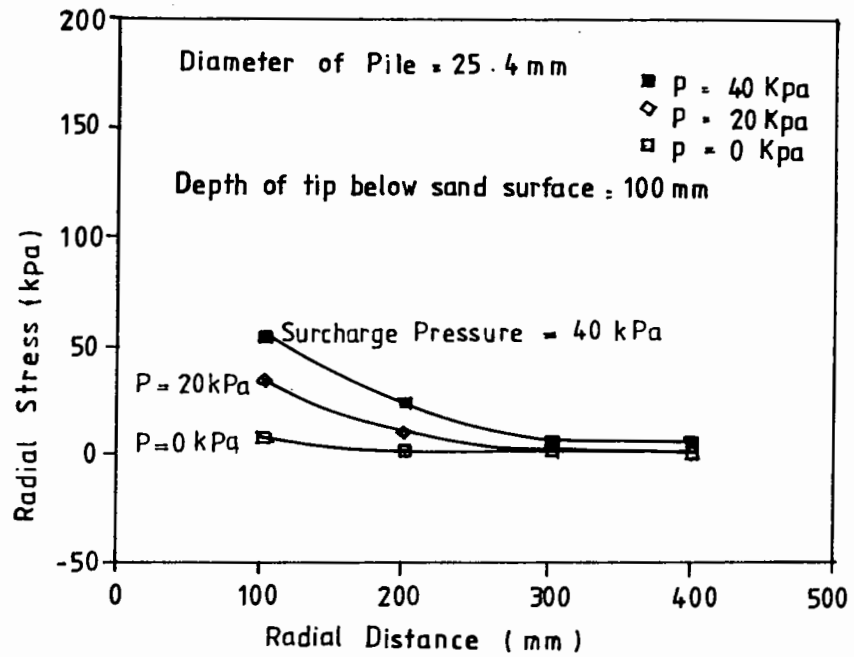


FIG. 6.5. STRESS VARIATION WITH RADIAL DISTANCE DURING THE PILE INSTALLATION (25.4 mm dia)

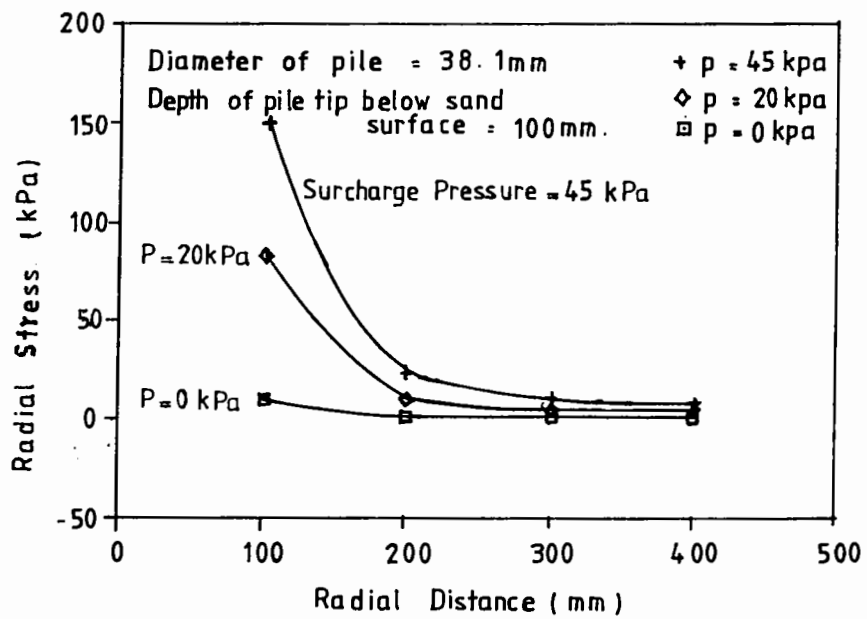
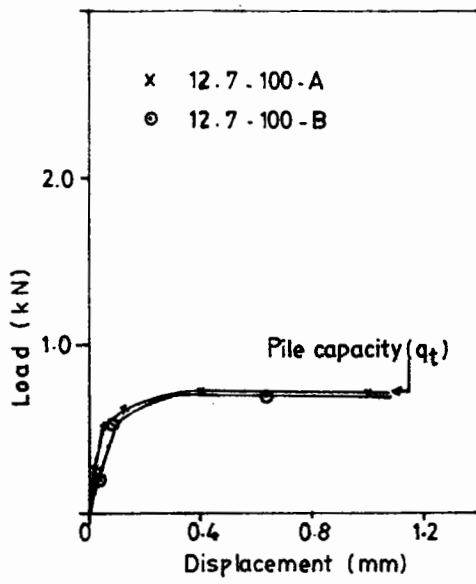
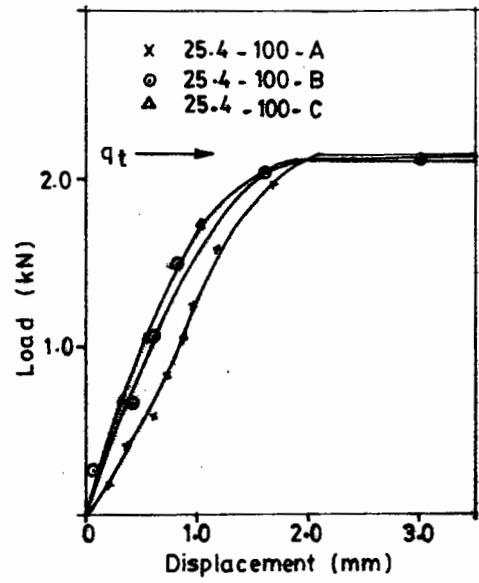


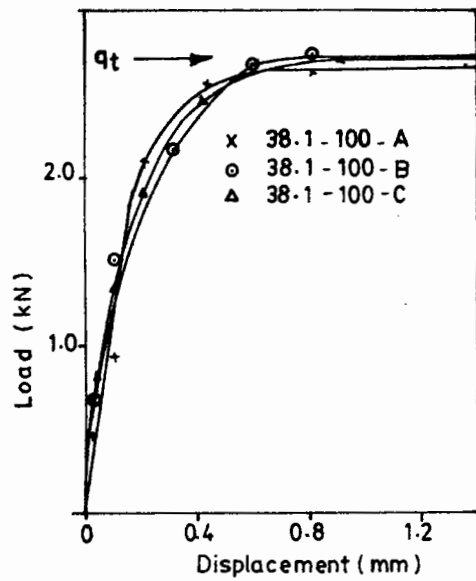
FIG. 6.6. STRESS VARIATION WITH RADIAL DISTANCE DURING THE PILE INSTALLATION (38.1 mm dia)



(a) 12.7 mm DIAMETER PILE



(b) 25.4 mm DIAMETER PILE



(b) 38.1 mm DIAMETER PILE

FIG.6.7. MONOTONIC TENSILE LOAD TEST RESULTS

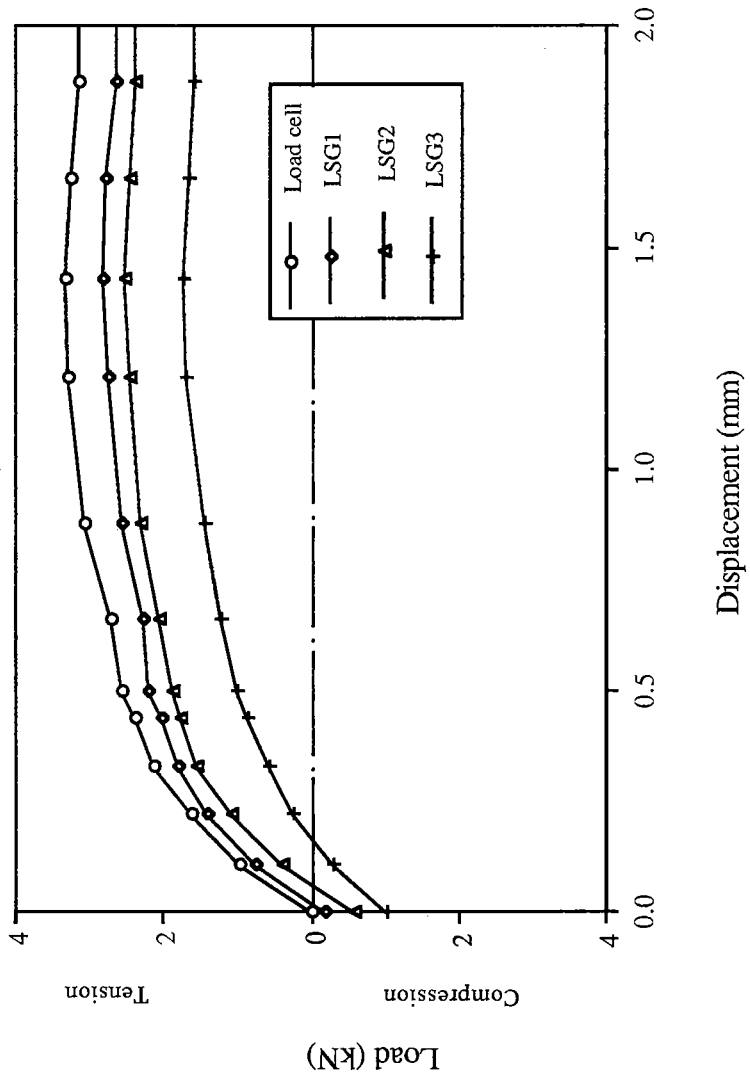


Fig.6.8. Loads Along the Instrumented Pile During a Monotonic Tension Test

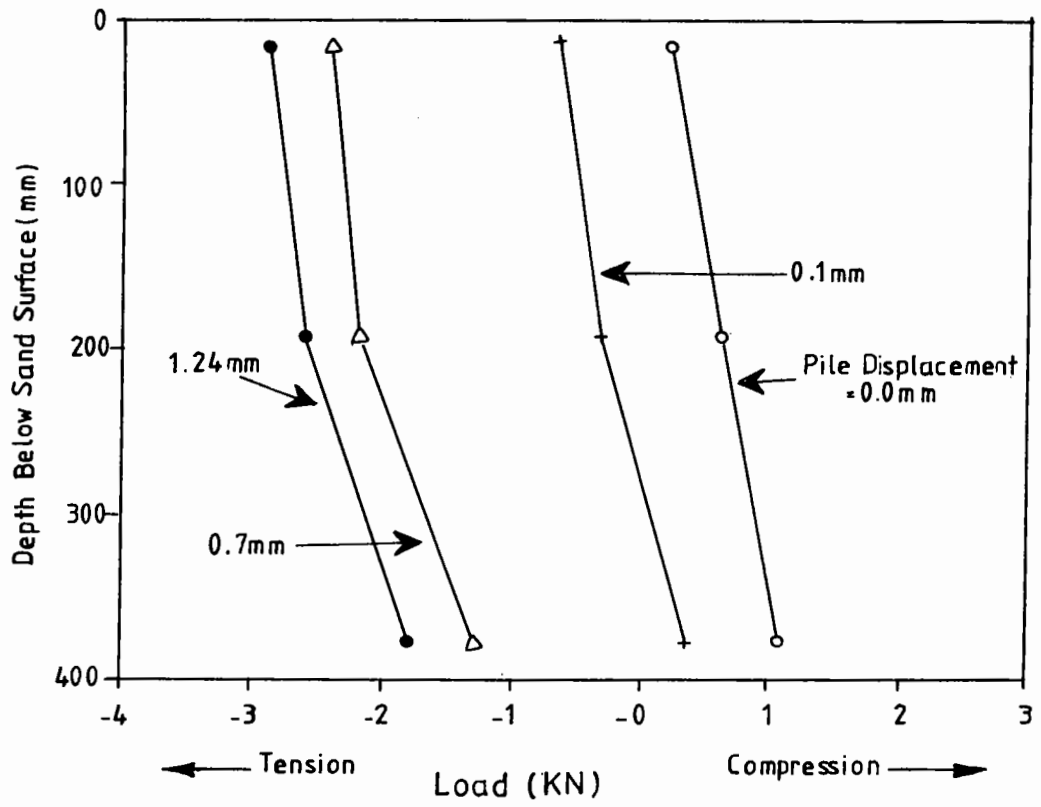


Fig.6.9. Load Distribution During Monotonic Tension Test
(38.1*100 - B)

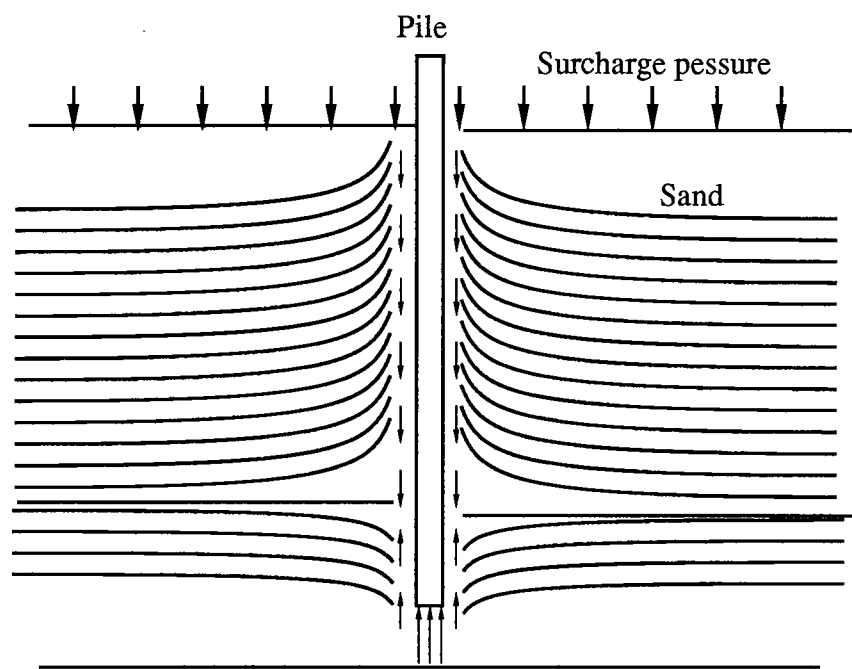


Fig. 6.10. Simple Representation of the Settlement of the Sand Due to a Surcharge Pressure

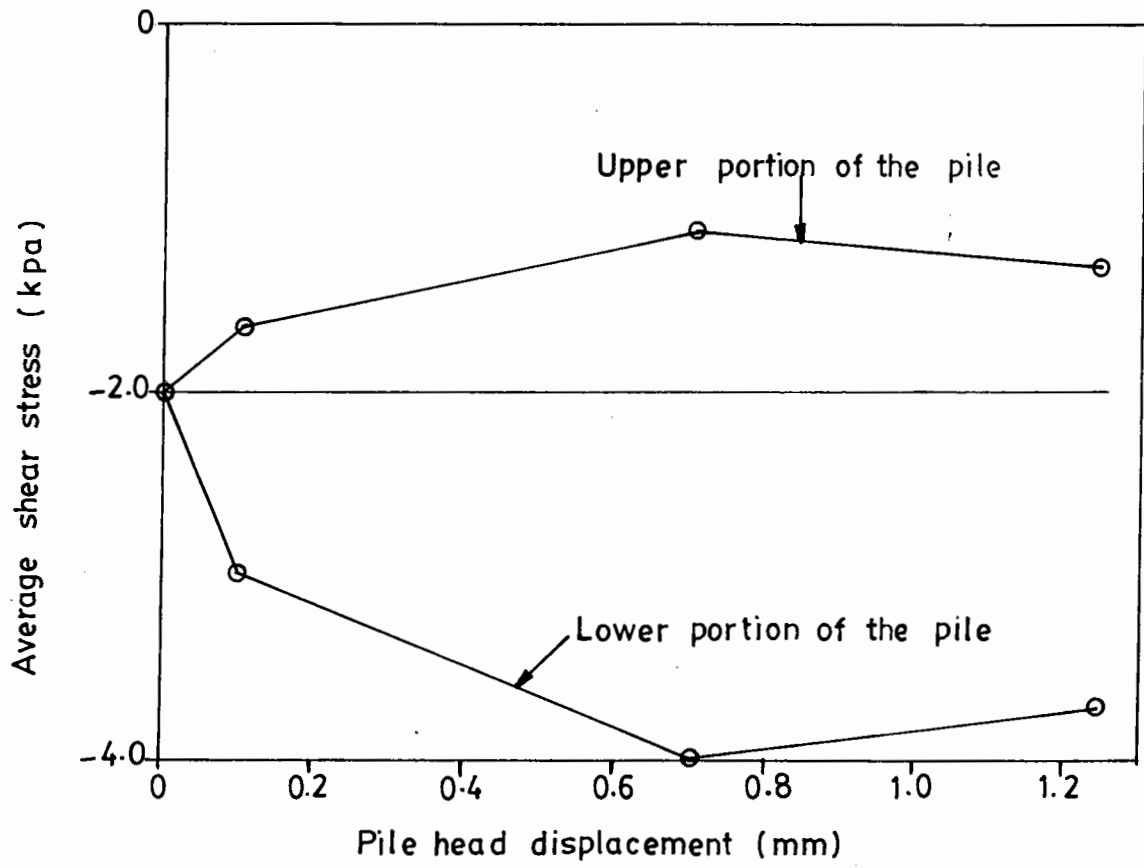


FIG. 6.11. AVERAGE SHEAR STRESS DISTRIBUTION
 During monotonic tension test
 (38-1* - 100 - B)

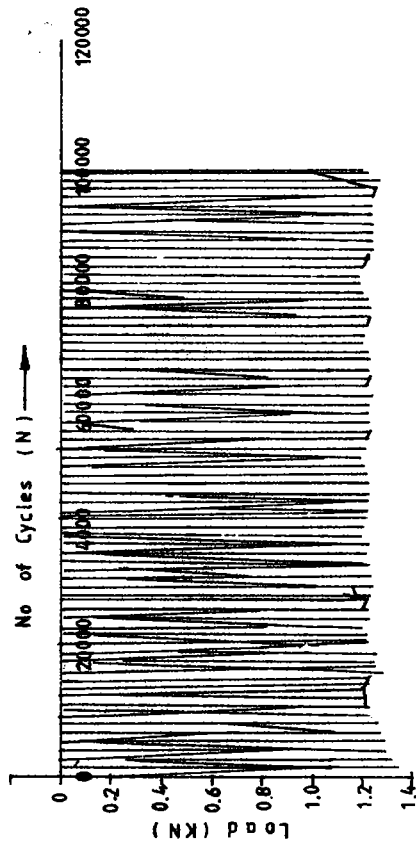
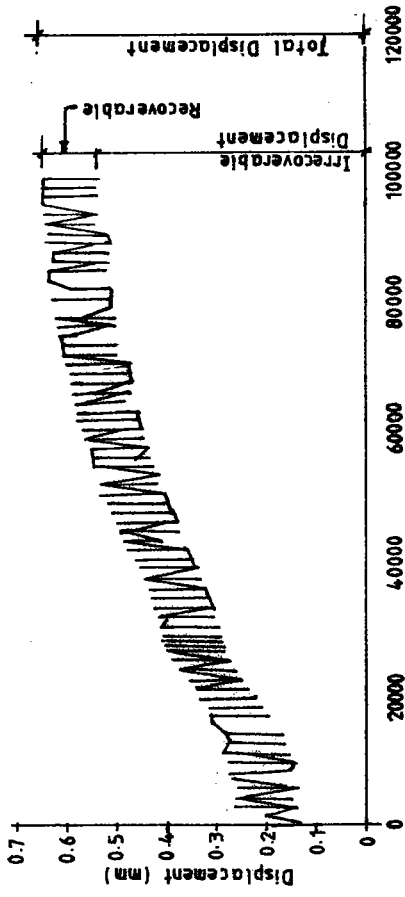


Fig.6.12.Load Displacement During a Constant Cyclic Load Test.

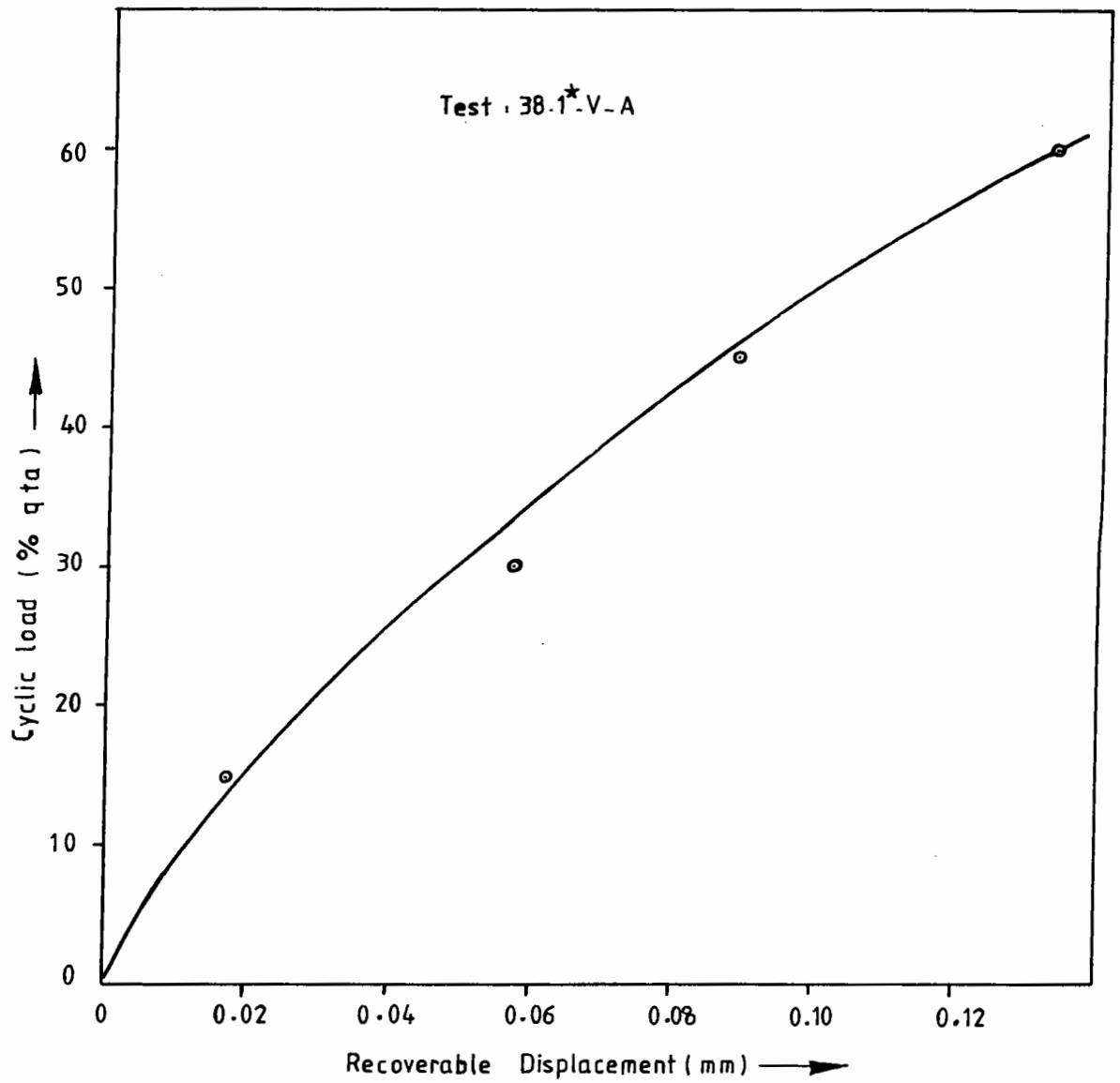


Fig.6.13. Variation of Recoverable Displacement With Cyclic Load

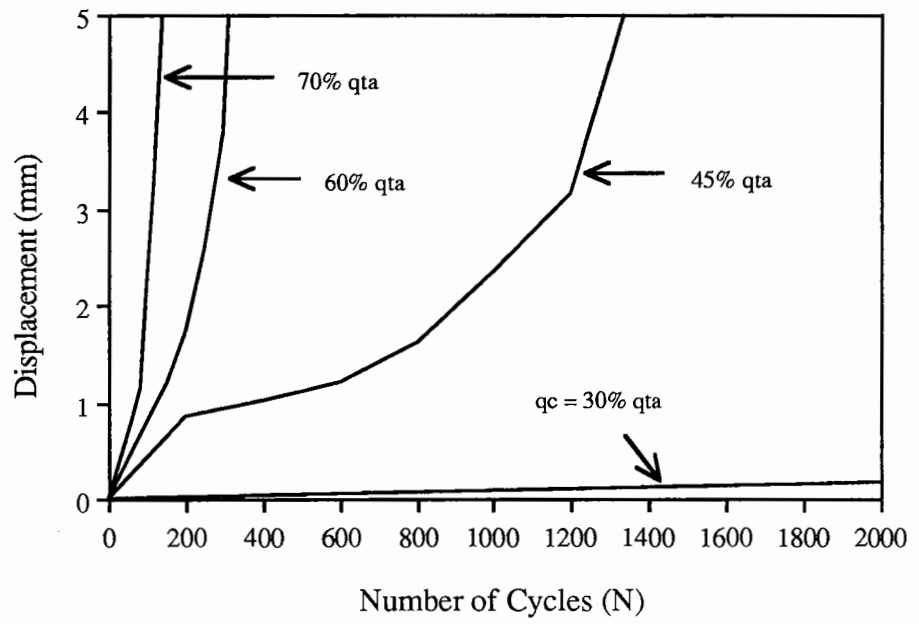


Fig. 6.14 · Total Displacement with Number of Cycles
(12.7 mm Diameter Pile)

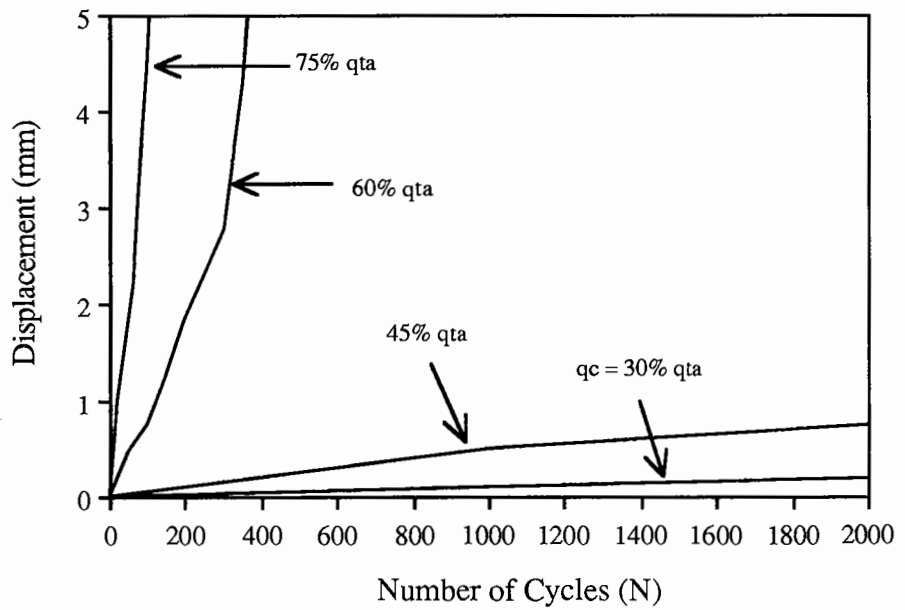


Fig. 6.15 · Total Displacement with Number of Cycles
(25.4 mm Diameter Pile)

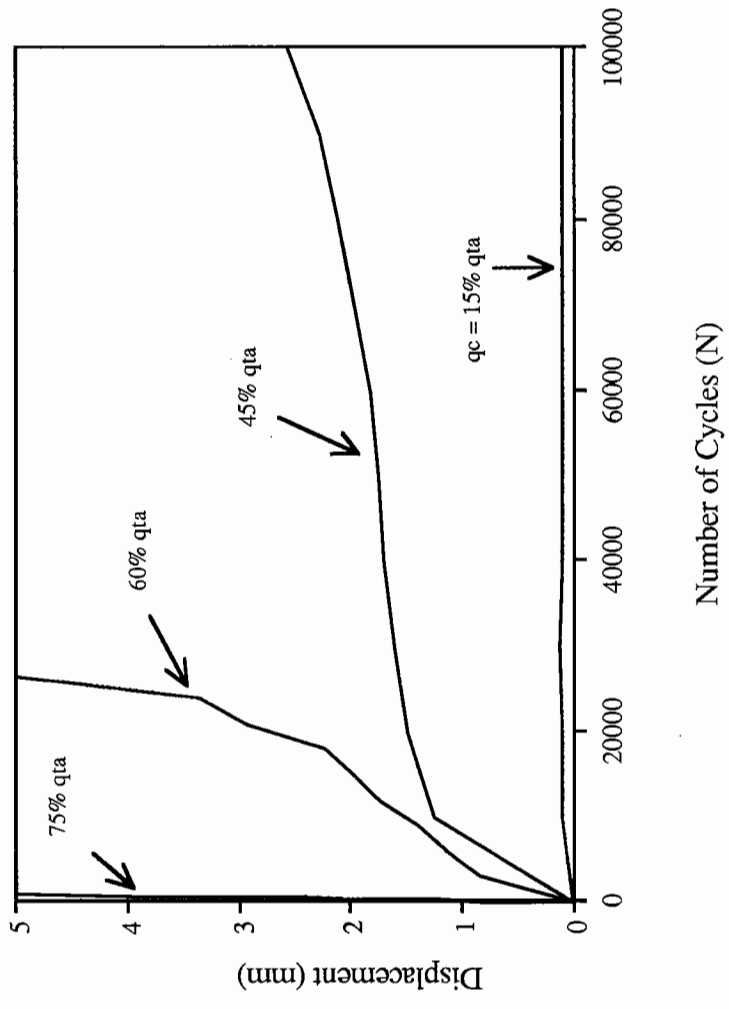
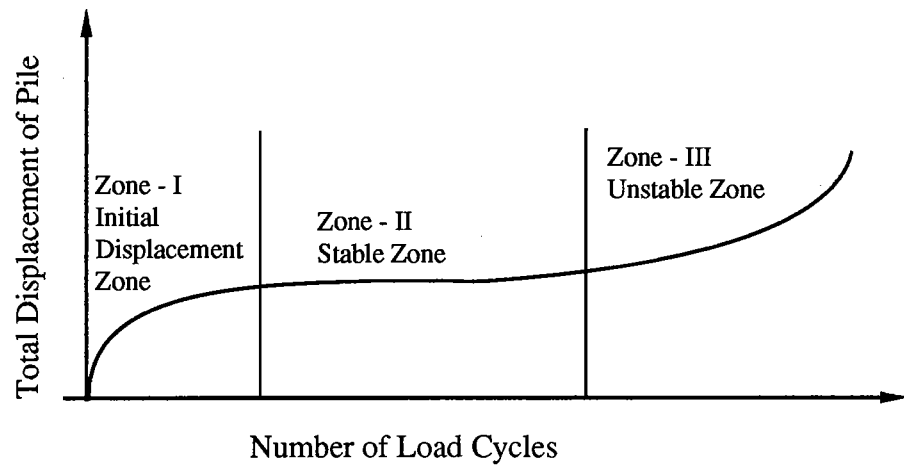
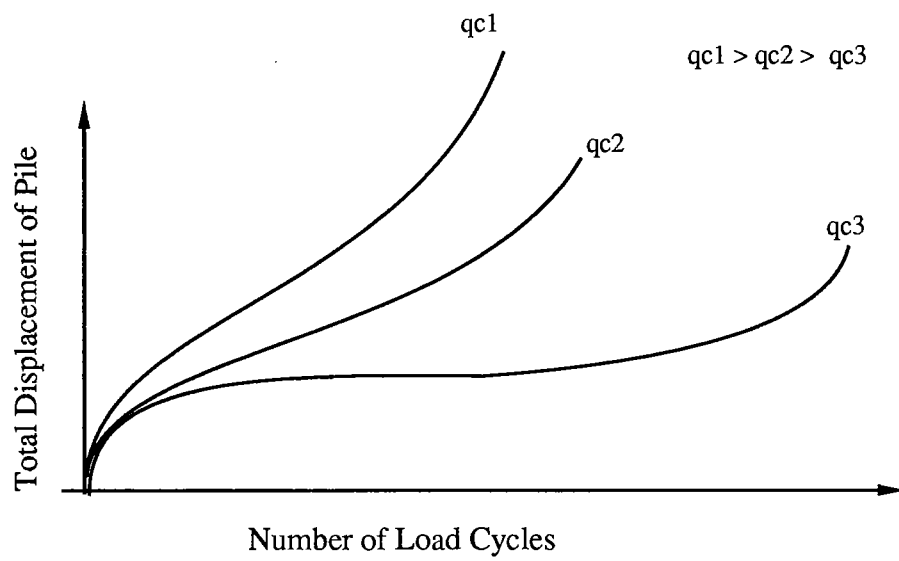


Fig. 6. 16. Total Displacement with Number of Cycles
(38.1 mm Diameter Pile)



(a) Displacement Zones for Pile Under Cyclic Loading



(b) Effect of Cyclic Load Magnitude on the Displacement of the Pile

Fig. 6.17. Displacement of Pile Under Cyclic Loading (an illustration)

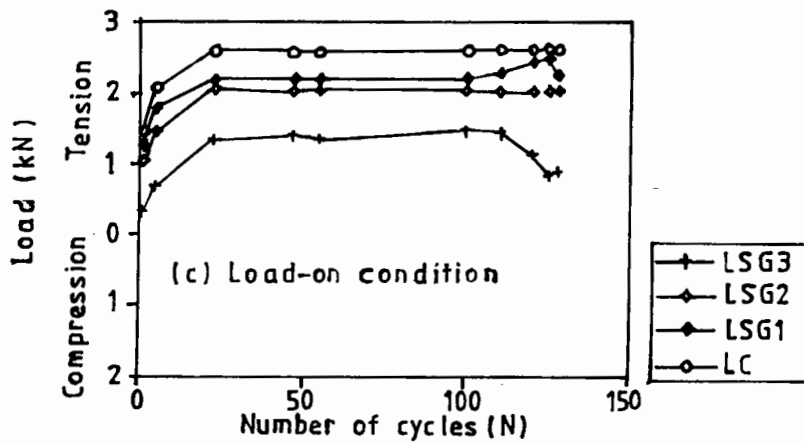
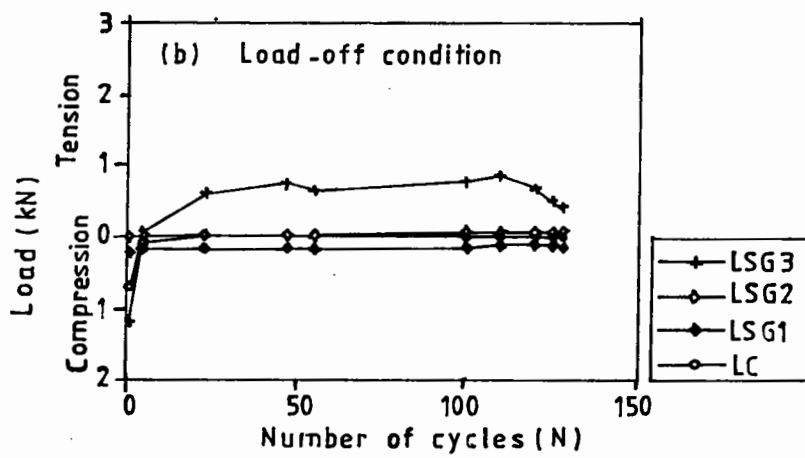
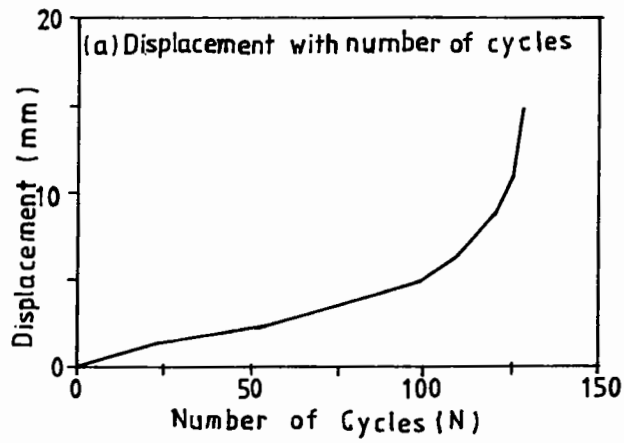


FIG. 6.18. LOAD VARIATION ALONG THE INSTRUMENTED PILE DURING CYCLIC LOADING (75 % q_{ta})

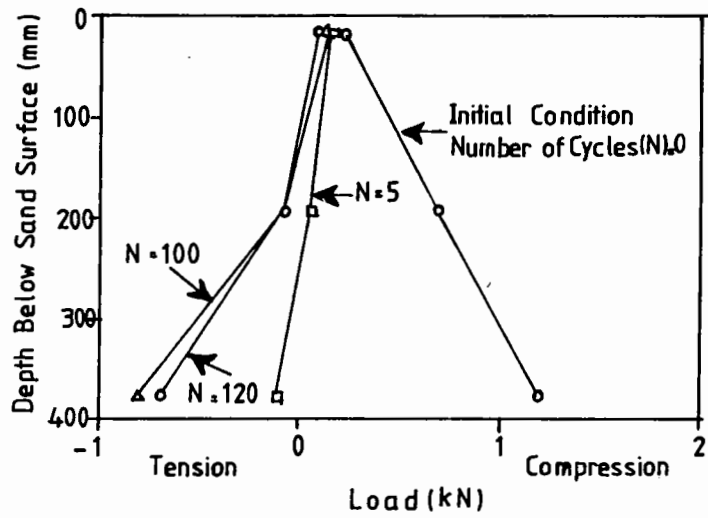


Fig.6.19. Load Distribution Load Off Condition
(Test 38.1*75-A)

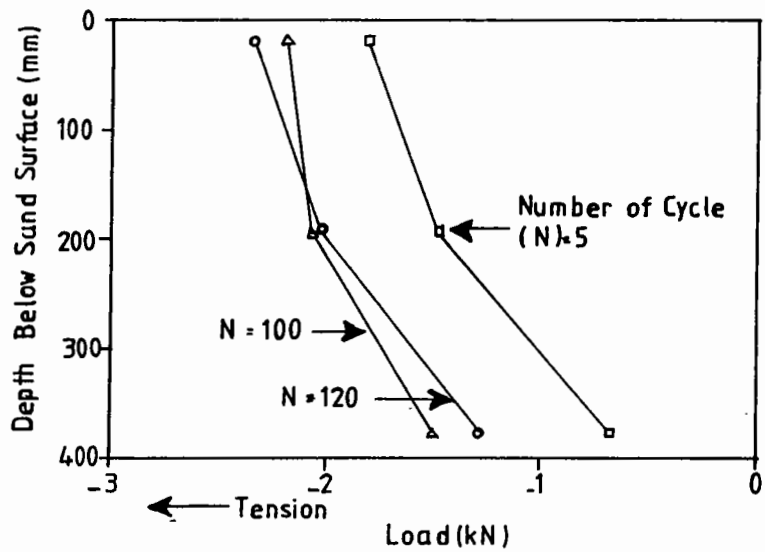
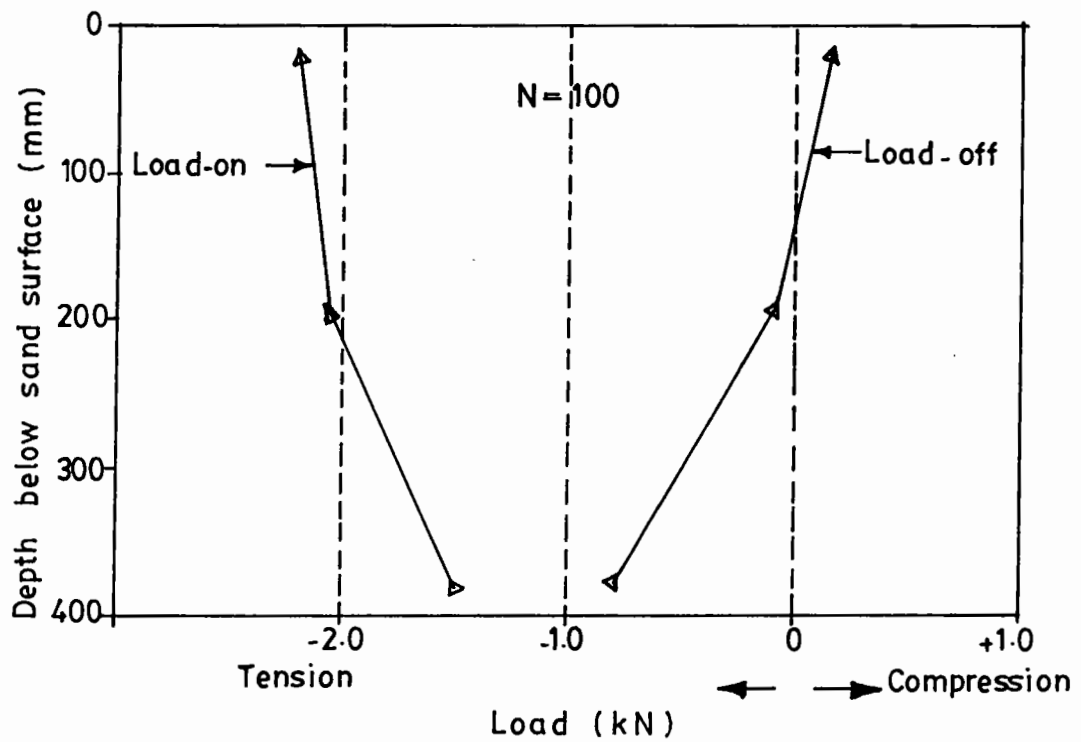
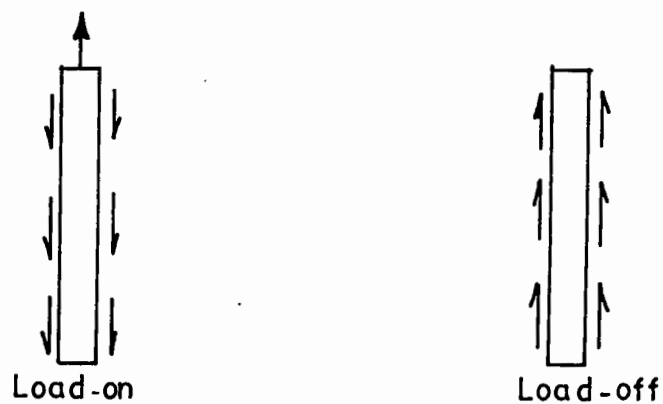


Fig.6.20. Load Distribution Load On Condition
(Test 38.1*75-A)



(a) LOAD DISTRIBUTION



(b) SHEAR STRESS CONDITIONS

FIG. 6.21. LOAD DISTRIBUTION AND SHEAR STRESS CONDITION DURING LOAD OFF AND LOAD ON CONDITIONS AT N=100

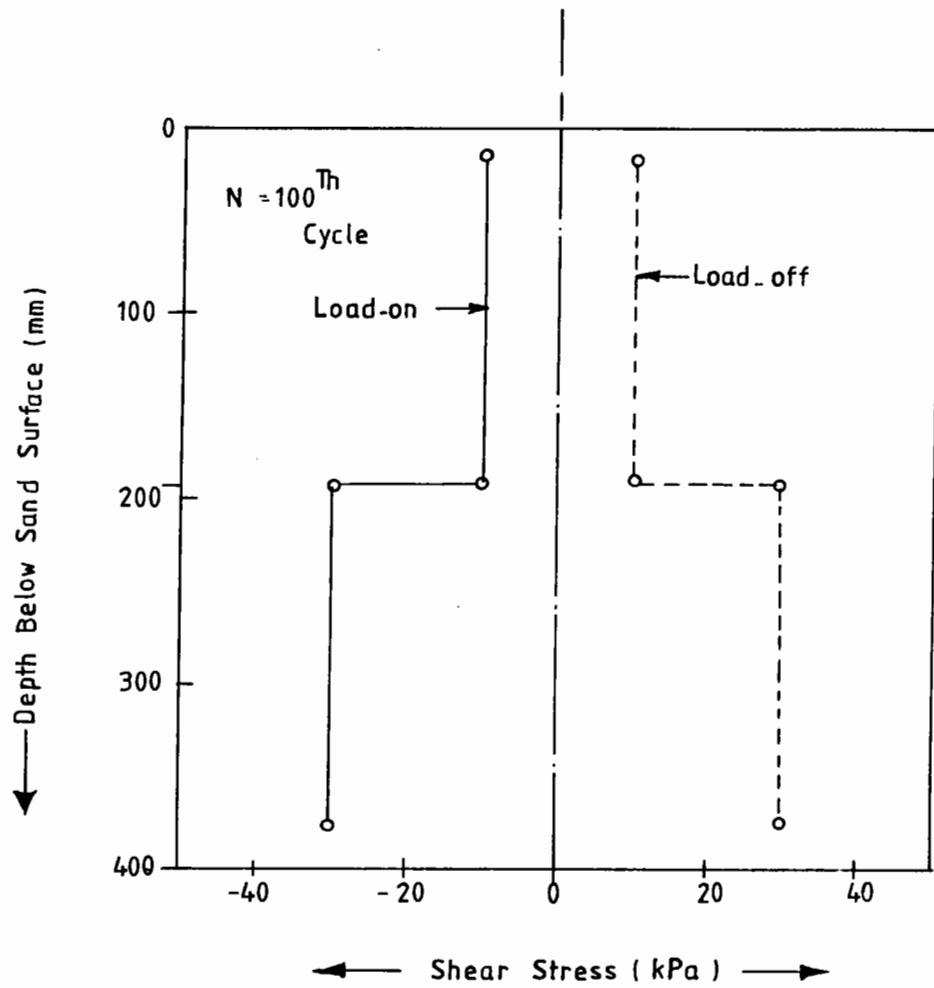
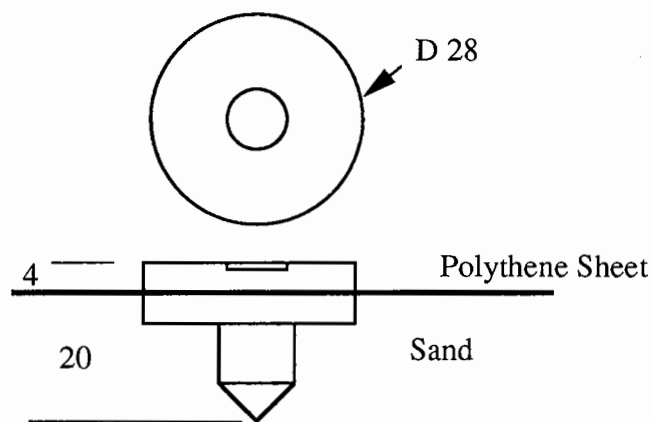


Fig. 6.22. Shear Stress Distribution Along The Pile
 During a Cyclic Load Test
 (38-1^{*}-75 - A)



All Dimensions are in mm

Fig. 6.23. Aluminum Tip Used to Monitor Movement of the Sand Surface

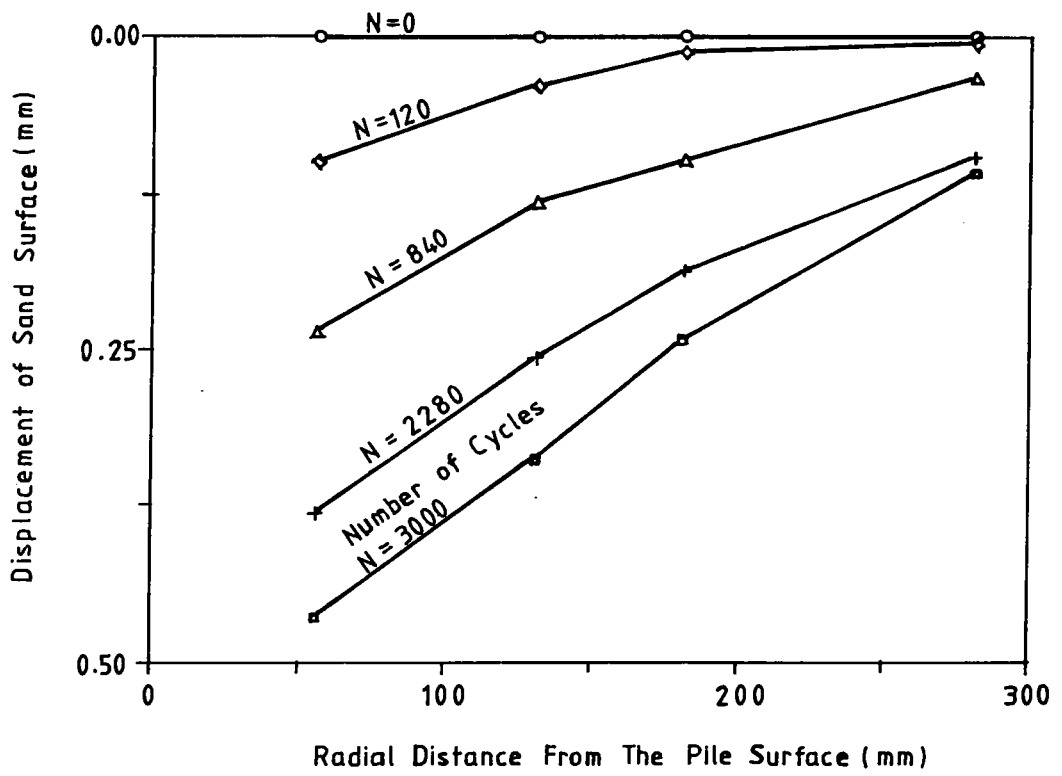


Fig. 6.24. Displacement of the Sand Surface During Tensile Cyclic Load Test (38.1 mm Dia Pile.)

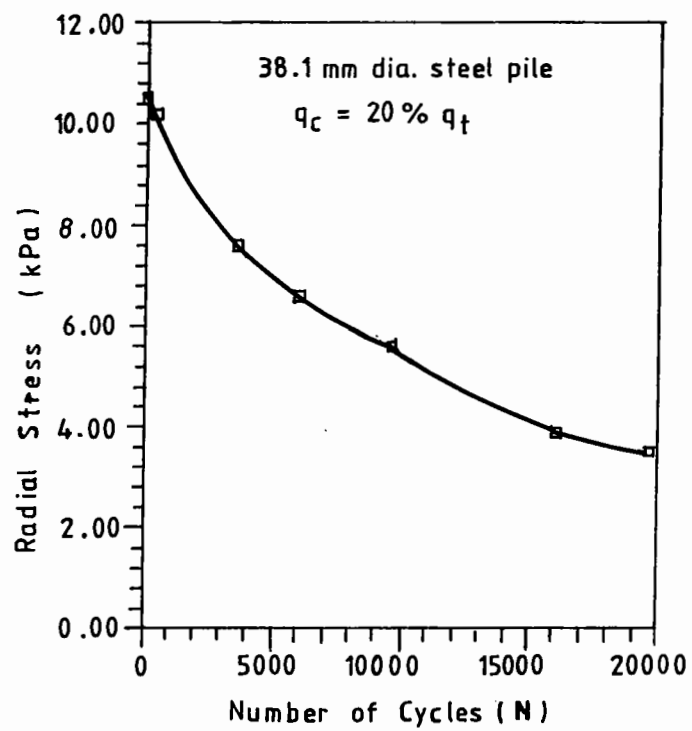


Fig. 6.25. Variation of Radial Stress in Sand Around the Pile During a Cyclic Load Test

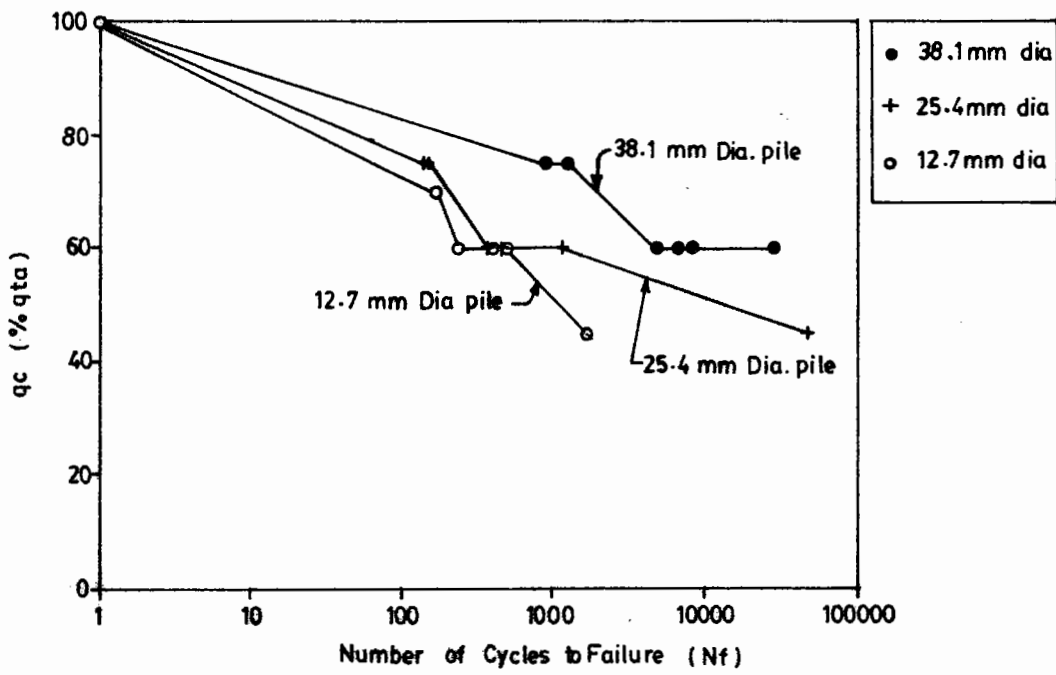


FIG. 6.26. NUMBER OF CYCLES TO FAILURE Vs q_c (as % q_{ta})

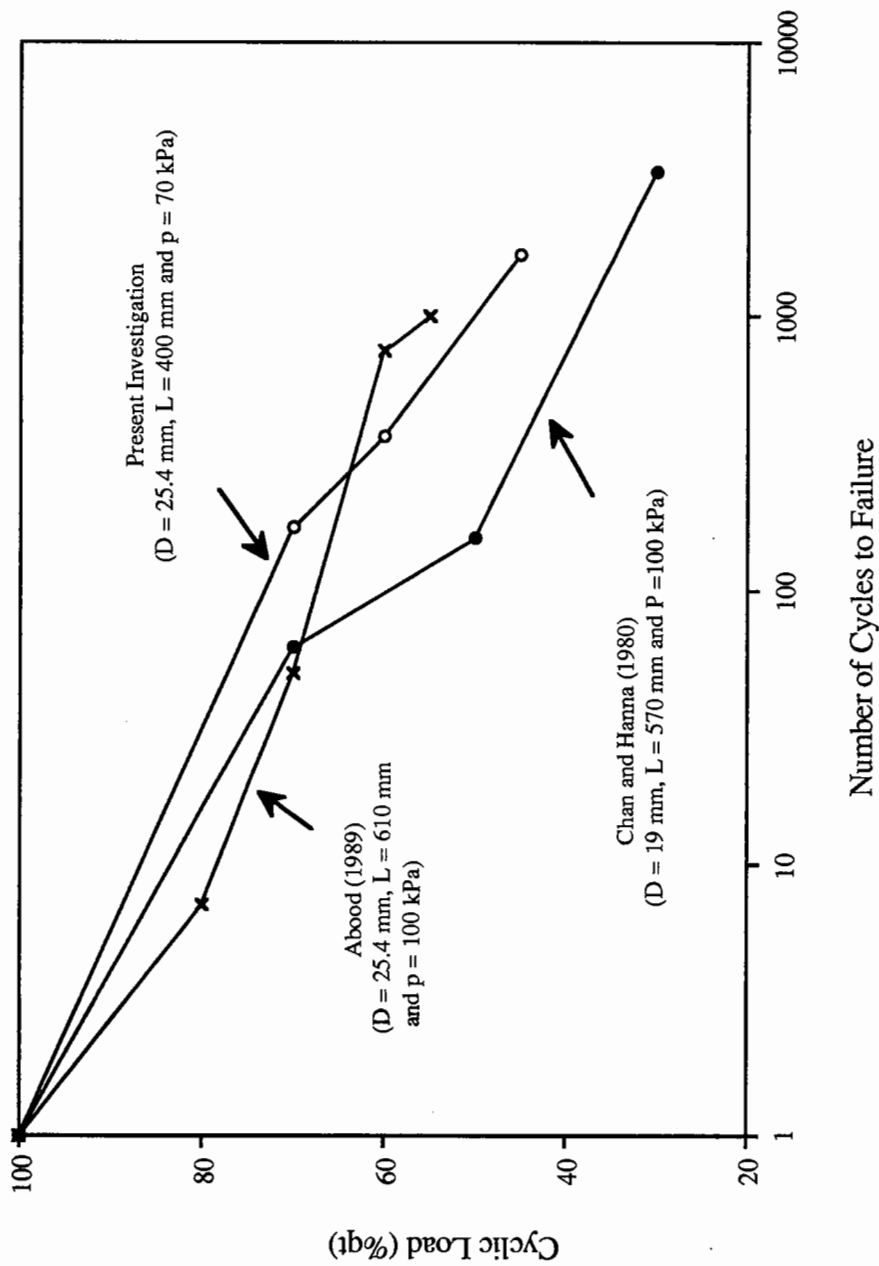


Fig. 6.27. Comparison of Cyclic Load Test Results With Existing Literature

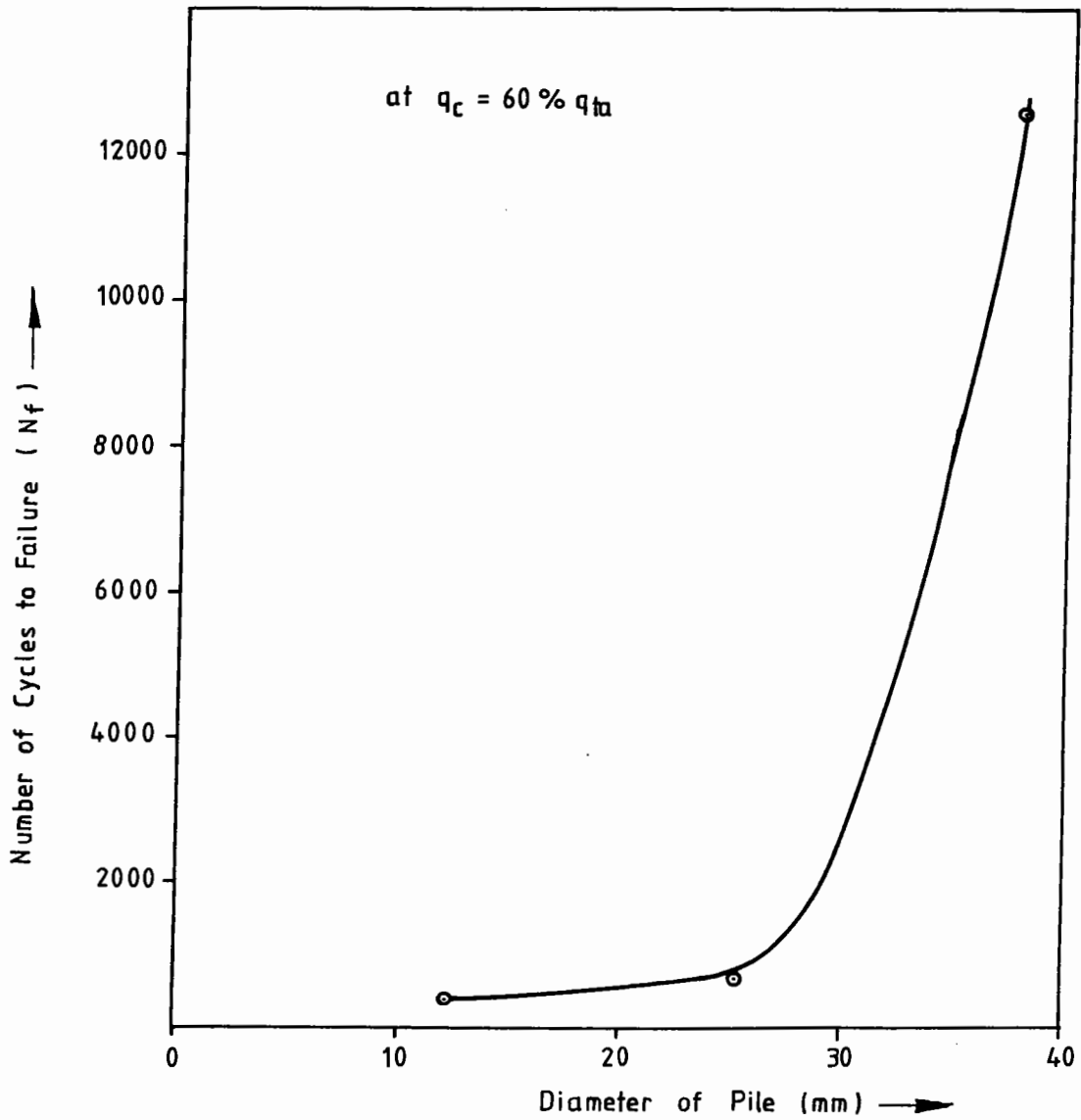
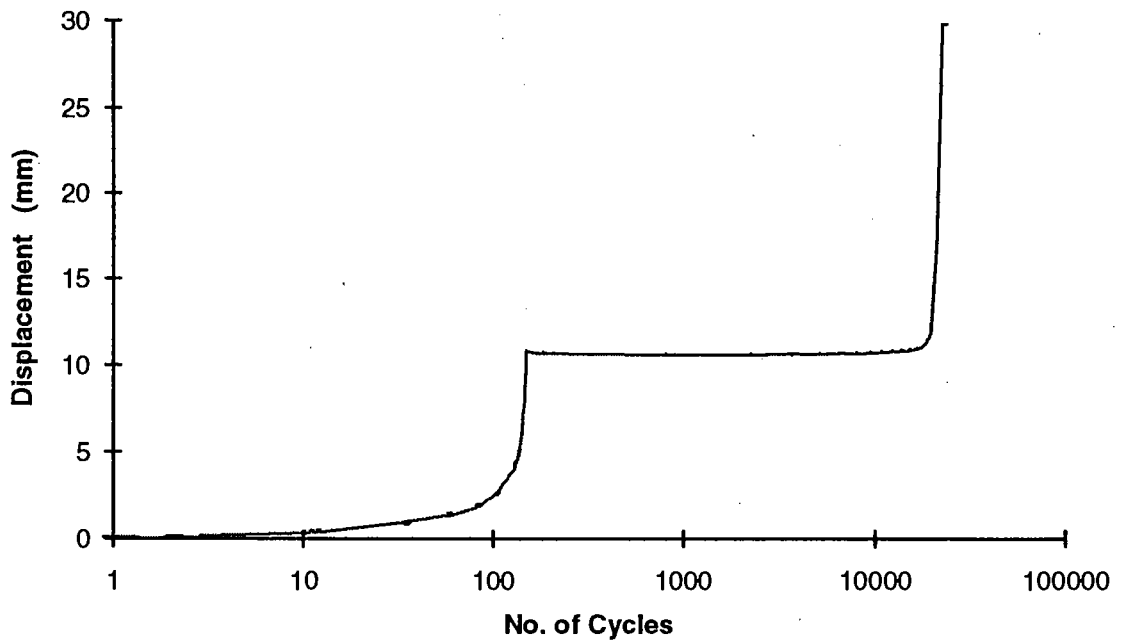


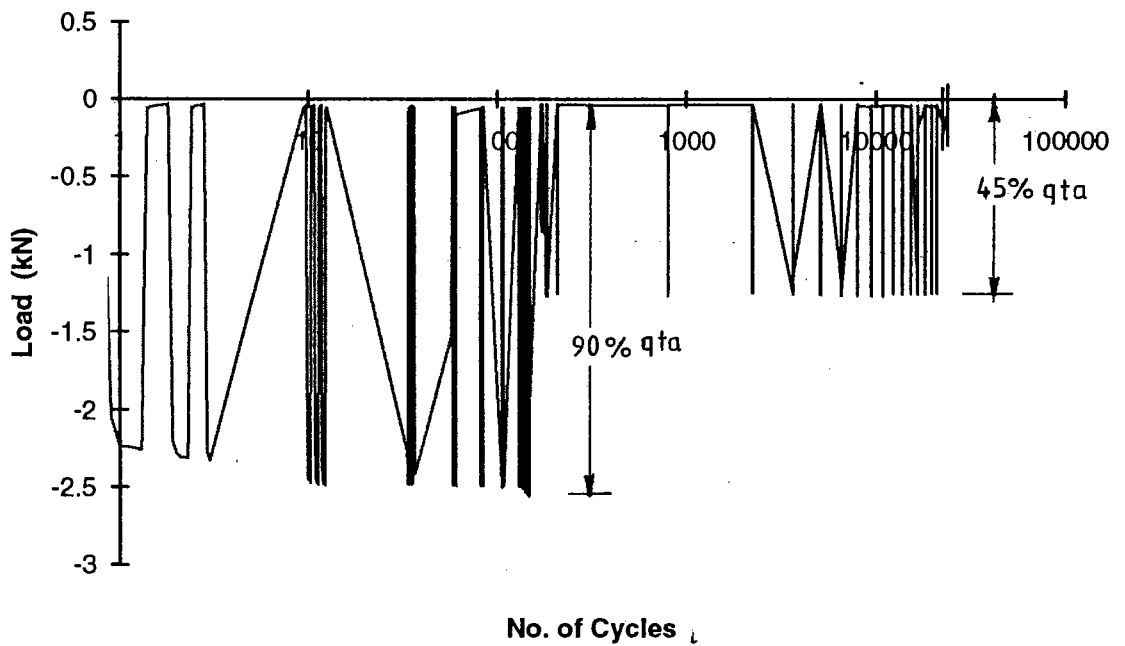
Fig.6.28. Effect of Pile Diameter on Number of Cycles to Failure

Test Identity 38.1 - V - A



(a)

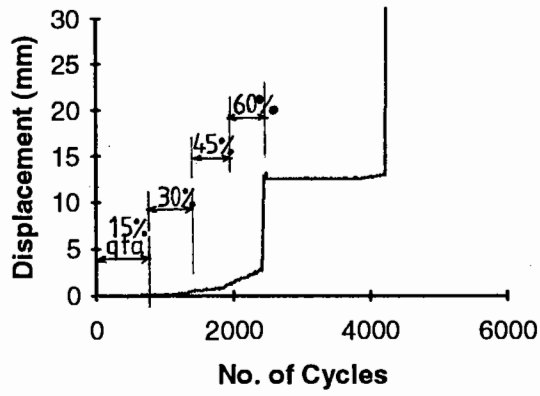
Test Identity 38.1 - V - A



(b)

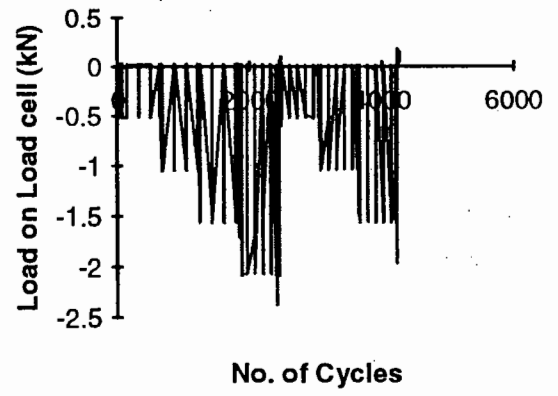
Fig. 6.29. Varying Cyclic Load Test Results for the 38.1 mm Diameter Pile

Test Identity 38.1* - V - B



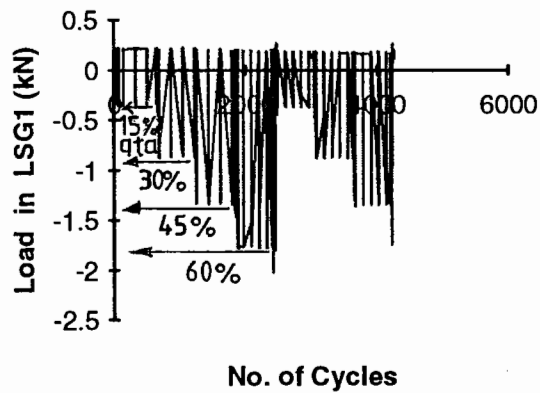
(a)

Test Identity 38.1* - V - B



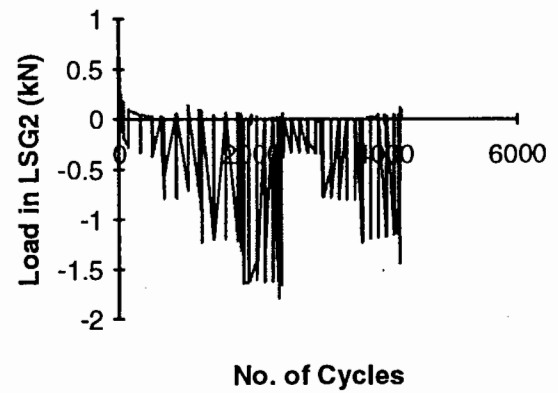
(b)

Test Identity 38.1* - V - B



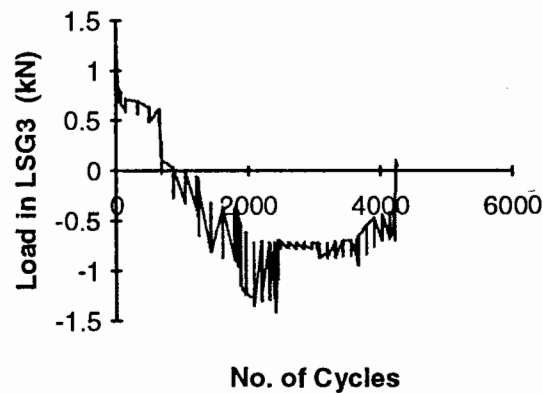
(c)

Test Identity 38.1* - V - B



(d)

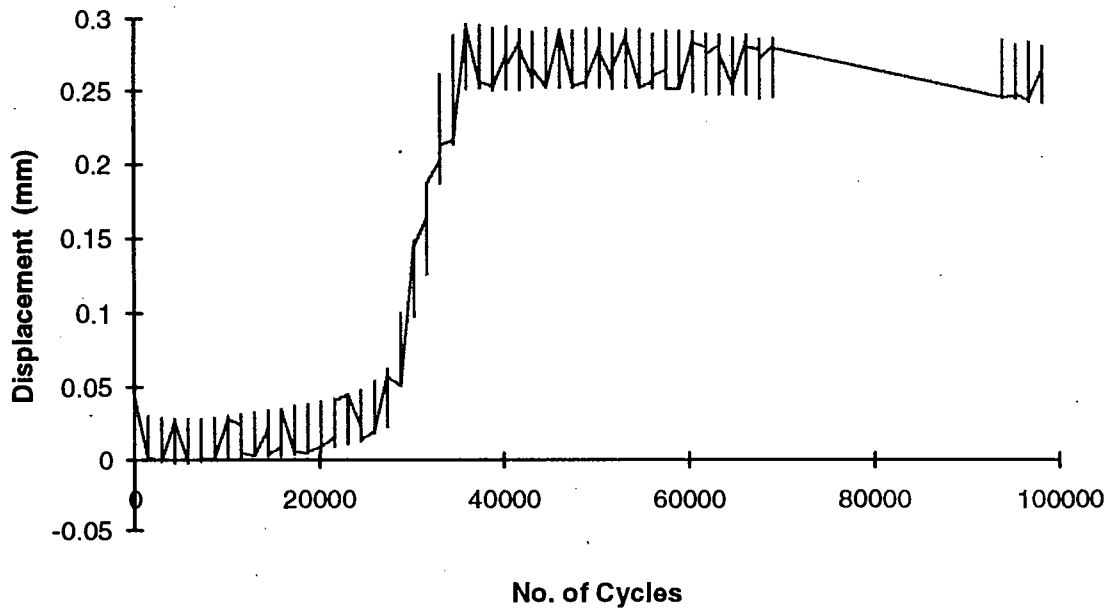
Test Identity 38.1* - V - B



(e)

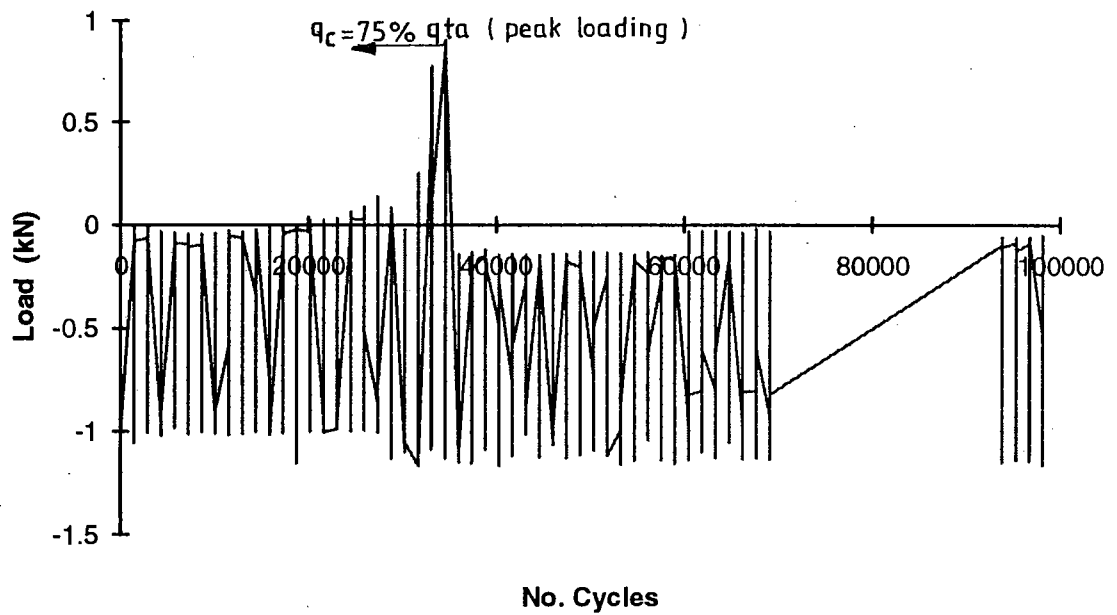
Fig. 6.30. Varying Cyclic Load Test Results for the Instrumented Pile (38.1*-V-B)

Test Identity 38.1 - 38 - A



(a)

Test Identity 38.1 - 38 - A



(b)

Fig. 6.31. Cyclic Load Test Results for the 38.1 mm Diameter Pile (38.1-38-A)

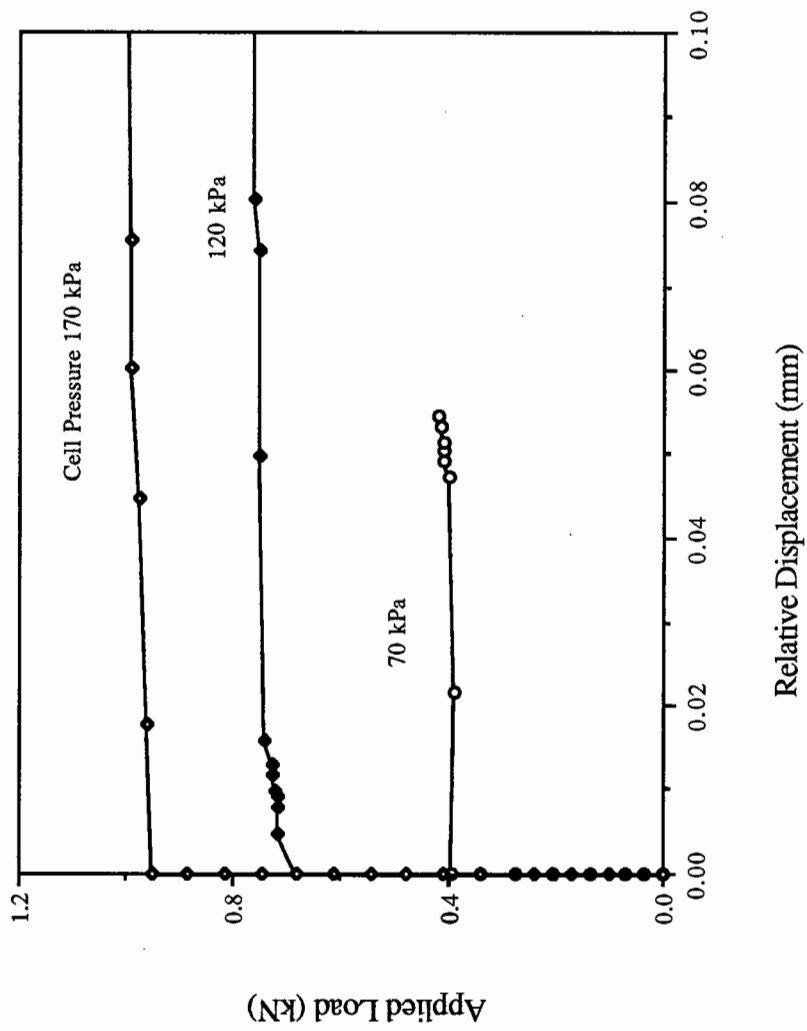


Fig. 6.32 . Pile Element Test Results (25.4 mm Diameter)

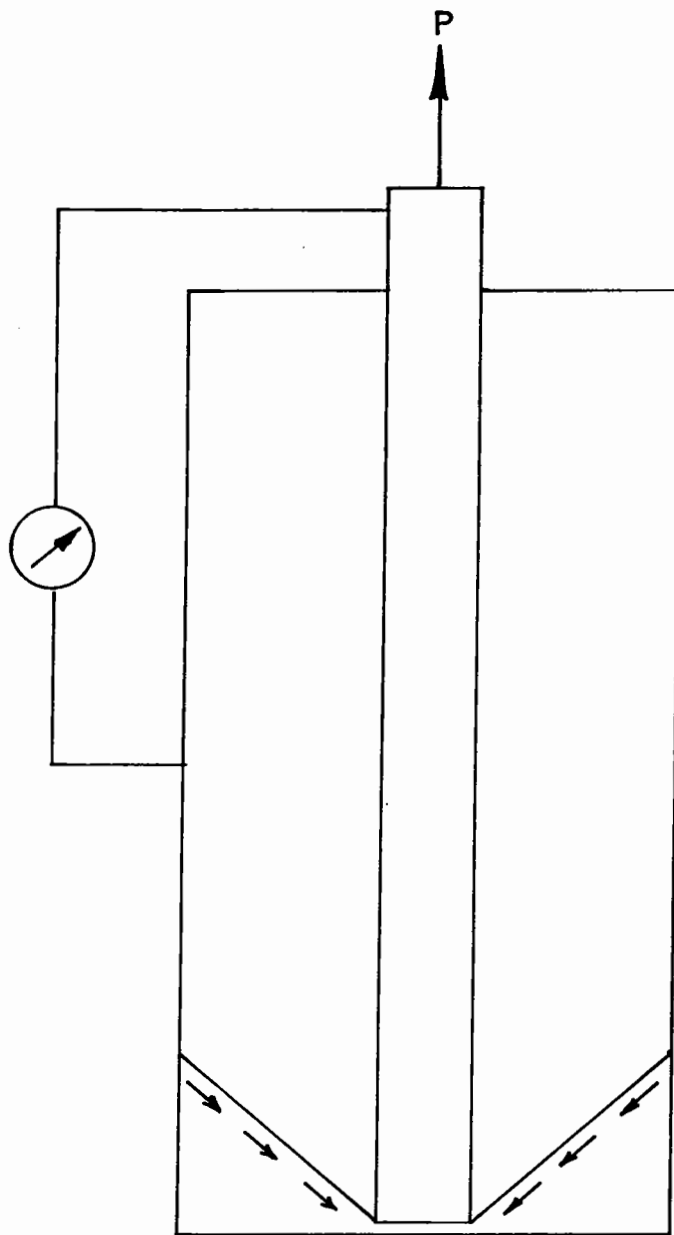


FIG.6.33. POSSIBLE LOAD TRANSFER MECHANISM TAKING PLACE IN SOIL-PILE-SLIP TEST APPARATUS

**Theoretical Studies on the Behaviour of Pile
Under Tensile Loading**

7.1 Introduction

The review of literature shows that a simple method of estimating the load-displacement behaviour of tension piles in sand was proposed by Sulaiman and Coyle (1976) using T-Z curves. The details of the method are presented in Chapter Two. Though the method is simple, it suffers from a few limitations. Therefore, the method has been modified to achieve a better prediction of load-displacement behaviour of tension piles. The modified method is programmed and solutions to a number of illustrative problems have been obtained to bring out:

- i) The salient features of the proposed method
- ii) The need for considering the elastic deformation of the pile in the estimation of skin resistance mobilised along the pile surface
- iii) The effect of the method of computing radial stress on the estimated pile capacity.
- iv) The sensitivity of the estimated load-displacement relationship to the assumed T-Z curve and

The program is also employed to estimate the load-displacement behaviour of a set of field piles. The results are compared with the observed values and with those predicted by the Sulaiman and Coyle method. It was observed that the present model provides a better predictions to the observed values than those predicted by the Sulaiman and Coyle method. Based on the shear stress distribution estimated by the present model, and considering the mechanism of the load transfer in the pile a procedure is suggested for estimating a safe cyclic load for a

pile. This helped to suggest a design method for piles subjected to cyclic tensile loads.

7.2 Limitations of the Sulaiman and Coyle (1976) Model

The model proposed by Sulaiman and Coyle (1976) for the prediction of load-displacement behaviour of tension piles in sand has the following features:

i) The elastic deformation of pile is ignored in estimating the mobilised skin friction.

ii) The computation starts with an assumed value of displacement at the pile tip.

iii) A constant value for the coefficient of lateral earth pressure (k) has been assumed for the computation of the radial stress.

The implications of the above features are examined in the following paragraphs.

i) The displacement of a pile consists of two components namely a) the rigid pile displacement and b) the elastic deformation of the pile. The skin friction mobilised is a function of the total displacement. However, in the method suggested by Sulaiman and Coyle, the mobilised skin friction is estimated considering only the rigid displacement of the pile. The rigid pile displacement, the elastic deformation and the total displacement of a field pile (about 16m long) as estimated by Sulaiman and Coyle are shown in Fig.7.1. It can be observed from Fig.7.1 that, the elastic deformation of the pile is the predominant component of the total displacement. For example, the rigid-pile displacement corresponding to 30t load is about 0.2mm against the corresponding elastic deformation of about 2mm (Fig.7.1). By considering only the rigid-pile displacement, the mobilised friction gets estimated from the initial portion of the

T-Z curves shown in Fig.7.2. On considering the total displacement, the mobilised skin friction gets estimated from the residual stress level (horizontal portion) of the T-Z curves. Hence, computing the shear mobilisation ignoring the elastic deformation of the pile introduces a significant discrepancy.

ii) It is reported that at low load levels, in long compressible piles, the load transfer is restricted up to a certain length of the pile only i.e., the entire length of the pile does not experience displacement. In Sulaiman and Coyle method, the computation starts by assuming a tip displacement (the whole length of the pile undergoes displacement), which implies load transfer to the full length of the pile therefore the load-displacement under low load levels can not be estimated by this method.

(iii) The radial stress ($\bar{\sigma}_r$) on the pile surface is computed as

$$\bar{\sigma}_r = k \bar{\sigma}_v \quad (7.1)$$

where

$\bar{\sigma}_r$ = effective radial stress on pile surface

k = co-efficient of lateral earth pressure

$\bar{\sigma}_v$ = effective vertical stress at the depth under consideration

As discussed in Section 6.2, $\bar{\sigma}_r$ at any location along the pile length is not only a function of vertical overburden pressure ($\bar{\sigma}_v$) at that point but also its distance from the pile tip (h). Hence, there is a need to consider the effect of 'h' in computing the radial stress $\bar{\sigma}_r$.

Keeping in view the above limitations, a modified procedure as below has been suggested to predict the load-displacement behaviour of pile under monotonic tensile load.

7.3 Estimation of Load-Displacement Behaviour of Piles Under Tensile Loads - A Modified Method

The present method provides a procedure of computing load-displacement behaviour of piles under tensile loads considering the following:

i) The total displacement including the elastic deformation of the pile is considered in computing mobilised skin friction

ii) The computation starts with a trial value of pile head displacement this results in the estimation of load-displacement behaviour for small load levels under which the load transfer does not extend to the full length of pile

iii) The radial stress is computed considering the affect of pile tip location and the relative density of sand.

According to the present method, the pile length is divided into a number of segments. The effective radial stress $\bar{\sigma}_r$ acting at the centre of each of the pile segment is computed using the following Eq. (7.2), which accounts for the affect of the pile tip location and the relative density of sand.

$$\bar{\sigma}_r = 0.7 (\bar{\sigma}_v)^{0.89} e^{(2.91 DR)} (h/R_0)^{-0.33} \quad (7.2)$$

(Lehane, 1992)

where $\bar{\sigma}_v$ = effective vertical stress

DR = relative density of sand

h = distance between the point under consideration and the pile tip

R₀ = radius of pile

Performing the miniature pile test, as suggested by Coyle and Sulaiman (1967), at confining pressures equal to the radial stresses ($\bar{\sigma}_r$) estimated for different locations along the pile length, T-Z curves are obtained.

A small upward pile head displacement is assumed and the shear stress mobilised along the length of the pile is estimated using the T-Z curves, accounting for elastic deformation. Knowing the shear stress mobilised along the pile length, the load at the pile head corresponding to the assumed pile head displacement is computed. These values provide a point on the load-displacement curve of the pile. By repeating the procedure with different pile head displacements, the complete load-displacement curve for the pile is estimated.

A flow-chart for the present method is shown in Fig.7.3 and the detailed computational procedure is presented step wise in the following algorithm

7.3.1 Algorithm

Step 1: Divide the pile into N-segments, as shown in Fig. 7.4 and calculate $\bar{\sigma}_r$ at the centre of each segment using Eq.(7.2).

Step 2: Obtain T-Z curves, by conducting miniature pile tests, for the soil-pile-interface at confining pressures equal to different $\bar{\sigma}_r$ values estimated in step 1 as shown in Fig. 7.5.

Step 3: Assume a tensile load P on the pile head and guess an upward pile head displacement y. Thus, the load at the top of the pile segment1 (P1) = P and the displacement at the top of segment1 (y1) = y.

Step 4: Considering the average tensile load acting on the pile segment1 as P1, estimate the initial elastic deformation in segment1 (e1) as

$$e1 = (P1 * DZ1) / (A * E) \quad (7.3)$$

where

A = cross-sectional area of the pile
 E = Young's modulus of the pile material and
 $DZ1$ = length of the pile segment1

Step 5: The displacement ($\Delta y1$) at the centre of the segment1 is computed as

$$\Delta y1 = y1 - (e1/2)$$

Step 6: Referring to a T-Z curve corresponding to σ_{r1} (the radial stress at the centre of the segment1), obtain the value of τ_1/σ_{r1} and hence τ_1 corresponding to the displacement $\Delta y1$.

Step 7: Compute the load transferred by the pile segment1 ($S1$) as

$$S1 = \tau_1 * (2 * \pi * R_o) * DZ1 \quad (7.4)$$

where R_o = radius of the pile.

Step 8: The average load acting on segment1 = $P1 - (S1/2.0)$. For this average load, compute the revised elastic deformation in the pile segment1 ($e1$) as

$$e1 = ((P1 - (S1/2)) * DZ1) / (A * E) \quad (7.5)$$

Step 9: If the difference between the initial value of elastic deformation ($e1$) (computed in step 4 in the first iteration) and the revised value obtained in step 8 is more than an acceptable limit, repeat the steps 5 to 8 with $e1$ calculated in step 8 as the revised initial value.

Step 10: When convergence is achieved in the value of $e1$ go to the next segment (segment2).

The load at the top of segment2 ($P2$) = $P1 - S1$

The displacement at the top of segment2 ($y2$) = $y1 - e1$

Step 11: Estimate the elastic deformation for segment2 (e_2) by assuming P_2 as the average tensile load acting on it. Compute the displacement at the centre of segment2 (Δy_2) as

$$\Delta y_2 = y_2 - (e_2/2) \quad (7.6)$$

Repeat steps 6 to 9 for the segment2.

Step 12: Repeat steps 6 to 11 for the segments 3, 4, etc. until either of the following conditions is encountered.

- i) load on top of a segment becoming zero or
- ii) displacement at the top of a segment becoming zero or
- iii) tip of the pile is reached.

Step 13: If the load at the top of an intermediate segment becomes zero, check the displacement at that point. If the displacement at that point is zero go to step 14; otherwise modify the assumed pile head displacement (y) and repeat steps 4 to 12.

If either the condition (ii) or (iii) is encountered, go to step14.

Step 14: Compute the sum of loads shared by the pile segments (PS) as

$$PS = S_1 + S_2 + S_3 + S_4 + \dots \quad (7.7)$$

If the difference between the assumed load (P) and the computed load (PS) is more than an allowable limit, repeat the steps 4 to 13 with a modified pile head displacement (y).

Step 15: Convergence between P and PS will provide a load (PS) and the corresponding pile head displacement (y).

Step 16: On repeating the steps 3 to 15 for different loads, obtain the corresponding pile head displacements which provide the data for the load-displacement curve for the pile.

It may be pointed out here that by choosing small load values at the pile head, the situation corresponding to the load transfer extending only up to a certain length of the pile can be simulated and the corresponding points on the load-displacement curve can be obtained.

A computer program has been developed using the above algorithm.

7.4 Results and Discussions

Using the computer programme developed, a number of illustrative problems have been solved and the results are discussed in the following paragraphs.

7.4.1 Response of a Pile Under Tensile Loads

A 15m long pile subjected to tensile loading is considered. The soil and the pile data considered are as follows:

Length of pile	= 15m
Outer diameter of pile	= 0.25m
Inner diameter of pile	= 0.24m
Young's modulus of pile material	= 2×10^8 kPa
Unit weight of sand	= 17 kN/m^3
Relative density of sand	= 60%
Soil-Pile interface friction angle	= 25°

Further, for simplicity, a single curve as shown in Fig. 7.6 is assumed to represent the T-Z relationship at different elevations of the pile.

The following results are obtained solving the above problem.

i) the load-displacement relationship at the pile head (Fig.7.7)

ii) the load distribution along the length of the pile (Fig.7.8) and

iii) the shear stress distribution along the length of the pile (Fig.7.9).

The load-displacement relationship and the load distribution obtained in Figs.7.7 and 7.8 respectively are similar to those usually obtained in a pile load test. The shear stress distribution along the length of a pile under various loads is shown in Fig.7.9. It can be observed from Fig.7.9 that the location of peak value of shear stress mobilised moves down as the applied load is increased. Further, it is observed that the shear stress values tend to increase as the pile tip is approached. This is due to the fact that the Eq. (7.2) estimates large normal stress values as the tip is approached.

The mobilised shear stress (τ) expressed as a percentage of the shear resistance (τ_{\max}) at different depths of the pile, for various load levels, is shown in Table 7.1. It can be observed from Table 7.1 that, when a load equal to 29% of ultimate tensile capacity of the pile is applied, the shear stress along the pile is not uniform at 29% τ_{\max} but it is decreasing with depth from a maximum value of 100% τ_{\max} near the pile head. As the applied load is increased, the depth of mobilisation of full shearing resistance ($\tau = \tau_{\max}$) increases. Thus, the failure progresses gradually from top to tip of the pile as the load on the pile is increased.

7.4.2 Parametric Study

In order to examine the present model, a parametric study has been carried-out by estimating the response of piles for the following situations:

i) when elastic deformations is considered in the computation

of mobilised skin friction

ii) when radial stress on the pile surface is computed using Eq. (7.1) and (7.2) and

iii) when different T-Z curves are used in the computations.

For the purpose of above study, the following soil and pile data are considered.

Properties of Sand:

Unit weight of sand = 17.0kN/m³

Relative density = 60%

Properties of Pile:

External diameter = 0.50m

Internal diameter = 0.46m

Length of the piles considered= 5m, 20m and 40m

Young's Modulus of pile

material = 2.0 x 10⁸ kPa

Soil-Pile interface friction

angle = 25°

7.4.2.1 Effect of Considering Elastic Deformation in Shear Mobilisation on the Response of Pile

The load-displacement relationships obtained for the two cases, namely, i) when the elastic deformation of the pile is considered (case 1) and ii) when only rigid displacement of the pile is considered (case 2) in estimating the mobilised skin friction are given in Fig.7.10. The shear distribution along the length of the pile for the above two cases are presented in Fig.7.11.

From Fig.7.10 it can be observed that the estimated load displacement curves for cases 1 and 2 are almost the same when the pile is short (5m long pile), where as, it is significantly different for long piles (20m and 40m long piles). For example,

in the case of 40m long pile, the displacement estimated in the case 1 for an applied load of 2000kN is about 7mm where as it is 11mm in case 2. Like wise, it can be seen from Fig.7.11 that the shear stress distribution curves estimated for cases 1 and 2 are almost the same for a short pile and significantly different for long piles. This is due to the fact that the elastic deformation constitutes a small portion of total displacements in a short pile where as it forms a significant proportion of total displacement in a long pile.

7.4.2.2 The Effect of Method of Computing Radial Stress

In the present model the radial stress is computed using Eq. (7.2) instead of Eq. (7.1). To examine the difference it makes in the pile response, results are obtained using Eqs. (7.1) and (7.2) for the estimation of σ_r . The curves showing variation of σ_r , obtained using Eqs. (7.1) and (7.2) are presented in Fig.7.12.

It can be seen from Fig.7.12 that, for the same set of values of k , γ , DR and pile radius, the values of σ_r estimated using Eq. (7.1) are less in the case of short piles and more in the case of long piles as compared to those estimated using Eq. (7.2), except near the pile tip. The load capacities estimated for different lengths of piles for the two cases (i.e., using Eqs. (7.1) and (7.2)) and presented in Fig.7.13. The results show that the rate of increase in pile capacity reduces with increase in length, in the case of long piles when Eq. (7.2) is used. This observation is consistent with the reported literature on the effect of pile length on pile capacity (Vesic, 1964, 1967, 1970; Mc Clelland, 1974, Meyerhof, 1970, 1976; Dennis and Olson, 1983; Toolan and Ims, 1988; Olson, 1990; Toolan *et al.*, 1990; Kraft, 1991 and Lehane *et al.*, 1993). Hence, adopting Eq. (7.2) for the computation of σ_r will result in a better estimation of pile capacity.

7.4.2.3 The Effect of T-Z Curves on Pile Response

To examine the role of T-Z curves, two different T-Z curves shown in Fig.7.14 are assumed. The load-displacement curves estimated using these two T-Z curves are shown in Fig.7.15. It may be pointed out here, that the maximum shear resistance kept the same in both the cases.

From Fig.7.15 it can be observed that the load-displacement curve obtained is sensitive in the case of short piles and less sensitive in the case of long piles to the T-Z curves are adopted. This is because, for long piles the total displacement, for most part of the pile length, is more than the displacement required for full mobilisation of skin friction. Hence, the use of either of the two T-Z curves, results in the estimation of same shear resistance over most part of the pile length. Hence, the estimated load-displacement behaviour is not affected by the T-Z curve adopted in the case of long piles.

7.4.3 Prediction of Load-Displacement Behaviour of a Field Pile

Sulaiman and Coyle (1976) predicted using their model, the load-displacement behaviour of four steel pipe piles and compared the results with the observed values. The properties of the soil and the pile are given in Table 7.2. The T-Z curves adopted are shown in Fig. 7.2.

Using the above data, the response of the above piles was re-estimated using the present model. In the present calculations, the value of specific gravity of sand particles as 2.65, the relative density (DR) as 0.55 (for the medium dense sand) and the value of E for the pile material (steel) as 2×10^8 kPa have been adopted.

The load-displacement plot obtained from the field load test

and the curves estimated by the Sulaiman and Coyle model and the present model for one of the piles (pile No. 1) are shown in Fig. 7.16. It can be seen from Fig. 7.16 that, the load-displacement behaviour predicted using the present model agrees more closely with the observed as compared to the model suggested by Sulaiman and Coyle (1976). A comparison of pile head displacements for loads upto about 50% of ultimate tensile capacity of the pile (working load level) is also shown in Table 7.3. The results show that the present model provides better estimation of displacement under working load levels.

For the other three piles, the displacement values at half the pile capacity have been reported (Sulaiman and Coyle, 1976). The displacement computations for these three piles have also been made using the present model and a comparison of these results is presented in Table 7.4. From Table 7.4 it can be observed that, except for the pile No. 3, the displacements at the half pile capacity estimated by the modified model are close to the actual observed values as compared to those estimated by the model suggested by Sulaiman and Coyle.

Thus, the above comparisons suggest that, the modifications incorporated in the present model appear to improve the prediction of the load-displacement behaviour of piles under tensile loading.

7.4.4 Estimation of Safe Cyclic Load Level - A critical Appraisal

Research to-date (Chan and Hanna, 1980,; Mc Anoy *et al.*, 1982; Puech, 1982; Poulos, 1988 and Abood, 1989), has tended to express the safe cyclic load level for a pile subjected to cyclic tensile loading as a percentage of its static tensile capacity (qt). The safe cyclic load suggested by different investigators varies considerably, ranging from 20% to 50% qt . This is because the soil properties and the piles and the number of load cycles

considered by them vary. From the present experimental investigation it was observed that the safe cyclic load level decreased with increase in number of load cycles. For the piles to be safe up to a maximum of 100,000 cycles, the safe cyclic load level was observed as 30% of its ultimate tensile capacity (q_t). However, the model piles may have experienced failure even under a cyclic load of 30% q_t , if the number of load cycles in the investigation was more than 100,000 cycles. Hence, it can not be stated that the 30% q_t as an absolute safe cyclic load for the model piles considered in this investigation. In order to obtain an absolute safe cyclic load, there is a need to understand the mechanism and the cause of failure of the pile under cyclic tensile loading.

From the results of the present experimental investigation and from the literature (Puech, 1982) it is observed that, when a pile in sand undergoes cyclic tensile loading it experiences a repeated shear on its surface and a reduction in normal stress leading to the pile failure. The rate of reduction in normal stress and hence the number of cycles to failure depend on the magnitude of cyclic shear stress on the pile surface. However, if the cyclic shear stress along the pile is less than a threshold value, it is possible that no progressive changes in soil properties take place with the increase in number of cycles, so that the pile remains safe irrespective of number of load cycles.

The theoretical studies of the present investigation indicate that that, even when the tensile load on the pile head is limited to a small percentage (29%) of tensile capacity of the pile, the shear stress along the pile surface reaches ^{ultimate} shearing resistance value to a certain depth below the ground level (Fig. 7.9 and Table 7.1). Further it has been reported by Karlsrud and Hauges (1983) that, in the case of a pile under cyclic tensile loading, degradation in skin frictional resistance along the pile surface takes place with increase in number of load cycles. This results

in a load transfer from the upper portion to the lower portion of the pile with increase in number of cycles.

The estimation of the safe cyclic load on a pile should account for, in some means, the above known behaviour of pile under cyclic tensile loads. With consideration of the above, an attempt has been made to evolve a procedure of estimating safe cyclic load which reflects the observed phenomena such as the degradation of shearing resistance in the top portion of the pile and the transfer of loads to lower portion of the pile with increase in load levels.

7.4.5 Suggested Procedure to Obtain Safe Cyclic Load

According to this procedure, an ultimate cyclic tensile capacity of the pile (q_{ct}) is estimated by considering load transfer mechanism. By dividing this load with a suitable factor of safety (SF), the safe cyclic load ($q_{c\text{safe}}$) is obtained.

$$q_{c\text{safe}} = q_{ct} / FS$$

where $q_{c\text{safe}}$ = safe cyclic load

q_{ct} = ultimate cyclic tensile capacity

FS = Factor of safety

In estimating the ultimate cyclic tensile capacity of the pile it is assumed that, when the cyclic shear stress (τ) at any point along the pile reaches shearing resistance (τ_{max}) the shear resistance at that point drops down to a limiting (residual) shear (τ_{limit}) due to degradation of shearing resistance and the load will be transferred to the lower portion of the pile. The maximum tensile load which do not bring the entire length of the pile to a residual value is termed as ultimate cyclic tensile capacity (q_{ct}) of the pile.

Procedure to Obtain Ultimate Cyclic Tensile Capacity:

The detailed procedure of obtaining ultimate cyclic tensile capacity of pile is outlined in the following steps and presented in the form of a flow chart in Fig.7.17. To illustrate the procedure the ultimate cyclic tensile capacity for the 40m long pile has been obtained using the procedure and the results are cited step wise.

Step 1: Obtain the properties of the soil and the pile including T-Z curves (for 40m long pile)

Step 2: Compute the shearing resistance (τ_{\max}) along the length of the pile using the following Eq.(7.8) (curve 1, Fig. 7.18)

$$\tau_{\max} = \sigma_r \tan \delta \quad (7.8)$$

Step 3: Assume a limiting value of shear stress (τ_{limit}) as a percentage of shearing resistance (τ_{\max}) (say $\tau_{\text{limit}} = 20\% \tau_{\max}$). Obtain τ_{limit} values along the depth of the pile (curve 2, Fig. 7.18).

Step 4: Assume a load P on the pile head. Use the present model and obtain the shear stress (τ) along the pile length (curve 3 in Fig.7.18). Compare the shear stress (τ) along the length of the pile with the corresponding limiting shear stress (τ_{\max}) value.

Step 5: If $\tau < \tau_{\max}$ at all points along the length of the pile (comparing the curves 1 and 3 of Fig. 7.18, $\tau < \tau_{\max}$ at all points along the pile length), then increase the load P on the pile head and repeat step 4; otherwise go to step 6. (curve 4 is obtained for P = 1700 kN; $\tau = \tau_{\max}$ upto a depth of about 7.0m below ground level).

Step 6: Reduce the shear resistance in the portion of the pile where $\tau = \tau_{\max}$ (i.e., by assuming $\tau = \tau_{\text{limit}}$ in this portion) and repeat step 4 with the same load P on the pile head and obtain the modified shear stress distribution along the pile length (curve 5 of Fig. 7.18). Assumption of $\tau = \tau_{\text{limit}}$ in a portion of the pile implies that the soil offers reduced resistance in that portion and the remaining load is transferred to the lower portion of the pile.

Step 7: Repeat the steps 4 to 6 by increasing loads on the pile head and obtain corresponding stress distribution (curves 6 to 8), until a load P is obtained such that when it is exceeded creates $\tau > \tau_{\max}$ in the portion of the pile offering resistance. This load P is considered as the ultimate cyclic tensile load on the pile head, which creates a shear stress at any point offering resistance within the specified stress limit (τ_{\max}) (P = 3190 kN, Fig. 7.18).

Figs. 7.19, 7.20 and 7.21 shows the shear stress distribution and safe cyclic loads for the 40m long pile for limiting shear stress $\tau_{\text{limit}} = 30\% \tau_{\max}$, $40\% \tau_{\max}$ and $50\% \tau_{\max}$ respectively.

A computer program has been developed for the above procedure. Using the computer program, the ultimate cyclic tensile capacity with different τ_{limit} values has been computed for the three piles (5m, 20m, and 40m long; Section 7.4.2), and the results are given in Table 7.5. It can be observed from Table 7.5 that the estimated ultimate cyclic tensile capacity (q_{ct}) of a pile is less than ultimate static tensile capacity (q_{t}) of the pile and is a function of τ_{limit} . Further, it can be observed that for a given value of τ_{limit} the corresponding q_{ct} (expressed as % q_{t}) is more for short pile (5m long) compared to long piles (20m and 40m). This is because the load transfer mechanism is effective in long piles, due to large elastic deformation, and is

insignificant in short piles (Fig.7.11).

7.4.6 A Suggested Design Procedure for a Pile Under Cyclic Tensile Loading

Based on the procedure presented in Section 7.4.5 the following design procedure is suggested for the piles subjected to cyclic tensile loading.

Step 1: Obtain the soil properties at the site, properties of the pile material and the T-Z curves for the soil pile interface.

Step 2: Obtain the limiting shear stress τ_{limit} to be maintained along the pile surface.

Step 3: Estimate the expected cyclic tensile load (P), on the pile head, for which the pile has to be designed.

Step 4: Assume a set of trial dimensions to the pile.

Step 5: For the properties of soil and pile and for the limiting shear stress (τ_{limit}) decided in step 2 and adopting a factor of safety(SF), calculate the safe cyclic load on the pile head using the routine explained in Section 7.4.5.

Step 6: Compare the computed allowable loads and the design load on the pile head to choose an appropriate set of dimensions of the pile.

In case of a pile which experiences a static tensile loading superimposed by cyclic tensile loads, such as TLP foundations, the procedure can be adopted with a few additional computations as shown in the flow chart Fig.7.22. For such pile, obtain the pile dimensions initially for the cyclic loads as explained above and

then estimate its static tensile capacity. If the estimated static capacity is less than the expected static tensile load, increase the pile dimensions to suite the required static capacity. If the estimated static capacity is more than or equal to the expected static load, retain the dimensions of the pile obtained from the cyclic load analysis.

7.5 Concluding Remarks

The theoretical studies of the present investigation resulted in the following conclusions:

1) A modified T-Z model has been presented for the prediction of load-displacement behaviour of tension piles. The present model considers the effect of elastic deformation of the pile and provides the load-displacement behaviour of pile under small loads which do not cause pile tip displacement.

2) The sensitivity of the present model has been examined by conducting a parametric study.

3) The present model is found to estimate the load displacement behaviour of some field piles more closely than the existing T-Z model proposed by Sulaiman and Coyle (1976).

4) Based on the modified T-Z model a procedure of estimating the safe cyclic load for a pile has been suggested.

Table 7.1 Shear Stress Distribution Along the Pile

Depth below ground level (m)	τ_{max} (kPa)	Shear stress under a load P (kPa)					
		P = 145 kN (29 % q_t) *		P = 305 kN (61% q_t)		P = 425 kN (85% q_t)	
		τ	% τ_{max}	τ	% τ_{max}	τ	% τ_{max}
0.63	3.04	3.04	100.0	3.04	100.0	3.04	100.0
1.9	8.34	8.34	100.0	8.34	100.0	8.34	100.0
3.1	13.57	7.60	56.0	13.57	100.0	13.57	100.0
4.4	19.00	9.50	50.0	19.00	100.0	19.00	100.0
5.6	24.80	10.90	44.0	24.80	100.0	24.80	100.0
6.9	31.00	11.90	38.0	31.00	100.0	31.00	100.0
8.1	38.10	12.70	33.0	38.10	100.0	38.10	100.0
9.4	46.20	13.60	29.0	46.20	100.0	46.20	100.0
10.6	56.10	14.10	25.0	29.10	52.0	56.10	100.0
11.9	69.20	15.30	22.0	31.40	45.0	69.20	100.0
13.1	89.50	17.60	20.0	36.20	41.0	54.70	61.0
14.4	140.00	25.10	18.0	51.80	37.0	81.90	59.0

* q_t - estimated tensile capacity of pile = 500 kN

Table 7.2 Properties of Soil and Piles
(Sulaiman and Coyle, 1976)

Pile No.	Diameter (m)	Embedded Length (m)	Cross-sectional Area (Sq.m)
1	0.324	16.17	0.0111
2	0.406	16.08	0.0154
3	0.508	16.14	0.0177
4	0.406	16.17	0.0154

Soil Properties:
 (i) Medium Dense Sand
 (ii) Void Ratio = 0.63

Table 7.3 Comparison of the Observed and Computed Pile Head Displacements

Load (kN)	Observed displacement (mm)	Computed displacement(mm)		% Error	
		Sulaiman & Coyle model	Present model	Sulaiman & Coyle model	Present model
100	0.29	0.59	0.35	+104	+ 4
200	0.68	1.27	0.75	+ 87	+ 10
300	1.27	2.05	1.30	+ 61	+ 2
400	1.95	2.91	1.90	+ 49	- 3

Table 7.4 Comparison of pile head displacement at half-load carrying Capacity

Pile No.	Half-load Carrying Capacity (kN)			Displacement of pile at half-load Carrying Capacity				
	Actual	Sulaiman & Coyle model	Present model	Displacement (mm)			Error (%)	
				Actual	Sulaiman & Coyle	Present model	Sulaiman & Coyle	Present model
1	350	320	340	1.70	2.41	1.62	+41.80	- 4.70
2	455	455	455	3.30	1.78	1.52	-46.10	-53.90
3	450	500	615	2.03	2.29	1.80	+12.50	-11.30
4	435	455	462	1.52	1.78	1.52	+16.70	0.00

Table 7.5 Ultimate Cyclic Tensile Capacity of Piles for Different Limiting Shear Stresses (τ_{limit})

Length of pile (m)	Computed Tensile Capacity of pile (q_t (kN))	Ultimate cyclic tensile capacity (q_{ct}) at different limiting shears							
		$\tau_{limit} = 20\% \tau_{max}$		$\tau_{limit} = 30\% \tau_{max}$		$\tau_{limit} = 40\% \tau_{max}$		$\tau_{limit} = 50\% \tau_{max}$	
		q_{ct}	% q_t	q_{ct}	% q_t	q_{ct}	% q_t	q_{ct}	% q_t
5	240	184.0	77.00	188.0	78.00	192.0	80.00	198.0	83.00
20	2000	1250.0	63.00	1360.0	68.00	1480.0	74.00	1550.0	78.00
40	6000	3190.0	53.00	3550.0	59.00	3800.0	63.00	4100.0	68.00

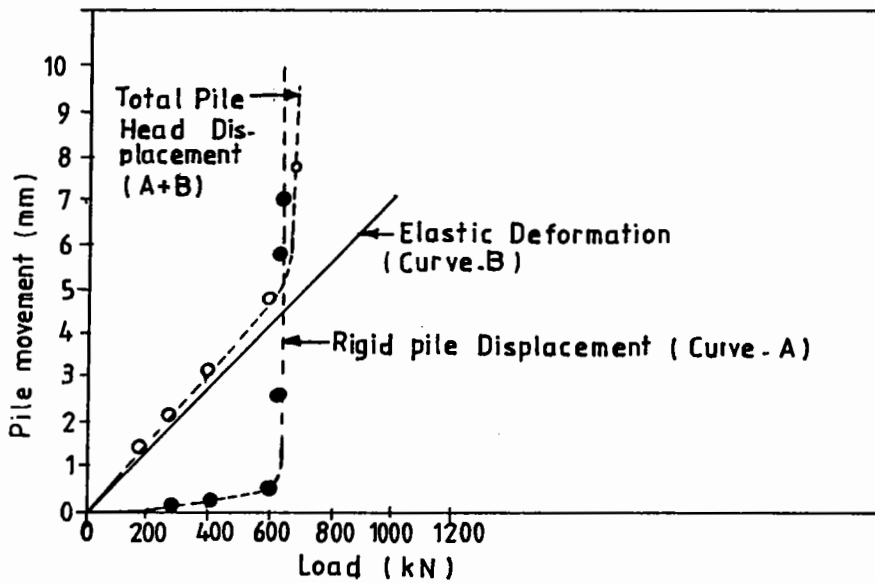


FIG.7.1. COMPONENTS OF PILE HEAD DISPLACEMENT ESTIMATED BY T-Z MODEL (Sulaiman and Coyle , 1976)

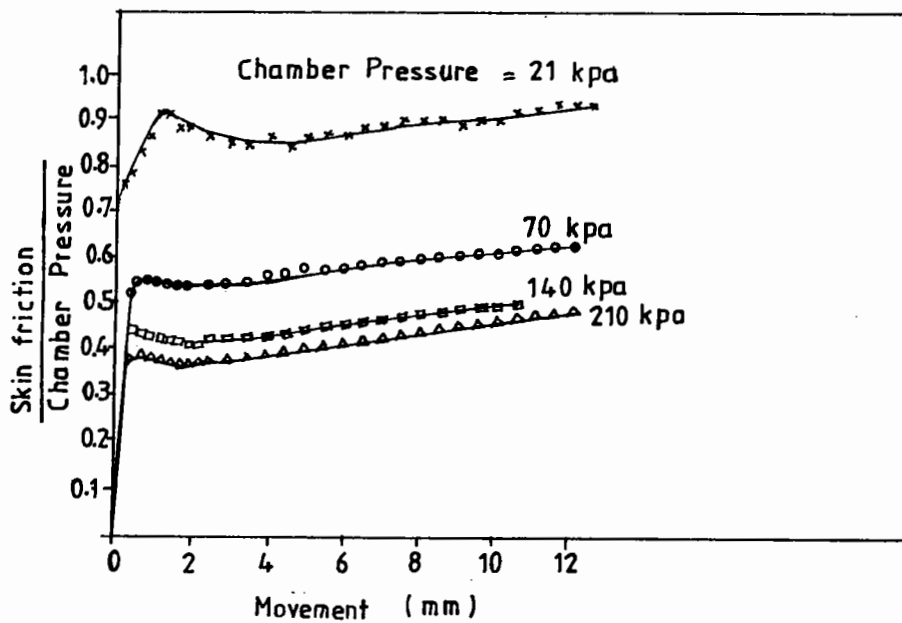


FIG.7.2. T-Z CURVES FOR THE SOIL PILE INTERFACE (Sulaiman and Coyle , 1976)

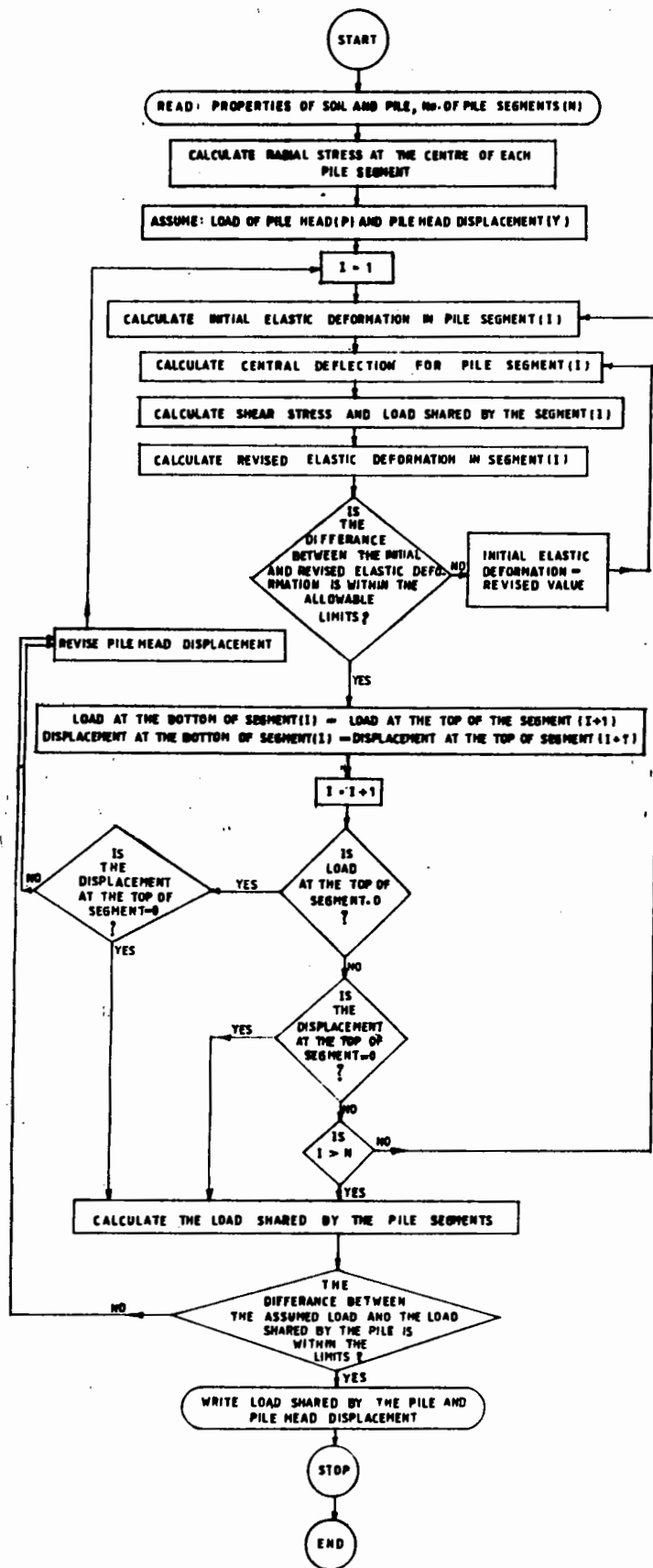


FIG. 7.3 FLOW CHART FOR MODIFIED T-Z MODEL

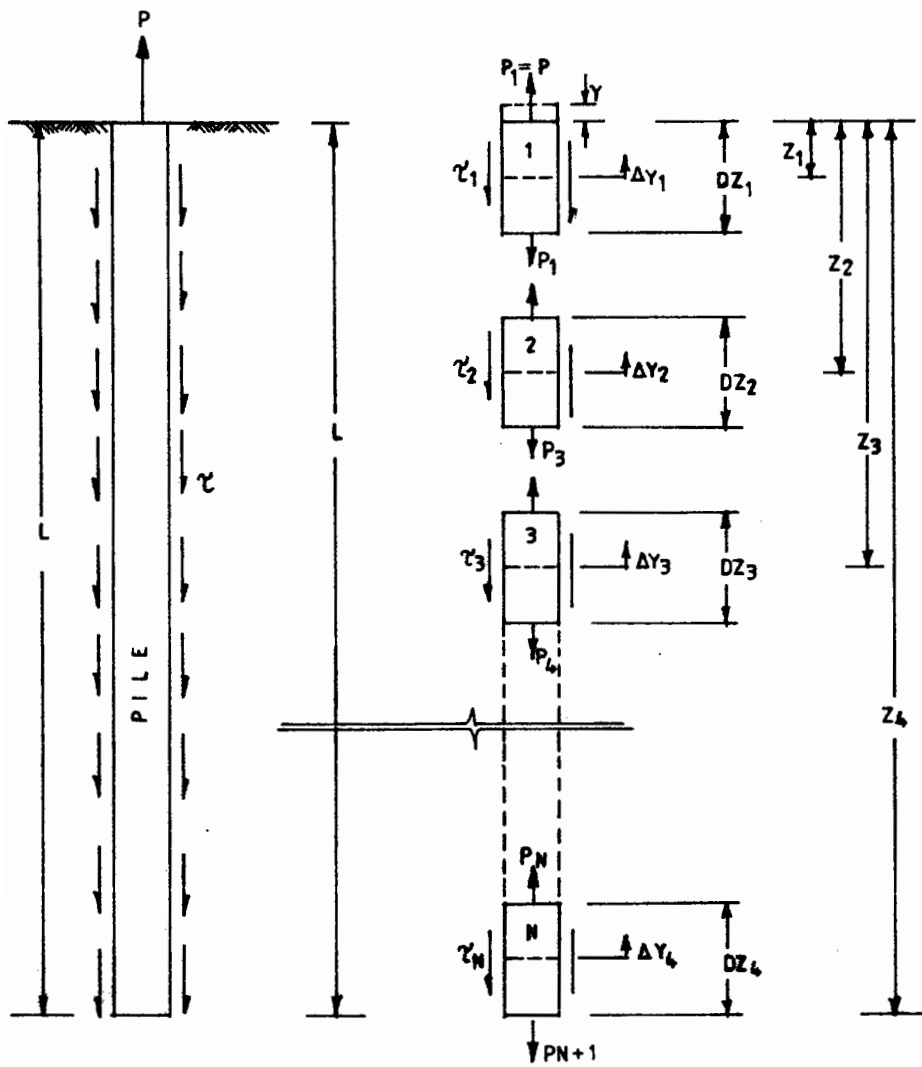


FIG.7.4. LOAD DISPLACEMENT COMPUTATION ALONG THE PILE
(Modified T-Z model)

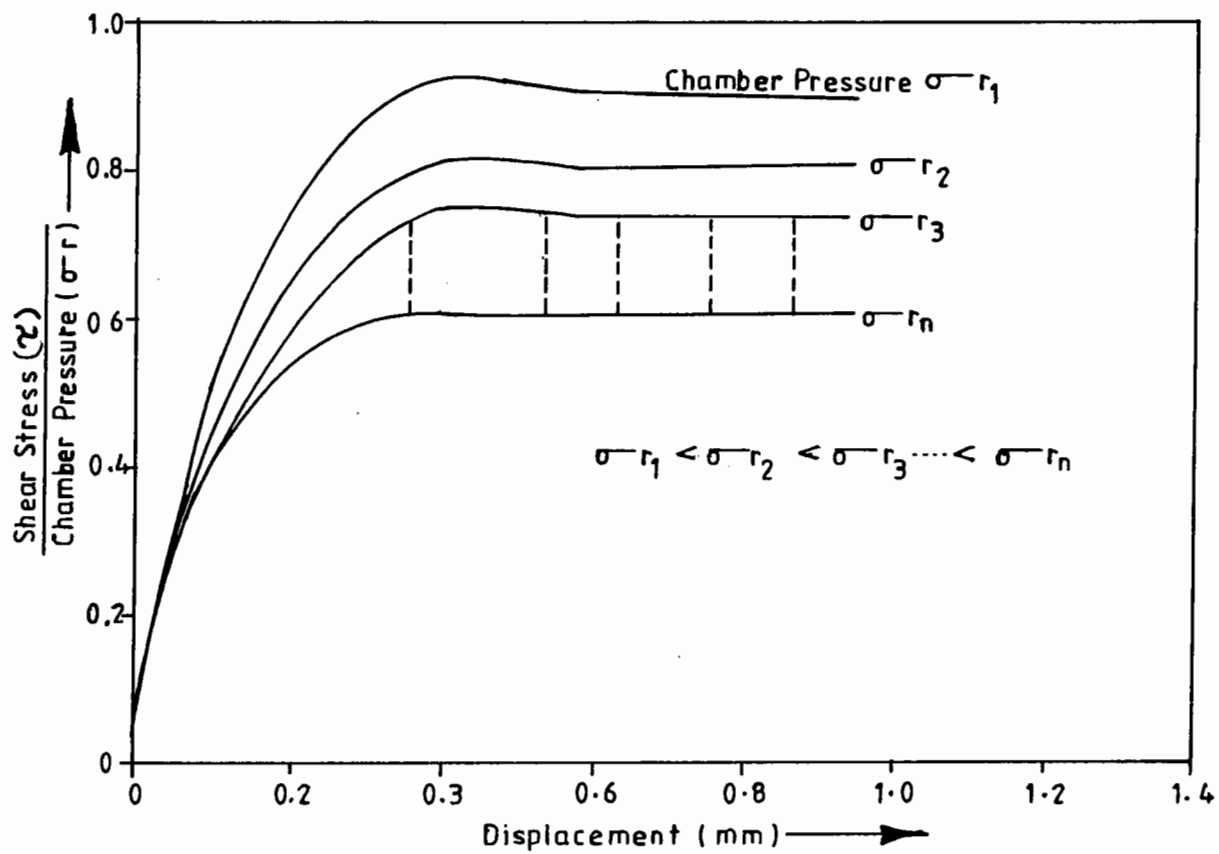


FIG. 7.5. T - Z CURVES (An Illustration)

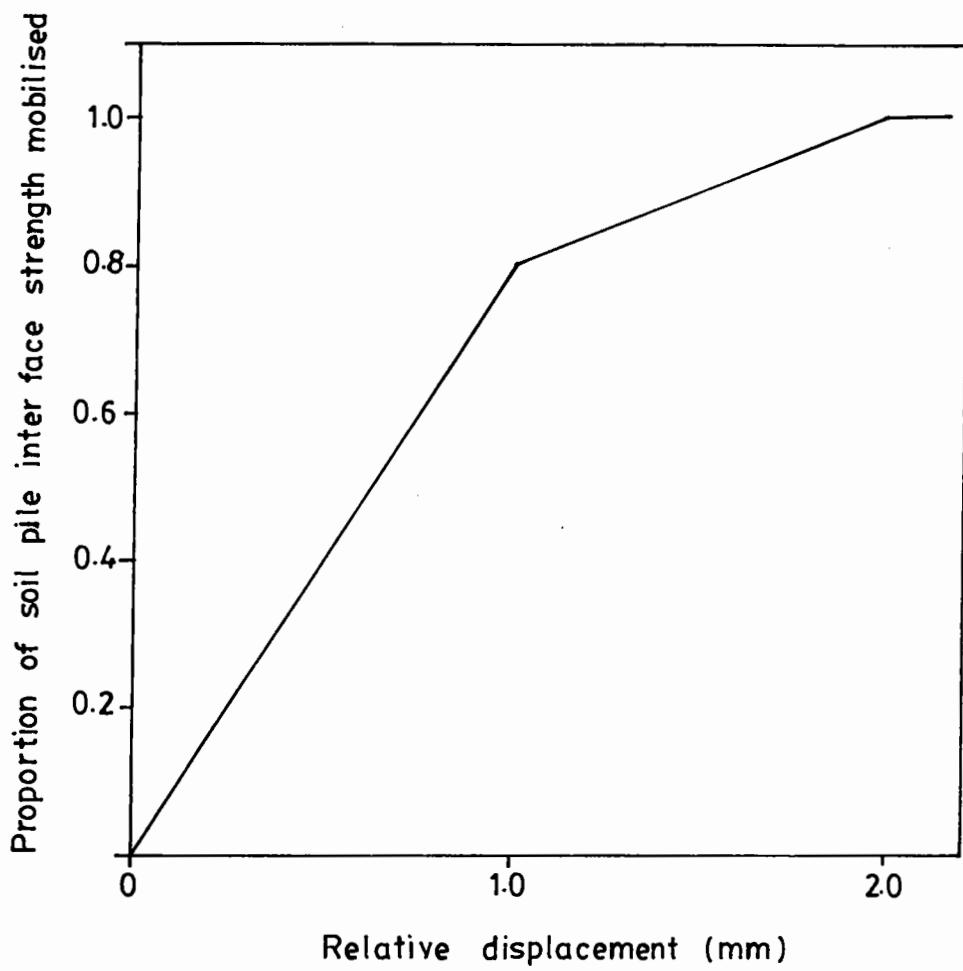


FIG. 7.6. T-Z CURVE USED

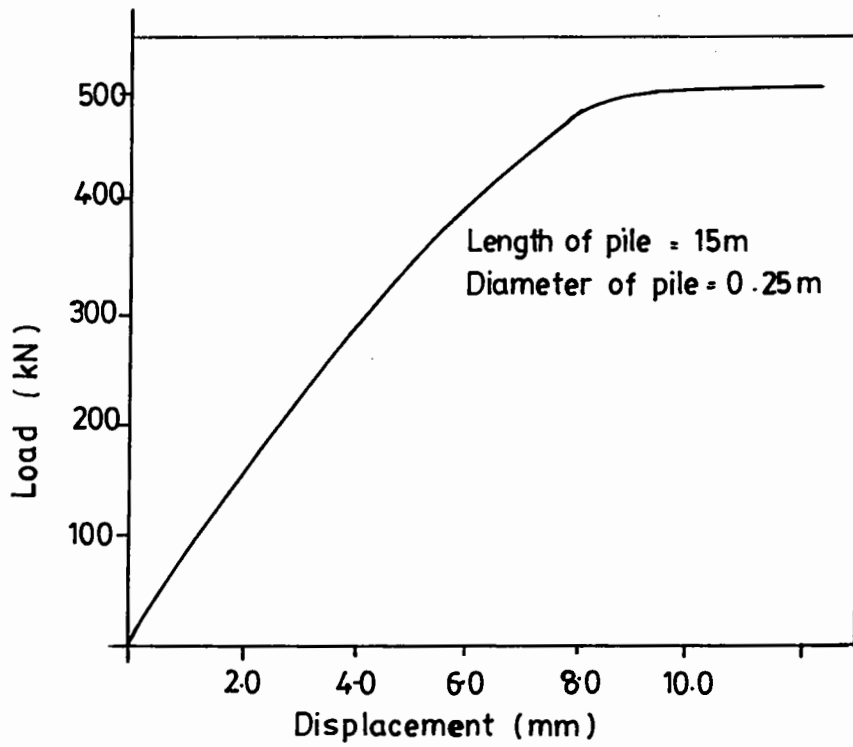


FIG. 7.7. LOAD DISPLACEMENT CURVE

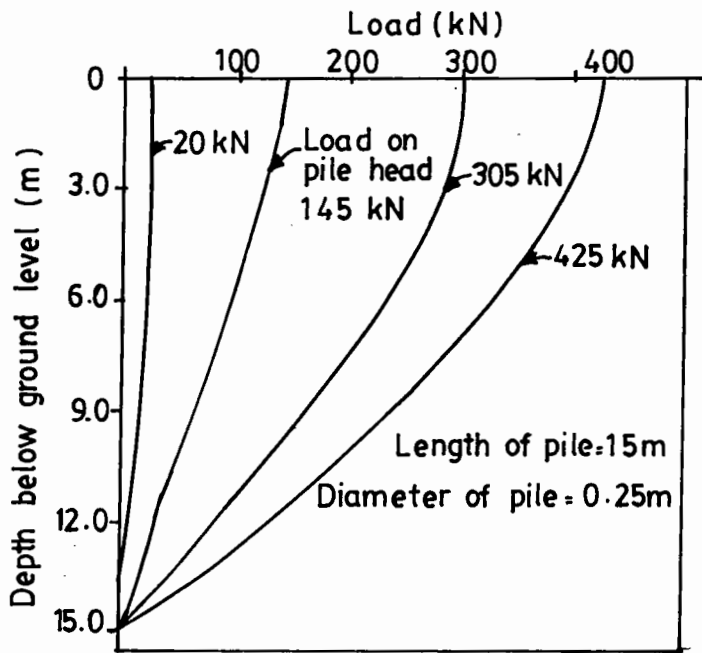
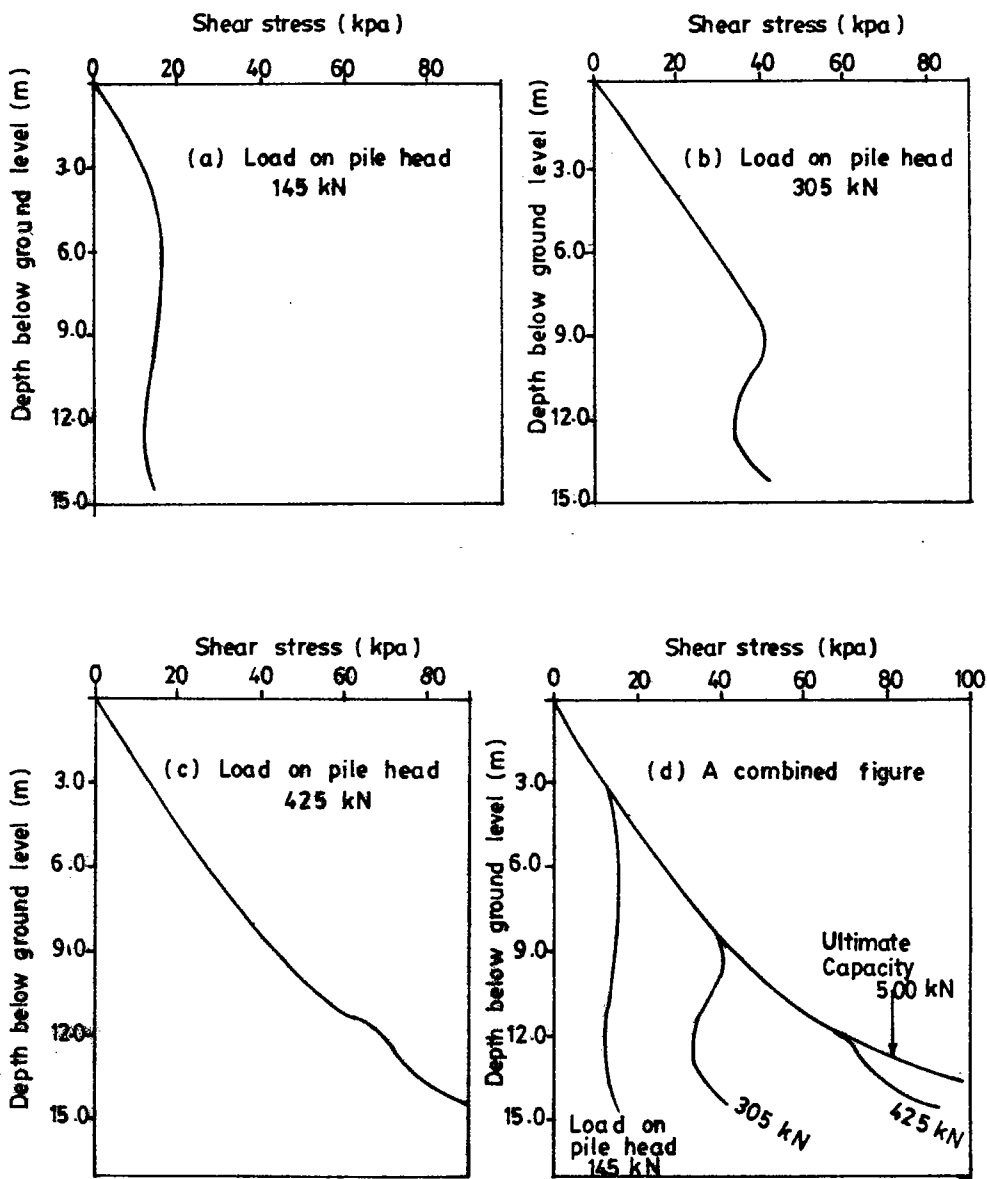


FIG. 7.8. LOAD DISTRIBUTION ALONG THE PILE LENGTH



Length of pile = 15 m
 Diameter of pile = 0.25m
 Ultimate capacity of pile = 500 kN

FIG. 7.9. SHEAR STRESS DISTRIBUTION UNDER DIFFERENT PILE HEAD LOADS

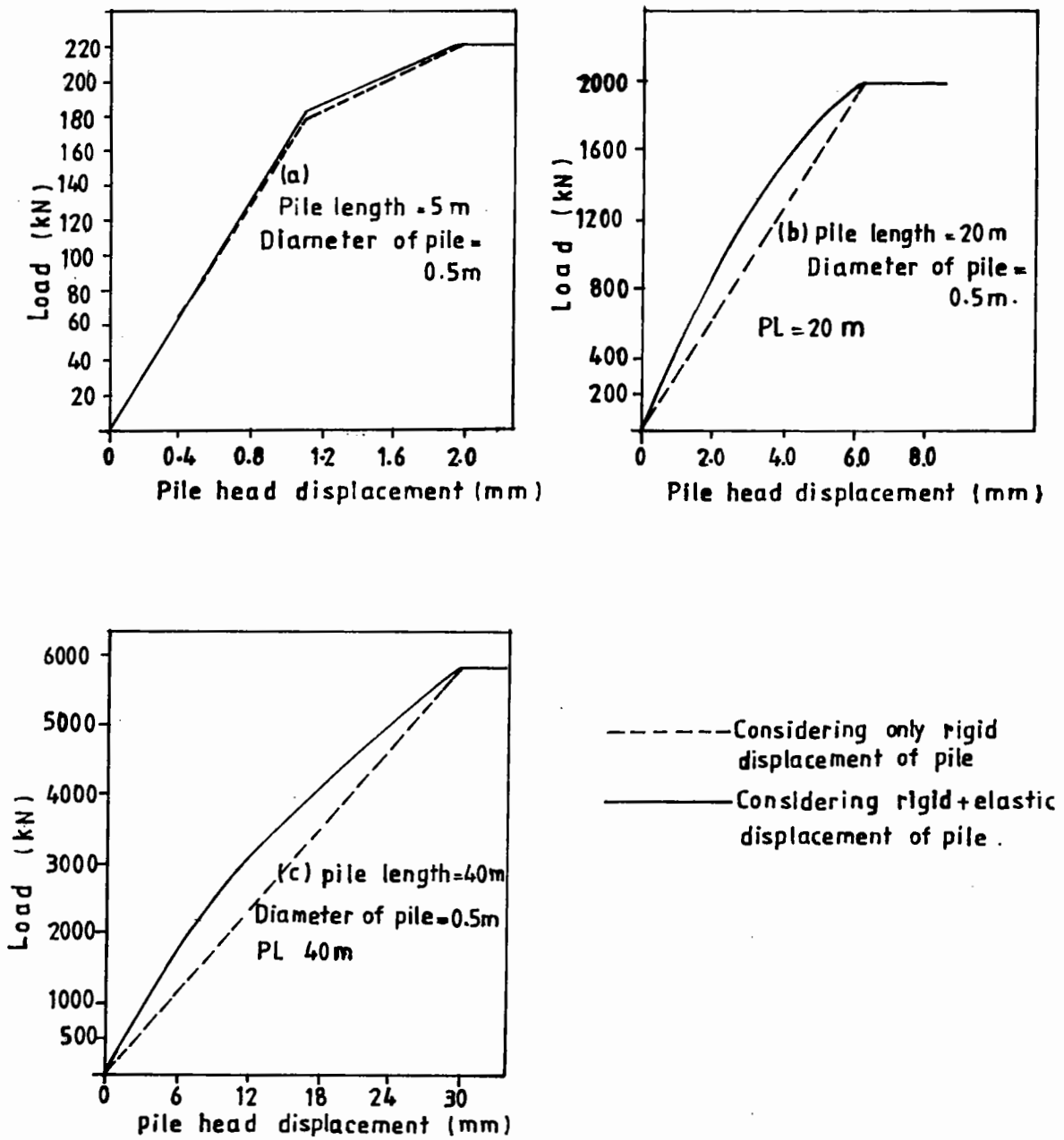


FIG.7.10. LOAD DISPLACEMENT BEHAVIOUR OF PILES OF DIFFERENT LENGTHS— EFFECT OF CONSIDERING ELASTIC DEFORMATION OF PILE

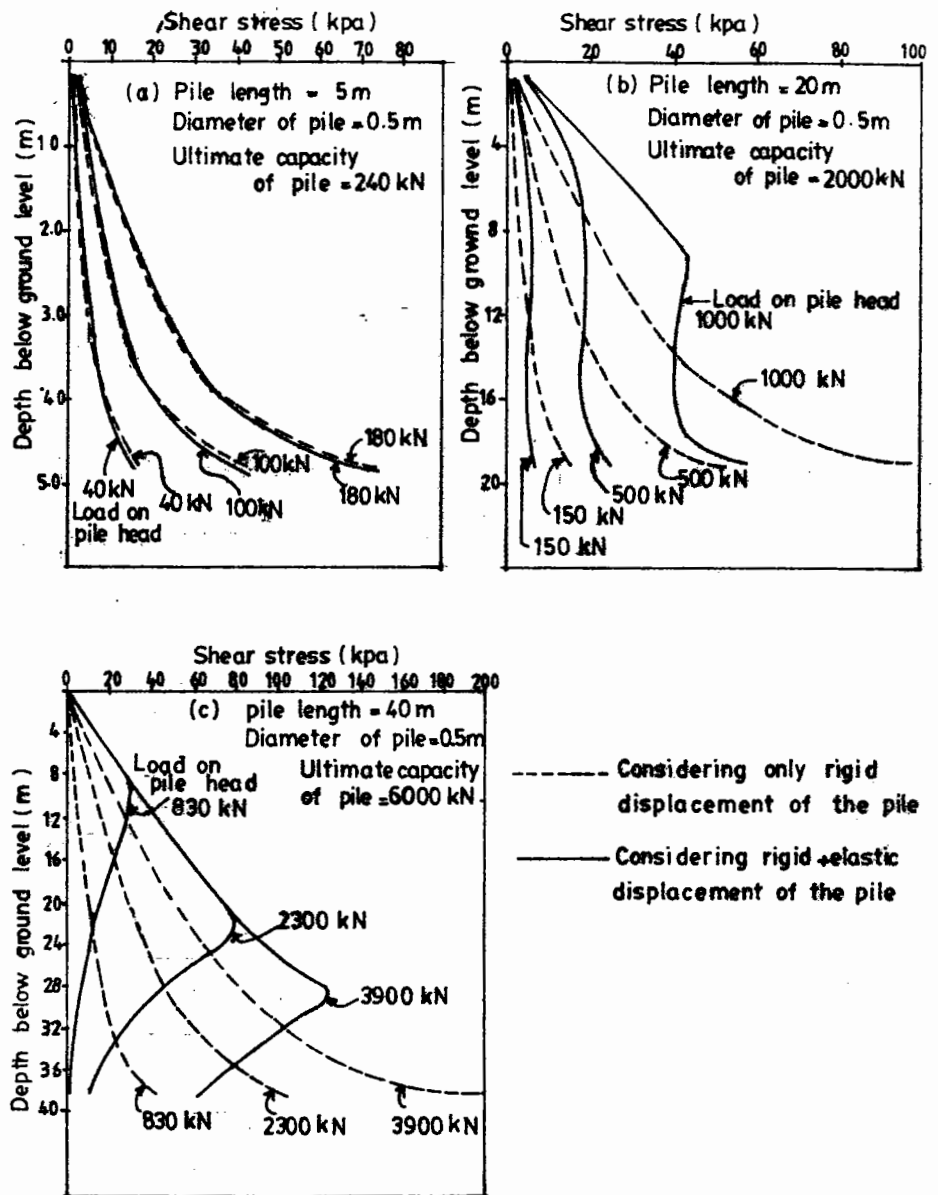
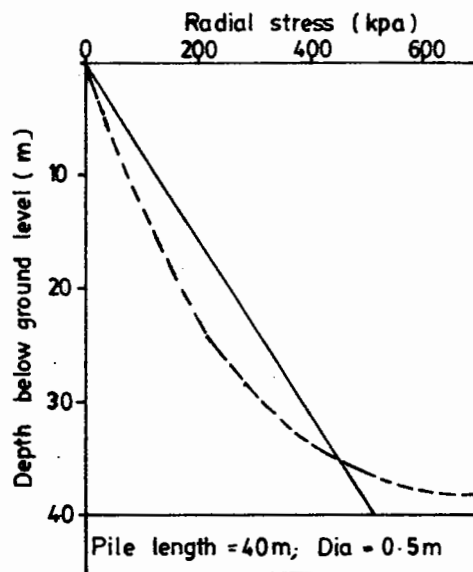
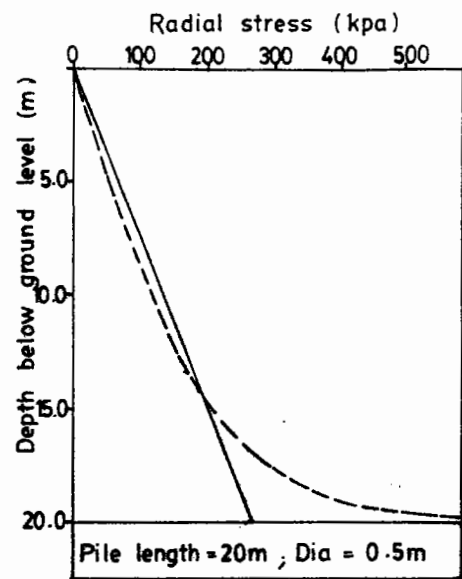
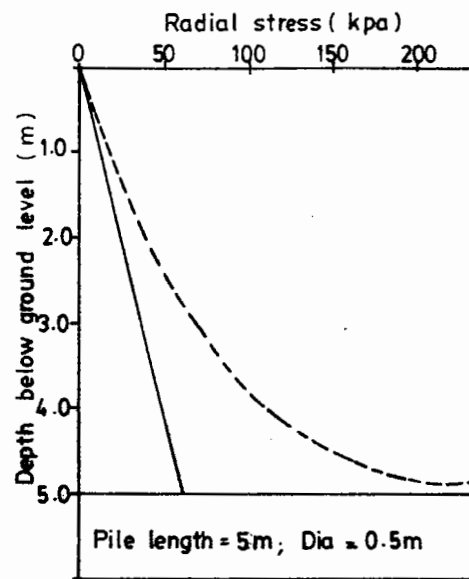


FIG. 7.11. SHEAR STRESS DISTRIBUTION ALONG THE LENGTH OF PILES - EFFECT OF CONSIDERING ELASTIC DEFORMATION OF PILE



————— From Equation (7.1)

----- From Equation (7.2)

$$\sigma_r = 0.75 \sigma_v \text{ ----- Eq. (7.1)}$$

$$\sigma_r = 0.7(\sigma_v)^{0.89} e^{(2.91 DR)} (h/R_0)^{-0.33}$$

----- Eq.(7.2)

FIG.7.12. RADIAL STRESS DISTRIBUTION FOR DIFFERENT PILE LENGTHS.

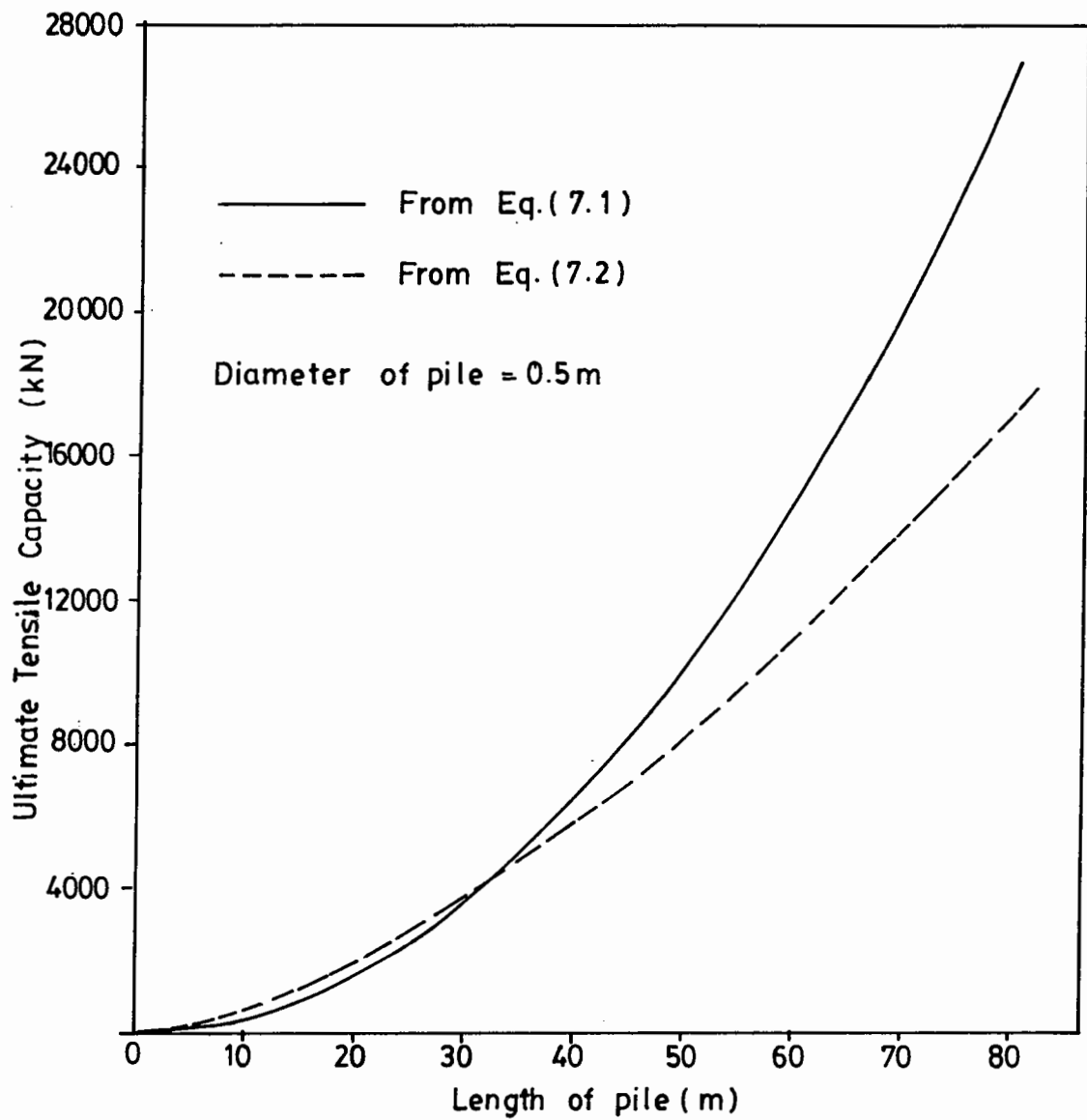


FIG. 7.13. VARIATION IN PILE CAPACITY—EFFECT OF METHOD OF COMPUTING RADIAL STRESS

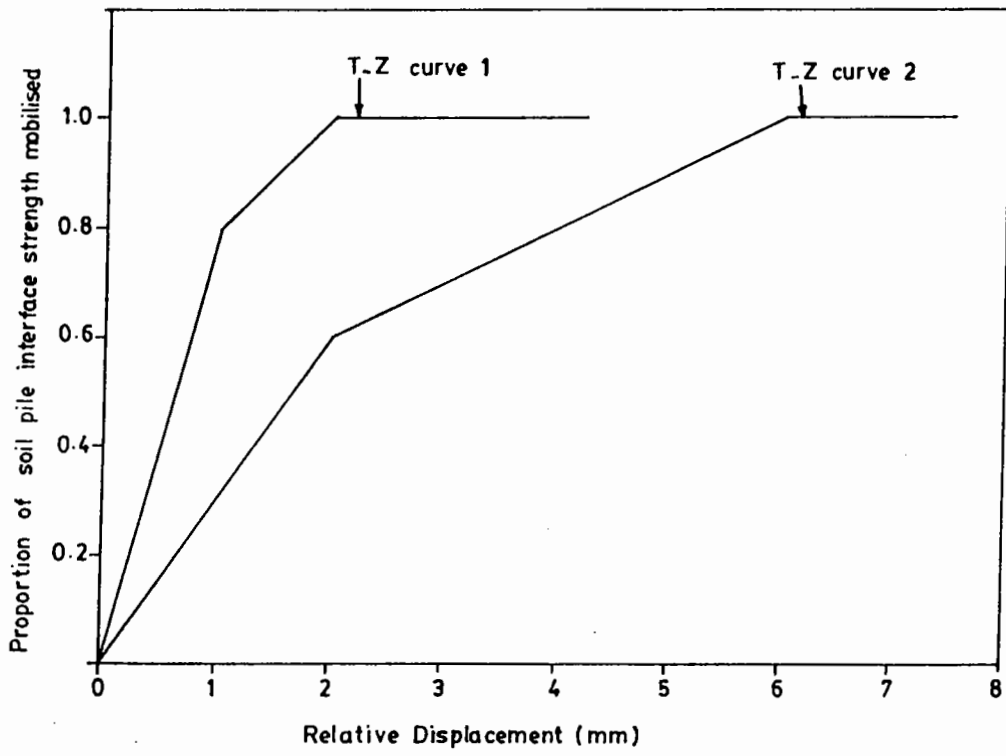
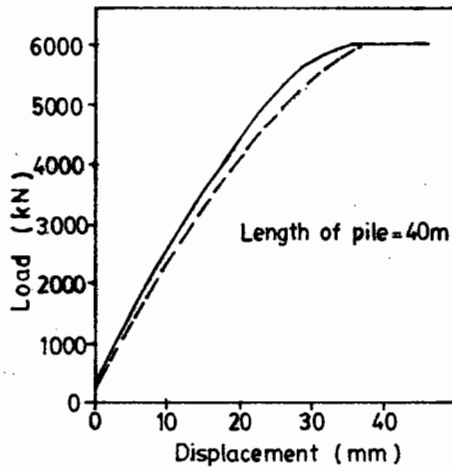
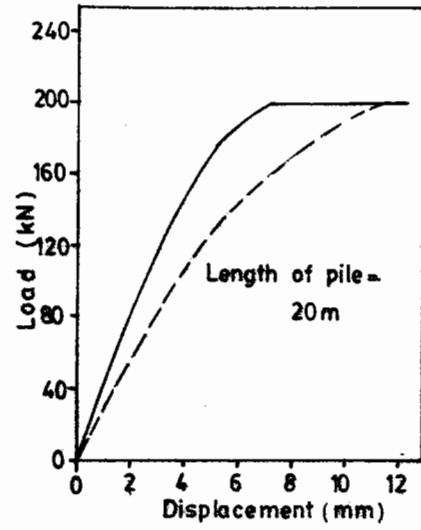
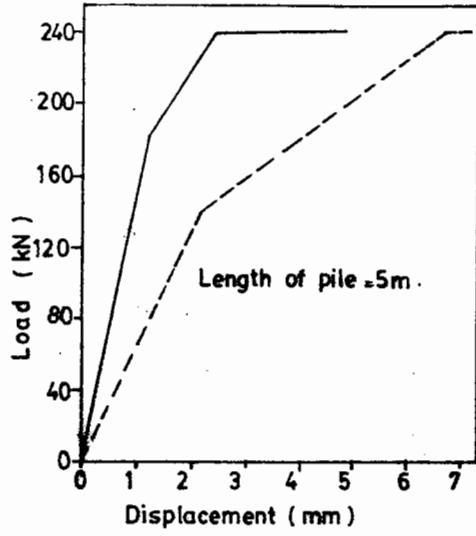


FIG. 7.14. T-Z CURVES USED FOR COMPARISON



— Using T-Z Curve -1 .
 - - - Using T-Z Curve -2

FIG.7.15. LOAD DISPLACEMENT BEHAVIOUR OF PILES OF DIFFERENT LENGTHS - EFFECT OF T-Z CURVE .

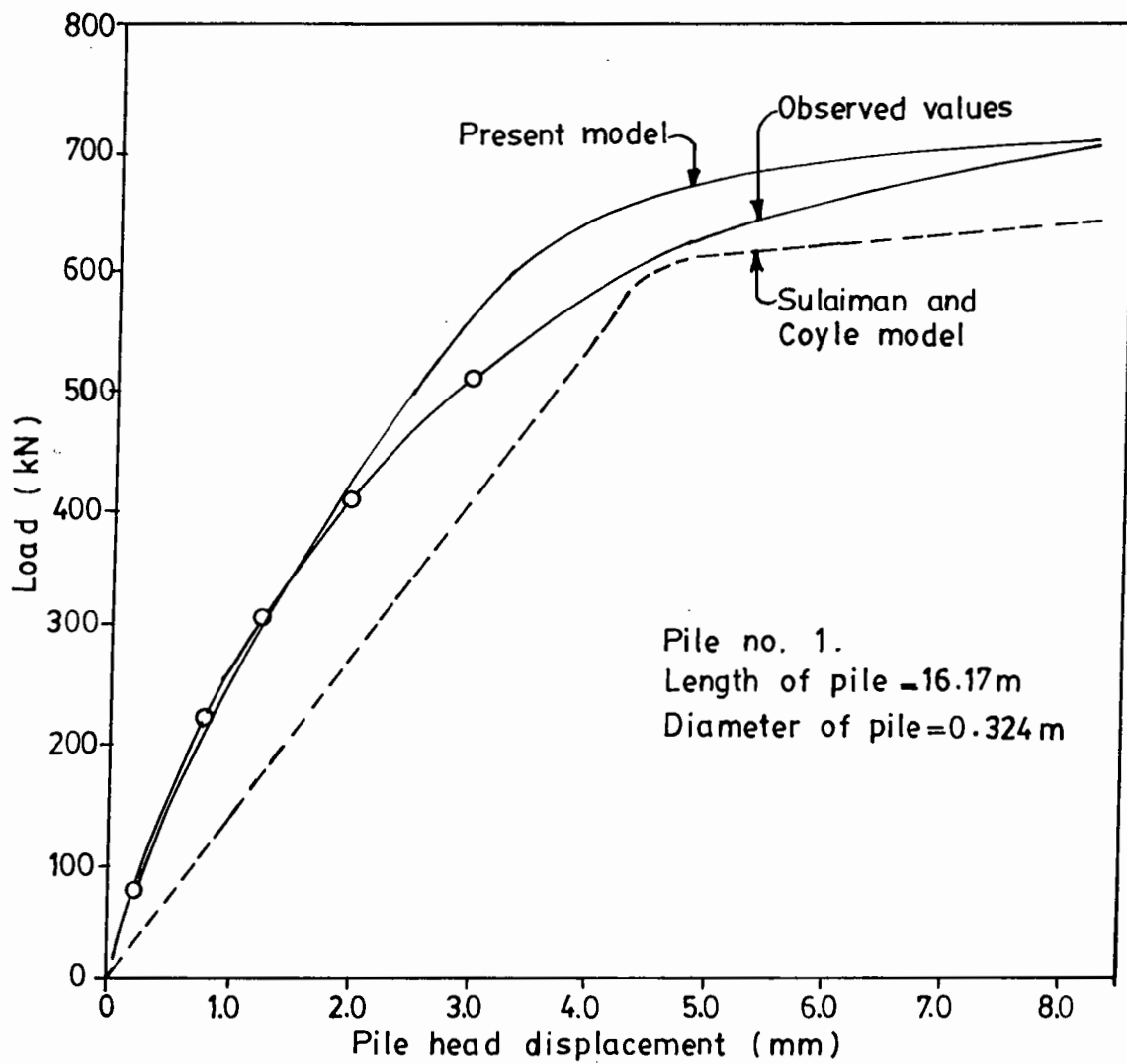


FIG. 7.16. COMPARISON OF LOAD DISPLACEMENT BEHAVIOUR OF A FIELD PILE

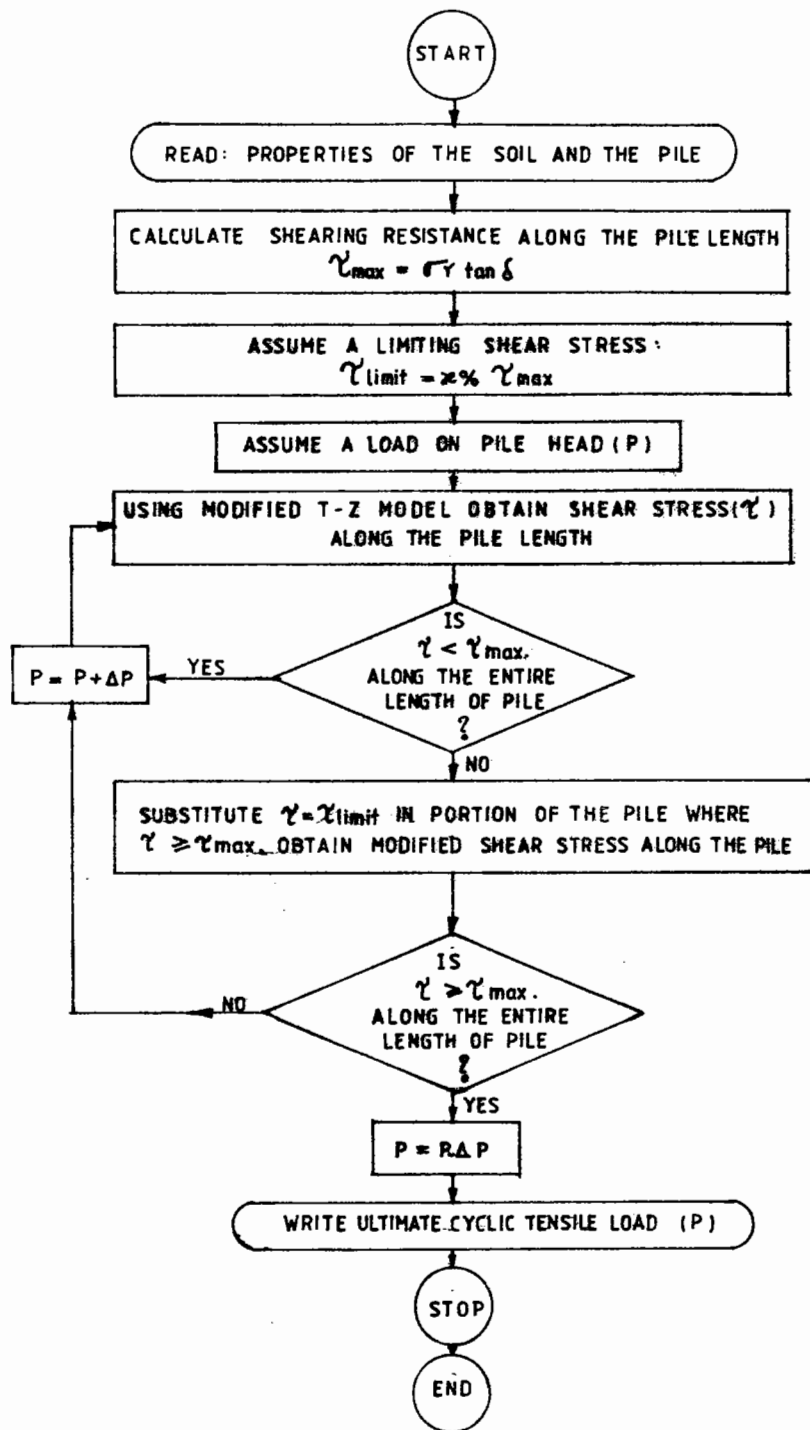


FIG. 7.17. FLOW CHART TO OBTAIN AN ULTIMATE CYCLIC TENSILE LOAD

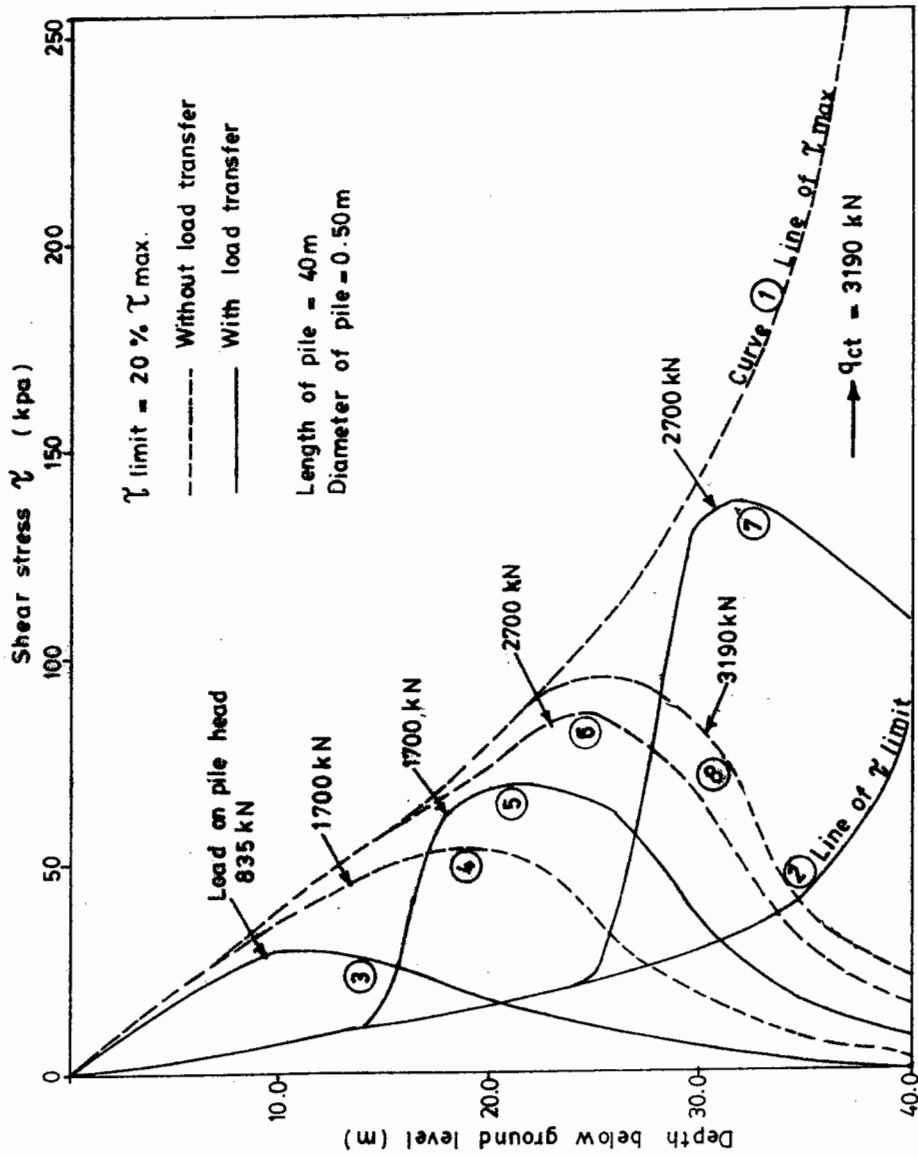


FIG. 7.18. SHEAR STRESS DISTRIBUTION WITH AND WITHOUT CONSIDERING LOAD TRANSFER MECHANISM (τ limit = 20% τ max.)

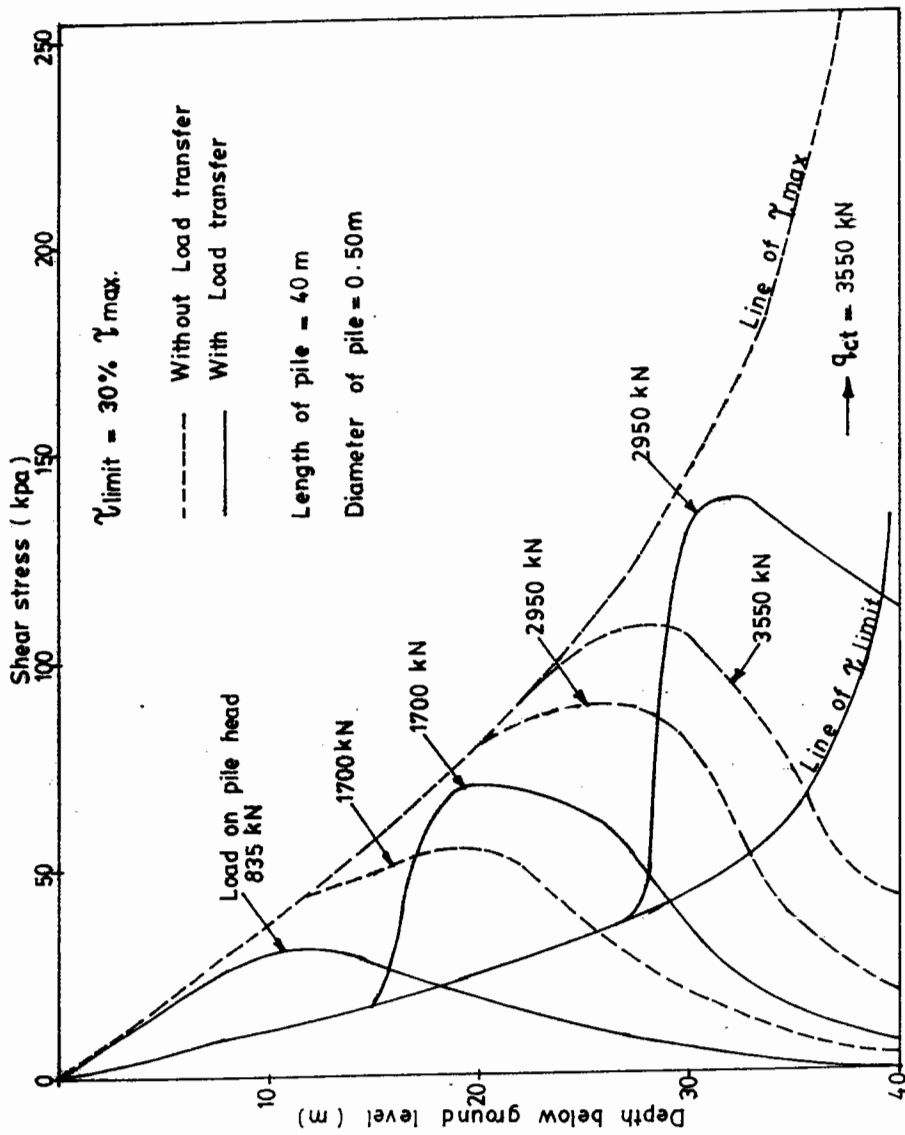


FIG.7.9. SHEAR STRESS DISTRIBUTION WITH AND WITHOUT CONSIDERING LOAD TRANSFER MECHANISM ($\tau_{limit} = 30\% \tau_{max}$.)

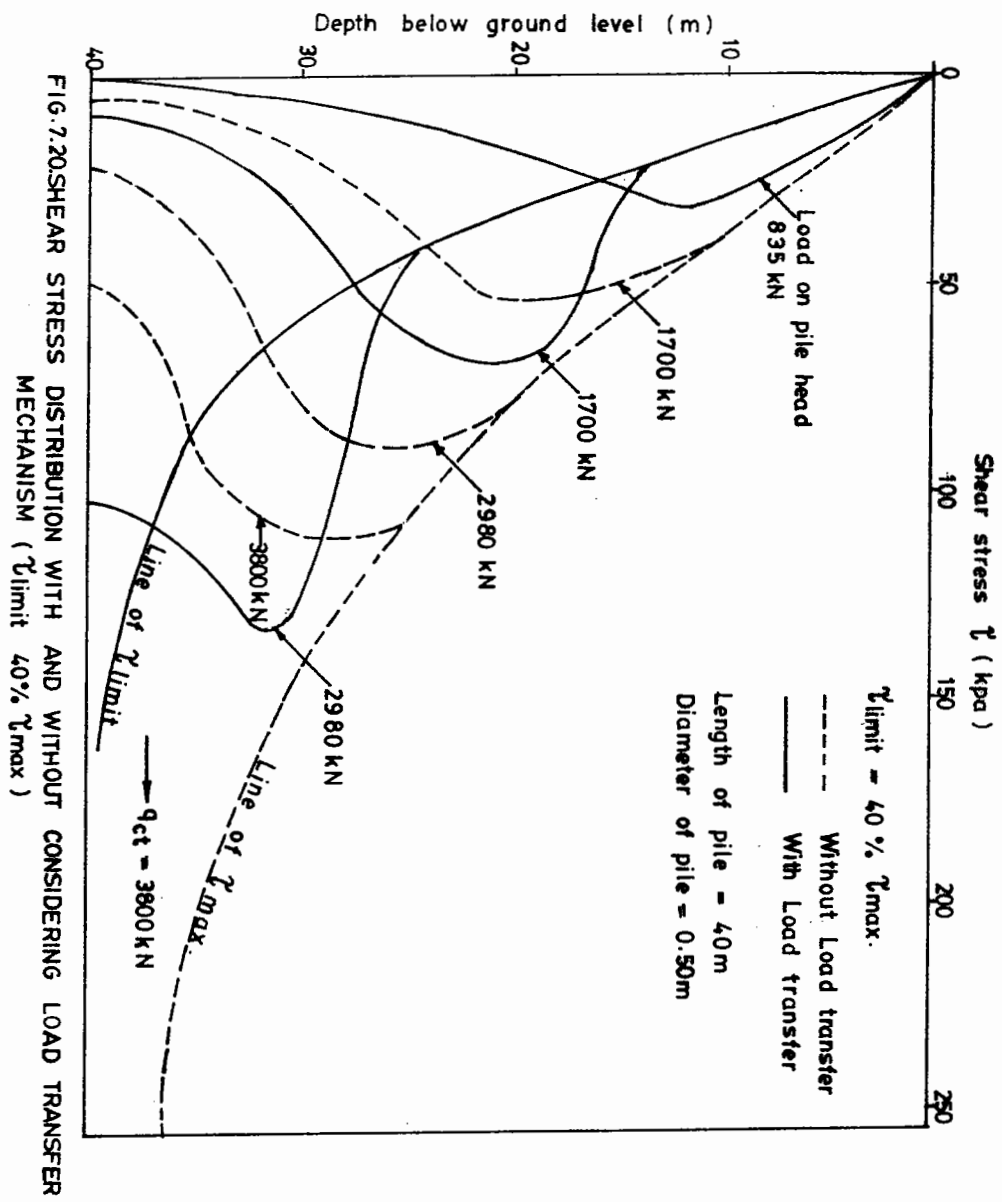


FIG.7.20.SHEAR STRESS DISTRIBUTION WITH AND WITHOUT CONSIDERING LOAD TRANSFER MECHANISM (τ_{limit} 40% τ_{max})

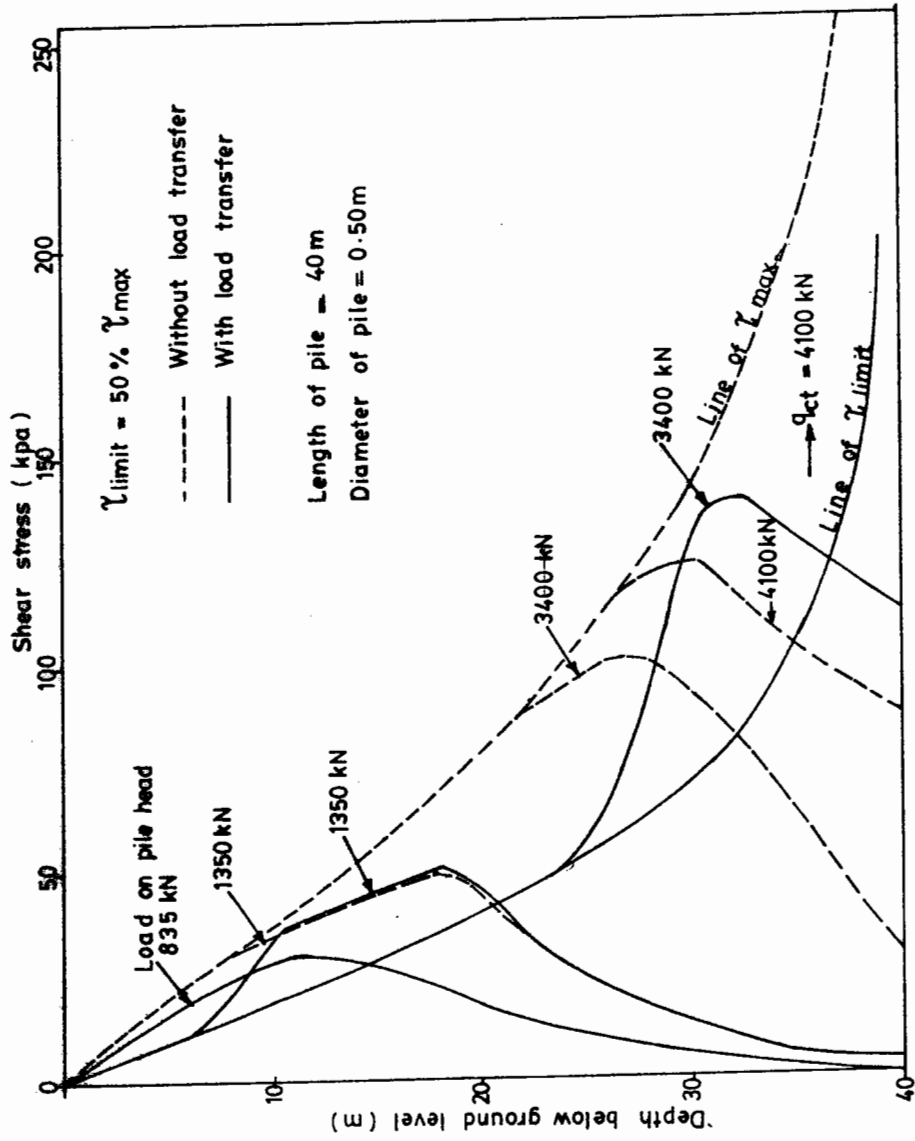


FIG.7.21.SHEAR STRESS DISTRIBUTION WITH AND WITHOUT CONSIDERING LOAD TRANSFER MACHANISM ($\tau_{limit} = 50\% \tau_{max}$.)

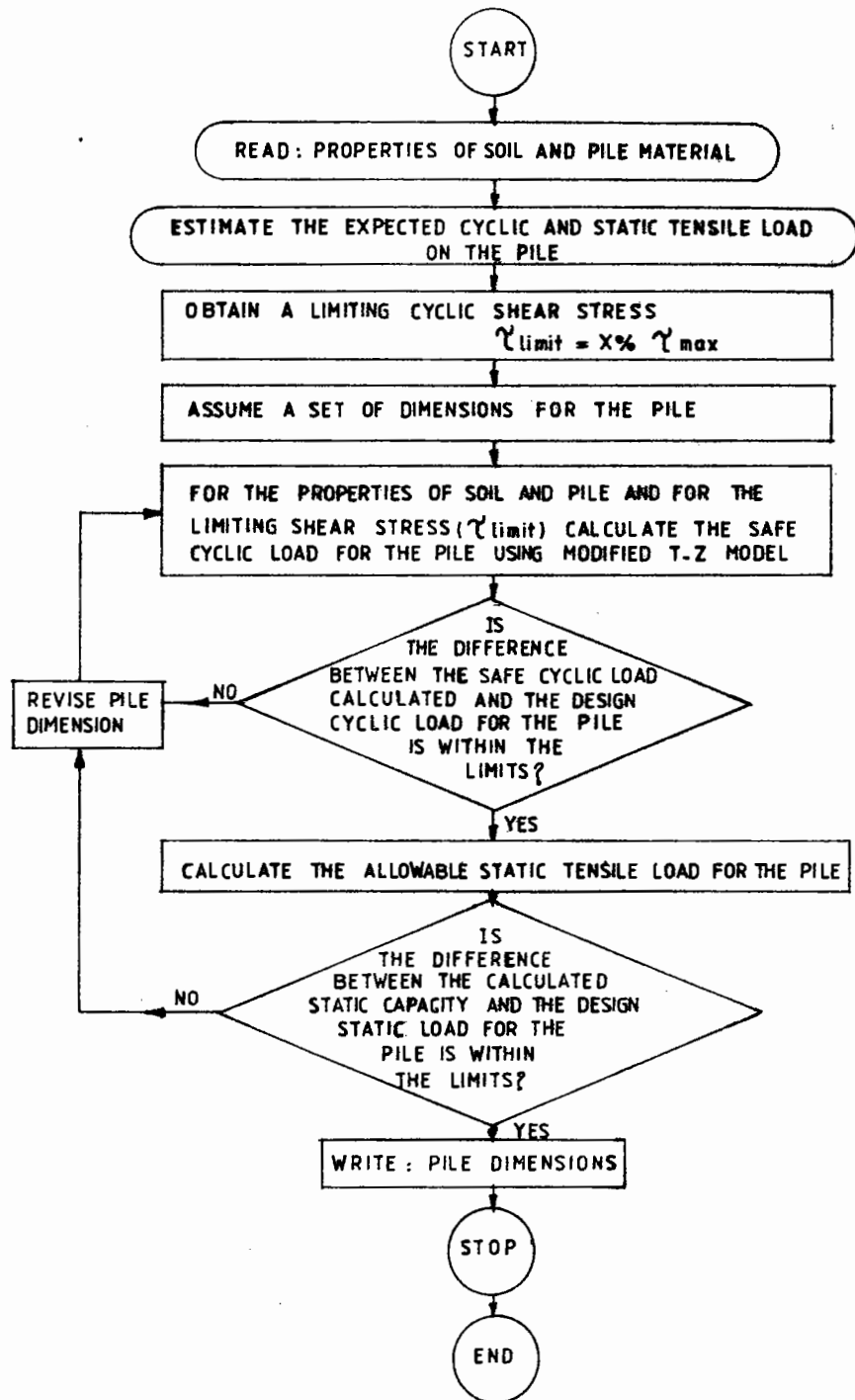


FIG.7.22.FLOW CHART FOR THE DESIGN OF PILE UNDER CYCLIC TENSILE LOAD

CONCLUSIONS

While most piles are subjected to compression during service, there are a number of situations where piles are required to carry tension. These include foundations of transmission towers, gas holders, mooring systems for ocean surface or submerged platforms. However, serious attempts to understand the behaviour of piles under monotonic and cyclic tensile loading have been made with the development of Tension Leg Platforms (TLP) for deep offshore oil fields as an economical alternative structure. The piles used for TLP foundation are subjected to static pull-out force superimposed by a cyclic tensile force. Further, an offshore foundation is subjected, majority of the time, to small cyclic loads and at some times the load reaches a peak value. Thus, there is a need to understand the behaviour of pile not only under a constant cyclic load but also subsequent to a peak loading. There is very limited literature available on the behaviour of pile under cyclic tensile loading, particularly for piles embedded in sand. Hence, the present investigation was directed towards a comprehensive study on piles in sand subjected to cyclic tensile loading to understand:

1. the displacement of pile under cyclic tensile loading
2. the mechanism of pile failure under cyclic tensile loading
and
3. the response of pile subsequent to peak loading.

The objective was planned to be met through a comprehensive laboratory study on model piles. Based on a critical analysis of the details of existing model pile test apparatus reported in literature, a model pile test apparatus was designed and developed. The apparatus was specially designed to effect an uniform increase in effective stresses in the test bed by creating vacuum into the sand-bed. Further, it had facility to measure

stresses in sand using pressure cells and settlement of sand surface. The working conditions of the apparatus was examined by conducting a set of preliminary experiments and necessary improvements were effected. Monotonic and cyclic tensile load tests were conducted on different diameter model piles and measurements of pile head displacement, variation of radial stress in sand-bed, settlement of sand surface and load distribution along the pile length were made. The results of these tests enabled understanding of the load-displacement behaviour of pile and the mechanism of pile failure under cyclic tensile loading. In a few tests, the pile was initially subjected to a large cyclic load for a few cycles and then the load was reduced to a small cyclic load. Results of these tests have thrown light on the behaviour of pile subsequent to peak loading.

Based on the results of the experimental investigation, it was considered necessary to modify the existing T-Z model suggested by Sulaiman and Coyle (1976) for the estimation of load-displacement behaviour of pile under monotonic tensile loads. Accordingly, the modified T-Z model has been proposed. The proposed T-Z model was found to estimate the load-displacement behaviour of some field piles more closely than the existing T-Z model. Based on the modified T-Z model, a procedure of estimating the safe cyclic load for a pile has been suggested.

In addition an attempt was made to develop an apparatus, called the soil-pile-slip test apparatus, to obtain T-Z curves for tension piles. The tests carried out using this apparatus, though they could not produce the desired T-Z curves due to certain limitations realised at the analysis stage, provided information on the changes in radial stress during pile loading.

Based on the above investigations the following conclusions have been drawn:

1). The pile undergoes recoverable and irrecoverable displacement under cyclic loading. The recoverable displacement remains constant and the irrecoverable displacement increases with increase in number of cycles.

2). The displacement curve, for a pile under cyclic loading, exhibits three distinct zones. Initially, for a few cycles, the displacement increases rapidly and then becomes almost constant (Zone-I). Then follows a stable zone (Zone-II) where there is insignificant increase in displacement with increase in number of cycles. The stable zone continues for a very large number of cycles, if the cyclic load level is within the safe limits. However, if the magnitude of cyclic load is large, the width of the stable zone shrinks and becomes less well defined. Beyond the stable zone, the pile head displacement increases at a faster rate till failure. This zone of large displacement is termed as unstable zone (Zone-III).

3). In tests carried out up to a maximum of 100,000 cycles, the safe cyclic load was observed to be 30% of ultimate tensile capacity of the pile.

4). Even under one-way (tensile) cyclic loading, the soil around the pile undergoes two-way shear.

5). Under monotonic tensile loading, the sand around the pile undergoes slip dilation resulting in an increase in radial stress on the pile surface where as under cyclic tensile loading, the sand around the pile undergoes reduction in volume accompanied by a reduction in radial stress on the pile surface.

6). The sequence of events leading to failure of a pile under cyclic tensile loading is as follows: The application of cyclic tensile loading causes two-way shear and a reduction in normal stress on the pile surface causing a reduction in the

shearing resistance leading to the failure of the pile.

7). The behaviour of a pile subsequent to a peak cyclic loading is not adversely affected as long as the displacement of the pile is within the stable zone of the displacement curve. However, if the pile reaches a state of failure under the peak cyclic loading its response to a subsequent reduced load level deteriorates substantially.

8). The T-Z model proposed by Sulaiman and Coyle (1976) has been modified to obtain the load-displacement behaviour of piles under tensile loading. This modified model provides better estimate of the load displacement behaviour of piles than the existing T-Z model.

9). Based on the modified T-Z model, a procedure of estimating the safe cyclic tensile load and a design method have been proposed for piles under cyclic tensile loads.

8.1 RECOMMENDATIONS FOR FUTURE WORK

Based on the experience gained through the present investigation, further investigation on the behaviour of piles under cyclic tensile loading in the following direction is suggested.

1). The present investigation suggests that, cyclic loading causes a reduction in normal stress on the pile surface leading to failure. Further, load transfer from upper portion to the lower portion of the pile is predicted by the present numerical model and also observed by Karlsrud and Haugen (1983) in field in the case of pile subjected to cyclic tensile loads. Additional evidence on the above obtained through an experimental investigation on large scale model piles, instrumented at closer intervals along the pile, can improve our confidence in the known

failure mechanism of the pile failure under cyclic tensile loading.

2). The present investigation was carried out using silica sand. The offshore fields of countries such as India, Australia, Indonesia, Mexico and USA (Rodgers, 1957) have calcareous soils for considerable depths below the sea-bed. The calcareous soils are found to be liable to reduction in strength considerably during cyclic loading (Datta et al., 1982; Demars et al., 1982 and Murff, 1987). The behaviour of piles in calcareous soils under cyclic loading could be different and this needs investigation.

3). During the present investigation, a method of estimating safe cyclic load for a pile is proposed. The method envisages limiting of shear stress (τ_{limit}) along the pile surface to a percentage of the shearing resistance (τ_{max}). However, at the present juncture no definite value of τ_{limit} could be assigned. Back analysis of some of the working piles subjected to cyclic tensile loads using the modified T-Z model suggested in the present investigation can help assign a τ_{limit} value for the design purpose.

4). The soil-pile-slip test apparatus developed during the present investigation could not produce the desired T-Z curves. However, it has provided the possibility of improving the method of measurements. Hence, the experience suggest that the existing miniature pile test apparatus designed by Coyle and Sulaiman (1967) may be adopted with certain modifications such as placing of the load cell and the LVDT within the triaxial cell as shown in the soil-pile-slip test apparatus (Fig.3.14). Such an arrangement is expected to provide reliable T-Z curves.

REFERENCES

Abedi, A. F.Y., (1978), "The behaviour of two soils in repeated triaxial compression", MSc thesis, Queen's university, Kingsyon, Canada.

Abood, A.S., (1989), "Load capacity of piled foundation under non-cyclic and cyclic uplift loading", PhD thesis, University of Wales.

Airey, D. W., Al-Douri, R. H. and Poulos, H. G., (1992), "Estimation of pile friction degradation from shearbox tests", Geotechnical Testing Journal, Vol. 15, No. 4, 388-392.

Al-Jumaily, F.A., (1981), "Further studies on the repeated loading of piles in sand", Ph.D thesis, University of Sheffield. U.K.

Andersen, K. H., (1991), "Foundation design of offshore gravity structures", In: Cyclic loading of soils, Eds. O'Reilly and Brown, Blackie, London.

Andersen, K. H., Lacasse, S., Aas, P. M. and Andenseas, E., (1982), "Review of foundation design principles for offshore gravity platforms", BOSS-82', Vol. 1, 243-261.

Angelides, D. C., Chen, C. Y. and Will, S. A., (1983), "Dynamic response of tension leg platform", BOSS-83', Vol. 2, 100-120.

Angemeer, J., Carlson, E. and Klick, J. H., (1973), "Techniques and results of offshore pile load testing in calcareous soils", 5th Offshore Technology Conference, paper No. OTC 1894.

Ansell, P and Brown, S. F., (1978), "Cyclic simple shear apparatus for dry granular material", Geotechnical Testing Journal, Vol. 2, p82-92.

ASTM (1970), "Annual book of American Society for testing and materials", Philadelphia, Pa., 1970.

Audibert, J. M. E. and Bamford, S. R., (1989), "TLP foundation design and analysis", Tension leg platforms: A state of the art review, Edited by Zeki Demirbilek, Published by ASCE, 77-117.

Baghdadhi, Z. A., Ghazali, F. M and Khan, A. M., (1991), "Model pile testing in carbonate sediments of the Red Sea", Canadian geotechnical journal, No. 28, p423-433.

Bea, R. G., Dover, A. R. and Audibert, J. M. E., (1982), "Pile foundation design considerations for deep-water structures", BOSS-82', Vol. 1, 125-140.

Bond, A. J., (1989), "Behaviour of displacement piles in an over consolidated clay", PhD thesis, University of London.

Bond, A. J. and Jardine, R. J., (1989), "Cannon park piling project: The behaviour of displacement piles in over consolidated clay", OTH Report, HMSO, London.

Bond, A. J. and Jardine, R. J., (1991), "Effects of installing displacement piles in a high-OCR clay", Geotechnique 41, No. 3.

Bond, A. J., Jardine, R. J. and Dalton, J. C. P., (1991), "Design and performance of the imperial college instrumented pile", Geotechnical Testing Journal, ASTM, Vol. 4, No. 4, 413-424.

Boulon, M., Desrues, J., Foray, P. and Forgue, M., (1980), "Numerical model for foundation under cyclic loading application to piles", Proc. Int. Symp. on soils under cyclic and transient loading, Swansea, Vol. 1, 681-694.

Boulon, M. and Foray, P., (1986), "Physical and numerical simulation of lateral shaft friction along offshore piles in sand", Proc. 3rd Int. Conf. on numerical methods in offshore piling, Editions Technir, Paris, France, p127-148.

Boyce, J. R., (1976), "The behaviour of a granular material under repeated loading", PhD thesis, University of Nottingham.

Boyce, J. R., (1980), "A non-linear model for the elastic behaviour of granular materials under repeated loading", Proc. Int. Symp. on soils under cyclic and transient loading, Swansea, U. K. p285-294.

Bradshaw, H., Barton, R. R. and McKenzie, R. H., (1984), "The Huton foundation design", 16th Offshore Technology Conference, paper No. OTC 4807.

Briaud, J. L. and Audibert, J. M. E., (1990), "Some thoughts on API RP2A for vertically loaded piles", 22nd Offshore Technology Conference, Paper No. OTC 6418, 9-16.

Brown, S. F., (1977), "state-of-the-art report on field instrumentation for pavement experiments", In: Multiple aspects of soil mechanics, Transportation Research Record 640, National academy of Sciences, Washington, 13-28.

Brown, S. F. and Brodrick, B. V., (1973), "The performance of stress and strain transducers for use in pavement research, Science Research Council, University of Nottingham, Research report.

Brown, S. F., Lashine, A. F. F. and Hyde, A. F. L., (1975), "Repeated load triaxial testing of a silty clay", Geotechnique 25, No.1, 95-114.

BS 1377 (1990), "British standards for Soil testing".

Chan, F. W. K., (1990), "Permanent deformation resistance of granular layers in pavement", Ph.D thesis, University of Nottingham. U.K.

Chan, S. F., (1976), "The behaviour of piles subjected to static and repeated loads", PhD thesis, University of Sheffield, U. K.

Chan, S. F. and Hanna, T. H., (1980), "Repeated loading on simple piles in sand", Journal of Geotechnical Engineering, ASCE, Vol. 106, No. GT2, 171-188.

Chaudhuri, K. P. R. and Symons, M. V., (1983), "Uplift resistance of model single piles", Proc. Conf. on Geotechnical practice in Offshore Engineering, Univ. of Texas; Sponsored by geotechnical engineering division, ASCE., 335-355.

Cooke, R. W., (1974), "The settlement of friction pile foundations", Conference on tall buildings, Kuala Lumpur, 7-19.

Cooke, R. W. and Price, G., (1973), "Strains and displacement around friction piles", Proc. 8th Int. Conf. on SMFE, Vol. 2.1, 53-60.

Coop, M. R., (1987), "The axial capacity of driven piles in clay", DPhil thesis, University of Oxford, U. K.

Coop, M. R. and Wroth, C. P., (1989), "Field studies of an instrumented model pile in clay", Geotechnique 39, No. 4, 679-696.

Coyle, H. M. and Castello, R. R., (1981), "New design

correlations for piles in sand", Journal geotechnical engineering division, ASCE, Vol. 107, No. GT7, p965-986.

Coyle, H. M and Reese, L. C., (1966), "Load transfer for axially loaded piles in clay", Journal of soil mechanics and Foundation Engineering, ASCE, Vol. 92, No. SM2, 1-26.

Coyle, H. M. and Sulaiman, I. H., (1967), "Skin friction for steel pile in sand", Journal of soil mechanics and foundation engineering, ASCE, Vol. 93, No. SM6, 261-278.

Dailey, J. E., Karsan, D. E. and Kypke, D. A., (1979), "Comparative study of offshore structure concepts for deep water applications", Pacific coast joint chapter meeting, American petroleum institute, California.

Datta, M., Gulhati, S. K. and Rao, G. V., (1979), "Crushing of calcareous sands during shear", 11th Offshore Technology Conference, paper No. OTC 3525.

Datta, M., Rao, G. V. and Gulhati, S. K., (1980), "Development of pore water pressure in dense calcareous sand under repeated compressive stress cycles", Proc. Int. Symp. on soils under cyclic and transient loading, Swansea, U. K.

Datta, M., Gulhati, S. K. and Rao, G. V., (1982), "Engineering behaviour of carbonate soils on India and some observations on classification of such soil", Geotechnical properties, behaviour and performance of calcareous soils, ASTM STP, 777, 113-140.

Demars, K. R., (1982), "Unique engineering properties and compression behaviour of deep-sea calcareous sediments", Geotechnical properties, behaviour and performance of calcareous soils, ASTM STP, 777, 97-112.

Dennis, Jr. N. D. and Olson, R. E., (1983), "Axial capacity of steel pipe piles in sands", Proc. Conf. on geotechnical practice in offshore engineering, Univ. Texas, Sponsored by geotechnical engineering division of ASCE.

Diyaljee, V. A. and Raymond, G. P., (1982), "Repetitive load deformation of cohesion less soils", the Journal of Geotechnical Engineering, ASCE, Vol. 108, No. GT10, 1215-1229.

Dorby, R. and Vucetic, M., (1987), "Dynamic properties and seismic response of soft clay deposits", Int. Symp. on Geotechnical engineering of soft soils, Soc. Mexicane Mec. Suelos, Vol. 2.

Fitzpatrick, C., (1977), "Repeated loading on saturated Ottawa sand in triaxial test", Report presented to Queen's university, Kingston, Canada.

Francescon, M., (1983), "Model pile tests in clay stresses and displacements due to installation and axial loading", PhD thesis, Churchill college, University of Cambridge, U. K.

Gallager, K. A., (1984), "Tensile loading of piles in a glacial Till", PhD thesis, University of Sheffield, U. K.

Georgiannou, V. N., Hight, D. W. and Burland, J. B., (1991), "Behaviour of clayey sands under cyclic triaxial loading", Geotechnique, Vol. 41, No. 3, p383-393.

Grosch, J. J. and Reese, L. C., (1980), "Field tests on small-scale pile segments in a soft clay deposit under repeated axial loading", 12th Offshore Technology Conference, Paper No. OTC 3869.

Hamilton, J. and Perrett, G. R., (1986), "Deepwater tension

leg platform design", Int. Symp. on Developments in deeper waters, London, Paper No. 9.

Hanna, T. H. and Tan, R. H. S., (1973), "The behaviour of long piles under compressive loads in sand", Canadian geotechnical journal, Vol. 10, p311-340.

Hettler, A., (1982), "Approximation formulae for piles under tension", Proc. Conf. on deformation and failure of granular materials, Int. Union of theoretical and Applied Mechanics (IUTAM), 603-608.

Ishihara, K., (1982), "Evaluation of soil properties for use in earthquake response analysis", Numerical modelling in Geomechanics., R. Dungar, G. N. Pande and J. A. Studer (Eds.), 237-259.

Jardine, R. J., (1985), "Investigation of pile-soil behaviour with special refernce to the foundations of offshore structures", PhD thesis, University of London.

Jardine, R. J., (1991), "The cyclic behaviour of large piles with special reference to offshore structures", In: Cyclic loading of soils, Eds. O'Reilly and Brown, Blackie, London.

Jardine, R. J., Bond, A. J and Lehane, B. M., (1992), "Field experiments with instrumented piles in sand and clay", Conference on Piling: European practice and worldwide trends, Thomas Telford, London, 59-66.

Jardine, R. J. and Christoulas, S., (1991), "Recent Developments in defining and measuring static piling parameters", General report, Proc. Int. Conf. on Deep foundations, Paris, 713-746.

Jardine, R. J., Hight, D. W. and McIntosh, W., (1988), "Hutton tension leg platform foundations: Measurement of pile group axial load-displacement relations", *Geotechnique* 38, No. 2, 219-230.

Jardine, R. J., Everton, S. J. and Lehane, B. M., (1992), "Friction coefficients for piles in cohesionless materials", *Offshore site investigations and foundation behaviour, proc. SUT Int. Conf.*, Kluwer, Dordrecht, p661-680.

Jardine, R. J. and Potts, D. M., (1988), 'Hutton tension leg platform foundations: Prediction of driven pile behaviour', *Geotechnique* 38, No. 2, 231-252.

Jardine, R. J. and Potts, D. M., (1992), "Magnus foundations: Soil properties and prediction of field behaviour", *Proc. Conf. Recent large-scale fully instrumented pile tests in clay*, Institution of Civil Engineers, London, 69-83.

Jardine, R. J., Potts, D. M., Fourie, A. B. and Burland, J. B., (1986), "Studies of the influence of non-linear stress-strain characteristics in soil-structure interaction", *Geotechnique* 36, No. 3, 377-396.

Jardine, R. J., Symes, M. J. and Burland, J. B., (1984), "The measurement of soil stiffness in the triaxial apparatus", *Geotechnique* 34, No. 3, 323-340.

Karlsrud, K. and Haugen, H., (1983), "Cyclic loading of piles and pile anchors-field model tests" Final report: Summary and evaluation of test results, Norwegian Geotechnical institute Report 40018-11 (see Jardine, 1991)

Karlsrud, K.; Kalsnes, B. and Nowacki, F., (1992), "Response of piles in soft clay and silt deposits to static and cyclic

loading based on recent instrumented pile load tests", Int. Conf. on offshore site investigation and foundation behaviour, organised by society for under water technology.

Karlsrud, K., Nadim, F. and Haugen, H., (1986), "Piles in clay under cyclic loading. Field tests and Computational methods", Proc. 3rd Int. Conf. on Numerical methods in Offshore Piling, Nantes, 165-190.

Kavvadas, M. and Baligh, M. M., (1982), "Non-linear consolidation analysis around pile shafts, Proc. 3rd Int. Conf. on Behaviour of Offshore structures, Boston, Hemisphere pub., Washington, Vol. 1, 325-337.

Kraft, L. M., (1991), "Performance of axially loaded pipe piles in sand", Journal of geotechnical engineering, ASCE, Vol. 117, No. 2, p272-296.

Lacy, J. E., Crull, C. M. and Stockard, D. M., (1986), "TLP foundation design and installation for 2000 to 4000 ft water depths", 18th Offshore technology conference, paper No. OTC 5327.

Lau, J. S. O., (1975), "Repeated loading triaxial tests in sand", Msc thesis, Queen's university, Kingston, Canada.

Lavadoux, J. N and Baligh, M. M., (1982), "Consolidation after undrained piezocone penetration I : Prediction, Journal of Geotechnical Engineering, Vol. 112, No. 7; 707-726.

Lebegue, M. Y., (1964), "Etude experimental des efforts d'arrachage et de frottement negatif sur les pieux en milieu pulverulant", Annales de l'institute du batiment et de travaux publics, serie sols et fondations, 17. annee, pp 199-200. (see Jardine and Christoulas, 1991)

Lehane, B. M., (1992), "Experimental investigation of pile behaviour using instrumented field piles", PhD thesis, University of London.

Lehane, B. M., Jardine, R. J., Bond, A. J. and Frank, R., (1993), "Mechanism of shaft friction in sand from instrumented pile tests", Journal of Geotechnical Engineering, ASCE, Vol. 119, No. 1, 19-35.

Lentz, R. W. and Baladi, G. Y., (1980), "Simplified procedure to characterize permanent strain in sand subjected to cyclic loading", Proc. Int. Symp. on soils under cyclic and transient loading, Swansea, U. K.

Luong, M.P., (1980), "Stress-strain aspects of cohesionless soil under cyclic and transient loading", Int. Symp. on Soils under cyclic and transient loading, Swansea, Vol. 1, 315-324.

Mangiavacchi, A., Abbott, P. A., Hanna, S. Y. and Suhendra, R., (1980), "Design criteria of a pile founded Guyed tower", 12th Offshore Technology Conference, Paper No. OTC 3882.

Marr, A. W. Jr. and Christian, T. J., (1981), "Permanent displacement due to cyclic wave loading", the Journal of Geotechnical Engineering, ASCE, Vol. 107, No. GT8.

Martins, J. P., (1983), "Shaft resistance of axially loaded piles in clay", PhD thesis, Imperial college of science and technology, University of London, U. K.

McAnoy, R. P. L., Cashman, A. C. and Purvis, D., (1982), "Cyclic tensile testing of a pile in glacial till", 2nd Int. Conf. on Numerical Methods in Offshore Piling, 257-291.

McClelland, B., (1974), "Design of deep penetration piles for

Ocean structures", Journal of the Geotechnical Engineering, ASCE, Vol. 100, No. GT7, 709-747.

Meyerhof, G. G., (1970), "Pile capacities and load distribution of pile soil systems", Conference on design and installation of pile foundations and cellular structures, Lehigh university, Pennsylvania.

Meyerhof, G. G., (1976), "Bearing capacity and settlement of pile foundations", Journal of geotechnical engineering division, ASCE, Vol. 102, GT3, p197-228.

Murff, J. D., (1987), "Pile capacity in calcareous sands state of the art", Journal of Geotechnical Engineering, ASCE, Vol. 113, No. GT5, 490-507.

Nauroy, J. F. and Le Tirant, P., (1983), "Model tests of piles in calcareous sand", Proc. Conf. on Geotechnical practice in Offshore Engineering, Univ. of Texas, Sponsored by ASCE, 356-369.

Norwacki, F., Karlsrud, K. and Sparrevik, P., (1992), "Comparison of recent tests on OC clay and implications for design", Proc. Conf. Recent large-scale fully instrumented pile tests in clay, Institution of civil engineers, London, 511-537.

Norwegian Geotechnical Institute (1987), "Summary, interpretation and analyses of the pile load tests at the pentre test site", NGI report 52523-27.

Norwegian Geotechnical Institute (1988a), "Summary, interpretation and analyses of the pile load tests at the Onsoy test site", NGI report 52523-23.

Norwegian Geotechnical Institute (1988b), "Summary, interpretation and analyses of the pile load tests at the

Lierstranda test site", NGI report 52523-26.

Norwegian Geotechnical Institute (1989), " Design of offshore piles in clay-field tests and computational modelling, final report, summary and recommendations test site", NGI report 52523-28.

Offshore Engineer, (1993), "Heidrum moves into construction phase", Offshore engineer, April, 1993, p100-102.

Olson, R. E., (1990), "Axial load capacity of steel pipe in sand", 22nd Offshore Technology conference, Paper No. OTC 6419, 17-24.

Ooi Teik Aun, (1980), "The loading behaviour of long piles", PhD thesis, University of Sheffield, U. K.

O'Reilly, M. P., (1985), "Mechanical properties of granular material for use in thermal energy stores", PhD thesis, University of Nottingham.

O'Reilly, M. P. and Brown, S. F., (1992), "Observations on the resilient shear stiffness of granular materials", Geotechnique, Vol. 42, No. 4, p631-633.

Pappin, J. W., (1979), "Characteristics of granular material for pavement analysis", PhD thesis, University of Nottingham.

Patel, M. H., (1989), "Dynamics of Offshore structures", Butterworths, London.

Perrett, G. R. and Webb, R. M., (1980), "Tethered Buoyant platform production system", 12th Offshore Technology Conference, Paper No. OTC 3881.

Poulos, H. G., (1979a), "An approach for the analysis of offshore pile groups", Proc. of Int. Conf. on Numerical methods in Offshore Piling, 119-126.

Poulos, H. G., (1979b), "Development of an analysis for cyclic axial loading of piles", Proc. 3rd Int. Conf. on Numerical methods in geomechanics, Aachen, 1513-1530.

Poulos, H. G., (1981a), "Cyclic and axial response of single pile", Journal of the Geotechnical Engineering, ASCE, Vol. 107, No. GT1.

Poulos, H. G., (1981b), "Some aspects of skin friction of piles in clay under cyclic loading", Geotechnical Engineering, Vol. 12, 1-17.

Poulos, H. G., (1983), "Cyclic axial response-alternative analysis", Proc. Conf. on Geotechnical practice in Offshore Engineering, Univ. of Texas, 403-421.

Poulos, H. G., (1984), "Cyclic degradation of pile performance in calcareous soils", Analysis and design of pile Foundations, ASCE, 99-118.

Poulos, H. G., (1988), "Cyclic stability diagram for axially loaded piles", Journal of the Geotechnical Engineering, ASCE, Vol. 114, No. 8, 887-895.

Poulos, H. G., (1989a), "Pile behaviour-theory and application", Geotechnique 39, No. 3, 365-415.

Poulos, H. G., (1989b), "Cyclic axial loading analysis of piles in sand", Journal of the Geotechnical Engineering, ASCE, Vol. 115, No. GT6, 836-852.

Proctor, D. C. and Khaffaf, J. H., (1987), "Cyclic axial displacement tests on model piles in clay", *Geotechnique*, Vol. 37, No. 4, p505-509.

Puech, A. A., (1982), "Basic data for the design of tension piles in silty soils", *BOSS-82*, Vol. 1, 141-157.

Puech, A. A., Boulon, M. and Meimon, Y., (1982), "Tension piles: Field data and numerical modeling", *Proc. 2nd Int. Conf. on Numerical methods in Offshore Piling*, 293-312.

Randolph, M. F., (1977), "A theoretical study of the performance of piles", PhD thesis, Cambridge University, England.

Randolph, M. F., (1983), "Design considerations for offshore piles", *Proc. Conf. on geotechnical practice in offshore engineering*, University of Texas, sponsored by ASCE.

Randolph, M. F. and Worth, C. P., (1978), "Analysis of deformation of vertically loaded piles", *the journal of the Geotechnical Engineering*, ASCE, Vol. 104, No. GT12, 1465-1488.

Robinsky, E. I. and Morrison, C. F., (1964), "Sand displacement and compaction around model friction piles", *Canadian Geotechnical Journal*, Vol. 1, No. 2, 81-93.

Rodgers, J., (1957), "The distribution of marine carbonate sediments: A review", *Regional aspects of carbonate deposits*, special publication of society of ECONOMIC PALEONTOLOGISTS and mineralogists, No. 5, p2-14.

Sagaseta, C., Cuellar, V. and Pastor, M., (1991), "Cyclic loading", *10th European conference on soil mechanics and Foundation engineering*, Italy, 981-999.

Sangrey, D. A., Henkel, D. J., and Esrig, M. I., (1969), "The effective response of a saturated clay soil to repeated loading", Canadian Geotechnical Journal, Vol. 6, No. 3, 241-252.

Schnaid, F. and Houlsby, G. T., (1991), "An assesment of chamber size effects in the calibration of in-situ tests in sand", Geotechnique, Vol. 41, No. 3, p437-445

Seed, H. B. and Idriss, I.M., (1970), "Soil modulie and damping factors for dynamic response analysis", Report No. EERC 70-10, Earthquake engineering research centre, University of california, Berkeley.

Shaw, P., (1980), 'Stress-strain relationship for granular materials under repeated loading", PhD thesis, Univ. of Nottingham.

Smith, I. M., (1979), "A survey of numerical methods in Offshore piling", Proc. Int. Conf. on Numerical methods in Offshore piling.

St. John, H. D., Randolph, M. F., McAnoy, R. P and Gallagher, K. A., (1983), "Design of piles for tethered platforms", Design of Offshore structures, Thomas telford Ltd. London, Paper No. 6

Sulaiman, I. H. and Coyle, H. M., (1976), "Uplift resistance of piles in sand", journal of geotechnical engineering, ASCE, Vol. 102, No. GT5, p559-562.

Tan, R. H. S., (1971), "Piles in tension and compression", PhD thesis, University of Sheffield, U. K.

Tan, R. H. S. and Hanna, T. H., (1974), "Long piles under tensile loads in sand", Geotechnical Engineering, Vol. 5, 109-124.

Tetlow, J. H., Ellis, N. and Mitra, J. K., (1983), "Hutton tension leg platform", Proc. Conf. Development in the design and construction of offshore structures, London, Paper No. 14.

Thornton, D., (1979), "A general review of future problems and their solution", 2nd Int. Conf. on behaviour of offshore structures, BOSS'79, London, p773-782.

Toolan, F. E. and Ims, B. W., (1988), "Impact of recent changes in the API recommended practice for offshore piles in sand and clays", Underwater Technology, Vol. 14, No.1.

Toolan, F. E., Lings, M. L. and Mizra, U. A., (1990), "An appraisal of API RP2A recommendations for determining skin friction of piles in sand", 22nd Offshore technology conference, paper No. OTC 6422.

Uchida, K., Sawada, T. and Hasegawa, T., (1980), "Dynamic properties of sand subjected to initial shear stress", Proc. of Int. Symp. on soils under cyclic and transient loading, Swansea, p121-133.

Uesugi, M. and Kishida, H., (1986), "Influential factors of friction between steel and dry sands", Soils and Foundations, Vol. 26, No. 1, 33046.

Vanimpe, W. F., (1991), "Deformation of deep foundations", 10th European Conf. on soil mechanics and foundation engineering, Italy, p1031-1062.

Vesic, A. S., (1963), "Bearing capacity of deep foundations in sand". National academy of sciences, National research council, Highway research record 39, p112-153.

Vesic, A. S., (1965), "Ultimate loads and settlements of deep

foundations in sand", Proc. Symp. on Bearing capacity and settlement of foundations, held at Duke university, p53-68.

Vasic, A. S., (1967), "A study of bearing capacity of deep foundations", final report, project B-189, Georgia Institute of Technology, Atlanta, Ga.

Vesic, A. S., (1970), "Load transfer in pile-soil system", Conf. on design and installation of pile foundations and cellular structure, Lehigh University, Pennsylvania, p47-73.

Werching, S. N., (1987), "The development of shaft friction and end bearing for piles in homogeneous and layered soils", PhD thesis, Polytechnic of South Wales.

Whittle, A. J., (1987), "A Constitutive model for over consolidated clays with application to the cyclic loading of friction piles", PhD thesis, Massachusetts Institute of Technology.

Williams, D. J., (1979), "The behaviour of model piles in dense sand under vertical and horizontal loading", Phd thesis, Churchill college, University of Cambridge, U. K.

Youd, T. L., (1970), "Densification and shear of sand during vibration", Journal of the soil mechanics and foundation division, ASCE, Vol. 96, No. SM3, 863-880.

Youd, T. L., (1972), "Compaction of sand by repeated shear straining", Journal of soil mechanics and foundation engineering, ASCE, Vol. 98, No. SM7, 707-725.

BIBLIOGRAPHY

Arthur, J. R.F., Chua, K. S. and Dunstan, T., (1977), "Induced anisotropy in sand", Geotechnique 27, No. 1, 13-20.

API (1981), "American petroleum institute recommended practice for planning, designing and construction of fixed offshore platforms", API production division, 211 North Ervay, Suite 1700, Dallas, Texas 75201.

API (1984), "Recommended practice for planning, designing and construction of fixed offshore platforms", API RP2A, 15 Edition.

API (1987), "Recommended practice for planning, designing and construction of fixed offshore platforms", American petroleum institute, RP2A

API (1989), "Recommended practice for planning, designing and construction of fixed offshore platforms", American petroleum institute, RP2A, 18th Edition, Washington.

Atkinson, J. H. and Bransby, P.L., (1978), "The mechanics of soils an introduction to critical state soil mechanics", McGraw Hill Book Company.

Baligh, M. M., (1984), "The simple-pile approach to pile installation in clays", In: Analysis and design of pile foundations, Ed. Meyer, J. R. Proc. Symp. on codes and standards, ASCE National Conv. San Francisco, 310-330.

Barton, Y. O., (1982), "Laterally loaded model piles in sand : Centrifuge tests and finite element analysis", PhD thesis, University of Cambridge, UK.

Bea, R. G. and Audibert, J. M.E., (1979), "Performance of

dynamically loaded pile foundations", BOSS'79, 728-745.

Briaud, J. L. and Tucker, L. M., (1988), "Measured and predicted axial response of 98 piles", Journal of geotechnical engineering, ASCE, Vol. 114, No. 9, 984-1001.

Briaud, J. L. and Tucker, L. M. and Ng. E. S., (1989), "Axially loaded 5 pile group and single pile in sand", Int. Conf. on SMFE, Balkema, Rotterdam, 1121-1124.

Broms, B. B., (1972), "Bearing capacity of cyclically loaded piles", Swedish geotechnical institute publication No. 44, on the bearing capacity of driven piles, Paper No. 4.

Brown, S. F., Andersen, K. H., and Mcelvaney, J., (1977), "The effect of drainage on cyclic loading of clay", Proc. of the 9th Int. Conf. on SMFE, Tokyo, Vol. 2, 195-200.

Burland, J., (1973), "Shaft friction of piles in clay - a simple fundamental approach", Ground Engineering, Vol. 6, No. 3, 30-42.

Chateau, G. M., (1982), "Oil and gas production facilities for very deep water fixed structures", BOSS'82, Vol. 1, 125-140.

Chaudhuri, K. P. R., (1977), "Uplift resistance of foundations", PhD thesis, University of Wales, Institute of Science and Technology, Cardiff, UK.

Chauduri, K. P. R., Ghataora, G. S. and Symons, M. V., (1982), "Uplift resistance of model piles and pile groups", Proc. of Int. Conf. on Num. methods in Offshore piling, Texas, 239-256.

Curis, L. B., (1984), "How Conoco developed the tension leg platform", Ocean industry, Vol. 19, No. 8, 35-42.

Das, B. M., (1983), "A procedure for estimation of uplift capacity of rough pile", Soils and Foundations, Vol. 23, No. 3, 122-126.

Das, B. M., Seely, G. R. and Pfeifle, T. W., (1977), "Pullout resistance of rough rigid piles in granular soil", Soils and foundations, Vol. 17, 72-77.

Davidson, J. L. and Boghrat, A., (1983), "Displacement and strains around probes in sand", Proc. Conf. on geotechnical practice in offshore engineering, Univ. of Texas, 181-202.

Dennis, N. D., (1982), "Development of correlations to improve the prediction of axial pile capacity", PhD thesis, University of Texas.

Ellis, N., Tetlow, J. H., Anderson, F. and Woodhead, A. L., (1982), "Hutton TLP vessel-structural configuration and design features", 14th Offshore Technology Conf., Paper No. OTC 4427.

Erb, P.R., (1986), "Conoco's TLP weathers North Sea storms", Oil and gas Journal, Vol. 84, No. 43, 71-75.

Fayans, B. L., Yastrebov, P.I., Lutckovsky, I. G. and Lekymovyrch, G. S., (1980), "Pile resistance to the repetitive lateral loads", Proc. of Int. Symp. on soils under cyclic and transient loading, Swansea, 747-750.

Flemings, W. G. K., (1992), "A new method for single pile settlement prediction and analysis", Geotechnique, Vol. 42, No. 3, 411-425.

Garas, F. K., (1979), "The behaviour of tension piles for offshore applications with reference to a particular tethered buoyant structure (ARCOLPROD)", BOSS'79, Paper No. 37.

Gie, T. S. and De Boom, W. C., (1981), "The wave induced motions of a tension leg platform in deep water", 13th OTC, Paper No. OTC 3869.

Hanna, T. H. and Tan, R. H. S., (1971), "The load movement behaviour of long piles", Journal of materials, JMLSA, Vol.3, 532-554.

Hansen, J. B., (1968), "A theory for skin friction on piles", Danish geotechnical Institute Bulletin No. 25, 5-12.

Hicks, R. G., (1970), "Factors influencing the resilient response of granular materials", PhD Thesis, University of California.

Ireland, H. O., (1957), "Pulling tests on piles in sand", Proc. 4th Int. Conf. on SMFE, Vol. 2, 43-45.

Jardine, R. J. and Bond, A. J. (1989), "Behaviour of displacement piles in a heavily consolidated clay", Proc. of 12th Int. Conf. on SMFE, 1147-1152.

Jardine, R. J., Lehane, B. M. and everton, S. J., (1992), "Friction coefficient for piles in sands and silts", Proc. of Society for under water technology conference - offshore site investigation and foundation behaviour, London.

Jardine, R. J., Potts, D. M., Hight, D. W. and Burland, J. B., (1985), "Assessing the safety of offshore piles by displacement monitoring", Proc. Conf. on Behaviour of Offshore structures.

Kerisel, J., Bassett, R. H., Andersen, K. H., Ovesen, N. K., Mair, R.J., Clegg, D. P. and Houlsby, G. T., (1979), " The use of physical models in design", 7th Europ. Conf. on SMFE, Vol. 4,

315-360.

Kraft, L., Focht, J. A., Jr. and Amerasinghe, S. F., (1981), "Friction capacity of piles driven into clay", Journal of the geotechnical engineering, ASCE, Vol. 107, No. GT11, 1521-1541.

Kraft, L. M., Jr., Ray, R. P. and Kagawa, T., (1981), "Theoretical t-z curves", Journal of the geotechnical engineering, ASCE, Vol. 107, GT11, 1543-1561.

Lassoudiere, F., Meimon. Y., Hujeux, J. C. and Auby, D., (1983), "Cyclic behaviour of soils and application to offshore foundation calculations", BOSS'83, Vol. 2, 392-400

Lee, G. C., (1968), "Offshore structures, past, present, future and design considerations", Proc. of OECON, new Orleans, 169-196.

Lee, G. C., (1980), "Recent advances in design and construction of deep-water platforms - part1", Ocean Industry, Nov. 1980, 71-80.

Malek, A. M., Azzouz, A. S., Baligh, M. M. and Germaine, J. T., (1989), "Behaviour of foundation clays supporting compliant offshore structures", the Journal of geotechnical engineering, ASCE, Vol. 115, No. 5, 615-636.

Marr, A. W., Urzua, A. and Bouckovalas, G., (1982), "A numerical model to predict permanent displacement from cyclic loading of foundations", BOSS'82, Vol. 1., 297-312.

Martin, j. P. and Potts, D. M., (1982), "A numerical study of skin friction around driven piles", BOSS'82, Vol. 1, 283-293.

Matlock, H. and Foo, S. H. C., (1979), "Axial analysis of

piles using a hysteretic and degrading soil model", Proc. of Int. Conf. on Num. methods in offshore piling, 127-134.

Mazurkiewicz, B. K., (1968), "Skin friction on model piles in sand", Danish geotechnical Institute Bulletin No. 25, 13-48.

Mc Iver, D. B., (1981), "The static offset in waves of tension leg platforms", 13th OTC, paper No. OTC 4070.

Meimon, Y. and Hicher, P. Y., (1980), "Mechanical behaviour of clays under cyclic loading", Int. Symp. on soils under cyclic and transient loading, Swansea, 77-88.

Mercier, J. A., Branch, D. W., Vories, D. W. and Marr, T. O., (1982), "Design of Hutton TLP", Offshore South East Asia 82 Conf., Singapore.

Mercier, J. A., Goldsmith, R. G. and Curtis, L. B., (1980), "The Hutton TLP; A preliminary design", European Offshore Petroleum Conf. and Exhibition, London, Paper No. EUR 264.

Mercier, J. A., Leverette, S. J., and Bliault, A. L., (1982), "Evaluation of Hutton TLP response to environment loads", 14th OTC, Paper No. OTC 4429.

Mercier, J. A., and Marshall, R. W., (1981), "Design of a Tension Leg Platform", A one-day Symp. on offshore engineering, Middlesex, organised by the Royal Institute of Naval Architects, Offshore engineering group, Paper No. 5.

Meyerhof, G. G., (1983), "Scale effects of ultimate pile capacity", Journal of geotechnical engineering, ASCE, Vol. 109, No. GT6, 797-806.

Ng, E. S., Briaud, J. L. and Tucker, L. M., (1988), "Pile

foundation: the behaviour of single pile in cohesionless soils", Vol. 1 and 2 Federal Highway Administration report FHWA-RD-88-081.

Ocean Industry, (1984), "How the TLP was installed in only 78 hours", Vol. 19, No. 8, Aug. 1984.

Ocean Industry, (1984), "TLP Design for deep water off Northern Norway", Vol. 19, No. 8, Aug. 1984.

Ocean Industry, (1985), "Concrete TLP for 3,300 ft water has unique features", Vol. 20, No. 4, April. 1985.

Offshore research focus (1981), "Tension piles new testing programme", No.23.

Offshore research focus (1983), "Tension piles as anchors for buoyant structures", No.40.

Offshore research focus (1985), "Piles as anchors as buoyant structures", No.49.

Offshore research focus (1986), "Tension pile research published", No.51.

Offshore research focus (1987), "Tension pile research in Britain and Norway", No.57.

O'Neill, M.W., (1983), "Group action in offshore piles", Proc. Conf. on Geotechnical Practice in Offshore Engineering, University of Texas, 25-64.

O'Reilly, M.P. and Al-Tabbaa, A., (1990), "Heave induced pile tension: a simple one dimensional analysis", Ground Engineering, June 1990, 28-33.

O'Reilly, M. P., Broen, S. F. and Overy, R. F., (1991), "Cyclic loading of silty clay with drainage periods", Journal of the geotechnical engineering, ASCE, Vol. 117, GT2, 354-362.

O'Riordan, N. J., (1982), "The mobilisation of shaft adhesion down a bored, cast-in-situ pile in the Woolwich and Reading beds", Ground engineering, April, 1982, 17-26.

Pappin, J.W., Brown, S.F. and O'Reilly, M.P. (1992), "Effective stress behaviour of saturated and partially saturated granular material subjected to repeated loading", Geotechnique 42, No. 3, 485-497.

Parry, R.H.G., (1980), "Literature review of offshore loading effects on axial pile capacity in soft cohesive soils", Report, University of Cambridge, UK.

Puech, A. and Jezequel, J.F. (1980), "The effects of long time cyclic loading on the behaviour of a tension pile", Proc. of 12th, OTC, paper No. OTC3870.

Randolph, M.F. (1983), "Settlement considerations in the design of axially loaded piles", Ground Engineering, May 1983, 28-32.

Rees, L. C. and Cox, W. R., (1976), "Pull-ut tests on piles in sand", 18th OTC, paper No. OTC2472.

Sangrey, D.A., (1977), "Response of offshore piles to cyclic loading", OTC2944.

Schofield, A. N., (1980), "Cambridge geotechnical centrifuge operations", Geotechnique, No.3.

Sparks, C. Manesse, J.P., Jardinier, R., Perol, Ch. and

Martin, J. (1985), "PLTB 1000- A concrete tension leg platform", Proc. of 4th, int. offshore mechanics and arctic engineering symp. Vol. 1, New York, ASME, 14-21.

Stranchan, T., (1985), "Hutton TLP: So creative a work of art", Scottish petroleum annual 1985.

Sutherland, H. B., Finley, T. W. and Fadl, M. O., (1983), "Uplift capacity of embedded anchors in sand", BOSS'83, Vol. 2, 451-263.

Symes, M. J. P. R., Gens, A. and Hight, D. W., (1984), "Undrained anisotropy and principle stress rotation in saturated sand", Geotechnique 34, No.1, 11-27.

Tejchman, A., (1976), "Skin resistance of tension piles", 6th European Conf. on SMFE, Vienna, 573-577.

Trbojevic, U. M. J., Danishch, R. and Delinic, K., (1981), "Pile-soil-pile interaction analysis for groups ", Proc. of 6th SMIRT, Paris, Paper No. k5/4.

Vesic, A. S. and Clough, G. W., (1968), "Behaviour of granular materials under high stresses", Journal of SMFE, ASCE, Vol. 94, No. SM3, 661-688.

Vijayvergiya, V. N., (1979), "Soil response during pile driving", Int. Conf. on Num. methods in offshore piling, 53-58.

White, C. N., Erb, P. R. and Botros, F. R., (1988), "The single - leg Tension-leg platform : A cost-effective evolution of the TLP Concept", 20th OTC, Paper No. OTC 5637.

White, G. J., Preston, S. and Mc Kenzie, R. H., (1985), "The Hutton TLP foundation installation", 17th OTC, Paper No. OTC 4949.

Whitman, R. V. and Luscher, U., (1962), "Basic experiments into soil-structure interaction", Journal of the SMFE, ASCE, Vol. 88, No. SM6, 135-167.

LIST OF RESEARCH PAPERS PRODUCED

1. *A software to predict the behaviour of tension piles*, paper accepted for publication in the Journal of Computers and Structures.
2. *Modified T-Z model- A software for tension piles*, paper under review for publication in the Journal of Computers and Structures.
3. *A computer package for the design of piles under cyclic tensile loads*, paper under review for publication in the Journal of Computers and Structures.
4. *Tensile capacity of a driven pile in sand*, paper communicated to division of Geotechnical Engineering Journal ASCE.
5. *Displacement and failure mechanism of piles in sand under cyclic tensile loading*, paper under review for publication in the journal of Geotechnical Engineering Division, A.S.C.E.

CALIBRATION OF MEASURING EQUIPMENT

The measuring equipment used in the present investigation were all calibrated before starting the experiments. All calibrations were repeated at least three times on each of the equipment to study the repeatability of the results and the average of these results were used to obtain the calibration factors. The calibration curves shown are the average curves obtained for each equipment. Most of the calibration was done using the existing equipment such as necessary, such as calibration of the load cell pile segments, pressure cells, new piece of apparatus were built or the existing equipment were modified for the calibration. The following sections presents the procedure adopted and the results of the calibration.

A.1 Calibration of 25 kN Load Cell

The 25 kN load cell was calibrated for both compression and tension. Calibration was done using a compression testing machine having a load range of 30 kN and a least measuring unit of 0.05 kN. The compression load was applied through a seating weight. The output of the load cell was recorded in mV for every 1 kN increase in load. The repeatability of the load cell behaviour was studied by repeating the loading and unloading process three times.

To calibrate the load cell under tension, a threaded shaft with enlarged base was fitted on to the bottom side of the load cell. With this shaft, the cell was placed upside down in the same compression testing machine. Since the load applied was transferred through the threads of the load cell in reverse direction, it produced a tension in the load cell. The loading sequence was carried out in the same way as for the compression loading. The calibration results are presented in Fig.A.1. The

conversion factor for the load cell both in compression and tension was observed to be same and equal to + or - 680 kN/V (+ve for compression and -ve for tension).

A.2 Calibration of Load Cell Pile Segment

Each of the load cell pile segments was calibrated separately. The calibration was done both in compression and tension. The compression testing machine used for the calibration of 25 kN load cell was used to apply compressive loads. The response of the load cell segments was observed during both loading and unloading.

To calibrate the load cell segment in tension the 25 kN load cell was used as a reference. For calibration, a load cell segment was fitted with two cylindrical attachments on either end to form a combined cylinder as shown in Fig.A.2. The 25 kN load cell was fitted through a steel plate to one end of this cylinder. The other end was clamped to a rigid support. The top of the load cell was subjected to tensile load as shown in fig.A.2. The load was applied with respect to the 25 kN load cell and the output of load cell pile segment was recorded. The results of the load cell pile segment calibration are presented in Fig.A.3. The response of the three load cell segments was very close to each other and hence an average value was considered. The average calibration factor was obtained as 588 kN/V.

A.3 Calibration of LVDTs

LVDT1 and LVDT2 were calibrated with a micrometer having a least measuring unit of 0.01 mm. These LVDTs had a two-way travel. The output voltage of these LVDTs was zero at the middle of travel, -ve for compression and +ve for extension of the plunger. It was observed that, for a given displacement, the output voltage of LVDT1 and LVDT2 was the same. The average calibration curve for these two LVDTs is shown in Fig.A.4(a). A common calibration factor of + or - 5mm/V was obtained for LVDT1

and LVDT2.

LVDT3 was calibrated using a micrometer with a least count of 0.00254 mm. The calibration curve of LVDT3 is shown in Fig.A.4(b). The calibration factor for LVDT3 was obtained as 6.14 mm/V.

A.4 Calibration of the Pressure Cells

The pressure cells used had a common calibration factor of 188 kPa/mV at 10 V input. This value was obtained by calibrating the cells using hydraulic pressure. Since the pressure cells were to be used in sand (a particulate structure) they were calibrated, separately for the present investigation, using sand as the pressurising media. To calibrate the pressure cells using sand, a separate piece of apparatus was developed. This was achieved by modifying an existing Rowecell.

A.4.1 Apparatus for the Calibration of the Pressure Cells

For the calibration of the pressure cells, a 150 mm diameter Rowecell was modified. The standard cylindrical cell of the Rowe cell was replaced with a cylinder having 150 mm diameter and 165 mm high as shown in Fig.A.5. A 5 mm hole was provided in the wall of the cylinder at its mid height to take the pressure cell cable out.

A.4.2 Calibration Procedure

The pressure cells were calibrated using the sand as pressurising media. A 3500 g of sand, used in the main model pile tests, was weighed to fill into the modified Rowecell cylinder. The modified was positioned on the base of the Rowecell and 1750 g of sand was filled into the cylinder and compacted with a small rammer, used for the sample preparation for direct shear test. The surface of the sand was then levelled and a pressure cell was centrally placed on the sand surface to record axial pressure (σ_a). Now the remaining 1750 g of sand was filled into the

cylinder and compacted to a total sand height of 115 mm. The top 50 mm clearance was left for the Bellowframe to expand during pressurising the cell. The top cap of the Rowe cell with Bellowframe was fitted with nut and bolts. The Bellowframe was pressurised using compressed air. The compressed air pressure was measured using a pressure gauge. The pressure in the cell was increased from 0-150 kPa in steps of 10 kPa and the out put of pressure cell was recorded. After reaching the pressure to 150 kPa the pressure was reduced to zero and the sand was refilled as explained earlier for the second trial on the same pressure cell. Each pressure cell was calibrated three times. In each trial the pressure cells shown reasonably consistent output. The out put of the four pressure cells was very close to each other. The average curve for all the pressure cells is shown in Fig.A.6.

The calibration factors obtained for various measuring equipment were consolidated in Table.A.1.

Table A.1 Calibration Factors for the Measuring Equipment Used in the Present Investigation.

Measuring Equipment	Calibration Factor
25 kN Load Cell	680 kN/V
Load Cell Pile Segments	
LSG1, LSG2 and LSG3	588 kN/V
LVDT1 and LVDT2	5 mm/V
LVDT3	6.14 mm/V
Pressure cells	
PC1, PC2, PC3 and PC4	220 kPa/mV (at 10 V input)

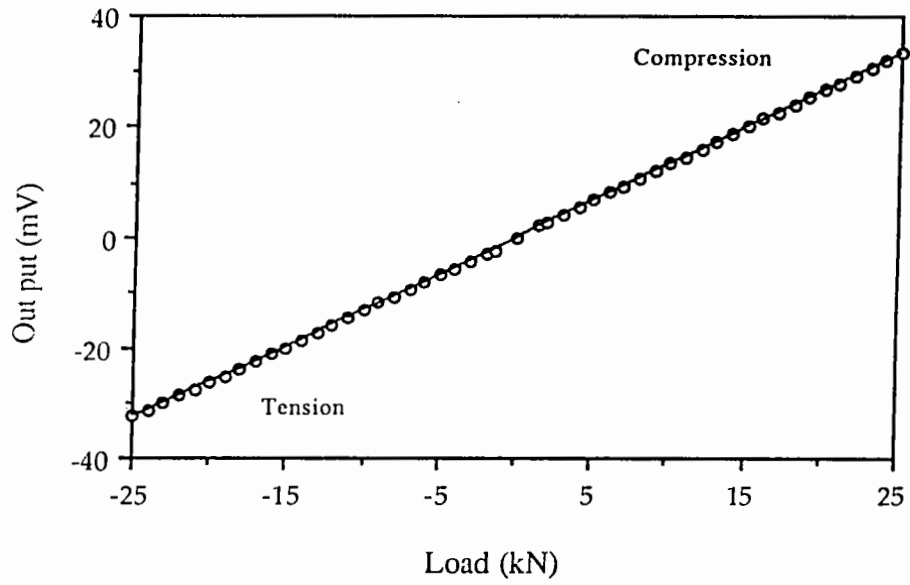


Fig. A.1 Calibration Data of 25 kN Load cell

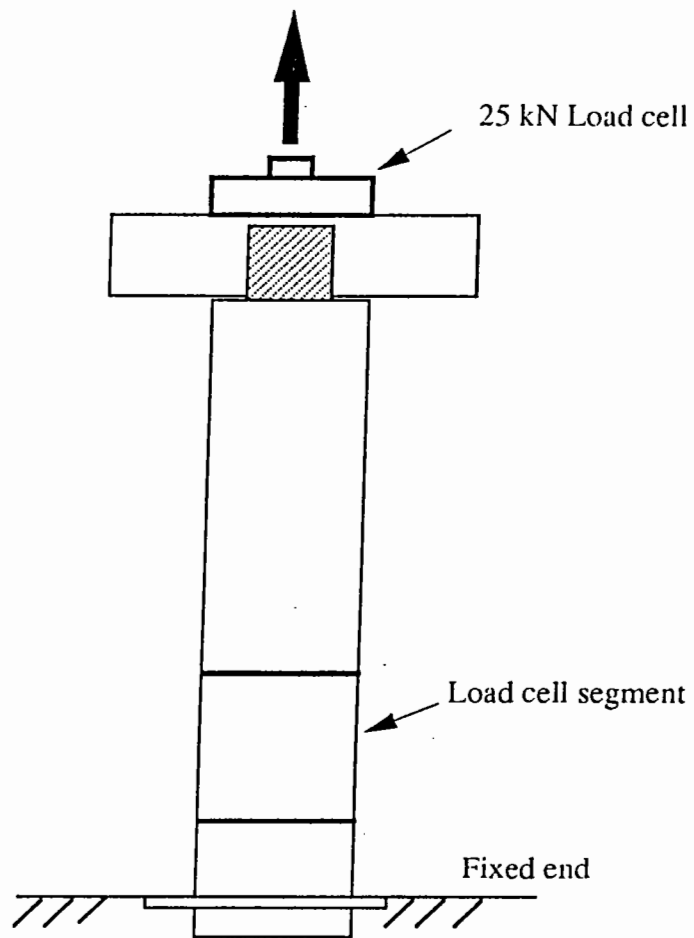


Fig. A.2 Calibration of Load cell segment in tension

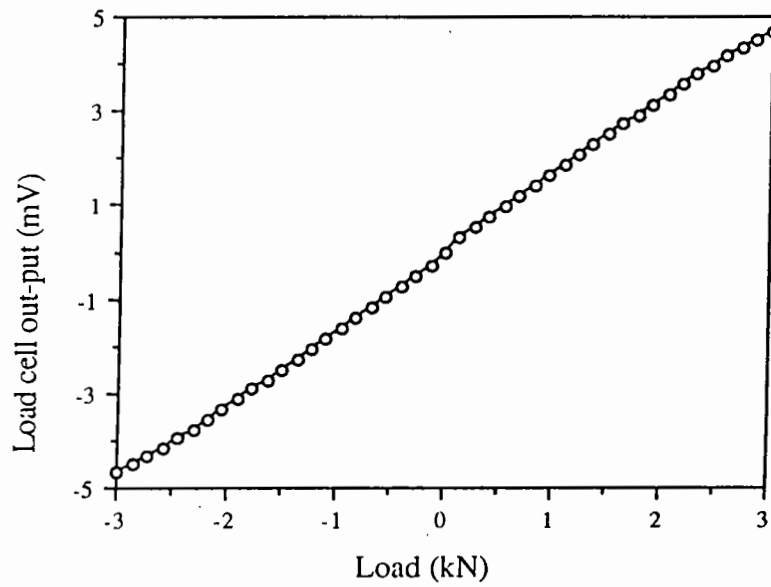
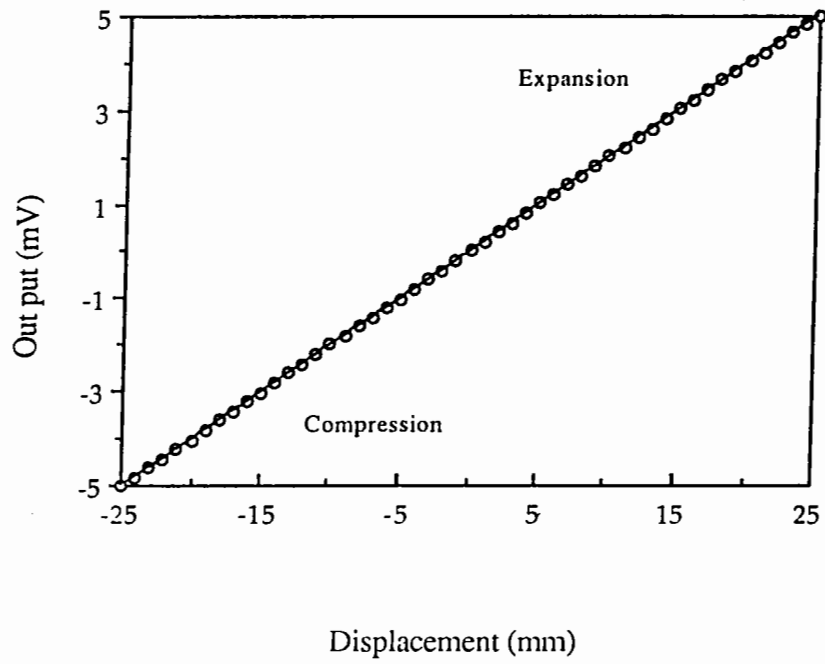


Fig. A.3 Calibration data of Load cell pile segments



(a) LVDT1 and LVDT2

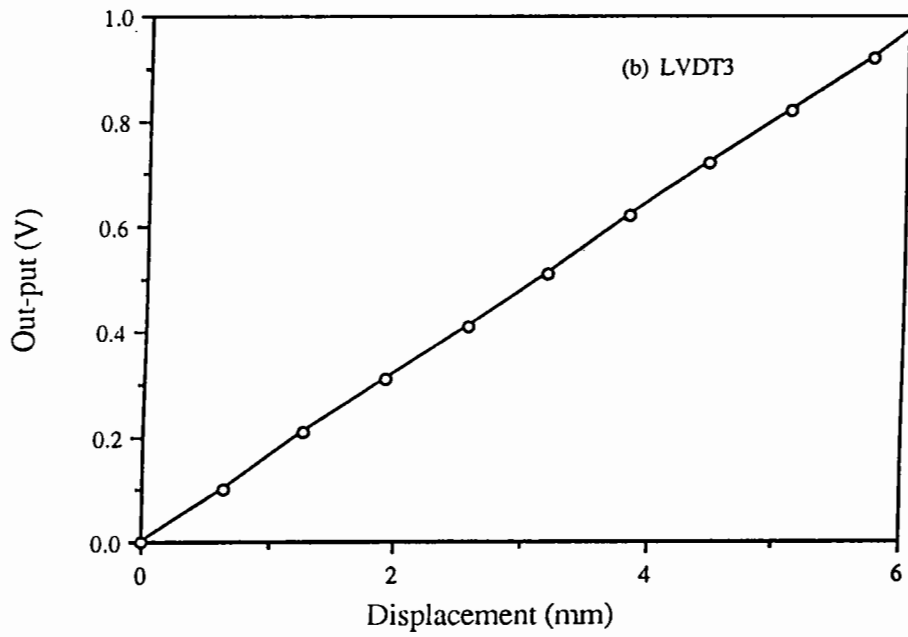
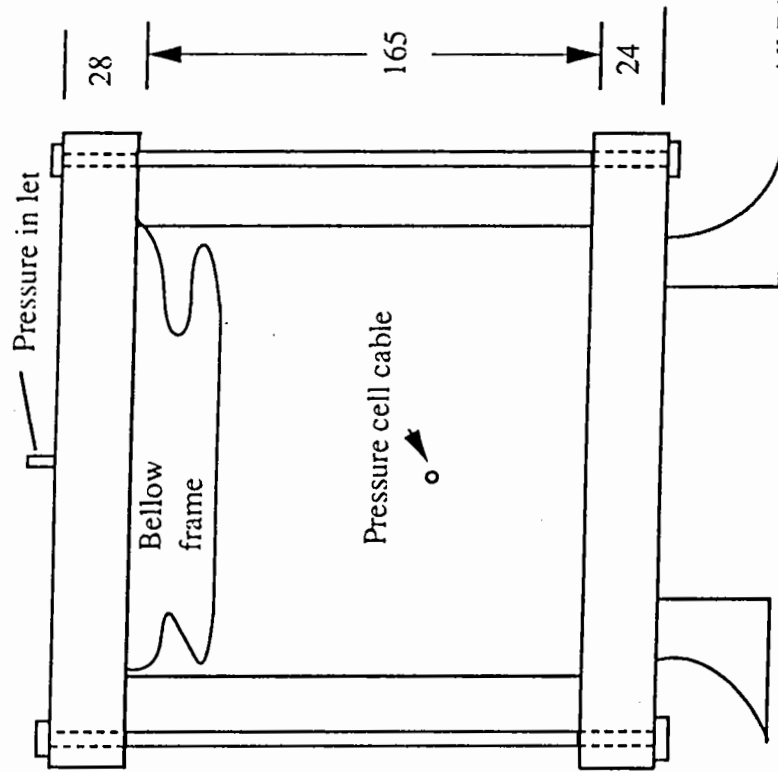


Fig. A.4 Calibration Results of LVDTs



All Dimensions are in mm

Fig. A.5 Modified Row Cell for the Calibration of Pressure cells

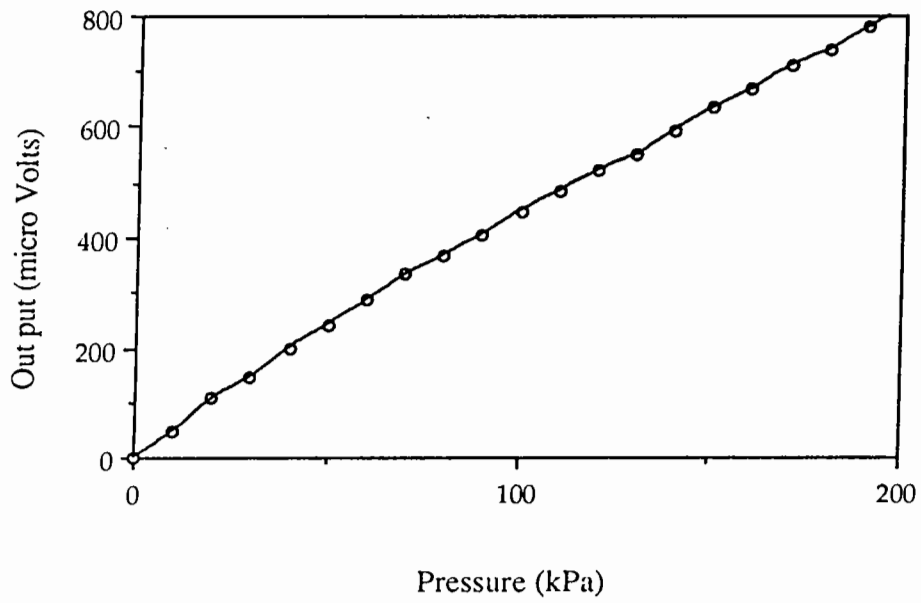


Fig. A.6 Calibration of Pressure Cells

APPENDIX B

Sample Print-Out from the Data Logger

```
D T 3
C 011 029.935 MM
C 006-01.2959 MM
C 005-00032.1 KN
C 003 00.1773 KN
S T 3 07:03:22.0
D T 3
C 011 029.935 MM
C 006-00.1986 MM
C 005-00229.9 KN
C 003 00.1774 KN
S T 3 07:03:21.0
D T 3
C 011 029.936 MM
C 006 01.2525 MM
C 005-00333.5 KN
C 003 00.1758 KN
S T 3 07:03:20.0
D T 3
C 011 029.926 MM
C 006 02.2582 MM
C 005-00513.3 KN
C 003 00.1751 KN
S T 3 05:33:24.0
D T 3
C 011 029.926 MM
C 006 03.1752 MM
C 005-00490.4 KN
C 003 00.1752 KN
S T 3 05:33:23.0
D T 3
C 011 029.926 MM
C 006 03.4295 MM
C 005-00464.0 KN
C 003 00.1756 KN
S T 3 05:33:22.0
D T 3
C 011 029.925 MM
C 006 03.4588 MM
C 005-00391.3 KN
C 003 00.1753 KN
S T 3 05:33:21.0
D T 3
C 011 029.927 MM
C 006 03.9825 MM
C 005-00361.7 KN
C 003 00.1739 KN
S T 3 05:33:20.0
```

A P P E N D I X C

Complete Set of Laboratory Results

The complete set of experimental results presented here are divided as under:

- 1) Preliminary experimental results
 - a) Horizontal pressure distribution during the installation of the model piles Fig. C.1 and C.2
 - b) Monotonic test results Fig. C.3 and C.4
 - c) Cyclic load test results Fig. C.5
- 2) Main experimental results
 - a) Monotonic test results Fig. C.6 to Fig. C.10
 - b) Pressure distribution during the installation of 76.2mm diameter pile Fig. C.11
 - c) Cyclic load test results Fig. C.12 to Fig. C.21
 - d) Results of soil displacement Fig. C.22 and C.23

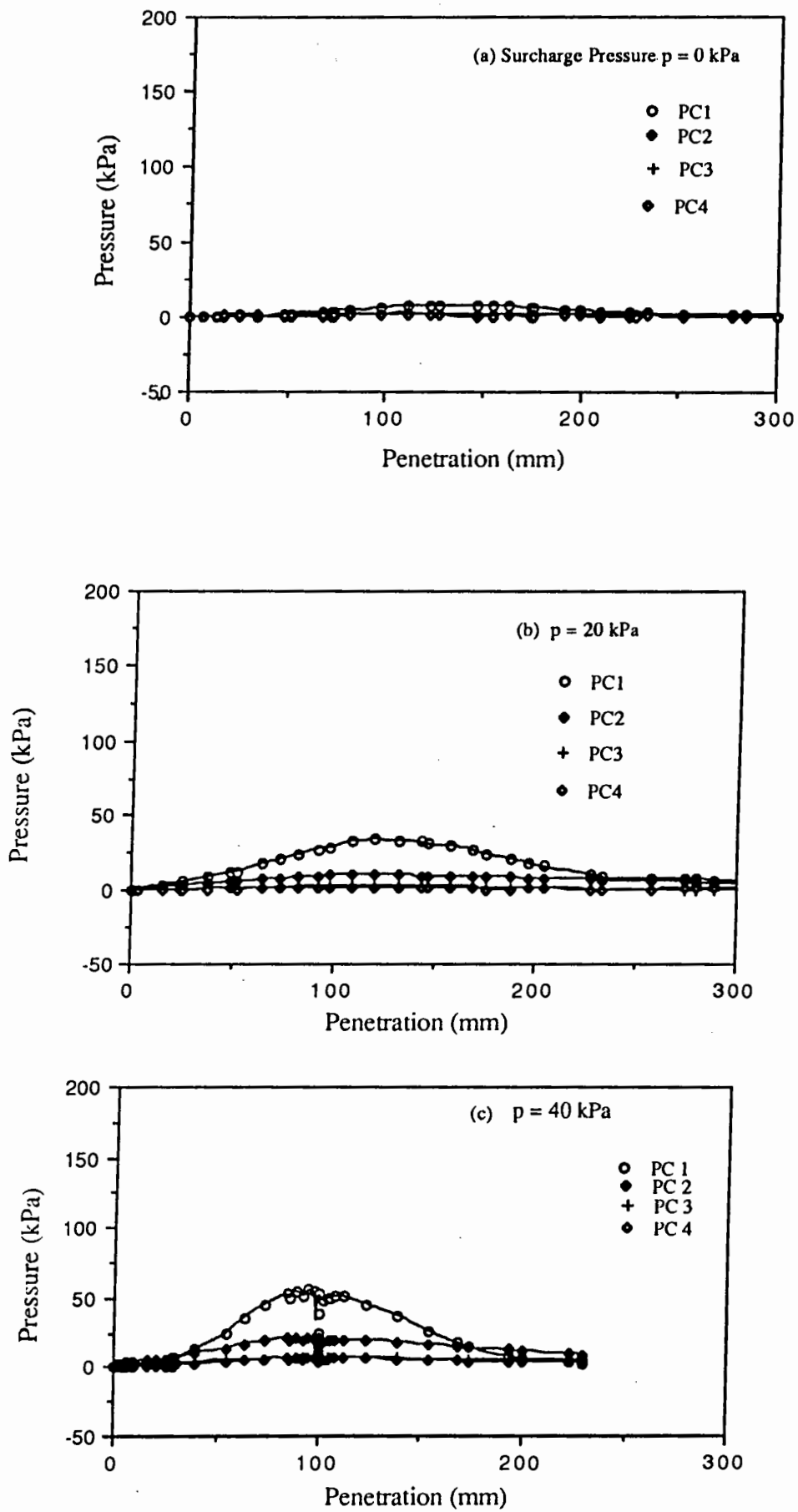


Fig. C.1 Horizontal Pressure Distribution in the Sand During the Installation of the 25.4 mm Diameter Pile

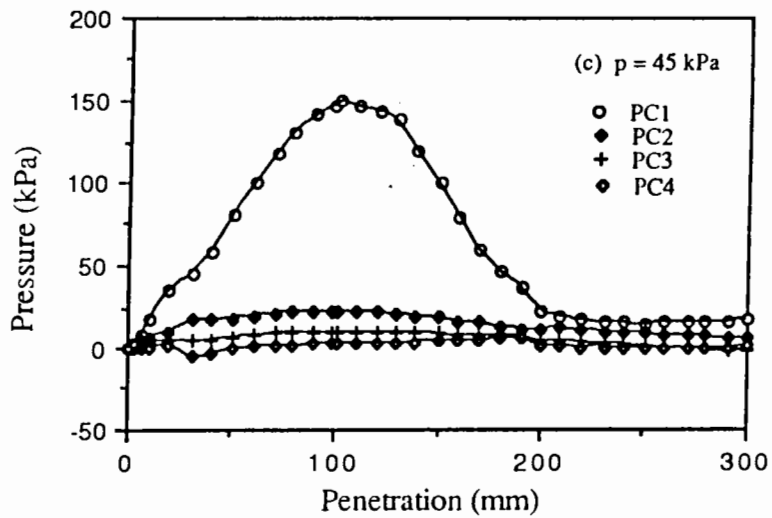
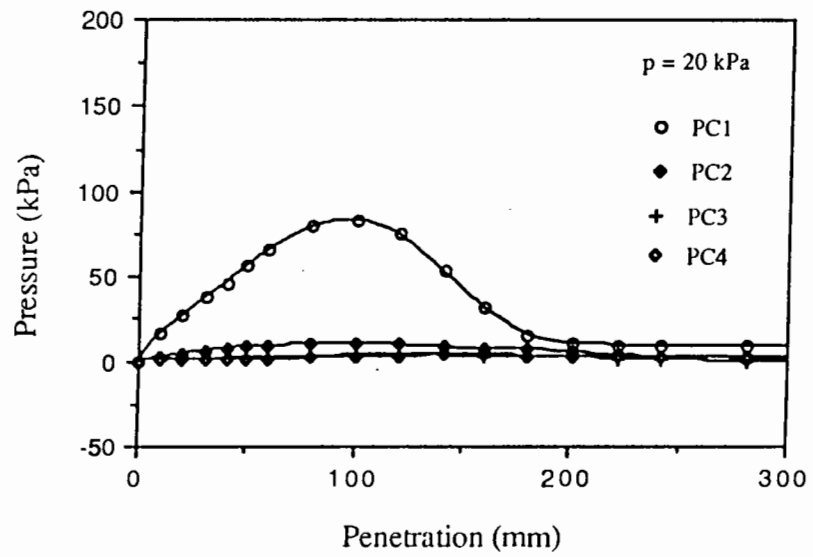
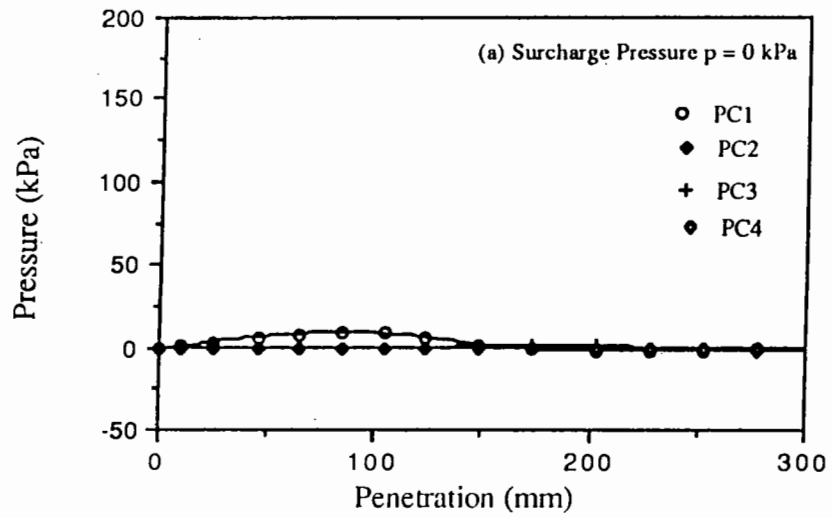


Fig. C.2 Horizontal Pressure Distribution in the Sand During the Installation of 38.1 mm Diameter Pile

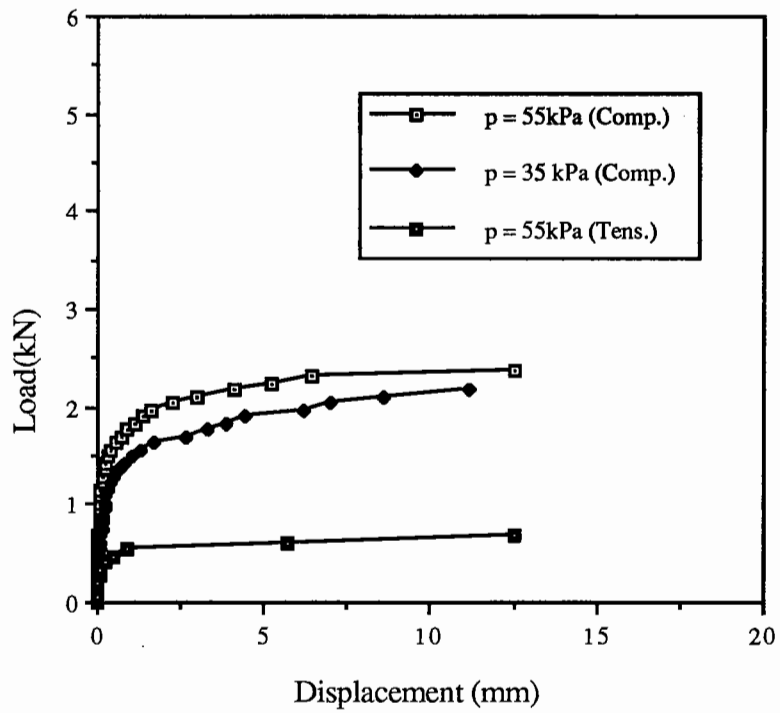


Fig. C.3 Monotonic Test Results for 25.4 mm Diameter Steel Pile

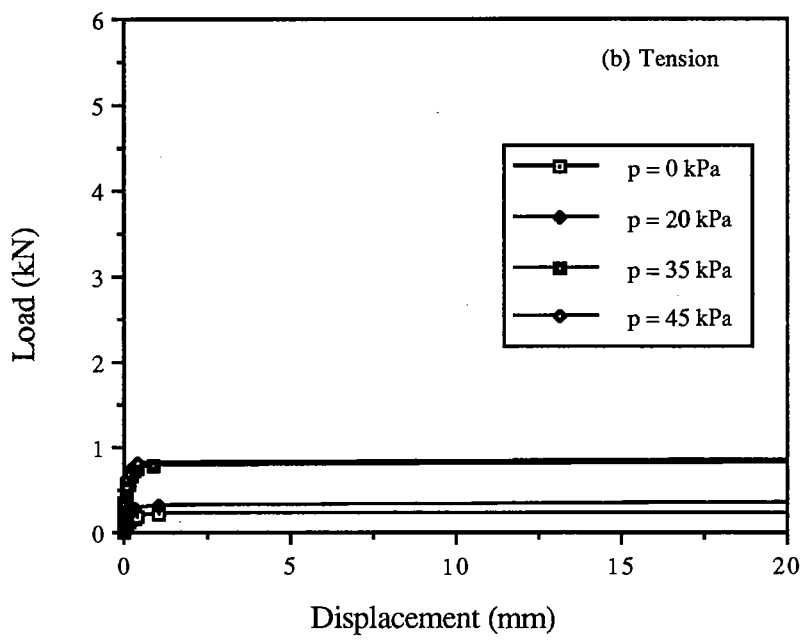
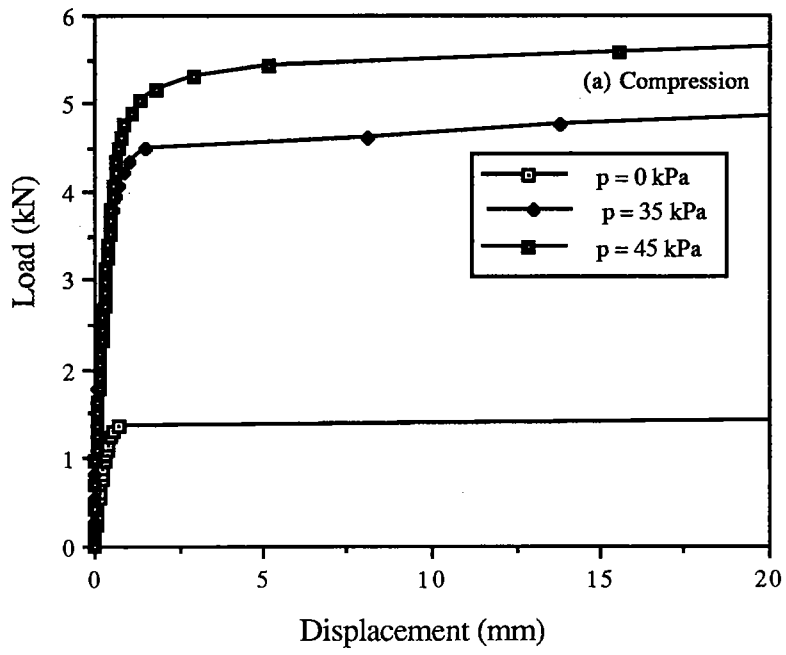
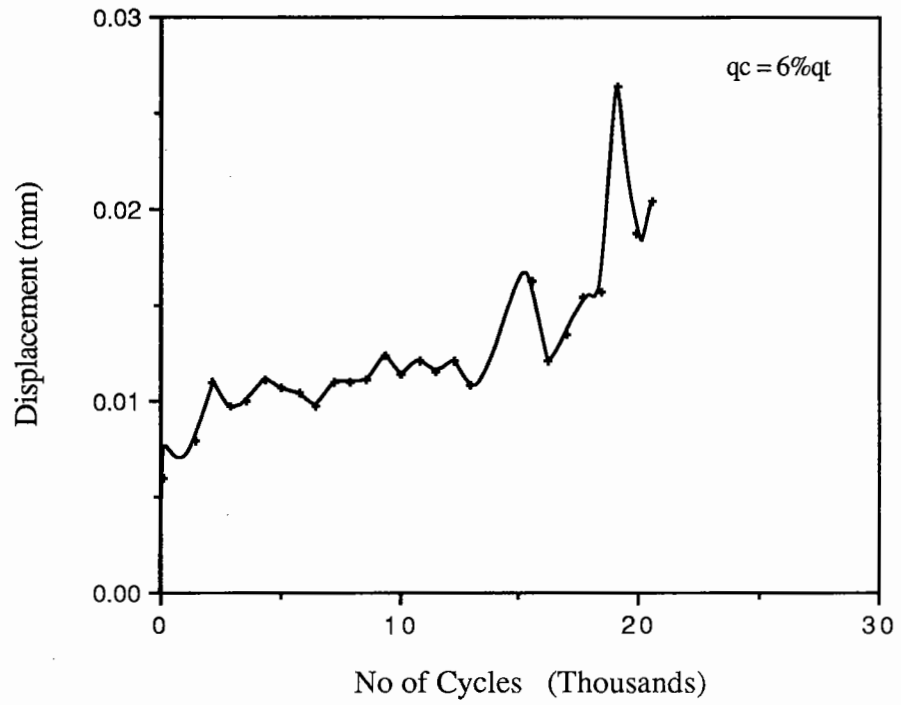


Fig. C-4 Monotonic Test Results for 38.1 mm Diameter Steel Pile



Cyclic Load Test Results
(25.4 mm Diameter Steel Pile)

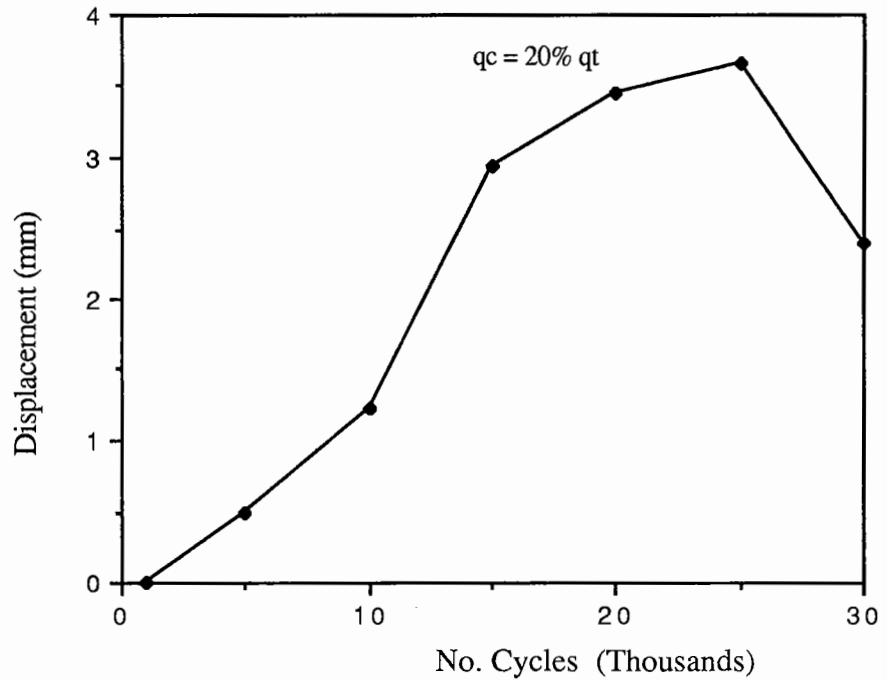


Fig. C-5 Cyclic Load Test Results
(38.1 mm Diameter Steel Pile)

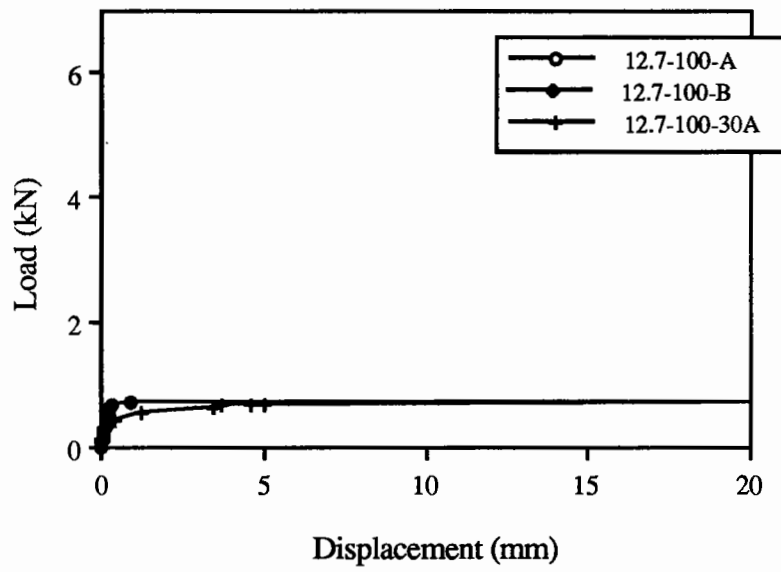


Fig. C-6 Monotonic Test Results for the 12.7 mm Diameter Pile

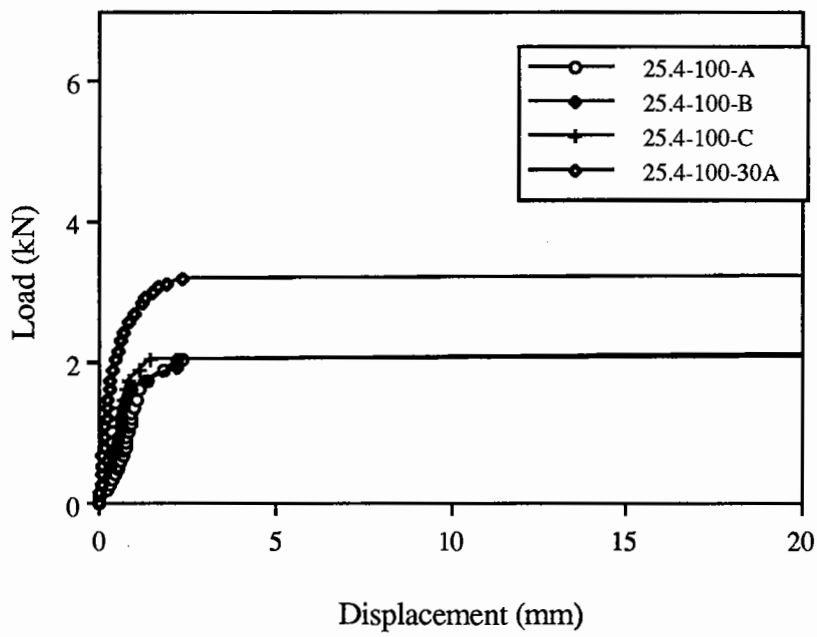


Fig. C-7 Monotonic Test Results for the 25.4 mm Diameter Pile

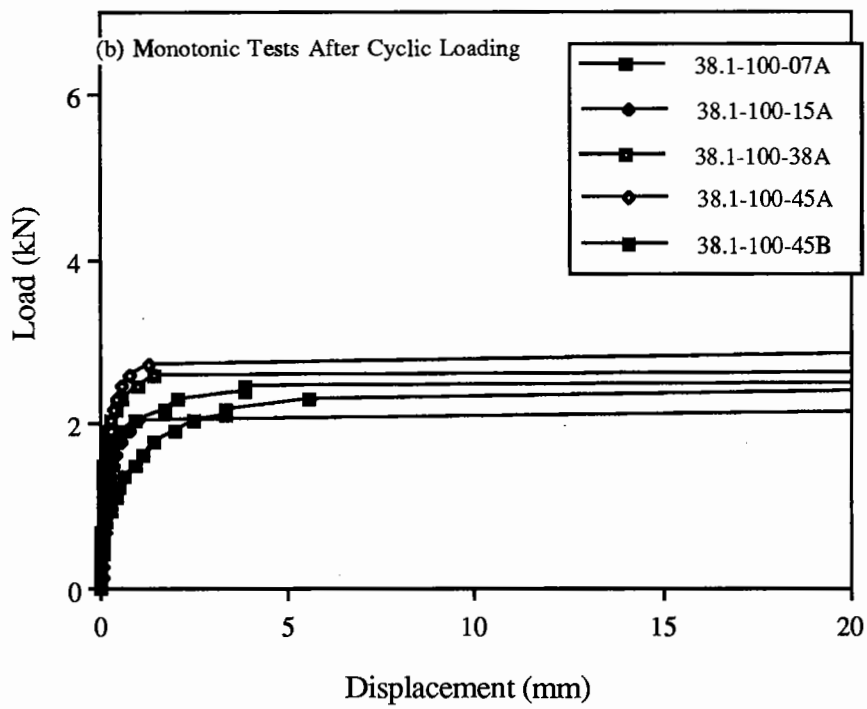
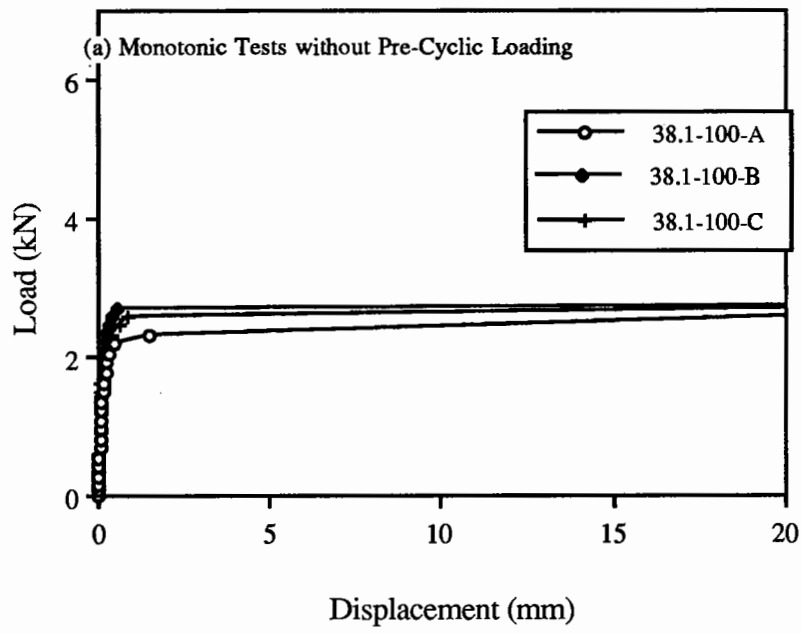


Fig. C-8 Monotonic Test Results for the 38.1 mm Diameter (Semi-Instrumented Pile)

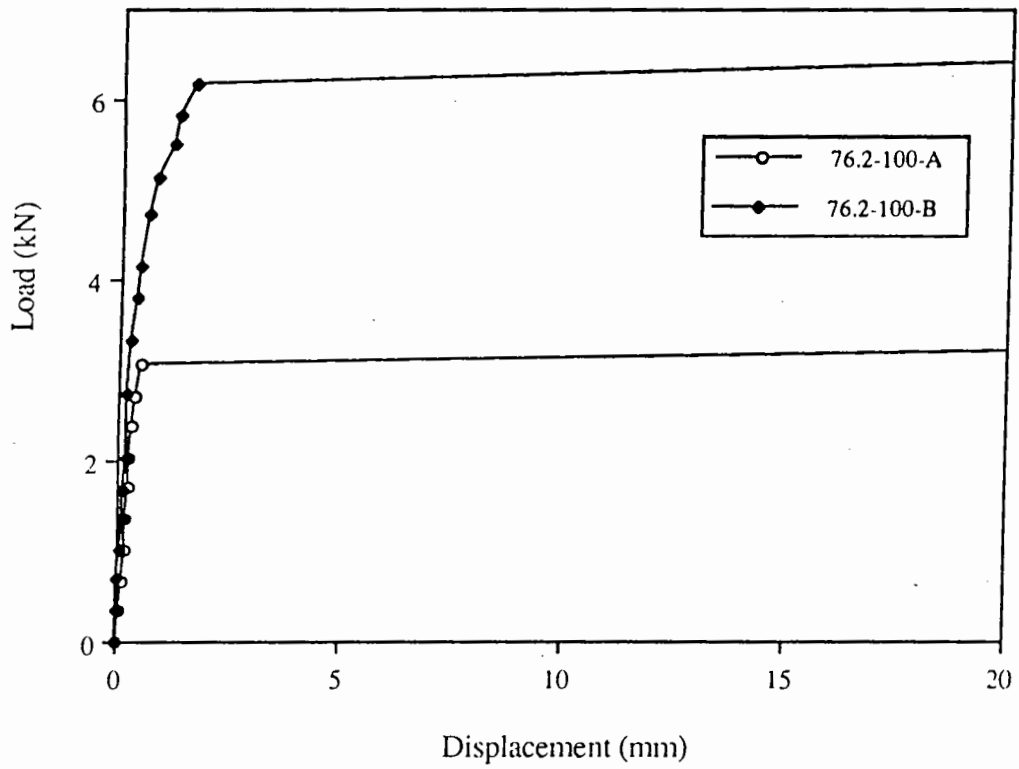


Fig. C.9 Monotonic Test Results for the 76.2 mm Diameter Pile

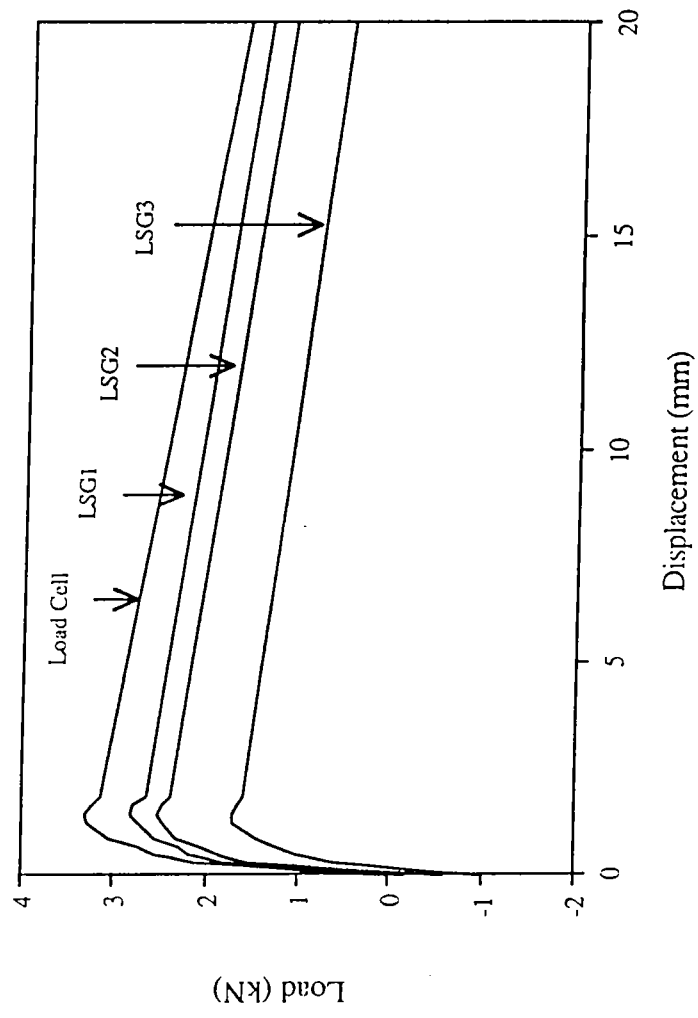


FIG. C. 10 Montonic Test Results for the Instrumented Pile

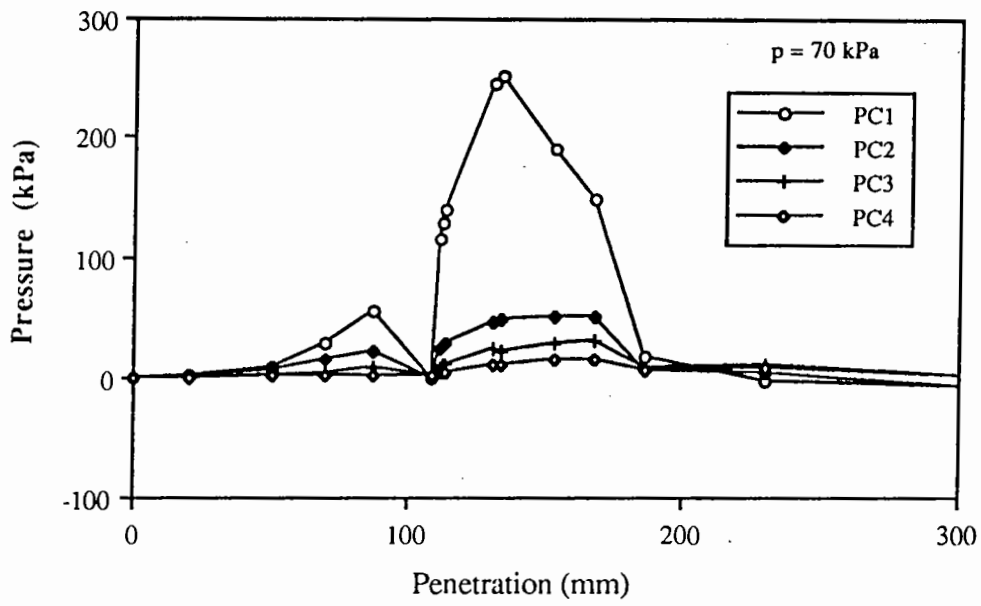


Fig. C.11 Horizontal Pressure Distribution During the Installation of 76.2 mm Diameter Pile

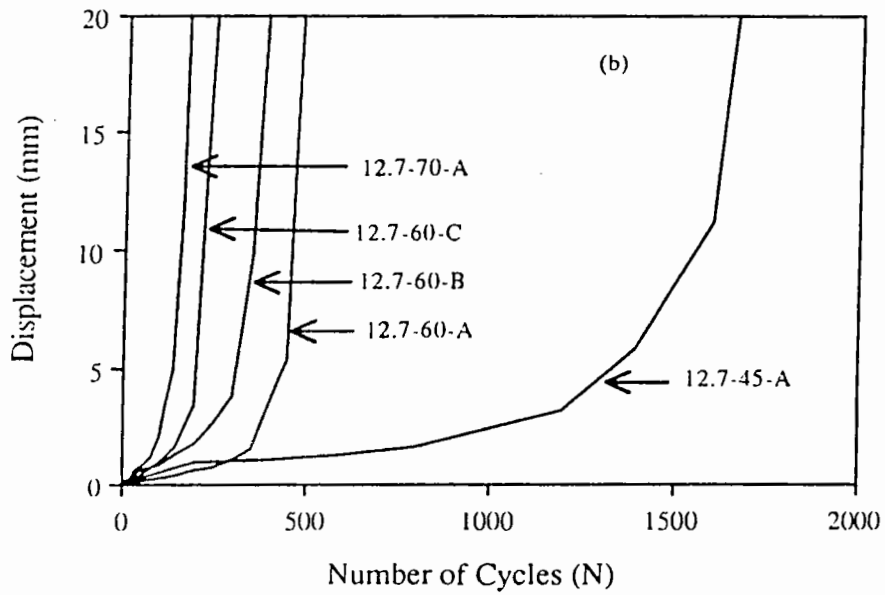
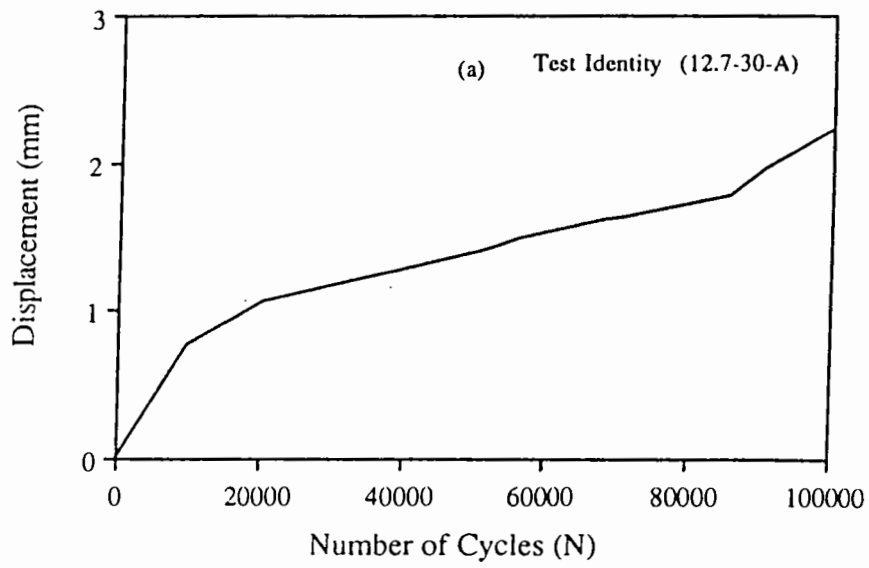


Fig. C . 12 Number of Cycles Versus Total Displacement (12.7 mm Diameter Pile)

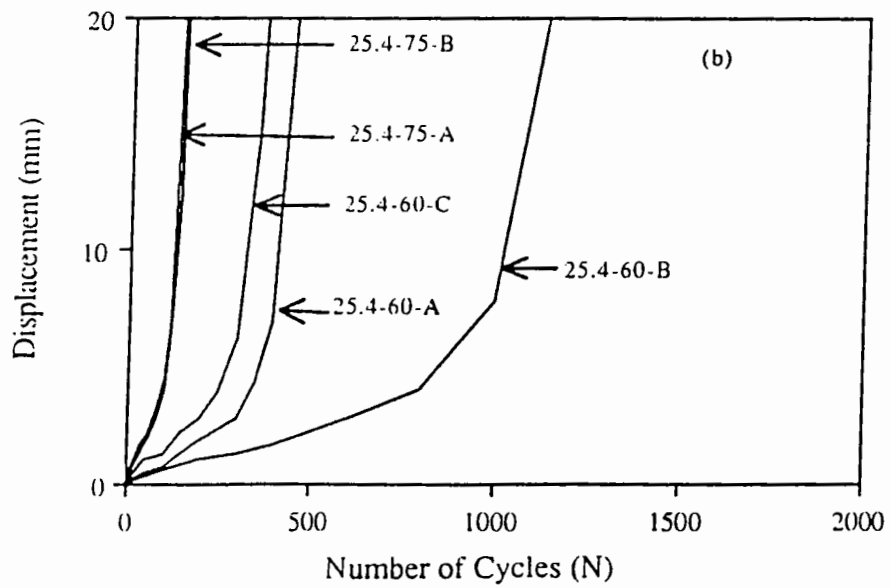
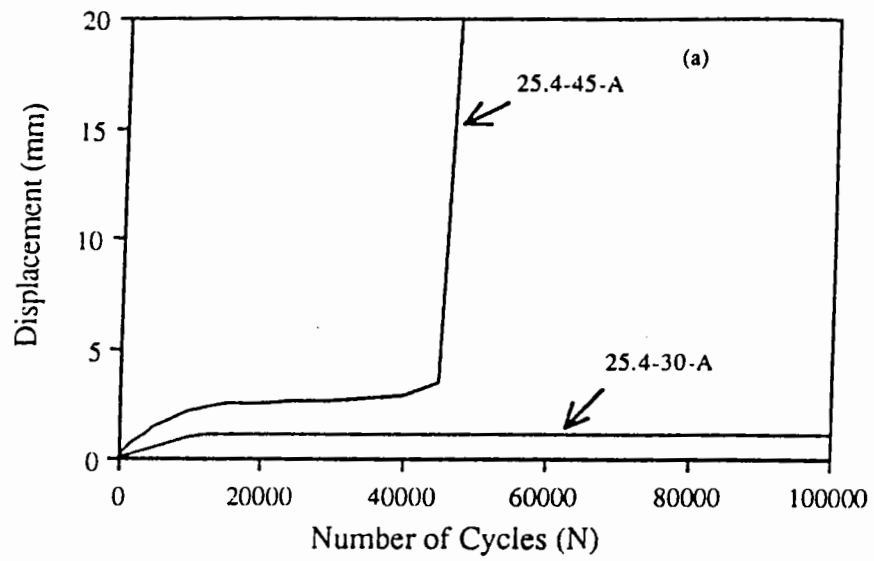
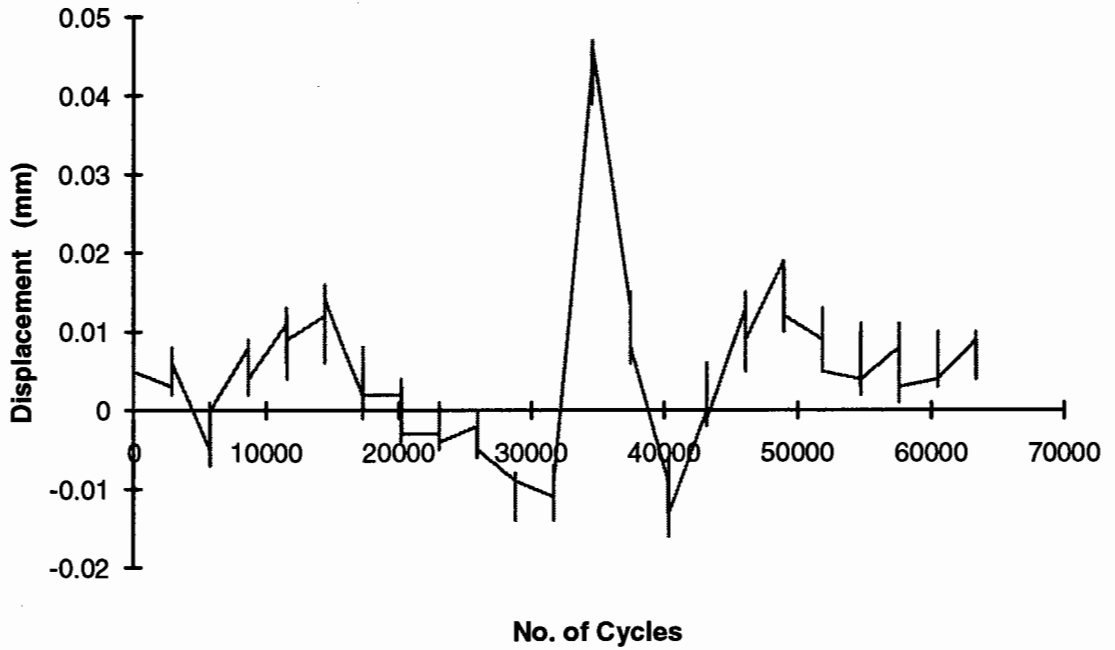
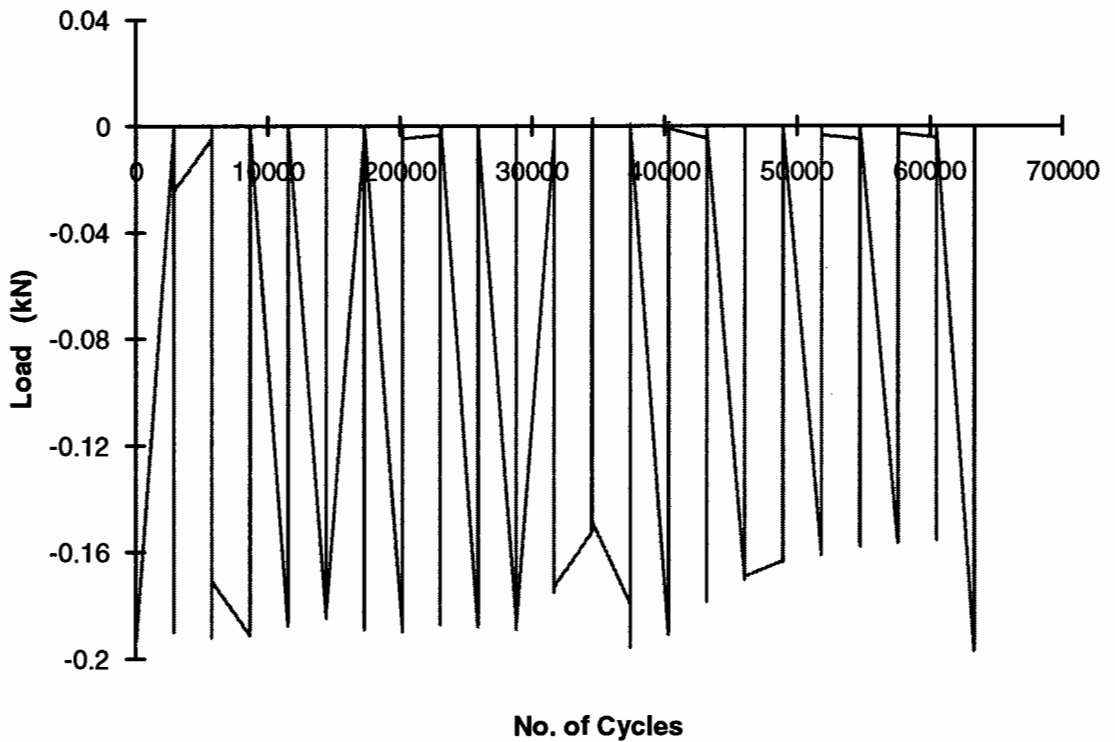


FIG. C.13 Number of Cycles Versus Total Displacement (25.4 mm Diameter Pile)

Test Identity 38.1 - 07 -A



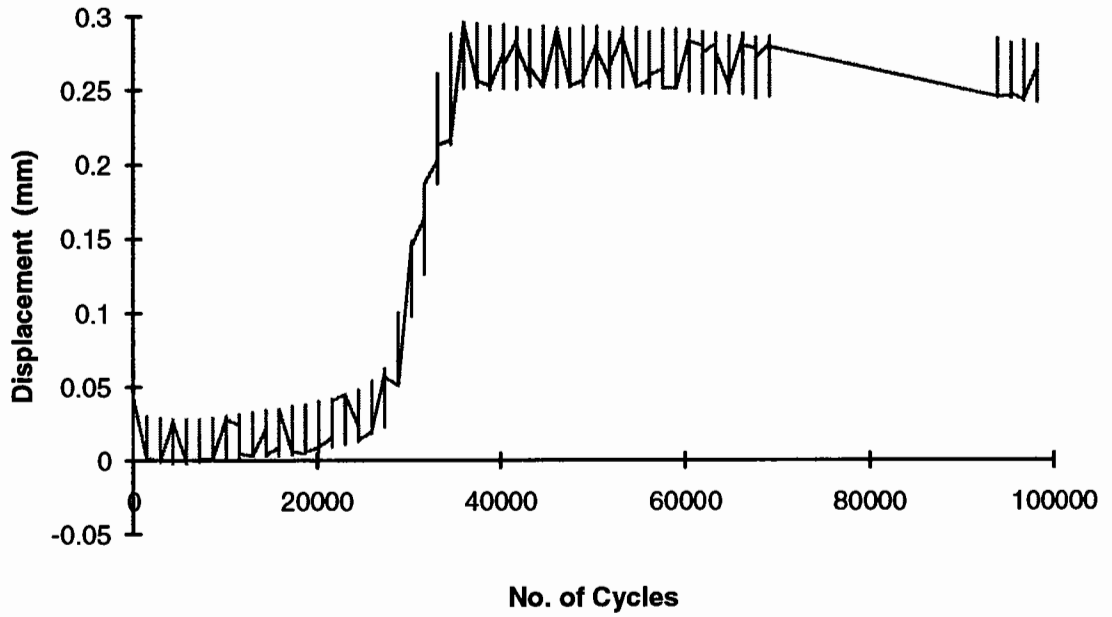
(a)



(b)

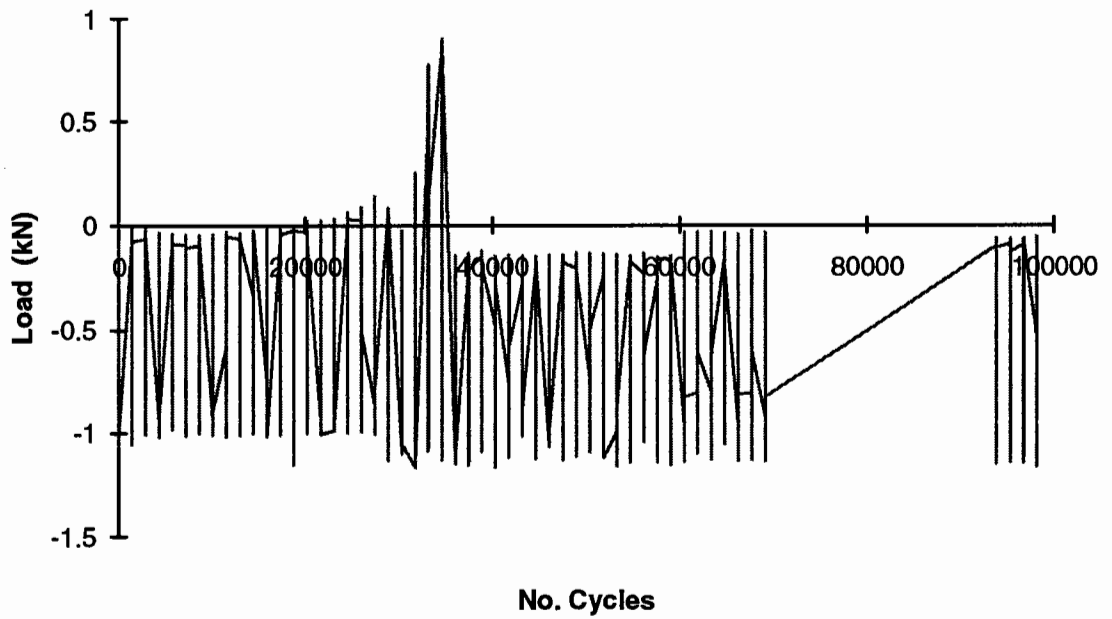
Fig. C.14 Cyclic Load Test Results for the 38.1 mm Diameter Pile (38.1-07-A)

Test Identity 38.1 - 38 - A



(a)

Test Identity 38.1 - 38 - A



(b)

Fig. C.15 Cyclic Load Test Results for the 38.1 mm Diameter Pile (38.1-38-A)

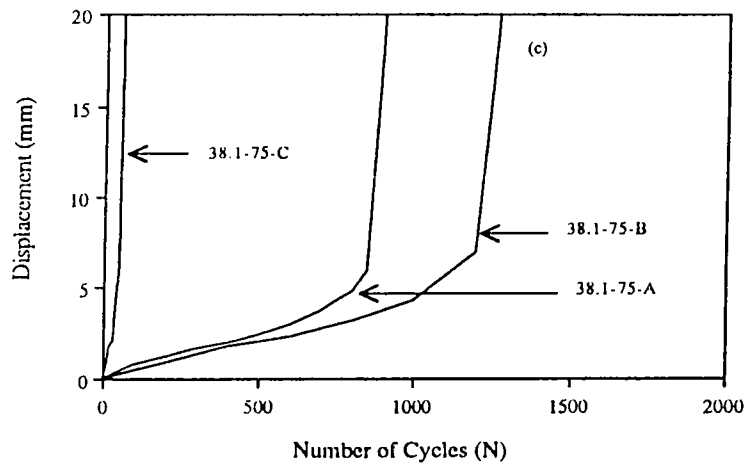
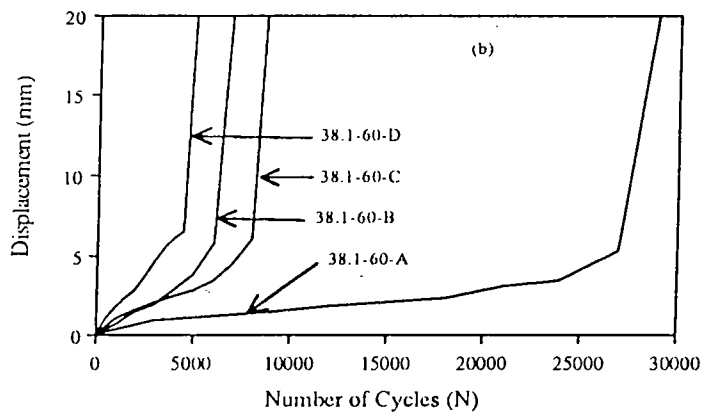
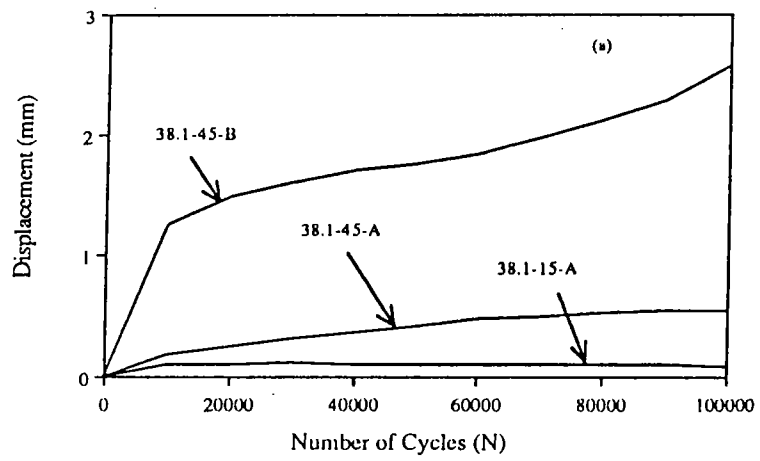
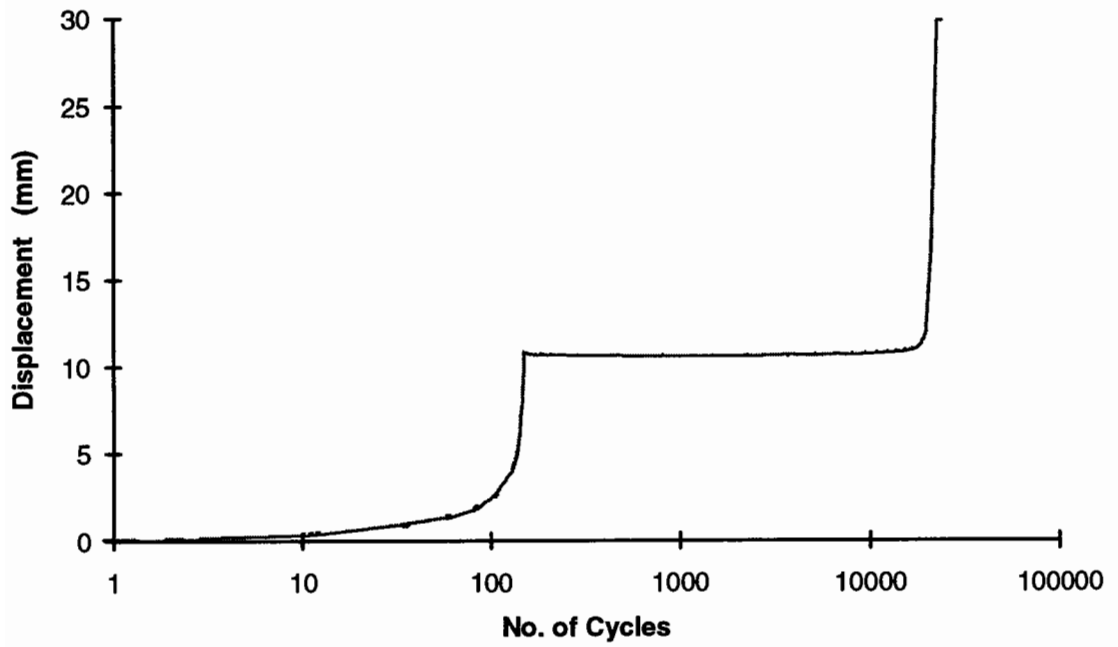


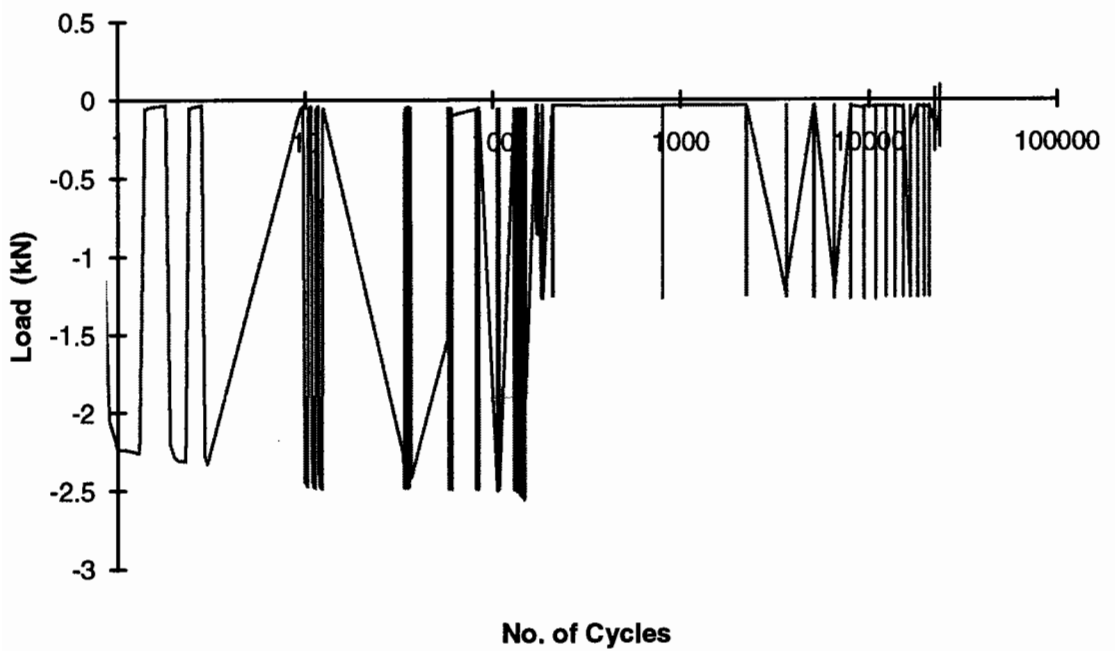
Fig. C .16 Number of Cycles Versus Total Displacement (38.1 mm Diameter Pile)

Test Identity 38.1 - V - A



(a)

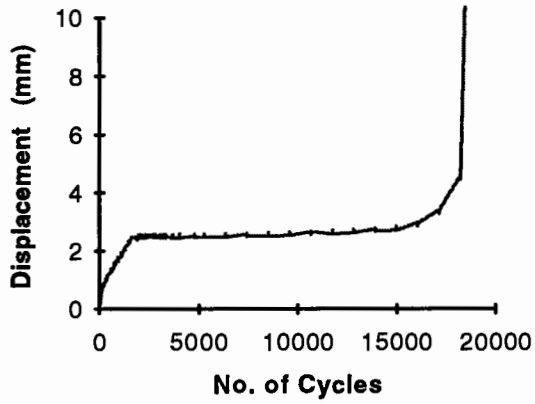
Test Identity 38.1 - V - A



(b)

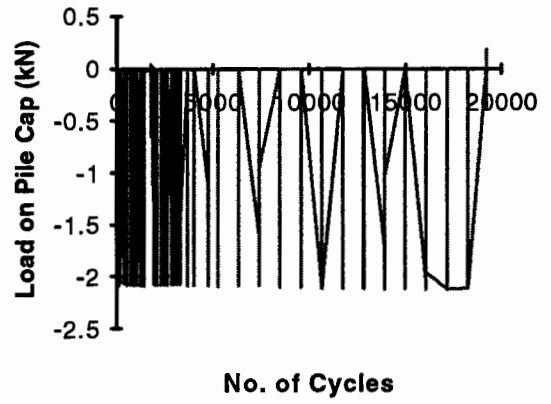
Fig. C.17 Varying Cyclic Load Test Results for the 38.1 mm Diameter Pile

Test Identity 38.1* - 60 - A



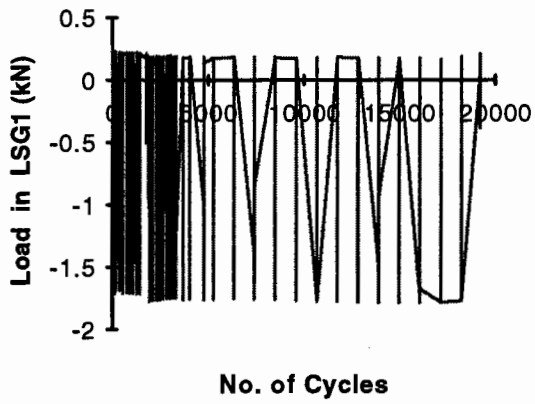
(a)

Test Identity 38.1* - 60 - A



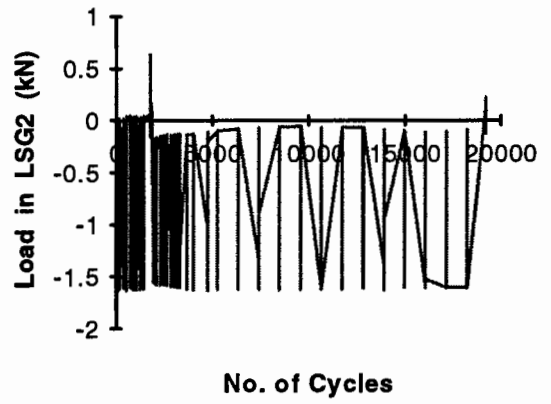
(b)

Test Identity 38.1* - 60 - A



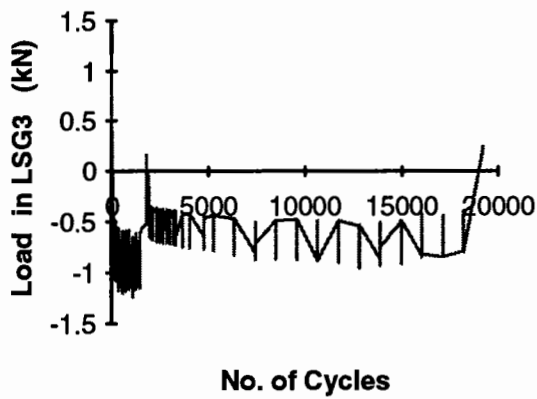
(c)

Test Identity 38.1* - 60 - A



(d)

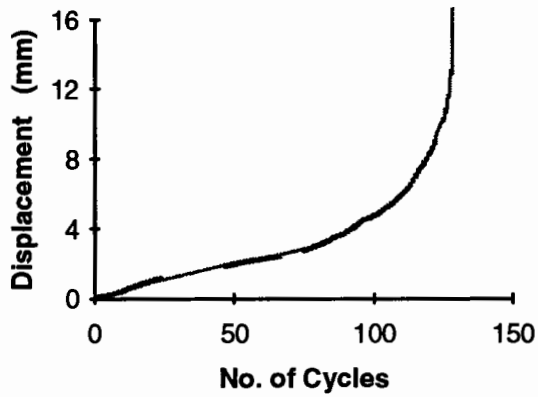
Test Identity 38.1* - 60 - A



(e)

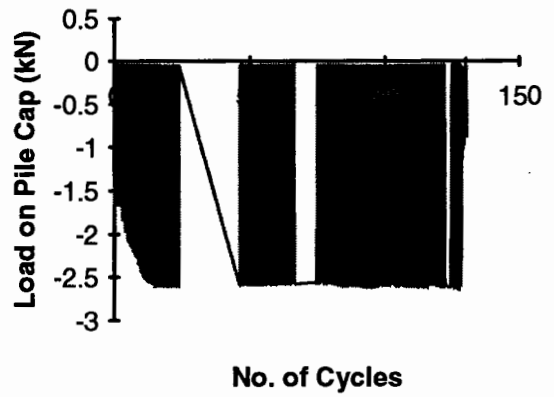
Fig. 18 Constant Cyclic Load Test Results for the Instrumented Pile(38.1*-60-A)

Test Identity 38.1* - 75 - A



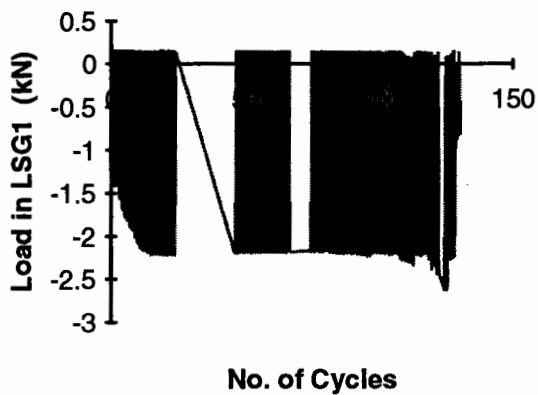
(a)

Test Identity 38.1* - 75 - A



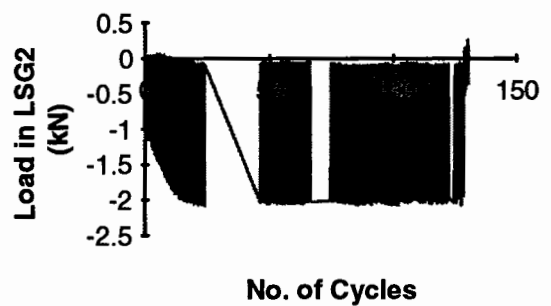
(b)

Test Identity 38.1* - 75 - A



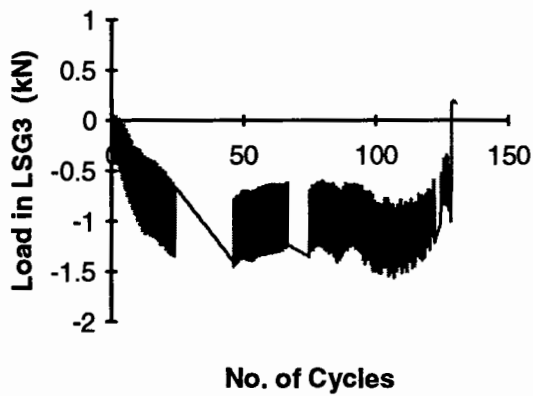
(c)

Test Identity 38.1* - 75 - A



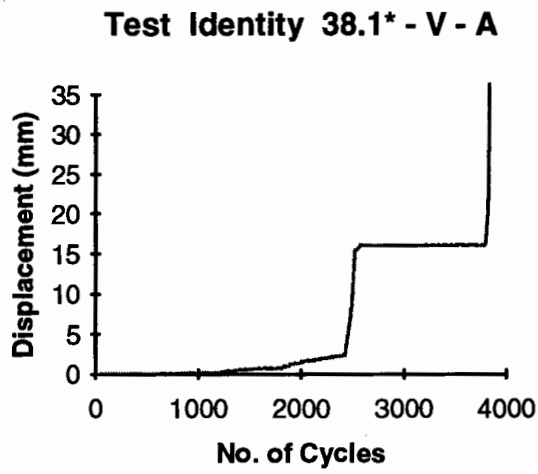
(d)

Test Identity 38.1* - 75 - A

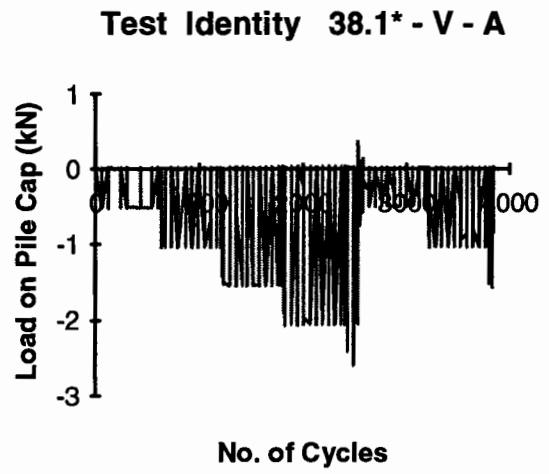


(e)

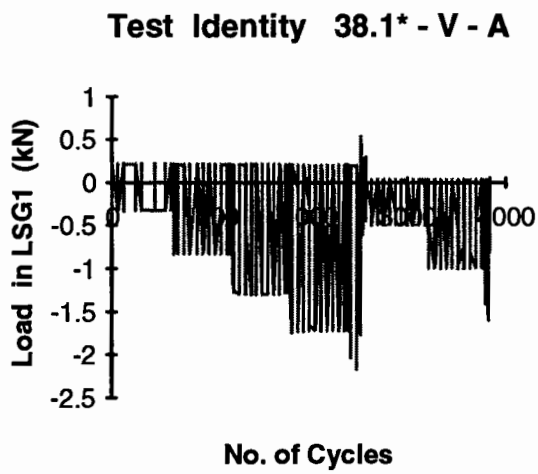
Fig. C.19 Constant Cyclic Load Test Results for the Instrumented Pile(38.1*-75-A)



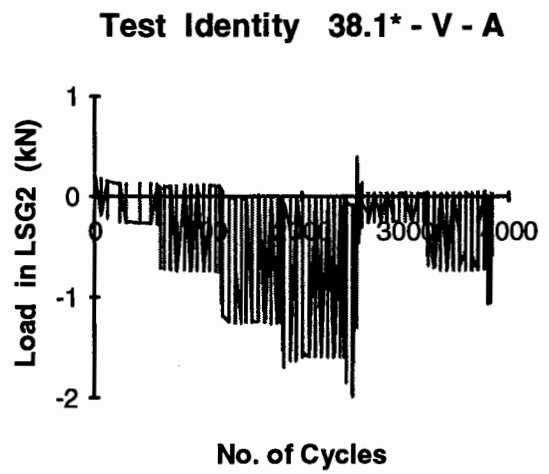
(a)



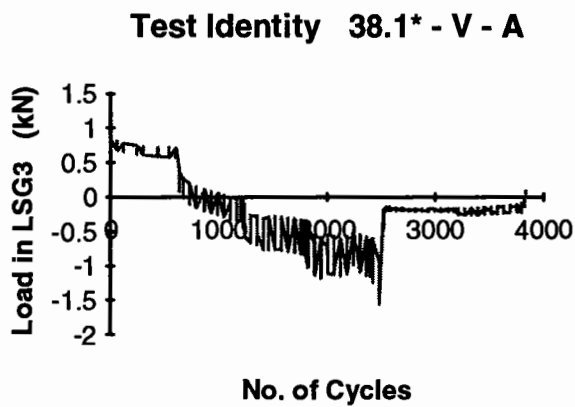
(b)



(c)



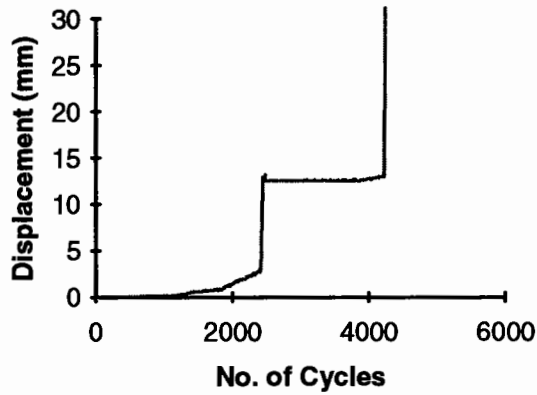
(d)



(e)

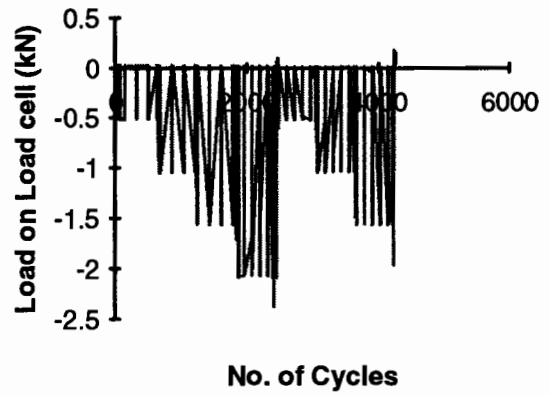
Fig. C.20 Varying Cyclic Load Test Results for the Instrumented Pile (38.1*-V-A)

Test Identity 38.1* - V - B



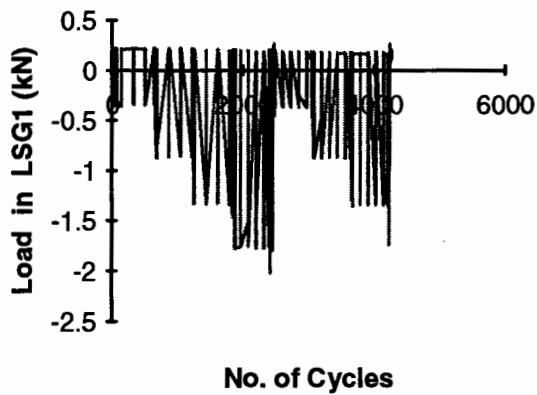
(a)

Test Identity 38.1* - V - B



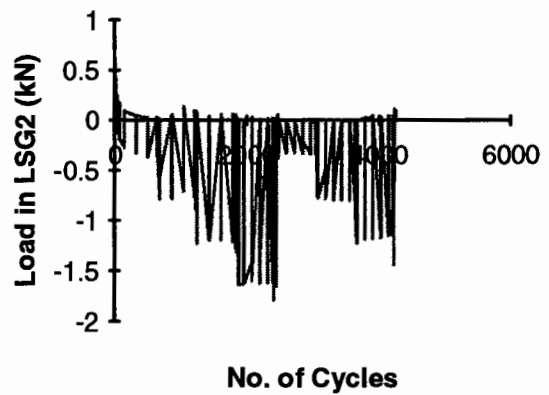
(b)

Test Identity 38.1* - V - B



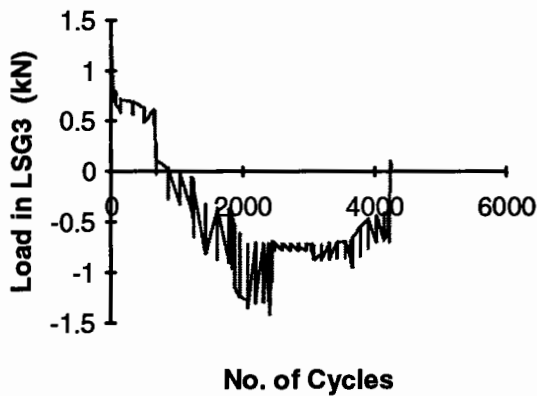
(c)

Test Identity 38.1* - V - B



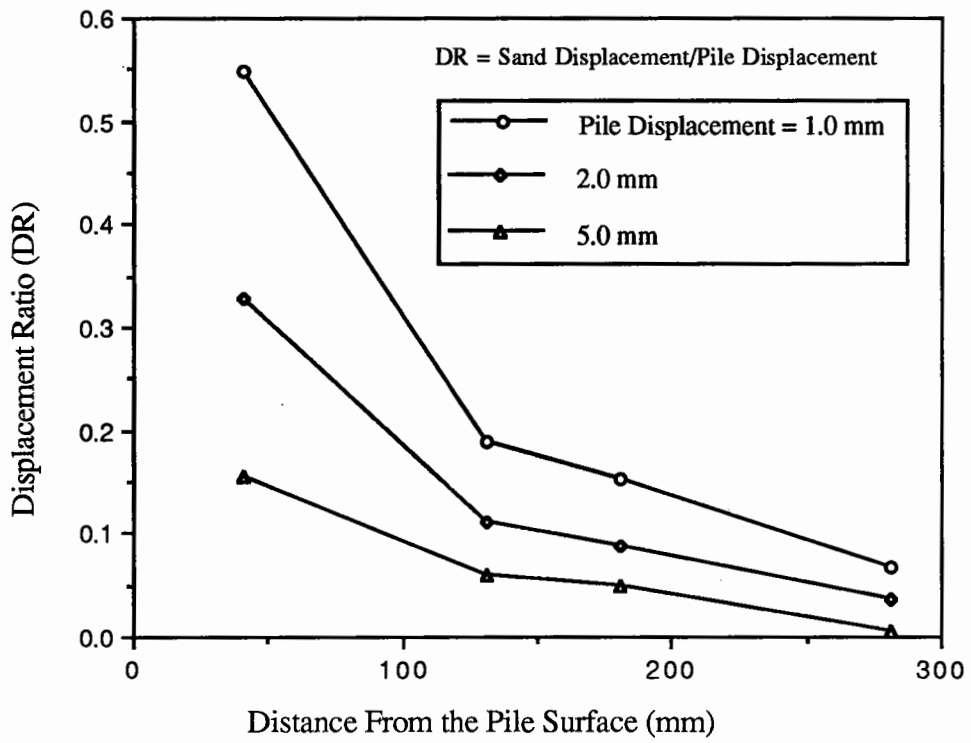
(d)

Test Identity 38.1* - V - B



(e)

Fig. c.21 Varying Cyclic Load Test Results for the Instrumented Pile (38.1*-V-B)



Displacement of the Sand During Monotonic Compression Test

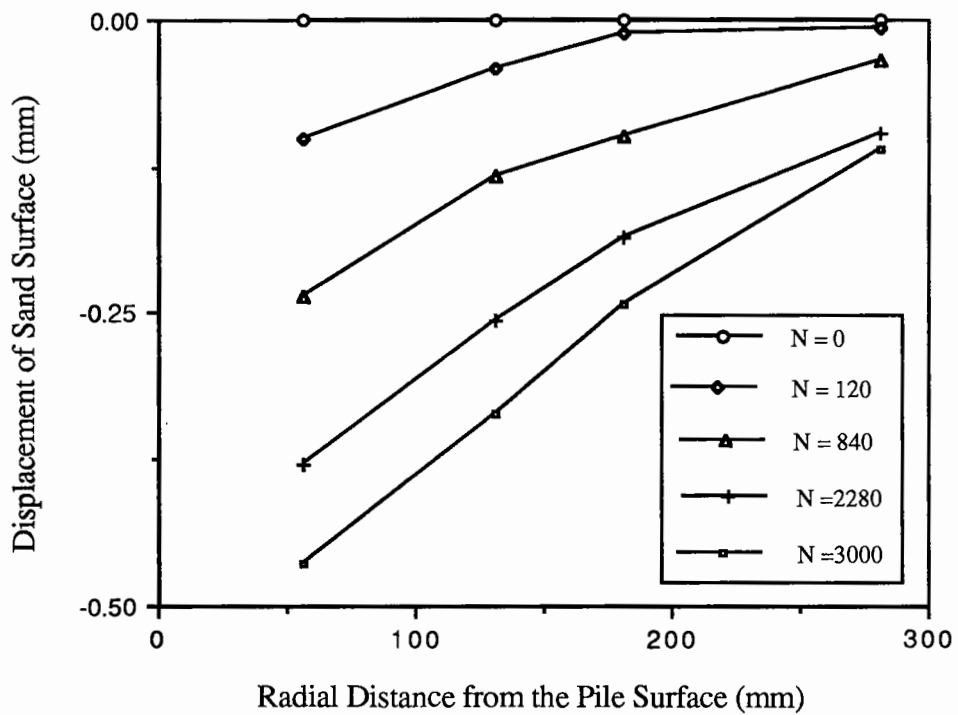


Fig. C.22 Displacement of the Sand Surface During Tensile Cyclic Load Test (38.1 mm Dia. Pile)